

UNIVERSITÄT
BAYREUTH



Importance of Thioarsenates for Rice Plants

Dissertation

zur Erlangung des akademischen Grades
einer Doktorin der Naturwissenschaften (Dr. rer. nat.)
in der Bayreuther Graduiertenschule für Mathematik und Naturwissenschaften
(BayNAT) der Universität Bayreuth

vorgelegt von:

Carolin Franziska Kerl
(MSc. Geoökologie)

geboren in Eichstätt

Bayreuth, August 2019

Die vorliegende Arbeit wurde in der Zeit von Februar 2016 bis August 2019 in Bayreuth am Lehrstuhl Umweltgeochemie unter Betreuung von Frau Professorin Dr. Britta Planer-Friedrich angefertigt.

Vollständiger Abdruck der von der Bayreuther Graduiertenschule für Mathematik und Naturwissenschaften (BayNAT) der Universität Bayreuth genehmigten Dissertation zur Erlangung des akademischen Grades einer Doktorin der Naturwissenschaften (Dr. rer. nat).

Dissertation eingereicht am: 13.08.2019

Zulassung durch das Leitungsgremium: 26.08.2019

Wissenschaftliches Kolloquium: 29.11.2019

Amtierender Direktor: Professor Dr. Dirk Schüler

Prüfungsausschuss:

Prof. Dr. Britta Planer-Friedrich (Gutachterin)

Prof. Dr. Martin Obst (Gutachter)

JProf. Dr. Johanna Pausch (Vorsitz)

Prof. Dr. Angelika Mustroph

Weitere Gutachter Prof. Dr. Adrien Mestrot

Acknowledgements

First of all, I would like to express my sincere gratitude to my advisor Prof. Dr. Britta Planer-Friedrich her great support during the last years. I am especially thankful for numerous helpful discussions and comments about my results and manuscripts. Moreover, I would like to thank her for giving me the opportunity and support to attend several international conferences, workshops, sampling campaigns, and beamtimes on three continents.

I am particularly grateful for the support of my second supervisor Prof. Dr. Stephan Clemens from the Plant physiology Department numerous valuable discussions and helpful contributions to the manuscripts. Additionally, I would like to thank the whole Plant physiology Department for supporting me during rice growth.

I am thankful for a three-year PhD stipend by the German Academic Scholarship Foundation and numerous travel grants to the ICOBTE conferences in 2017 (Zürich), 2019 (Nanjing), and to the Goldschmidt Conference 2018 in Boston. Additionally, I would like to thank the University of Bayreuth Graduate School for a three-month 'Feuerwehrfonds' position as well as for contribution to the travel grant to the ICOBTE conferences 2019 in Nanjing.

My sincere thanks also go to my collaborators Dr. Tiziana Boffa Balera from the Bavarian Geoinstitute for XRD measurements and Colleen Rafferty from the Plant physiology Department for training in rice plant growth and preparation of protein extracts. Furthermore, I would like to thank my supervised students Andrea Colina Blanco, Ruth Alina Schidele, Lena Brüggewirt, und Sonja Pinzer for their help and great cooperation during experiments.

Special thanks should be given to all current and former members of the Environmental Geochemistry Group for their support and greatly appreciated discussions. In particular, I would like to thank Johannes Besold, Dr. Judith Mehlhorn, Jiajia Wang, Anne Eberle, Dr. Jörg Schaller, Dr. Kerstin Hockmann, and Dr. Samer Bachmaf. The assistance for IC-ICP-MS analysis provided by Stefan Will was greatly appreciated. Additionally, I would like to thank my Hiwis Kai Jansen, Kai Hao Tiew, Nathalia Ceron Espejo, Philipp Knobloch, Christin Wirth, Shubi Aurora, and Eva Voggenreither for their help with lab work and great cooperation.

Finally, I would like to sincerely thank my family and friends for supporting me during the last years.

Abstract

Rice (*Oryza sativa* L.) is a staple food for more than half of the world's population; however, it accumulates 10 times more toxic arsenic (As) in its grains than other cereals. Arsenic is ubiquitously present in the environment and mobilized in paddy fields during reductive dissolution of iron (Fe)-minerals under anoxic conditions in flooded paddy soils. Commonly, only inorganic arsenite and arsenate, as well as organic monomethylarsenate (MMA^V) and dimethylarsenate (DMA^V) are considered to be important As species in paddy soils, even though sulfate-reducing, methanogenic conditions are reported in paddy soil pore-water. Thioarsenates, As species where oxygen atoms were replaced by sulfur atoms, have been found under sulfate-reducing conditions in geothermal and terrestrial environments before but have never been reported in paddy fields up to now.

The aim of this thesis was to investigate the occurrence of inorganic and methylated thioarsenates in paddy fields and to study their transformation, uptake, accumulation, and translocation by rice plants. Additionally, the mobility of methylated thioarsenates in presence of Fe(oxyhydr)oxide was examined and it was tested whether roots covered with Fe(oxyhydr)oxide could be a barrier for the uptake of methylated thioarsenates in rice plants.

In the first study, methylated and inorganic thioarsenates were detected in the pore-water of a large variety of paddy soils from different origins and throughout the whole growing season in Italian soils. The contributions of thioarsenates to total As concentrations were similar to methylated oxyarsenates. By determining the thiolation potential in anoxic lab incubations, the soil pH was found to be an easy to measure indicator for the formation of methylated or inorganic thioarsenates. Sulfur-fertilization increased thiolation and methylation in soil but lowered the total As concentration in the pore-water. Increased shares of methylated and thiolated As with decreasing total As indicated that mobility of thioarsenates in the rhizosphere could be higher than that of inorganic As.

The following two studies revealed that thioarsenates could be taken up and transported by hydroponically grown rice plants, nevertheless, differences were observed for the individual thioarsenates. Inorganic monothioarsenate (MTA) was taken up in rice roots and rapidly transformed to arsenite by a so far unknown enzyme, however, this transformation was not complete and MTA was detected in the xylem, as well as in roots and shoots. Higher translocation from roots to shoots, compared to the non-thiolated analog arsenate implied that different, so far unknown, enzymes and transporters were involved in the uptake, reduction, and translocation of MTA. Monomethylmonothioarsenate (MMMTA) is oxygen-sensitive and was partly transformed to its non-thiolated analog MMA^V outside the rice root

by root oxygen loss. No transformation was detected inside the root cells and MMMTA was partly transported to the xylem. The overall As uptake and translocation of rice plants exposed to MMMTA was similar to MMA^V, indicating effective As sequestration in roots, even though the exact mechanism for MMMTA sequestration remained unknown. Dimethylmonothioarsenate (DMMTA) was not transformed by root oxygen loss and taken up inside the rice roots. However, DMMTA was partly transformed to DMA^V in roots but non-transformed DMMTA was partly transported to the xylem. The transformation of DMMTA was most likely a chemical disproportionation in the presence of glutathione to DMA^V and dimethyldithioarsenate (DMDTA). High As accumulation in roots and shoots when plants were exposed to DMMTA revealed that the detoxification and translocation of DMMTA is clearly different from its non-thiolated analog DMA^V.

The fourth study confirmed the assumption from the pore-water speciation in study 1 that methylated thioarsenates were sorbed less to Fe(oxyhydr)oxides than inorganic or methylated As species. Goethite-rich iron plaque formed around rice roots, was no barrier for the uptake of MMMTA and DMMTA in rice roots, as they were not sorbed effectively. Lab studies with goethite and ferrihydrite revealed that methylated thioarsenates have to be transformed to the non-thiolated analogs MMA^V and DMA^V prior to sorption. Especially DMMTA was poorly sorbed in all treatments due to its slow transformation to DMA explaining its high mobility in the rhizosphere.

Altogether, the four studies demonstrated the importance of thioarsenates in paddy soils and for the uptake, translocation, and accumulation in rice plants. Thus, adequate analytical methods that can detect thioarsenates should be included in further studies and their contribution to As accumulation in rice grains should be evaluated, especially as the highly toxic DMMTA has already been detected in rice grains before.

Zusammenfassung

Reis (*Oryza sativa* L.) ist ein wichtiges Grundnahrungsmittel für mehr als die Hälfte der Weltbevölkerung, allerdings nimmt Reis auch 10-mal mehr Arsen (As) als andere Getreidesorten auf. Arsen kommt ubiquitär in der Umwelt vor und wird unter reduzierenden Bedingungen, wie sie in gefluteten Reisfeldern vorkommen, durch die Auflösung von Eisen (Fe)-Mineralen mobilisiert. Üblicherweise werden in Reisfeldern nur anorganische (Arsenit und Arsenat) und organische (Monomethylarsenat; MMA^V und Dimethylarsenat; DMA^V) As-Verbindungen als wichtig erachtet, obwohl in Reisfeldern sulfatreduzierende, methanogene Bedingungen herrschen. Thioarsenate sind As-Verbindungen, bei denen Sauerstoff- durch Schwefelatome ersetzt wurden und diese Verbindungen wurden bereits unter sulfatreduzierenden Bedingungen in Geothermalwässern und terrestrischen Ökosystemen nachgewiesen, allerdings noch nie in Reisfeldern.

Ziel der vorliegenden Arbeit war es, das Vorkommen von anorganischen und methylierten Thioarsenaten in Reisfeldern zu analysieren und ihre Umwandlung, Aufnahme, Akkumulierung und Translokation in Reispflanzen zu untersuchen. Außerdem wurde die Mobilität von methylierten Thioarsenaten in Gegenwart von Fe(oxyhydr)oxiden untersucht und getestet, ob die Bildung von Fe(oxyhydr)oxidbelägen entlang von Wurzeln die Aufnahme von methylierten Thioarsenaten verhindern kann.

In der ersten Studie konnten methylierte und anorganische Thioarsenate in Porenwasser verschiedener Reisböden und im Verlauf der gesamten Vegetationsperiode italienischer Reisböden nachgewiesen werden. Thioarsenate hatten einen ähnlichen Anteil an den Gesamtarsengehalten wie methylierte Oxyarsenate. In anoxischen Laborversuchen, die das Thiolierungspotenzial von Böden ermitteln sollten, war der Boden pH-Wert ein einfach zu messender Indikator für die Bildung von methylierten oder anorganischen Thioarsenaten. Zusätzliche Schwefeldüngung der Reisböden erhöhte den Anteil an thiolierten und methylierten As-Spezies, konnte aber gleichzeitig die Gesamtarsengehalte im Porenwasser senken. Allerdings zeigt die Erhöhung des Anteils an thioliertem und methyliertem As, dass diese As-Spezies im Porenwasser mobiler sein könnten als anorganische As-Spezies.

Die folgenden zwei Studien zeigten, dass Thioarsenate von hydroponisch gezogenen Reispflanzen aufgenommen und transportiert werden können, auch wenn es Unterschiede zwischen den einzelnen Thioarsenaten gab. Anorganisches Monothioarsenat (MTA) wurde in die Wurzeln aufgenommen und rasch durch ein unbekanntes Enzym zu Arsenit umgewandelt, jedoch war diese Umwandlung nicht vollständig und MTA konnte sowohl im Xylem als auch in den Wurzeln und im Spross nachgewiesen werden. Eine im Vergleich

zum nicht-thiolierten Arsenat höhere MTA-Translokation von den Wurzeln in den Spross legt nahe, dass bisher unbekannte Enzyme und Transporter an der Aufnahme, Reduktion und Translokation von MTA beteiligt sind. Monomethylmonothioarsenat (MMMTA) ist sauerstoffsensitiv und wurde teilweise außerhalb der Reisswurzel durch die Sauerstoffabgabe der Wurzeln in das nicht-thiolierte Analogon MMA^V umgewandelt. MMMTA wurde in den Wurzeln nicht weiter umgewandelt und teilweise weiter ins Xylem transportiert. Die Gesamtarsenaufnahme und As-Translokation war für Reispflanzen, die MMA oder MMMTA ausgesetzt waren, ähnlich und lässt darauf schließen, dass As effektiv in den Wurzeln zurückgehalten wurde, obwohl die Mechanismen für MMMTA bis jetzt noch unbekannt sind. Dimethylmonothioarsenat (DMMTA) wurde in die Reisswurzeln aufgenommen, ohne durch die Sauerstoffabgabe der Wurzeln umgewandelt zu werden. Allerdings wurde DMMTA in den Wurzeln teilweise zu DMA^V umgewandelt, aber ein Teil des verbleibenden DMMTAs wurde weiter ins Xylem transportiert. DMMTA zerfällt wahrscheinlich in Gegenwart von Glutathion durch chemische Disproportionierung zu DMA^V und Dimethyldithioarsenat (DMDTA). Wenn Pflanzen DMMTA ausgesetzt wurden, nahmen sie hohe As-Gehalte in den Spross und in die Wurzeln auf, was zeigt, dass sich die Detoxifizierung und Translokation von DMMTA klar von DMA^V unterscheidet.

Die vierte Studie konnte die Vermutungen aus der ersten Studie bestätigen, dass methylierte Thioarsenate schlechter an Fe(Oxyhydr)oxide sorbieren als anorganische oder methylierte As-Spezies. Goethithaltige Eisenbeläge entlang von Reisswurzeln konnten keine Barriere für die Aufnahme MMMTA und DMMTA bilden, da diese Verbindungen nicht effektiv sorbiert wurden. Laborstudien mit Goethit und Ferrihydrit zeigten, dass methylierte Thioarsenate erst in ihre nicht-thiolierten Analoga MMA^V und DMA^V umgewandelt werden müssen, bevor sie sorbiert werden können. DMMTA wurde besonders schlecht sorbiert, da die Umwandlung zu DMA^V nur sehr langsam geschieht, wodurch sich seine hohe Mobilität erklärt.

Zusammen konnten die vier Studien die Wichtigkeit von Thioarsenaten in Reisböden und für die Aufnahme, Translokation und Akkumulation in Reispflanzen zeigen. Deswegen sollten in folgenden Studien adäquate Analysemethoden verwendet werden, die auch Thioarsenate nachweisen können. Die Rolle von Thioarsenaten bei der Akkumulierung von As in Reiskörnern muss weiter untersucht werden, da einzelne Studien bereits das hochgiftige DMMTA in Reiskörnern nachweisen konnten.

Table of content

Acknowledgements.....	V
Abstract	VII
Zusammenfassung	IX
Table of content	XI
List of abbreviations	XIII
List of Figures	XV
Extended summary	1
1. Introduction.....	1
1.1. General problem of arsenic in rice.....	1
1.2. Arsenic in soil and pore-water of paddy fields	2
1.3. Arsenic uptake and transport in rice plants.....	6
1.4. Arsenic accumulation in rice grains	8
1.5. Arsenic mitigation strategies.....	10
1.6. Objectives	11
2. Methods.....	13
2.1. Experiments for detecting thioarsenates in paddy soil pore-water	13
2.2. Hydroponic culture	13
2.3. Transformation of thioarsenates.....	14
2.4. Uptake and translocation of thioarsenates.....	14
2.5. Sorption of thioarsenates to Fe-minerals	15
2.6. As-measurements	15
3. Results and discussion	17
3.1. Occurrence of inorganic and methylated thioarsenates in paddy fields on different scales and parameters influencing their formation (study 1).....	17
3.2. Transformation of inorganic and methylated thioarsenates by rice plants (study 2 and 3)	18
3.3. Uptake, accumulation and translocation of inorganic and methylated thioarsenates by rice plants (study 2 and 3).....	20
3.4. Mobility of methylated thioarsenates in presence of iron plaque and Fe(oxyhydr)oxide minerals (study 4).....	23
4. Conclusion.....	27

References	31
Contribution to studies 1 to 4.....	37
Appendix: Studies 1-4	39
Study 1: Thiolated arsenic species observed in rice paddy pore-waters	41
Study 2: Monothioarsenate Uptake, Transformation, and Translocation in Rice Plants .	109
Study 3: Methylated thioarsenates and monothioarsenate differ in uptake, transformation, and contribution to total arsenic translocation in rice plants	133
Study 4: Iron plaque of rice plants: no barrier for methylated thioarsenates.....	165
List of publications.....	193
Supervised theses.....	195
Bachelor	195
Master	195
(Eidesstattliche) Versicherungen und Erklärungen	197

List of abbreviations

ARPW	artificial rhizosphere pore-water
DIC	dissolved inorganic carbon
DMA ^{III}	dimethylarsenite
DMA ^V	dimethylarsenate
DMDTA	dimethyldithioarsenate
DMMTA	dimethylmonothioarsenate
DOC	dissolved organic carbon
DTA	dithioarsenate
DTPA	diethylenetriaminepentaacetic acid
DTT	dithiothreitol
EDTA	ethylenediaminetetraacetic acid
GSH	glutathione
IC	ion-chromatography
IC ₅₀	half maximal inhibitory concentration
IC-ICP-MS	ion-chromatography coupled to inductively coupled plasma mass spectrometry
ICP-MS	inductively coupled plasma mass spectrometry
IP	iron plaque
MMA ^{III}	monomethylarsenite
MMA ^V	monomethylarsenate
MMDTA	monomethyldithioarsenate
MMMTA	monomethylmonothioarsenate
MTA	monothioarsenate
OVT	ovular vascular trace
PBS	phosphate buffer saline
PC	phytochelatins
ROL	root oxygen loss
SRB	sulfate reducing bacteria
TTA	trithioarsenate
TTTA	tetrathioarsenate
XANES	x-ray absorption near edge structure
XAS	x-ray absorption spectroscopy
μ-XRD	micro x-ray diffraction

List of Figures

Figure 1: Schematic overview of major organic and inorganic As species investigated in rice research so far and environmental relevant organic and inorganic thioarsenates.	5
Figure 2: Schematic summary of lateral As transport in the rice root. Arsenite, MMA ^V , and DMA ^V are transported through the rice root by two aquaporin channels Lsi1 and Lsi2 and sequestered in the vacuoles after PC-complexation (except DMA ^V). Passive diffusion pathways are indicated by dashed arrows (Clemens and Ma, 2016).....	6
Figure 3: Arsenic distribution obtained by synchrotron x-ray fluorescence imaging for a mature rice grain. Rice plants were treated with a: 5 μM arsenate and b: 5 μM DMA ^V . The color chart displays the fluorescence density indicating high As concentrations by red color and the scaling bar equals 500 μm (Zheng et al., 2012).....	9
Figure 4 a: Summarized and simplified formation of inorganic thioarsenates (Planer-Friedrich et al., 2015) and methylated thioarsenates (Fan et al., 2018) in paddy soils. b: Uptake of thioarsenates in roots and shoots of rice plants without IP compared to the As uptake in shoots for rice plants covered with IP (no data for the MTA uptake available). Stability of methylated thioarsenates in the presence of oxygen and ferric Fe and sorption of thioarsenates to IP (goethite and ferrihydrite) and the resulting As mobility in the pore-water (Kerl et al., 2018; Kerl et al., 2019).....	28

Extended summary

1. Introduction

1.1. General problem of arsenic in rice

More than half of the world's population consumes rice (*Oryza sativa* L.) as a major staple food for their subsistence (Chen et al., 2017; Meharg et al., 2009). Besides all its nutritious benefits, rice is known to accumulate 10 times more arsenic (As) in its grains than other cereals (Williams et al., 2007a; Williams et al., 2007b). Especially people depending on a rice-based diet and young children have a higher exposure to As than the average population (BfR, 2014; Mantha et al., 2017). Arsenic was listed first in the substance priority list of the US Agency for Toxic Substances and Disease Registry (ATSDR) which takes the abundance, toxicity, and potential for human exposure of a toxic substance into account (ATSDR, 2017). Generally, As is classified as a human class 1 carcinogen (WHO, 2010) without a defined safe uptake limit that is not increasing the cancer risk (BfR, 2014). Uptake of As should, therefore, be limited to the lowest level possible.

The toxicity of As is strongly dependent on its redox-state and formation of different As species. Arsenic species in rice are separated in organic and inorganic As. Both inorganic arsenite and arsenate are cytotoxic with arsenite being even more toxic than arsenate (Naranmandura et al., 2011; Petrick et al., 2000) and both species are highly bioavailable during digestion in the human gut (Meharg and Zhao, 2012). Organic As is often used as a synonym for monomethylarsenate (MMA^{V}), dimethylarsenate (DMA^{V}), and tetramethylarsonium in rice grains (Hansen et al., 2011; Meharg and Zhao, 2012), but arsenobetain,- cholein, -sugars, -phosphates or -lipids are other common organic As species in food such as fish or mushrooms (Molin et al., 2015). Methylated oxyarsenates (MMA^{V} and DMA^{V}) are regarded as less toxic compared to inorganic As (Naranmandura et al., 2011; Naranmandura et al., 2007), however, both species can be reduced to their trivalent analogs during digestion and the acute toxicity of MMA^{III} und DMA^{III} is higher than that of arsenite (Bartel et al., 2011; Naranmandura et al., 2011; Naranmandura et al., 2007; Petrick et al., 2000; Styblo et al., 2002). Trivalent As species are generally more toxic than pentavalent species.

Threshold values for inorganic As in rice (200 $\mu\text{g}/\text{kg}$ for white rice) were introduced in the European Union and China to minimize the As uptake from rice consumption (Chen et al., 2018; European Commission, 2015). If rice is used for the production of baby food an even lower limit of 100 $\mu\text{g}/\text{kg}$ inorganic As was established in the European Union and the USA.

Taking the highly toxic metabolites of methylated oxyarsenate species into account, their exemption from food guidelines seems questionable.

After outlining the general problem of As accumulation in rice grains, the following sections will identify reasons and mechanisms for As occurrence in paddy fields, its uptake by plants and accumulation in rice grains.

1.2. Arsenic in soil and pore-water of paddy fields

Arsenic is ubiquitously present in the environment at low background levels resulting from weathering of As containing minerals, volcanic eruptions or discharge of geothermal waters (Alloway and Trevors, 2013). The global average of As in soils is about 5-7.5 mg/kg (Matschullat, 2000) but soil concentrations can reach up to hundreds of mg/kg in areas with As-rich bedrocks (Alloway and Trevors, 2013). Anthropogenic As contamination from mining, industry or use of As-containing pesticides or fertilizers can cause locally elevated As concentrations in soils or drinking water (Alloway and Trevors, 2013).

Under oxic soil conditions, used for growing most crops, the predominant As species in the pore-water is pentavalent arsenate. Arsenate is highly immobile due to sorption to iron (Fe)-, manganese (Mn)-, or aluminum (Al)(oxyhydr)oxides and uptake into crops is low (Goldberg and Johnston, 2001; Raven et al., 1998; Williams et al., 2007b). Rice, however, is grown under flooded soil conditions to increase nutrient availability, control weeds or pests, and avoid drought stress (Meharg and Zhao, 2012). Traditionally, rice fields are only drained shortly before harvest to ensure complete ripening of rice grains. Flooding induces several important processes in paddy fields, starting with the depletion of oxygen in soil followed by the reduction of nitrate, manganese oxides and Fe(oxyhydr)oxides. The reduction of ferric Fe is a common indicator for anoxic soil conditions under which sulfate is reduced to sulfide and methane production is enabled. Depending on the soil heterogeneity and different redox conditions in micro-pore sites, these reactions might occur simultaneously and not only step-wise. Solely decreasing redox potential is enough to enable all reactions, however, most reactions are catalyzed by microorganisms which accelerate slow reaction kinetics (Kirk, 2004). After flooding, the soil pH increases to 6.5 – 7 due to the proton consumption during ongoing reduction (Kirk, 2004). Flooding induces further indirect mobilization of nutrients or metals that were sorbed or incorporated in minerals, which were dissolved under reducing conditions. Arsenate or phosphate are for example released during reductive dissolutions of Fe(oxyhydr)oxides and accumulate in the pore-water (Takahashi et al., 2004; Zhang et al., 2003).

Arsenate released into the pore-water is unstable under anoxic conditions and reduced to thermodynamically stable arsenite (Masscheleyn et al., 1991). Speciation analysis in pore-

water samples from flooded paddy fields revealed that besides inorganic arsenite, methylated As species occurred (Takamatsu et al., 1982). Soil microorganisms or algae are able to biomethylate inorganic As by the enzyme As^{III} S-adenosylmethionine (SAM) methyltransferase and produce MMA^V and DMA^V (Fan et al., 2018; Lomax et al., 2012). Recent findings showed that especially sulfur-reducing bacteria (SRB) play an important role in the formation of MMA^V in paddy soils, while the demethylation of DMA^V is controlled by methanogenic archaea (Chen et al., 2019).

Reducing conditions in paddy fields do not only mobilize As into the pore-water but can also lead to As volatilization into the atmosphere (Mestrot et al., 2011). Methylated oxyarsenates formed under reducing conditions in the pore-water can be volatilized by microorganisms (Bentley and Chasteen, 2002) and mostly trimethylarsine, with small contributions of arsine, monomethylarsine, and dimethylarsine were detected above paddy fields or in the headspace of incubations with paddy soils (Mestrot et al., 2011). Rice plants were found to be additional trimethylarsine emitters when methylated As species were present in paddy soil and taken up by the rice plant (Jia et al., 2012). Compared to large As pools in paddy soils, only minor amounts of As are volatilized per year (less than 1% As) but biovolatilization still contributes up to 6% to natural As emissions (Mestrot et al., 2011).

Although flooded paddy fields are overall anoxic, redox potentials can vary on a very small scale for example in micro-pore sites or along rice roots. Rice roots release oxygen (ROL; root oxygen loss) through the aerenchyma to the rhizosphere to cope with anoxic soil conditions. Ferrous iron (Fe²⁺) that was mobilized during reductive dissolution of Fe-minerals after flooding is re-oxidized by the released oxygen and precipitates in nearby rhizosphere or along the roots where it is forming so-called iron plaque (IP). Typical Fe(oxyhydr)oxide minerals such as ferrihydrite, goethite, lepidocrocite, or siderite are found in IP and their contents vary depending on pore-water chemistry (Bacha and Hossner, 1977; Chen et al., 1980; Liu et al., 2006; Seyfferth et al., 2010; Seyfferth et al., 2011; Tripathi et al., 2014). Toxic metalloids (e.g. As) or nutrients (e.g. phosphate) that were mobilized before can be re-sorbed to the newly formed minerals and are therefore effectively removed from pore-water. The sorption of metalloids and nutrients is strongly dependent on pH, mineral crystallinity, competitive ions and their chemical speciation (Dixit and Hering, 2003; Lafferty and Loeppert, 2005; Raven et al., 1998).

Both arsenite and arsenate are sorbed to Fe(oxyhydr)oxides primarily by strong bidentate binuclear inner-sphere complexes (Manning et al., 1998; Ona-Nguema et al., 2005), however weaker outer-sphere complexes can be formed as well (Goldberg and Johnston, 2001). Similar to inorganic As, methylated oxyarsenates sorb to Fe(oxyhydr)oxides forming bidentate binuclear inner-sphere complexes and especially DMA^V forms additional outer-

sphere complexes via electrostatic interactions or hydrogen bonds (Lafferty and Loeppert, 2005; Shimizu et al., 2011). The sorption of all four As species is greater to amorphous Fe(oxyhydr)oxides than to crystalline Fe(oxyhydr)oxides due to the large differences in surface area (Dixit and Hering, 2003). Compared to inorganic As, the additional methyl groups of MMA^V and DMA^V decrease the sorption to Fe(oxyhydr)oxides and facilitate the desorption from Fe(oxyhydr)oxides when competing ions such as phosphate or sulfate are present (Lafferty and Loeppert, 2005).

Formation and behavior of inorganic or methylated As species in paddy soils have been intensively studied over the last decades. However, focusing only on these species might not account for all As species occurring in paddy field pore-water. Anoxic conditions after flooding (described above) are producing methanogenic environments in paddy soils (Kogel-Knabner et al., 2010) which implies that thermodynamically sulfate reduction was favored before methane is produced (standard redox potential for sulfide formation (-221 mV) vs methane formation (-243 mV) (Sigg and Stumm, 1994)). Nevertheless, sulfate reduction was often considered non-important in paddy soils due to the low sulfate concentration in soils (Wind and Conrad, 1997) and formation of mackinawite (Fe^{II}S) as a final S-sink (Ayotade, 1977). This concept omits the possibility of sulfur (S)-cycling, often termed “cryptic” S-cycle (Wind and Conrad, 1997). In this “cryptic” S-cycle, small amounts of sulfate are continuously reduced to sulfide and stepwise re-oxidized to zero-valent S, thiosulfate, and sulfate. None of the S-species is building up in larger quantities during this cycling, but the continuous resupply of S-species triggers many further reactions.

Anoxic, sulfide-rich aquatic environments are known to form As-S-compounds, so-called thioarsenates, where oxygen atoms are replaced by sulfur (Planer-Friedrich et al., 2007) and thioarsenate formation was also reported in terrestrial environments with low sulfide concentrations in the pore-water. Thioarsenate formation in terrestrial environment is most likely controlled by S surface-bound to minerals or organic matter that reacts with pore-water As (Besold et al., 2018; Planer-Friedrich et al., 2018). Thioarsenates are separated in inorganic and organic (methylated) species (Figure 1). Inorganic thioarsenates form at neutral to alkaline pH when S-reducing conditions lead to ligand exchange of OH⁻/SH⁻ at arsenite molecules followed by the addition of zerovalent sulfur (Planer-Friedrich et al., 2010; Stauder et al., 2005). Depending on how many oxygen atoms are substituted, mono-, di-, tri-, or tetrathioarsenate is formed (H₃AsS_nO_{4-n}, n=1-4). Inorganic thioarsenates are abbreviated as MTA, DTA, TTA, and TTTA depending on the number of S-atoms. Methylated thioarsenates form in contrast to inorganic thioarsenates primarily at acidic pH from MMA^V and DMA^V via ligand exchange of OH⁻ by SH⁻ (Conklin et al., 2008; Wallschläger and London, 2008). Four methylated thioarsenates have been found in the

1.3. Arsenic uptake and transport in rice plants

Uptake of non-essential As to rice plant roots is not actively controlled by the plants but As is rather hitchhiking through uptake transporters with similar essential nutrients (Clemens and Ma, 2016). If arsenate (pK_{a1} 2.2, pK_{a2} 6.9) is present in the pore-water, it is a structural analog to phosphate (pK_{a1} 2.1, pK_{a2} 7.1) sharing similar chemical properties. Uptake transporters for phosphate such as OsPht1;1 (Sun et al., 2012), OsPht1;4 (Cao et al., 2017; Ye et al., 2017), or OsPht1;8 (Wang et al., 2016) cannot distinguish between arsenate and phosphate and take up the arsenate unintentionally. Arsenite (pK_{a1} 9.2) occurs as an uncharged molecule at pH 7 in flooded pore-water similar to silicic acid (pK_{a1} 9.5). Silicic acid and arsenite are passively taken up through a nodulin 26-like intrinsic protein (NIP) aquaglyceroporins Lsi1 (OsNIP2;1; Figure 2) (Li et al., 2009; Ma et al., 2006; Ma and Yamaji, 2015; Ma et al., 2008; Zhao et al., 2010). Rice is known to accumulate high silicon (Si) concentrations in tissues as protection against grazing or abiotic stress and increase thereby the uptake of arsenite as well (Ma and Yamaji, 2015). Methylated oxyarsenates MMA^V (pK_{a1} 4.2) and DMA^V (pK_{a1} 6.1) are partly undissociated at a pore-water pH around 7 and can be taken up through the same aquaglyceroporin channel (OsNIP2;1, Figure 2) as arsenite (Li et al., 2009). The uptake of dissociated MMA^V and DMA^V via additional transporters has been hypothesized but no transporter was identified up to now (Meharg and Zhao, 2012).

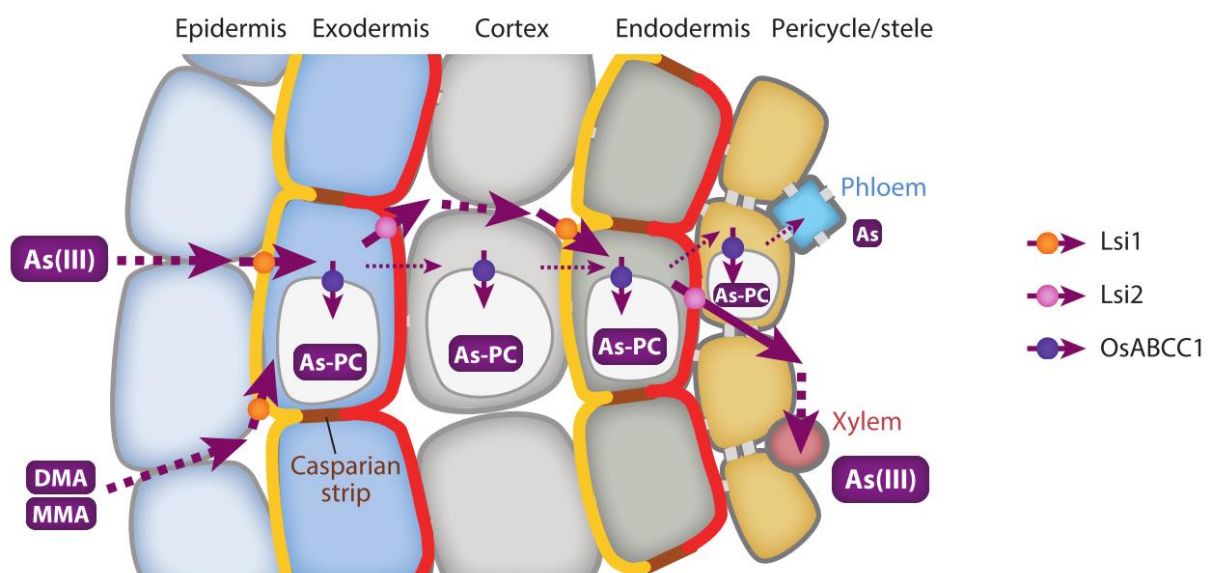


Figure 2: Schematic summary of lateral As transport in the rice root. Arsenite, MMA^V , and DMA^V are transported through the rice root by two aquaporin channels Lsi1 and Lsi2 and sequestered in the vacuoles after PC-complexation (except DMA^V). Passive diffusion pathways are indicated by dashed arrows (Clemens and Ma, 2016).

Especially inorganic As is toxic for rice plants and plants have developed two major detoxification strategies to cope with As uptake. Arsenic is either effluxed out of the root or sequestered in the root to avoid distribution to above-ground biomass. Non-charged As species (arsenite, MMA^{V} , and DMA^{V}) can be effluxed directly via the Lsi1 transporter (Clemens and Ma, 2016; Zhao et al., 2010). Arsenate has to be reduced to arsenite prior to efflux or sequestration and recently, several such arsenate reductases, for example, HAC1;1, HAC1;2, and HAC4 (Shi et al., 2016; Xu et al., 2017) have been identified in rice plants. Non-effluxed trivalent As species can be complexed with thiol ligands such as phytochelations (PC) due to their high affinity to SH^- -groups. Phytochelatin is synthesized in roots cells from glutathione (GSH) and has the general structure $(\gamma\text{-Glutamic acid Cysteine})_n\text{-Glycine}$ with $n=2\text{-}11$ (Cobbett and Goldsbrough, 2002). Arsenite is complexed by SH^- -groups from cysteine forming an $\text{As}^{\text{III}}\text{-PC}$ complex (Clemens, 2006; Mendoza-Cozatl et al., 2011; Pickering et al., 2000; Verbruggen et al., 2009). Besides arsenite, MMA^{V} can be reduced to MMA^{III} and complexed by PCs as $\text{MMA}^{\text{III}}\text{-PC}$ (Mishra et al., 2017; Raab et al., 2005), however, no $\text{DMA}^{\text{III}}\text{-PC}$ complexes have been found in rice roots so far (Raab et al., 2005). Solely, the complexation of As is not sufficient for effective detoxification and PC-complexes have to be sequestered in root vacuoles to avoid translocation to above-ground biomass. The transport of As-PC complexes to vacuoles is mediated by an OsABCC1 transporter (Song et al., 2014) and As-PC complexes are sequestered in vacuoles under acidic pH which enhances their stability (Schmöger et al., 2000).

Even though detoxification of As is quite efficient for inorganic As and MMA^{V} , not all As taken up is trapped in roots and the remaining As can be distributed to above-ground biomass via xylem and phloem. Rice roots developed an efficient system to transport the essential nutrient Si to the xylem and As is transported inevitably with Si. Besides the Lsi 1 transporter that mediates the Si and arsenite influx in the root cells, a similar Lsi 2 transporter mediates the efflux out of root cells and contributes to arsenite and Si loading into the xylem (Figure 1) (Ma et al., 2007; Ma et al., 2008). However, more transporters could be involved in the xylem loading (Clemens and Ma, 2016; Lindsay and Maathuis, 2016; Xu et al., 2015). Methylated oxyarsenates are known to reach the xylem but the involved transporters remain unknown until now (Li et al., 2016; Li et al., 2009).

The most important pathway for inorganic As to reach the rice grain is via phloem transport (around 90% of inorganic grain As and 55% DMA^{V}) while macronutrients (e.g. sugars or amino acids) are accumulated in the rice grains (Carey et al., 2010; Meharg and Zhao, 2012). Phloem and xylem are two separated systems and transfer from xylem to phloem requires active transporters, which can be found in the nodes. Especially node I is important for transferring As from the xylem to the phloem and then further to the grain (Clemens and

Ma, 2016). Phloem cells in the nodes can additionally help to sequester As by PC-complexation and storage of As in cell vacuoles limiting the further As translocation to grains (Song et al., 2014). Before macronutrients or toxicants reach the filial tissue (endosperm, aleurone layer, and embryo) they have to pass a symplastic discontinuity between maternal and filial tissue (ovular vascular trace, OVT) which could act as the last barrier for As accumulation (Meharg and Zhao, 2012).

All the different mechanisms outlined above contribute to As translocation from roots to shoots and further to grains. The transport of inorganic As is understood quite in detail, while much less is known about methylated oxyarsenates and nothing is known about thioarsenates, yet. Comparing the detailed transport (e.g. knowing the exact transporter) of different As species is often difficult and therefore simple As ratios (translocation factors) of two different tissues can already give valuable information about the different behavior of As species.

1.4. Arsenic accumulation in rice grains

Uptake, detoxification, and transport through the rice plant are different for each As species (see 1.3 for details). The As distribution in rice mirrors the different mobility of As species showing high accumulation of arsenite in roots with decreasing contents in stems, leaves, and grains. DMA^V, in contrast, is poorly retained in roots and shoots, but translocated to the grain efficiently (Carey et al., 2010; Zheng et al., 2011). Equal arsenite and DMA^V concentrations can therefore be found in rice grains even if DMA^V concentrations are 5 times lower in paddy soil pore-water than arsenite (Zhao et al., 2013). Arsenite and DMA^V are the dominant As species in rice grains, however, minor amounts of arsenate, MMA^V, DMMTA, and tetramethylarsonium were found in rice grains before (Ackerman et al., 2005; Hansen et al., 2011; Meharg and Zhao, 2012). The location of the two major compounds arsenite and DMA^V has been identified in rice grains by x-ray absorption spectroscopy (XAS) mapping. Arsenite accumulation is highest in the OTV (Figure 3a) while DMA^V is distributed throughout the whole endosperm (Figure 3b) (Zheng et al., 2012), which is in line with the high mobility of DMA^V in all rice tissues leading to accumulation in the terminal plant part. The As distribution in rice grains is also mirrored in the differences between brown and white (polished) rice where the bran and embryo are removed from the endosperm. White rice has lower As concentration and higher shares of DMA^V compared to brown rice (Sun et al., 2008).

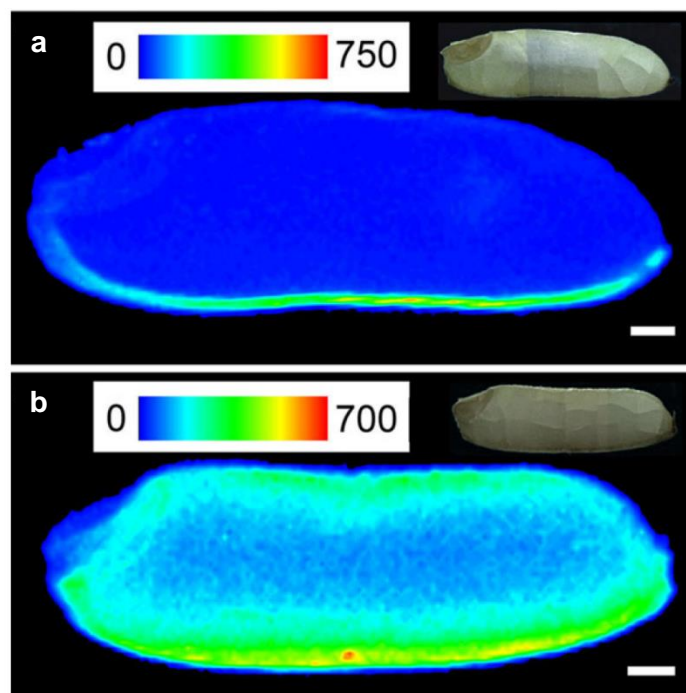


Figure 3: Arsenic distribution obtained by synchrotron x-ray fluorescence imaging for a mature rice grain. Rice plants were treated with a: 5 μM arsenate and b: 5 μM DMA^{V} . The color chart displays the fluorescence density indicating high As concentrations by red color and the scaling bar equals 500 μm (Zheng et al., 2012).

The As speciation in rice grains gave first hints, that As-S molecules (As^{III} -S complexes and DMMTA) can be found in the rice grain, when sophisticated analysis methods were used but it was not clear whether these As species were taken up in the rice plant or formed inside the plant. Analysis of intact rice grains with synchrotron-based X-ray absorption near edge structure (XANES) revealed that trivalent As can be complexed by thiol groups of sulfur-rich amino acid oligomers in rice grains (e.g. As^{III} -PC-complexes). These complexes were most likely formed inside the rice plant and not taken up from the rhizosphere. Analyzing the same rice grains with the standardized acidic digestion, the As-S complex was destroyed and quantified as arsenite (Lombi et al., 2009; Raab et al., 2004). An enzyme-based extraction method used to quantify bioavailable As detected DMMTA in several rice grains and further tests showed that DMMTA is transformed to DMA^{V} during acidic digestion (Mantha et al., 2017). If thioarsenates occur in the paddy soil pore-water, DMMTA might be taken up directly and transported to the rice grains but neither the occurrence of DMMTA in soil pore-water nor the plant uptake was investigated until now. The quantification of DMA^{V} instead of DMMTA is problematic especially as regulatory guidelines in Europe and China exempted organic As from their threshold values due to the lower toxicity compared to inorganic As. DMMTA, in contrast to DMA^{V} , is considered as

toxic as arsenite (Naranmandura et al., 2007) but not taken into account for consumer safety using the standard acidic digestion.

Based on the data from several market surveys around the world, the total As concentration in rice grains can reach from a few up to more than 800 µg/kg. Inorganic As species contribute between 10 to 100% of total As with the remaining 0 to 90% being DMA^V (Zhao et al., 2013). The As speciation showed different patterns between countries or continents with a higher share of inorganic As in Asia, similar shares of organic and inorganic As in Europe and highest shares of organic As in the USA. Rice grains from the USA and Europe often show decreasing percentage of inorganic As when the total As concentrations increased, however, no such trend is found in Asian rice samples (Zhao et al., 2013). The large regional variability could be either due to regional differences in planted rice varieties (genetic differences) or to differences in environmental conditions, especially different soil types. Several studies investigated the same rice variety growing on different soils or different rice varieties on the same soil, revealing that soil properties and water-management have great influence on the As speciation, but genetic differences between rice varieties contribute to the different As speciation as well (Norton et al., 2009; Syu et al., 2015; Zhao et al., 2013).

1.5. Arsenic mitigation strategies

Natural background levels of As in soil are sufficient to accumulate As concentrations in rice grains that are close to or even above the threshold values in Europe or China, especially when rice is intended as baby food (100 µg/kg inorganic As). Several strategies have been developed during the last years to mitigate the As uptake and accumulation in rice grains. Breeding new rice varieties that naturally take up less As or translocate As less efficiently to the grains would be the most effective strategy, however, breeding is a long-lasting and expensive process that will not solve the problem on the short-term. Modifying rice plants genetically (e.g. disabling certain transporters) could be faster (Clemens and Ma, 2016) but, at least in Europe, most consumers would not accept these rice varieties.

If the rice plants cannot be modified, the second strategy is to lower As concentrations in the pore-water and/or to hinder the uptake of As. The major problem of high As concentrations in paddy soil pore-water results from the rice cultivation under flooded conditions and the release of As during reductive Fe dissolution (see 1.2 for details). Changing the water management regime from constantly flooded conditions to altering periods of flooding and draining the soil, shows several benefits. Obviously, less irrigation water is used and no anoxic conditions are developed over a long period, which hinders Fe dissolution and mobilization of As and has the beneficial side effect of lowering methane production (Linquist et al., 2015). Grain As accumulation is reduced compared to constantly

flooded rice fields (Hu et al., 2015; Somenahally et al., 2011), however, the grain uptake of Cadmium (Cd) is increased as Cd mobility increases under oxic conditions (Hu et al., 2015). Observed losses in grain yields after draining soils might be another limitation of this strategy (Linguist et al., 2015).

A third method to mitigate the uptake of As in rice grains is additional soil fertilization for example with Si or S. Arsenite is taken up accidentally via Si transporters (see 1.3 for details) due to the high demand of Si by rice plants. Supplying rice plants with additional Si helps to downregulate the Si transporter and less arsenite is taken up (Ma et al., 2006; Seyfferth et al., 2016; Teasley et al., 2017). Recent findings show, that the uptake of DMA^V can be reduced by Si-fertilization as well (Limmer et al., 2018).

Sulfur-fertilization improves nutrient uptake and rice growth (Crusciol et al., 2013) while methane emissions are decreased (Minamikawa et al., 2005; Schütz et al., 1989). Compared to Si, S-fertilization decreases As uptake not by direct competition but reduces As concentration on the pore-water by enhanced formation of IP (Jia et al., 2015; Saalfield and Bostick, 2009) and newly formed Fe minerals (Jia et al., 2015; Saalfield and Bostick, 2009). Enhanced formation of PCs and arsenite-PC complexes (Dixit et al., 2015; Fan et al., 2013; Zhang et al., 2011) can further contribute to lowering the As accumulation in rice grains after S-fertilization (Fan et al., 2013), however, S-fertilization could not decrease As uptake in grains in Fe rich soils and even increased pore-water As compared to non-fertilized controls (Boye et al., 2017). These findings show that the results for S-fertilization are not fully conclusive, yet. One reason might be that the redox chemistry in paddy fields can favor the formation of thioarsenates (see 1.2 for details) and S-fertilization can further promote their formation by supplying a highly available S pool. Higher As concentrations in pore-water after S-fertilization could, for example, be due to less sorption affinity of inorganic thioarsenates to Fe-minerals (Couture et al., 2013; Suess and Planer-Friedrich, 2012). Before promoting S-fertilization as an effective mitigation strategy for As uptake in rice grains, the role of thioarsenates in paddy soils and their contribution to As uptake in rice plants should be evaluated.

1.6. Objectives

The main aim of this thesis was to elucidate the role of thioarsenates in paddy soils and their uptake, transformation, and translocation in rice plants. Thioarsenates have not been reported in paddy soil pore-water so far, although their formation could be expected under methanogenic, sulfate-reducing conditions in paddy fields (see 1.2 for detailed explanation). Therefore, the first step was to detect thioarsenates in paddy soil pore-water and reveal soil parameters that influence their formation. The second step of the current thesis was to evaluate whether inorganic and methylated thioarsenates can be taken up, translocated

and accumulated by rice plants and whether they are transformed during these processes. Finally, the influence of Fe(oxyhydr)oxide minerals on the mobility of methylated thioarsenates in the pore-water and the influence of IP on their uptake into rice plants was investigated. All these detailed investigations of the behavior of thiolated As species should help to improve our understanding of As accumulation in rice with the overall goal to find strategies for producing rice with low As in grains.

The specific objectives presented in this thesis were to:

- (1) investigate the occurrence of inorganic and methylated thioarsenates in paddy fields on different scales and identify the governing parameters driving their formation (study 1)
- (2) study the transformation of inorganic and methylated thioarsenates by rice plants (study 2 and 3)
- (3) evaluate the uptake, accumulation, and translocation of inorganic and methylated thioarsenates by rice plants (study 2 and 3)
- (4) investigate the mobility of methylated thioarsenates in presence of IP and Fe(oxyhydr)oxide minerals (study 4)

2. Methods

2.1. Experiments for detecting thioarsenates in paddy soil pore-water

After the first screening for thioarsenates in French and Italian paddy soils in August 2016, the occurrence of thioarsenates was studied in detail during the whole growing season (mesocosms) and for different soil types (incubations). The first screening revealed problems with poor recovery for As speciation and an improved method for sample stabilization was developed. Iron in pore-water samples for As speciation was complexed with 10 mM (DTPA diethylenetriaminepentaacetic acid) (neutralized to pH 7.5), flash-frozen and stored at -20°C until analysis by ion-chromatography coupled to inductively coupled plasma mass spectrometry (IC-ICP-MS). Basic soil parameters including pH, 0.5 M HCl-extractable Fe, total As, C, and N were determined for all paddy soils used in further experiments.

The two Italian paddy soils (Fornazzo and Veronica soil) selected for mesocosm experiments contained the highest concentrations of thioarsenates during the first screening. Twelve 0.82 m² containers were filled with each of the soils and installed at the rice research center Ente Nazionale Risi in Italy. All mesocosms were fertilized and amended with rice straw according to agronomic practice in Italy. Additionally, half the mesocosms were fertilized with sulfate and either dry or water seeded with rice seeds (*Oryza sativa* L. cv. Selenio). Pore-water in mesocosms was sampled using micro rhizon samplers (Rhizon MOM, Rhizosphere Research Products, The Netherlands) at seven rice growing stages (tillering, stem elongation, flowering, grain filling, dough, and mature stage). General pore-water parameters (pH, E_H, conductivity, DIC, DOC, Fe^{II}, and total As) were determined and the As-speciation was stabilized and analyzed as described above.

Thiolation potential of 31 Chinese paddy soils was evaluated with anaerobic incubations of 10 g air-dried soil amended with 2.5 mM glucose and 1.5 mM K₂SO₄ (3 mmol/kg sulfate) or without sulfate as a control treatment. After 14 days incubation at room temperature in the dark, pore-water was sampled. In addition to As-speciation, the aqueous phase was characterized by the following parameters: pH, redox potential, dissolved free sulfide, aqueous and soil-bound zero-valent S, total As and Fe.

2.2. Hydroponic culture

Hydroponic experiments were conducted with a European rice variety (*Oryza sativa* L. cv. Arelate) and two Chinese rice varieties (*Oryza sativa* L. cv. Yangdao 6 “YD” and Nongken 57 “NK”). After germination, rice seedlings were grown in 50 mL tubes (Sarstedt) containing a nutrient solution for 20 days (16 h of light and 8 h of darkness at 23°C and 110 μE) and the nutrient solution was exchanged bi-weekly to ensure sufficient supply with nutrients.

For some plants, IP formation was induced at 14-days-old plants by replacing chelated Fe in nutrient solution with 100 mg/L Fe^{II}Cl₂ (Sigma-Aldrich) and reducing the phosphate concentration to 1/20. The nutrient solution was exchanged daily for the following 7 days to ensure sufficient supply with Fe^{II} and nutrients. The IP composition was analyzed by micro-focused X-ray diffractometer (μ -XRD, Bruker, D8 DISCOVER).

2.3. Transformation of thioarsenates

To determine the species transformation of (methylated) thioarsenates in the nutrient solution, 20-day-old plants were exposed to 10 μ M arsenate, MTA, MMA^V, MMMTA, DMA^V, or DMMTA for 24 h and sub-samples for As-speciation were taken over time. Abiotic oxidation by oxygen was tested for 10 μ M of MTA, MMMTA, or DMMTA by purging As spiked nutrient solutions with pressurized air (\approx 40 mM O₂/h) for 24 h. All samples for As-speciation were flash-frozen and stored at -20°C until analysis by IC-ICP-MS unless stated otherwise.

Further, crude protein extracts were used to evaluate whether the transformation of (methylated) thioarsenates could be enzymatically driven (Bleeker et al., 2006; Duan et al., 2005; Wu et al., 2002). Proteins were extracted from flash-frozen rice roots using a protein buffer. As species transformation in crude protein extracts was studied by spiking 500 μ L root protein extract with 3.33 μ M MMMTA, DMMTA, or MTA under anoxic atmosphere (glovebox) and analyzing sacrifice samples over 120 min immediately by IC-ICP-MS. To account for matrix effects, As spiked protein buffer and denaturated protein extracts were analyzed as well.

2.4. Uptake and translocation of thioarsenates

Toxicity of arsenate, arsenite, and MTA was determined by obtaining growth inhibition curves for 5-225 μ M As during a 20-day growth period at two phosphate concentrations (1.8 and 0.9 mM P). A three-parameter-log-logistic dose-response model (Sigma plot) and IC₅₀ values were derived from the relative root and shoot lengths, as well as seedling fresh weights.

As-speciation in xylem sap was analyzed by IC-ICP-MS after rice plants were exposed to 10 μ M arsenate, MTA, MMA^V, MMMTA, DMA^V, or DMMTA for 24 h. Therefore, plants were cut 2 cm above the roots with a sharp blade and xylem was sampled for 1.5 h into a diluted ice-cold phosphate buffer saline (PBS, 2 mM NaH₂PO₄ (Grüssing) + 0.2 mM Na₂-EDTA (Grüssing); pH 6.0 (Xu et al., 2007)).

After testing the stability of MTA in different extractants and evaluating their extraction efficiency, a new method for MTA extraction in plant tissue was developed. Therefore, plant material was flash-frozen and ground in liquid nitrogen before 0.01-0.06 g was extracted in

1.5 mL PBS (Xu et al., 2007). The samples were boiled for 5 min to reduce MTA transformation, before vortexing them for 55 min under anoxic conditions inside a glovebox. The As speciation was analyzed immediately after extraction by IC-ICP-MS.

Uptake and translocation of 10 μM arsenate, MTA, MMA^{V} , MMMTA , DMA^{V} , or DMMTA in rice roots and shoots was studied over 72 h. After exposure to As, roots were washed with 1 mM KH_2PO_4 , 5 mM $\text{Ca}(\text{NO}_3)_2$, 5 mM MES for 10 min to remove As sorbed to root surface (Xu et al., 2007). Additional uptake experiments were conducted for rice plants covered with and without IP, exposing the plants to 10 μM MMA^{V} , MMMTA , DMA^{V} , or DMMTA for 8 h. Total As concentrations of all samples were determined by ICP-MS after microwave digestion (0.01-0.08 g plant material was digested in concentrated HNO_3 and 30% H_2O_2 (ratio 1.5:1) using a CEM Mars 5 microwave digestion system (CEM Corp., Matthews, NC). For rice seedlings exposed to arsenate and MTA, the As speciation was analyzed by IC-ICP-MS using the newly developed method. Translocation factors from roots to shoots were calculated ($\text{As-shoot}/\text{As-root}$).

2.5. Sorption of thioarsenates to Fe-minerals

Laboratory sorption experiments of methylated thioarsenates on goethite and ferrihydrite, the two most common components of IP, were conducted under anoxic conditions. After pre-equilibration for 16 h, MMA^{V} , MMMTA , DMA^{V} , or DMMTA were spiked to goethite or ferrihydrite and equilibrated. Samples for As speciation and total As (stabilized with 2.5% 7 M HNO_3) were taken after centrifuging for 5 min (5000 rpm; Hettich) and the pH was measured in the remaining samples. Three different sorption experiments were conducted. First, the kinetic sorption was evaluated by spiking 5 μM MMA^{V} , MMMTA , DMA^{V} , or DMMTA at pH 6.5 to both minerals and taking sacrifice samples over 72 h. Sorption isotherms were obtained at pH 6.5 by spiking 0.5-500 μM MMA^{V} , MMMTA , DMA^{V} , or DMMTA to mineral suspensions and equilibration for 2 h. The pH-dependent sorption was determined by spiking 5 μM MMA^{V} , MMMTA , DMA^{V} , or DMMTA at pH 4-12 for 2 h to goethite and ferrihydrite. All sorption experiments were conducted in an electrolyte that mimics the rhizosphere pore-water (called ARPW, artificial rhizosphere pore-water) and can sustain rice plant growth.

2.6. As-measurements

Pore-water samples stabilized with DTPA were diluted 1:5 with deionized water prior to analysis. Arsenic species for all experiments were analyzed by IC (Dionex ICS-3000) coupled to ICP-MS (XSeries2, Thermo-Fisher) using oxygen as reaction gas (AsO^+ m/z 91). Pore-water and laboratory samples containing (methylated) thioarsenates were separated using an AS16 column (Dionex AG/AS16 IonPac column, 2.5–100 mM NaOH, flow rate 1.2

mL/min) and 2.4% methanol was added for pore-water samples to enhance detection limits (Wallschläger and London, 2008). As speciation in laboratory samples without methylated thioarsenates was determined by using a PRP-X100 column (Hamilton, 10 mM NH_4NO_3 , 10 mM $\text{NH}_4\text{H}_2\text{PO}_4$ and 500 mg/L $\text{Na}_2\text{-EDTA}$ at a flow rate of 1.0 mL/min) at the IC-ICP-MS (Van de Wiele et al., 2010). All samples for determination of total As (AsO^+ m/z 91) and Fe (Fe^+ m/z 56 using -2V kinetic energy discrimination with helium as collision gas) were analyzed by ICP-MS and Rhodium (Rh^+ m/z 103) was used as an internal standard correction for signal drift.

3. Results and discussion

3.1. Occurrence of inorganic and methylated thioarsenates in paddy fields on different scales and parameters influencing their formation (study 1)

Thioarsenates were detected throughout the whole growing cycle in the pore-water of mesocosms with and without S-fertilization as well as in all soil incubations regardless of the soil type. Up to 19% (4.1% on average; all values calculated as the share of total As) thioarsenates and up to 33% (6.5% on average) methylated species were found in the pore-water of mesocosms during the rice growth (see appendix study 1, Figure 2 and 3). Among the thioarsenates, the share of inorganic thioarsenates was higher than that of methylated thioarsenates (19 compared to 8.2%, respectively). Additionally, the thiolation and methylation potential of paddy soils was determined in soil incubation experiments, without rice plants to eliminate additional effects of As uptake and changing redox-conditions by ROL. There, the maximum share of total thiolation with 56% (9.6% on average) and total methylation with 38% (7.5% on average) was higher than in mesocosms (study 1, Figure 4). Similar to the mesocosms, more inorganic thioarsenates were found compared to methylated thioarsenates (40 compared to 32%, respectively).

Both field and lab experiments revealed that thioarsenates could occur in paddy soil pore-water; however, parameters driving their formation were unknown until now. Our results showed that inorganic and methylated thioarsenates have to be evaluated separately as their formation is influenced by different parameters. Alkaline soil pH and soil zero-valent S showed a positive correlation with the formation of inorganic thioarsenates, while the share of methylated oxyarsenates and acidic soil pH showed the best correlation with the formation of methylated thioarsenates (study 1, Figure 4). Soil bound zero-valent S was shown to control the formation of inorganic thioarsenates in terrestrial low sulfide environments (Besold et al., 2018; Planer-Friedrich et al., 2018) and soil zero-valent S increased with soil pH in our experiments. The positive correlation of soil pH and formation of inorganic thioarsenates was therefore mainly caused by the strong correlation between soil pH and soil zero-valent S, mirrored in our data where zero-valent S predicted the formation of inorganic thioarsenates best. The pedogenic (0.5 M HCl-extractable) Fe had little influence on the formation of inorganic thioarsenates because only low concentrations of Fe were dissolved due to the high pH (study 1, Figure 4).

In contrast to inorganic thioarsenates, the formation of methylated thioarsenates was mainly correlated to the share of methylated oxyarsenates. Acidic soil pH was enhancing the formation of methylated oxyarsenates that are preferably formed at pH 3.5 to 5.5 (Baker et al., 1983) and additionally enhanced the formation of methylated thioarsenates as they are

formed under acidic pH by a nucleophilic attack of reduced S to the As atom (Conklin et al., 2008). However, the influence of pedogenic Fe was greater on methylated than on inorganic thioarsenates, as more Fe was soluble at low pH. Moreover, low total As concentrations in soil were a powerful predictor for high (thio)methylation because only the absolute concentrations of inorganic As species increased with increasing soil As and the share of (thio)methylated As species stayed constant (study 1, Figure 4).

Besides the natural soil properties discussed above, As concentrations and thiolation were further influenced by S-fertilization. Sulfur-fertilization in mesocosms decreased the total pore-water As compared to treatments without additional S (study 1, Figure 2), which is in line with previously published data (Jia et al., 2015; Saalfield and Bostick, 2009). Additional sulfate stimulated SRBs and with this enhanced the sulfide production and formation of Fe-minerals (Jia et al., 2015; Saalfield and Bostick, 2009). Newly formed Fe^{II}Fe^{III} or FeS minerals were sinks for especially inorganic As species while inorganic and methylated thioarsenates, as well as methylated oxyarsenates sorbed to a lower extent and their relative contribution to total pore-water As increased with S-fertilization (see study 4 for discussion about sorption to Fe minerals). Additionally, S-fertilization enhanced the As thiolation because more zero-valent S was available and the pore-water Fe concentration, as well as the redox potential, were decreased. The effects of S-fertilization were most pronounced in soils with very low zero-valent S. One of these soils was the Italian soil Veronica used for mesocosms and lab incubations. There, S-fertilization increased zero-valent S by 49% compared with non-fertilized soil and total thiolation increased from 28.7 to 56.1% in incubation and from 1.9 to 6.2% in mesocosms. The second Italian soil, Fornazzo, had a higher zero-valent S concentration and S-fertilization increased the soil-bound zero-valent S only by 13%. Sulfur-fertilization did not increase the As thiolation in this soil (study 1, Figure 3 and 4).

3.2. Transformation of inorganic and methylated thioarsenates by rice plants (study 2 and 3)

After we detected thioarsenates and proved their importance in paddy fields (study 1), we were interested in their transformation and uptake by rice plants. To investigate the interaction of thioarsenates with rice plants, we conducted all further experiments in hydroponic culture to simplify the system and amended the nutrient solution with thioarsenates. We selected the inorganic species MTA and the two methylated thioarsenates MMMTA and DMMTA as model compounds that were synthesized in our lab.

In first experiments, we monitored the As speciation in nutrient solution spiked with thioarsenates over time to estimate whether the As species can be transformed by rice

plants (via uptake or by ROL). We could show that all rice cultivars transformed MTA to arsenite or arsenate while MTA remained stable in the control treatment without plants (Kerl et al., 2018; Kerl et al., 2019). Surprisingly, different compositions of the nutrient solutions in study 2 (without phosphate and only 50% Fe) and 3 (complete nutrient solution) led to MTA transformation either to arsenite (study 2, Figure 4) or to mainly arsenate (study 3, Figure 2). Additional tests without plants revealed that higher phosphate and Fe concentrations could slightly increase the oxidation of arsenite to arsenate but it remained unclear whether this could explain the observed differences in MTA transformation. Based on knowledge about arsenate reduction to arsenite and arsenite efflux by plants as part of their As detoxification process (Xu et al., 2007; Zhao et al., 2009), the transformation of MTA to arsenite instead of arsenate was more likely. We further analyzed the As speciation in crude protein extracts of rice roots to separate the processes and interactions of the nutrient solution from the reactions inside the rice roots. Crude protein extracts transformed MTA to arsenite rapidly in all cultivars, while MTA remained stable in denatured crude protein extracts (study 3, Figure 3). Our results were explained best by an enzymatic transformation of MTA to arsenite inside rice roots similar to the reduction of arsenate to arsenite by HAC-family enzymes (Shi et al., 2016; Xu et al., 2017). However, up to now, no enzyme is known that can reduce MTA to arsenite and further studies need to identify the responsible enzyme.

Both methylated thioarsenates were transformed by rice plants when they were spiked to the nutrient solution, but the underlying mechanisms were different from the enzymatic transformation of MTA. Rice plants transformed MMMTA, present in the nutrient solution, faster to MMA^V than in the control treatment without plants (study 3, Figure 2). However, MMMTA was stable in crude protein extracts indicating that the transformation from MMMTA to MMA^V was not driven by enzymes (study 3, Figure 3). Pre-tests revealed that MMMTA was sensitive to oxygen and transformed into MMA^V when exposed to air (study 3, Figure 1) (Cullen et al., 2016; Kerl et al., 2019). Rice roots are known to release oxygen into the rhizosphere and this ROL most likely transformed MMMTA to MMA^V by oxidizing the sulfide bound in MMMTA outside the rice root.

Like MTA and MMMTA, DMMTA was transformed to DMA^V by rice plants when spiked to the nutrient solution, while the control without rice plants remained stable (study 3, Figure 2). Transformation of DMMTA in crude protein extracts was not significantly different from the transformations found in denatured controls (study 3, Figure 3). Further tests showed that DMMTA was disproportionated to DMA^V and DMDTA in the protein buffer without root material. A similar reaction was observed before where DMMTA disproportionated abiotically in the presence of glutathione (GSH) to DMA^{III} and DMDTA under neutral to basic

conditions and to DMA^{III}-GSH and DMDTA under acidic conditions (Raab et al., 2007b; Suzuki et al., 2008). Our protein buffer contained dithiothreitol (DTT) instead of GSH, but tests with DTT revealed that DMMTA was disproportionated to DMA^V and DMDTA in its presence as well. Compared to the enzymatic transformation of MTA and the oxidation of MMMTA by ROL, DMMTA was most likely transformed abiotically by the root matrix for example by disproportionation of DMMTA to DMDTA and DMA^{III} in the presence of GSH under neutral and slightly alkaline conditions as they occur in cytoplasm (pH 7.5) (Suzuki et al., 2008).

3.3. Uptake, accumulation and translocation of inorganic and methylated thioarsenates by rice plants (study 2 and 3)

The results of As species transformation in the nutrient solution gave first evidence that thioarsenates were taken up by rice plants, however, the direct proof of thioarsenate uptake in plants was still missing. Growth inhibition curves of rice seedlings with MTA in comparison to arsenite and arsenate revealed that MTA (IC₅₀: 50 µM for shoot weight) was at least as toxic as arsenate (IC₅₀: 190 µM) but less toxic than arsenite (IC₅₀: 4 µM) and these results were additional evidence for MTA uptake (study 2, Figure 3) (Kerl et al., 2018). Similar toxicity of As species was found before for *A. thaliana* (arsenite>MTA>arsenate) indicating that MTA is toxic for different plant families (Planer-Friedrich et al., 2017).

The first direct evidence for uptake of thioarsenates in rice plants was found when xylem sap of rice plants exposed to thioarsenates was sampled. Up to 20±5% MTA, 18±1% MMMTA, and 7±1% DMMTA were detected in the xylem sap proving that these species were taken up intact by the rice roots and at least partially transported in the xylem (study 2, Figure 5 and study 3, Figure 4) (Kerl et al., 2018; Kerl et al., 2019). For MTA, we additionally developed an extraction method with which we can determine the As speciation in shoots and roots and found 12-19% MTA in roots and 4% MTA in shoots, respectively (study 2, Figure 6) (Kerl et al., 2018).

After we proved that MTA, MMMTA, and DMMTA were directly taken up and transported in the xylem, the next step was to quantify the accumulation and translocation of total As in roots and shoots when 20-day-old rice plants were exposed to 10 µM thioarsenates. Rice roots accumulated most total As (after 72 h) in plants when exposed to MMMTA (220±27 µmol/kg), MMA^V (146±5 µmol/kg), and DMMTA (130±22 µmol/kg), less total As when plants were exposed to MTA (57±2 µmol/kg) or DMA^V (14±1 µmol/kg). The order of total As accumulation in shoots was different and most As was taken up when plants were exposed to DMMTA (44±6 µmol/kg), followed by MTA (40±7 µmol/kg), MMMTA (17±8 µmol/kg), MMA^V (10±1 µmol/kg) and DMA^V (9±3 µmol/kg) (study 2, Figure 6 and study 3, Figure 5).

Combining the results from roots and shoots, the following root-to-shoot translocation factors were calculated: DMA^{V} (0.61 ± 0.15) = MTA (0.55 ± 0.14) \approx DMMTA (0.34 ± 0.03) > MMMTA (0.08 ± 0.03) = MMA^{V} (0.07 ± 0.01) (Kerl et al., 2018; Kerl et al., 2019).

Our results showed that uptake, accumulation, and translocation of thioarsenates were different from their non-thiolated analogs. Compared to organic and inorganic As (arsenate, arsenite, MMA^{V} , and DMA^{V}) which were studied intensively during the past, no information about uptake mechanisms, involved enzymes, or transporters was available for (methylated) thioarsenates. Arsenate ($\text{pK}_{\text{a}1}$ 2.2; $\text{pK}_{\text{a}2}$ 6.9), phosphate ($\text{pK}_{\text{a}1}$ 2.2; $\text{pK}_{\text{a}2}$ 7.2), and MTA ($\text{pK}_{\text{a}1}$ 3.3; $\text{pK}_{\text{a}2}$ 7.3) are structural analogs and the structural similarity inadvertently leads to arsenate uptake via phosphate transporters (Cao et al., 2017; Clemens and Ma, 2016; Wu et al., 2011). Our growth inhibition experiments showed that reduced phosphate concentrations in the nutrient solution increased the MTA toxicity for rice seedlings (IC_{50} : 50 μM compared to 7.5 μM) similar like for arsenate (IC_{50} : 190 μM compared to 25 μM ; study 2, Figure 3) (Kerl et al., 2018). Hence, the increased MTA toxicity with reduced phosphate concentration could be indirect evidence that MTA was taken up through phosphate transporters as well.

Compared to the anions arsenate, phosphate, and MTA, both MMA^{V} ($\text{pK}_{\text{a}1}$ 4.2) and DMA^{V} ($\text{pK}_{\text{a}1}$ 6.1) are taken up as non-charged molecules by the aquaporin channel OsNIP2;1 (Li et al., 2009). Depending on the pH in nutrient solution or pore-water (pH 5 for our experiments or in paddy soil pore-water 6.5-7), dissociated MMA^{V} and DMA^{V} become dominant at higher pHs and their uptake decreases with increasing pH (Li et al., 2009). No uptake transporter for methylated thioarsenates is known until now. Theoretical assumptions about a possible uptake transporter for methylated thioarsenates were more difficult than for MTA because no pK_{a} values were determined for MMMTA and DMMTA , yet. Nevertheless, the chromatographic behavior of DMMTA led to the assumption that the $\text{pK}_{\text{a}1}$ for DMMTA is between 6-7 and MMMTA might be similar to MMA^{V} (Raml et al., 2006). Uptake as non-charged molecules via aquaporin channels could be possible for both, MMMTA and DMMTA . However, systematic uptake experiments with varying composition of the nutrient solution are needed to identify possible transporters and additionally knockout mutants could be used to verify the uptake through a selected transporter.

Once phytotoxic As species are taken up into the rice root, the rice plant has two major defense mechanisms to avoid As transport and accumulation in shoots and grains. One mechanism is the efflux of As species out of the plant root and the other mechanism is As complexation and sequestration in root vacuoles. Both mechanism were discovered before for inorganic and organic As species, but no information was available about thioarsenates so far.

The first step in the detoxification of arsenate is its reduction to arsenite by enzymes from the HAC-family (Shi et al., 2016; Xu et al., 2017). This step is necessary because only arsenite can be efflux out of root cells via aquaporins (Zhao et al., 2009) or complexed by phytochelatins (PC) and further stored in root vacuoles (Clemens, 2006; Mendoza-Cozatl et al., 2011; Pickering et al., 2000; Verbruggen et al., 2009). Our results monitoring the MTA transformation in crude protein showed that MTA was rapidly reduced to arsenite, which could be complexed as As^{III}-PC in root vacuoles (study 3, Figure 3). We did not quantify the amount of PCs that were induced after exposure to thioarsenates, but previous experiments revealed that *A. thaliana* synthesized PCs after exposure to MTA (Planer-Friedrich et al., 2017). Whether MTA could be directly complexed by PC for example as MTA^{III}-PC is still unknown. Taking the As translocation and accumulation in shoots into account, we found higher translocation and accumulation for MTA than for arsenate exposed plants (study 2, Figure 6). This clearly showed that the detoxification of MTA is at least partly different from arsenate. Possible reasons for the observed differences could be that enzymes responsible for MTA reduction to arsenite were spatially separated in root tissue from arsenite PC complexation and were, therefore, less efficient in trapping MTA in root vacuoles compared to arsenate/arsenite. With this, MTA could be loaded to the xylem more efficiently and transported to the shoots.

The detoxification of MMA^V is similar to arsenate and involves the reduction of the pentavalent MMA^V to MMA^{III}, which can then be complexed by PCs as MMA^{III}-PC before its sequestration in root vacuoles (Mishra et al., 2017; Raab et al., 2007a). In contrast to MMA^V, DMA^V can not be reduced to its trivalent species and therefore no PC-complexes can be formed (Raab et al., 2007a). Our results for MMA^V and DMA^V uptake, accumulation, and translocation were in line with previous studies, showing that most MMA^V is sequestered in roots and only few As is translocated or accumulated in shoots, while DMA^V concentrations were low in roots but translocation and accumulation in shoots were high (study 3, Figure 5) (Mishra et al., 2017; Raab et al., 2007a).

No detoxification mechanisms for methylated thioarsenates are known, yet. Taking all our results obtained for MMMTA into account, high As concentrations in roots indicated that MMMTA could be sequestered in roots cells similar to MMA^V. However, the results from crude protein extracts showed that MMMTA was not transformed to MMA^V by root protein and the formation of a so far unknown MMMTA-PC complex would be necessary for sequestration (study 3, Figure 3). Another possibility is that MMMTA was partly transformed to MMA^V by ROL outside the root and then taken up as MMA^V. Translocation and accumulation in shoots were similar for MMMTA and MMA^V indicating that the detoxification processes might be comparable (study 3, Figure 5). Our results showed greater differences

between DMMTA and DMA^V than for MMMTA and MMA^V. Plants exposed to DMMTA had about 10 times more As in roots than plants exposed to DMA^V which could result from higher As uptake and /or higher As sequestration in roots (study 3, Figure 5). Similar to DMA^V, no PC complex has been reported for DMMTA but *Brassica oleracea* exposed to DMA^V contained a DMMTA-GSH complex (Raab et al., 2007b), however, no information about possible sequestration of this complex in root cells is available. Although DMMTA exposed plants accumulated high As concentrations in roots, translocation, as well as accumulation in shoots, was high, too, which is contradicting a quantitative complexation by thiols especially as the total As content in shoots was highest for plants exposed to DMMTA.

3.4. Mobility of methylated thioarsenates in presence of iron plaque and Fe(oxyhydr)oxide minerals (study 4)

The first three studies presented in this thesis revealed that thiolated arsenic species are occurring in paddy field pore-water over the whole growing season and under a broad variety of soil types and conditions (study 1) from where they are taken up by rice plants and transported further to the shoots (Kerl et al., 2018; Kerl et al., 2019). Sulfur-fertilization, applied to rice fields to reduce grain As content, enhanced the formation Fe-minerals and IP (Fan et al., 2013; Hu et al., 2007) and reduced total As concentrations in pore-water. Our mesocosm experiments showed an increasing share of methylated and thiolated As species after S-fertilization (study 1) which could be caused by preferential sorption of inorganic As species to the newly formed Fe-minerals and greater mobility of methylated and thiolated As species. Greater mobility of methylated oxyarsenates and inorganic thioarsenates was already shown in the presence of Fe(oxyhydr)oxide (Couture et al., 2013; Lafferty and Loeppert, 2005; Suess and Planer-Friedrich, 2012). Therefore, our aim was to get new insight into the sorption behavior of methylated thioarsenates to Fe(oxyhydr)oxide or IP and whether IP could act as a barrier for uptake of methylated thioarsenates into rice plants.

Uptake experiments with 20-day-old plants revealed that IP (mainly goethite) was no barrier for the uptake methylated thioarsenates spiked to the nutrient solution (pH 6.5) when comparing the As uptake in shoots to that in rice plants without IP covered roots. Little and no net As enrichment was found in IP for MMMTA and DMMTA, respectively and total As concentrations in shoots were not decreased for rice plants with IP (compared to plants without IP) when exposed to 10 µM MMMTA and DMMTA. In comparison to methylated thioarsenates, both methylated oxyarsenates MMA^V and DMA^V were sequestered in IP however, only the accumulation of MMA^V in shoots was decreased compared to rice plants without IP while DMA^V concentrations in shoots were even increased (study 4, Figure 1).

In order to improve the understanding of the sorption behavior of methylated thioarsenates, we conducted sorption experiments with the two synthetic end-members of

Fe(oxyhydr)oxides that occur in IP: amorphous ferrihydrite and highly crystalline goethite. Highest sorption was found for MMA^V both on goethite and on ferrihydrite but sorption to ferrihydrite was faster (within 10 min compared to 24 h), higher (30-50 times more), and the pH range of complete sorption was larger (pH<7.0 compared to <5.3) compared to goethite (study 4, Figure 3 and 4). The general sorption pattern for MMMTA was similar to MMA^V, however, especially the time-resolved sorption experiment to goethite revealed that sorption of MMMTA was slower than that of MMA^V (sorption maximum after 48 than 24 h) and therefore less MMMTA was sorbed in pH and concentration-dependent short-term experiments (study 4, Figure 3 and 4). Compared to MMA^V and MMMTA, less DMA^V was sorbed to goethite and slightly less to ferrihydrite. DMMTA was not sorbed to goethite quantitatively at any pH, concentration, or time (study 4, Figure 2, 3, and 4). DMMTA sorption to ferrihydrite increased over time to 32% after 72 h but short-term pH and concentration-dependent sorption were negligible (study 4, Figure 2).

Taking the results from all experiments into account, we found that IP was an effective barrier, which decreased the MMA^V accumulation in shoots by immobilizing MMA^V on IP (study 4, Figure 1). Sorption of MMA^V to mainly goethite containing IP was in line with our sorption experiments using synthetic Fe-minerals (study 4, Figure 2, 3, and 4) and previously published studies (Kersten and Daus, 2015; Lafferty and Loeppert, 2005). The sorption of DMA^V was lower to IP and Fe(oxyhydr)oxides but some DMA^V was still immobilized by IP. Nevertheless, the DMA^V accumulation in shoots was even higher when plants with IP were compared to plants without IP (study 1, Figure 1). The IP could act as a DMA^V reservoir where DMA^V is bound to Fe via weak outer-sphere complexes instead of stronger inner-sphere complexes like for MMA^V. Desorption and with this remobilization is higher for outer-sphere complexes than for inner-sphere complexes (Adamescu et al., 2010; Lafferty and Loeppert, 2005). Mobile DMA^V that is taken up by rice plants was not sequestered by PC complexation in roots and was translocated to shoots to a greater extent than MMA^V complexed as MMA^{III}-PC in root vacuoles which is limiting its translocation to shoots (see 3.3 for further details) (Mishra et al., 2017; Raab et al., 2007a).

The sorption behavior of MMMTA is more complicated than the behavior of MMA^V and DMA^V. Little As was sorbed to IP after MMMTA exposure, which seemed to contradict the much higher sorption of MMMTA on synthetic Fe(oxyhydr)oxides (study 4, Figure 1). Taking the MMMTA speciation results and the time lag in sorption to goethite into account, we propose that MMMTA was transformed to MMA^V first and then MMA^V was sorbed to the Fe-minerals (study 4, Figure 2). Results from study 2 and literature showed that oxygen could transform MMMTA to MMA^V (Cullen et al., 2016; Kerl et al., 2019; Wallschläger and London, 2008) and additional transformation was expected in presence of Fe^{III} as it is a stronger oxidant than oxygen. A continuous transformation of MMMTA to MMA^V would explain the

time lag in sorption to goethite and the smaller differences between MMMTA and MMA^V for the sorption to highly reactive ferrihydrite. Low sorption to IP is well explained assuming that MMMTA was not directly sorbed to IP, because transformation of MMMTA to MMA^V was hindered by exchanging the ARPW spiked with MMMTA every 2 h during uptake (results from study 2 showed that less than 10% MMMTA are transformed to MMA^V within 2 h).

No or very little DMMTA was sorbed to Fe(oxyhydr)oxides and the IP was no barrier for the uptake of DMMTA in rice plants (study 4, Figure 1). Similar to MMMTA, direct binding to Fe(oxyhydr)oxides seemed unlikely for DMMTA especially as one S and two methyl groups could hinder the binding sterically. DMMTA was more stable against oxidation compared to MMMTA and therefore less transformation to DMA^V was expected in the presence of oxygen or Fe^{III} (Kerl et al., 2019; Kim et al., 2016), explaining its poor sorption. Slightly higher sorption to highly reactive ferrihydrite than to crystalline goethite might be due to faster DMMTA transformation to DMA^V with higher surface area and reactivity of amorphous ferrihydrite (study 4, Figure 2).

Similar to inorganic thioarsenates, thiolation also decreased the sorption of methylated As species to Fe(oxyhydr)oxides, however, we found no evidence for direct sorption of methylated thioarsenates to Fe as it was reported before for inorganic thioarsenates (Burton et al., 2013; Couture et al., 2013; Suess and Planer-Friedrich, 2012). The extent of As sorption to IP in paddy fields is dependent on multiple factors that can de- or increase the sorption compared to the standardized lab experiments. Rice roots releasing oxygen in the rhizosphere will transform more oxygen-sensitive MMMTA to MMA^V than stabile DMMTA to DMA^V resulting in a higher mobility of DMMTA. Sulfate-reducing conditions in the rhizosphere sustain the precipitation of amorphous FeS, which could scavenge additional As from the pore-water. Unintended FeS precipitation during sorption experiments with more than 100 µM MMMTA (10-fold sulfide excess remaining after synthesis) revealed that at least MMMTA was sequestered through this mechanism, too (study 4, Figure 3). Another factor that had a great influence on the sorption of MMA^V, MMMTA, and DMA^V was the crystallinity of the Fe(oxyhydr)oxides. Natural iron plaque consisting mainly of ferrihydrite might increase sorption (30-50 times in our experiments) compared to our goethite rich IP, however, the sorption of DMMTA would not increase significantly in the presence of ferrihydrite (study 4, Figure 3). Besides these factors increasing the sorption to IP, experiments showed that competing ions, such as phosphate or sulfate decreased the sorption of methylated As species (Lafferty and Loeppert, 2005) and indirectly methylated thioarsenates. Increasing pH significantly reduced the sorption of methylated As species to Fe(oxyhydr)oxides. Our experiments were conducted at pH 6.5, which is the minimum of pH values occurring in paddy fields and a slight increase from 6.5 to 7 decreased the

sorption already by around 30% for MMTA and MMA^V and by around 20% for DMA^V on goethite (study 4, Figure 4). In order to disentangle the contribution of these different parameters hindering or enhancing the sorption of methylated thioarsenates, pore-water and IP of soil-grown rice plants will need to be monitored on a temporal and special scale.

4. Conclusion

Arsenic accumulation in rice grain is a well-known and intensively studied problem, however, past studies focused on inorganic and methylated arsenic species although the occurrence of thiolated arsenic species seemed highly plausible under sulfate-reducing conditions in flooded paddy fields. The present thesis aimed therefore to elucidate the role of thioarsenates in paddy soils and their uptake, transformation, and translocation in rice plants. A more detailed understanding of the As speciation in paddy field pore-water and rice plants will help to evaluate challenges or benefits of new strategies for producing low-level As rice grains (e.g. S-fertilization, water-management).

Methylated and inorganic thioarsenates could be determined in the pore-water of paddy soils from a large variety of soil types and throughout the whole rice-growing season (study 1). Thiolation of As species was a common process in paddy field pore-water with similar shares of thioarsenates and methylated oxyarsenates, revealing their importance for further investigations. Inadequate sample stabilization (e.g. HCl) or chromatographic separation methods (e.g. neutral pH) hindered the detection of thioarsenates in previous studies. Lab incubations, that determined the thiolation potential of soils, clearly showed that the soil pH was an effective predictor for the formation of inorganic or methylated thioarsenates. Inorganic thioarsenates were mainly formed at alkaline pH from arsenite via OH^- and SH^- ligand exchange and addition to zero-valent sulfur (Figure 4a). Methylated thioarsenates, in contrast, formed from methylated oxyarsenates via nucleophilic ligand exchange of OH^- and SH^- groups under acidic pH (Figure 4a). Natural S contents in paddy soils were sufficient for the formation of thioarsenates, however, additional S-fertilization promoted thiolation and methylation further. Beneficial effects of S-fertilization were detected when total As concentration in pore-water was decreased after fertilization, especially when the soil was low in zero-valent S. Even though the total As in pore-water was decreased, the share of methylated and thiolated As species was increased in the pore water. Sulfur-fertilization is known to increase the formation of Fe-minerals and IP along rice roots. Inorganic As, especially arsenate, has a high sorption affinity to Fe-minerals while methylated oxyarsenates and inorganic thioarsenates showed less sorption affinity. Sorption experiments with methylated thioarsenates revealed that these As species had very low sorption affinity to Fe(oxyhydr)oxides, especially to highly crystalline goethite (Figure 4b; study 4).

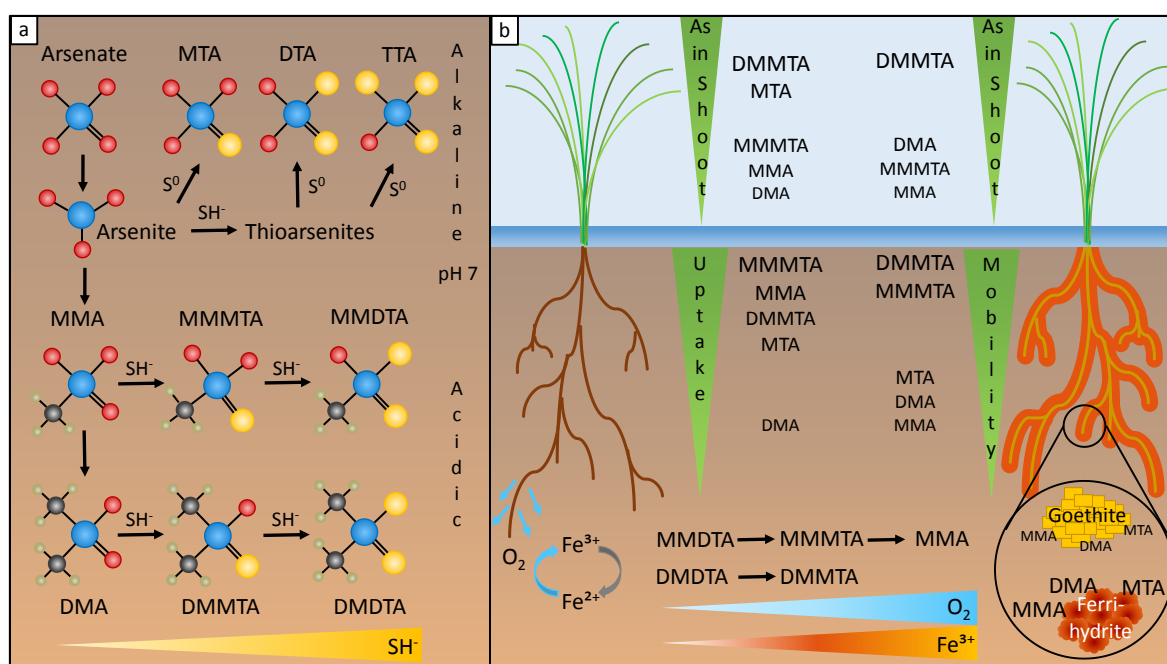


Figure 4 a: Summarized and simplified formation of inorganic thioarsenates (Planer-Friedrich et al., 2015) and methylated thioarsenates (Fan et al., 2018) in paddy soils. b: Uptake of thioarsenates in roots and shoots of rice plants without IP compared to the As uptake in shoots for rice plants covered with IP (no data for the MTA uptake available). Stability of methylated thioarsenates in the presence of oxygen and ferric Fe and sorption of thioarsenates to IP (goethite and ferrihydrite) and the resulting As mobility in the pore-water (Kerl et al., 2018; Kerl et al., 2019).

After detecting thioarsenates in paddy soils, their interaction with rice plants was evaluated. Hydroponic studies showed that inorganic and methylated thioarsenates were taken up by rice plants and were partly transported in the xylem and partly transformed to their non-thiolated analogs (study 2 and 3, Figure 4b). Different transformation pathways and accumulation patterns were identified for the individual thioarsenates. Monothioarsenate was taken up, possibly by a phosphate transporter and rapidly transformed to arsenite by a so far unknown enzyme in rice roots. Although most MTA was transformed to arsenite in roots, the remaining MTA could be detected in the xylem, roots, and shoots of rice plants and MTA translocation from roots to shoots was higher than for the non-thiolated analog arsenate (Figure 4b). The exact mechanisms and enzymes or transporters involved in MTA uptake, reduction, and translocation are still unknown but the results from this thesis clearly showed the different behavior of MTA and arsenate and the need for identification of the involved transporters and reductases.

Both methylated thioarsenates behaved differently from MTA in rice plants. The oxygen-sensitive MMMTA was partly transformed to MMA^V by ROL prior to uptake, but no transformation of MMMTA to MMA^V was detected inside roots. Speciation of xylem sap

proved that MMMTA was taken up into rice plants by a so far unknown transporter and that it could be partly translocated from roots to shoots. The As uptake and translocation of plants exposed to MMMTA was similar to its non-thiolated analog MMA^V. Both As species were efficiently sequestered in rice roots and few As was translocated to shoots, however the exact mechanisms for MMMTA are unknown similar to MTA (Figure 4b).

DMMTA was taken up into rice roots by an unknown transporter and partly transformed to DMA^V inside roots and partly transported in the xylem. Different from MTA and MMMTA, DMMTA was not transformed enzymatically or by ROL but disproportionated chemically in the presence of GSH to DMA^{III} and DMDTA. Plants exposed to DMMTA accumulated more As in roots and shoots than plants exposed to the non-thiolated analog DMA^V leading to the highest As accumulation in shoots and could possibly contribute to a high As accumulation in rice grains (Figure 4b).

The increasing share of methylated and thiolated As species in pore-water after S-fertilization in mesocosms indicated that these species were more mobile in the rhizosphere and the hydroponic studies showed that these species were taken up by rice plants and increased shoot accumulation of As. Therefore, the sorption behavior of MMMTA and DMMTA on Fe-minerals was tested and IP was evaluated as a possible barrier limiting their uptake in rice plants. The IP, containing mostly goethite, was no barrier for the MMMTA and DMMTA uptake in rice roots as methylated thioarsenates were not directly sorbed to IP but had to be transformed to the corresponding methylated oxyarsenates first (Figure 4b; study 4). The more detailed sorption experiments with goethite and ferrihydrite revealed that thiolation of methylated As species decreased sorption kinetics and lowered the extent of sorption because transformation to the methylated oxyarsenates was necessary prior to sorption. Especially, the DMMTA transformation to DMA^V was very slow resulting in poor sorption of DMMTA to Fe(oxyhydr)oxides and higher mobility of DMMTA than any other As species tested.

The four studies of this thesis revealed that thioarsenates were formed in paddy soils and were more mobile (especially DMMTA) in the pore-water due to their lower sorption affinity to Fe(oxyhydr)oxides. The more mobile thioarsenates were taken up by rice plants, where especially MTA and DMMTA increased the total As translocation to above-ground biomass. However, the most important question for rice consumers is whether any toxic thioarsenates can reach the rice grain and if thioarsenate accumulation increases the uptake of total As in rice grains. Accumulation of MTA or MMMTA in rice grains is less critical because MMA^V, the transformation product to MMMTA during sample digestion, is typically only found in traces in rice grains and arsenite and arsenate, the MTA transformation products, are regulated in the guideline values.

Highly toxic DMMTA is the As species of greatest concern since it was already detected in rice grains. Routine acidic sample digestion transforms DMMTA, which is then quantified as less toxic DMA^V and therefore excluded from the food guidelines. The contribution of thioarsenate uptake to total As accumulation in rice grains remains unclear up to now and more studies are needed that identify involved transporters and enzymes. Before S-fertilization is further advertised as beneficial for reducing inorganic As in rice grains, the contribution of thioarsenates, especially DMMTA, in grains should be further investigated. Therefore, sample stabilization and analytical methods have to be adapted to account for thioarsenates and the exemption of organic As from the food guidelines should be reevaluated.

Future rice production will face challenges such as the need to lower methane emissions, or save water, and adopt management to changing climate, besides lowering the concentrations of toxicants (As, Cd, Pb) in rice grains. To fulfill all these demands, one management strategy might not be enough, as most mitigation strategies have undesired side effects (yield loss, Cd increase, thioarsenates formation). Preliminary data from combined S-fertilization with alternate wetting and drying showed quite promising results that addressed most challenges (reduces grain As and Cd, formation of thioarsenates, methane production, water use) and might be an interesting option for the future.

References

- Ackerman, A.H. et al., 2005. Comparison of a Chemical and Enzymatic Extraction of Arsenic from Rice and an Assessment of the Arsenic Absorption from Contaminated Water by Cooked Rice. *Environ. Sci. Technol.*, 39(14): 5241-5246.
- Adamescu, A., Mitchell, W., Hamilton, I.P., Al-Abadleh, H.A., 2010. Insights into the surface complexation of dimethylarsinic acid on iron (oxyhydr)oxides from ATR-FTIR studies and quantum chemical calculations. *Environ. Sci. Technol.*, 44(20): 7802-7.
- Alloway, B.J., Trevors, J.K., 2013. Heavy Metals in Soils. In: Alloway, B.J. (Editor), *Trace Metals and Metalloids in Soils and their Bioavailability*. Springer Netherlands, pp. 614.
- ATSDR, 2017, The ATSDR (Agency for Toxic Substances and Disease Registry) 2017 Substance Priority List. <https://www.atsdr.cdc.gov/SPL/#2017spl>,
- Ayotade, K.A., 1977. Kinetics and reactions of hydrogen sulphide in solution of flooded rice soils. *Plant Soil*, 46(2): 381-389.
- Bacha, R.E., Hossner, L.R., 1977. Characteristics of Coatings formed on Rice Roots as Affected by Iron and Manganese Additions¹. *Soil Sci. Soc. Am. J.*, 41(5): 931.
- Baker, M.D., Inniss, W.E., Mayfield, C.I., Wong, P.T.S., Chau, Y.K., 1983. Effect of pH on the methylation of mercury and arsenic by sediment microorganisms. *Environmental Technology Letters*, 4(2): 89-100.
- Bartel, M., Ebert, F., Leffers, L., Karst, U., Schwerdtle, T., 2011. Toxicological Characterization of the Inorganic and Organic Arsenic Metabolite Thio-DMA in Cultured Human Lung Cells. *J Toxicol*, 2011: 373141.
- Bentley, R., Chasteen, T.G., 2002. Microbial methylation of metalloids: arsenic, antimony, and bismuth. *Microbiol Mol Biol Rev*, 66(2): 250-71.
- Besold, J. et al., 2018. Monothioarsenate Transformation Kinetics Determining Arsenic Sequestration by Sulfhydryl Groups of Peat. *Environ Sci Technol*, 52(13): 7317-7326.
- BfR, B.f.R., 2014. Arsen in Reis und Reisprodukten, Stellungnahme pp. 58.
- Bleeker, P.M., Hakvoort, H.W., Blik, M., Souer, E., Schat, H., 2006. Enhanced arsenate reduction by a CDC25-like tyrosine phosphatase explains increased phytochelatin accumulation in arsenate-tolerant *Holcus lanatus*. *Plant J*, 45(6): 917-29.
- Boye, K., Lezama-Pacheco, J., Fendorf, S., 2017. Relevance of Reactive Fe:S Ratios for Sulfur Impacts on Arsenic Uptake by Rice. *Soils*, 1(1): 1.
- Burton, E.D., Johnston, S.G., Planer-Friedrich, B., 2013. Coupling of arsenic mobility to sulfur transformations during microbial sulfate reduction in the presence and absence of humic acid. *Chemical Geology*, 343: 12-24.
- Cao, Y. et al., 2017. Knocking Out OsPT4 Gene Decreases Arsenate Uptake by Rice Plants and Inorganic Arsenic Accumulation in Rice Grains. *Environ. Sci. Technol.*, 51(21): 12131-12138.
- Carey, A.M. et al., 2010. Grain unloading of arsenic species in rice. *Plant Physiol*, 152(1): 309-19.
- Chen, C. et al., 2019. Sulfate-reducing bacteria and methanogens are involved in arsenic methylation and demethylation in paddy soils. *ISME J*.
- Chen, C.C., Dixon, J.B., Turner, F.T., 1980. Iron Coatings on Rice Roots: Mineralogy and Quantity Influencing Factors¹. *Soil Sci. Soc. Am. J.*, 44(3): 635.
- Chen, H., Tang, Z., Wang, P., Zhao, F.J., 2018. Geographical variations of cadmium and arsenic concentrations and arsenic speciation in Chinese rice. *Environ. Pollut.*, 238: 482-490.
- Chen, Y. et al., 2017. Arsenic Transport in Rice and Biological Solutions to Reduce Arsenic Risk from Rice. *Front. Plant Sci.*, 8: 268.
- Clemens, S., 2006. Toxic metal accumulation, responses to exposure and mechanisms of tolerance in plants. *Biochimie*, 88(11): 1707-19.
- Clemens, S., Ma, J.F., 2016. Toxic Heavy Metal and Metalloid Accumulation in Crop Plants and Foods. *Annu. Rev. Plant Biol.*, 67: 489-512.

- Cobbett, C., Goldsbrough, P., 2002. Phytochelatins and metallothioneins: roles in heavy metal detoxification and homeostasis. *Annu Rev Plant Biol*, 53: 159-82.
- Conklin, S.D., Fricke, M.W., Creed, P.A., Creed, J.T., 2008. Investigation of the pH effects on the formation of methylated thio-arsenicals, and the effects of pH and temperature on their stability. *Journal of Analytical Atomic Spectrometry*, 23(5): 711.
- Couture, R.M. et al., 2013. Sorption of arsenite, arsenate, and thioarsenates to iron oxides and iron sulfides: a kinetic and spectroscopic investigation. *Environ. Sci. Technol.*, 47(11): 5652-9.
- Crusciol, C.A.C., Nascente, A.S., Soratto, R.P., Rosolem, C.A., 2013. Upland Rice Growth and Mineral Nutrition as Affected by Cultivars and Sulfur Availability. *Soil Science Society of America Journal*, 77(1): 328.
- Cullen, W.R. et al., 2016. Methylated and thiolated arsenic species for environmental and health research - A review on synthesis and characterization. *J. Environ. Sci. (China)*, 49: 7-27.
- Dixit, G. et al., 2015. Sulfur mediated reduction of arsenic toxicity involves efficient thiol metabolism and the antioxidant defense system in rice. *J. Hazard. Mater.*, 298: 241-51.
- Dixit, S., Hering, J.G., 2003. Comparison of Arsenic(V) and Arsenic(III) Sorption onto Iron Oxide Minerals: Implications for Arsenic Mobility. *Environ. Sci. Technol.*, 37(18): 4182-4189.
- Duan, G.L., Zhu, Y.G., Tong, Y.P., Cai, C., Kneer, R., 2005. Characterization of arsenate reductase in the extract of roots and fronds of Chinese brake fern, an arsenic hyperaccumulator. *Plant Physiol*, 138(1): 461-9.
- European Commission, 2015. amending Regulation (EC) No 1881/2006 as regards maximum levels of inorganic arsenic in foodstuffs. In: Commission, E. (Editor).
- Fan, C., Liu, G., Long, Y., Rosen, B., Cai, Y., 2018. Thiolation in arsenic metabolism: a chemical perspective. *Metallomics*, 10(10): 1368-1382.
- Fan, J., Xia, X., Hu, Z., Ziadi, N., Liu, C., 2013. Excessive sulfur supply reduces arsenic accumulation in brown rice. *PSE*, 59(No. 4): 169-174.
- Goldberg, S., Johnston, C.T., 2001. Mechanisms of Arsenic Adsorption on Amorphous Oxides Evaluated Using Macroscopic Measurements, Vibrational Spectroscopy, and Surface Complexation Modeling. *J Colloid Interface Sci*, 234(1): 204-216.
- Hansen, H.R. et al., 2011. Identification of tetramethylarsonium in rice grains with elevated arsenic content. *J Environ Monit*, 13(1): 32-4.
- Hu, P. et al., 2015. Effects of water management on arsenic and cadmium speciation and accumulation in an upland rice cultivar. *J Environ Sci (China)*, 27: 225-31.
- Hu, Z.Y. et al., 2007. Sulfur (S)-induced enhancement of iron plaque formation in the rhizosphere reduces arsenic accumulation in rice (*Oryza sativa* L.) seedlings. *Environ. Pollut.*, 147(2): 387-93.
- Jia, Y., Bao, P., Zhu, Y.G., 2015. Arsenic bioavailability to rice plant in paddy soil: influence of microbial sulfate reduction. *JSS*, 15(9): 1960-1967.
- Jia, Y., Huang, H., Sun, G.X., Zhao, F.J., Zhu, Y.G., 2012. Pathways and relative contributions to arsenic volatilization from rice plants and paddy soil. *Environ Sci Technol*, 46(15): 8090-6.
- Kerl, C.F., Rafferty, C., Clemens, S., Planer-Friedrich, B., 2018. Monothioarsenate Uptake, Transformation, and Translocation in Rice Plants. *Environ. Sci. Technol.*, 52(16): 9154-9161.
- Kerl, C.F. et al., 2019. Methylated Thioarsenates and Monothioarsenate Differ in Uptake, Transformation, and Contribution to Total Arsenic Translocation in Rice Plants. *Environ. Sci. Technol.*, 53(10): 5787-5796.
- Kersten, M., Daus, B., 2015. Silicic acid competes for dimethylarsinic acid (DMA) immobilization by the iron hydroxide plaque mineral goethite. *Sci. Total Environ.*, 508: 199-205.
- Kim, Y.T., Lee, H., Yoon, H.O., Woo, N.C., 2016. Kinetics of Dimethylated Thioarsenicals and the Formation of Highly Toxic Dimethylmonothioarsinic Acid in Environment. *Environ. Sci. Technol.*, 50(21): 11637-11645.

- Kirk, G., 2004. *The Biogeochemistry of Submerged Soils*. John Wiley & Sons Ltd., pp. 282.
- Kogel-Knabner, I. et al., 2010. Biogeochemistry of paddy soils. *Geoderma*, 157(1-2): 1-14.
- Lafferty, B.J., Loeppert, R.H., 2005. Methyl arsenic adsorption and desorption behavior on iron oxides. *Environ. Sci. Technol.*, 39(7): 2120-7.
- Li, N., Wang, J., Song, W.Y., 2016. Arsenic Uptake and Translocation in Plants. *Plant Cell Physiol*, 57(1): 4-13.
- Li, R.Y. et al., 2009. The rice aquaporin Lsi1 mediates uptake of methylated arsenic species. *Plant Physiol.*, 150(4): 2071-80.
- Limmer, M.A., Wise, P., Dykes, G.E., Seyfferth, A.L., 2018. Silicon Decreases Dimethylarsinic Acid Concentration in Rice Grain and Mitigates Straighthead Disorder. *Environ Sci Technol*, 52(8): 4809-4816.
- Lindsay, E.R., Maathuis, F.J., 2016. Arabidopsis thaliana NIP7;1 is involved in tissue arsenic distribution and tolerance in response to arsenate. *FEBS Lett*, 590(6): 779-86.
- Linquist, B.A. et al., 2015. Reducing greenhouse gas emissions, water use, and grain arsenic levels in rice systems. *Glob Chang Biol*, 21(1): 407-17.
- Liu, W.J. et al., 2006. Arsenic Sequestration in Iron Plaque, Its Accumulation and Speciation in Mature Rice Plants (*Oryza Sativa*L.). *Environ. Sci. Technol.*, 40(18): 5730-5736.
- Lomax, C. et al., 2012. Methylated arsenic species in plants originate from soil microorganisms. *New Phytol.*, 193(3): 665-72.
- Lombi, E. et al., 2009. Speciation and distribution of arsenic and localization of nutrients in rice grains. *New Phytol*, 184(1): 193-201.
- Ma, J.F. et al., 2006. A silicon transporter in rice. *Nature*, 440(7084): 688-691.
- Ma, J.F., Yamaji, N., 2015. A cooperative system of silicon transport in plants. *Trends Plant Sci.*, 20(7): 435-42.
- Ma, J.F. et al., 2007. An efflux transporter of silicon in rice. *Nature*, 448(7150): 209-12.
- Ma, J.F. et al., 2008. Transporters of arsenite in rice and their role in arsenic accumulation in rice grain. *Proc. Natl. Acad. Sci. U.S A.*, 105(29): 9931-5.
- Manning, B.A., Fendorf, S.E., Goldberg, S., 1998. Surface Structures and Stability of Arsenic(III) on Goethite: Spectroscopic Evidence for Inner-Sphere Complexes. *Environmental Science & Technology*, 32(16): 2383-2388.
- Mantha, M. et al., 2017. Estimating Inorganic Arsenic Exposure from U.S. Rice and Total Water Intakes. *Environ. Health Perspect.*, 125(5): 057005.
- Masscheleyn, P.H., Delaune, R.D., Patrick, W.H., 1991. Effect of Redox Potential and Ph on Arsenic Speciation and Solubility in a Contaminated Soil. *Environ. Sci. Technol.*, 25(8): 1414-1419.
- Matschullat, J., 2000. Arsenic in the geosphere — a review. *Sci. Total Environ.*, 249(1-3): 297-312.
- Meharg, A.A. et al., 2009. Geographical Variation in Total and Inorganic Arsenic Content of Polished (White) Rice. *Environ. Sci. Technol.*, 43(5): 1612-1617.
- Meharg, A.A., Zhao, F.-J., 2012. *Arsenic & Rice*. Springer Netherlands, pp. 172.
- Mendoza-Cozatl, D.G., Jobe, T.O., Hauser, F., Schroeder, J.I., 2011. Long-distance transport, vacuolar sequestration, tolerance, and transcriptional responses induced by cadmium and arsenic. *Curr. Opin. Plant Biol.*, 14(5): 554-62.
- Mestrot, A. et al., 2011. Field fluxes and speciation of arsines emanating from soils. *Environ Sci Technol*, 45(5): 1798-804.
- Minamikawa, K., Sakai, N., Hayashi, H., 2005. The effects of ammonium sulfate application on methane emission and soil carbon content of a paddy field in Japan. *Agriculture, Ecosystems & Environment*, 107(4): 371-379.
- Mishra, S., Mattusch, J., Wennrich, R., 2017. Accumulation and transformation of inorganic and organic arsenic in rice and role of thiol-complexation to restrict their translocation to shoot. *Sci. Rep.*, 7: 40522.
- Molin, M., Ulven, S.M., Meltzer, H.M., Alexander, J., 2015. Arsenic in the human food chain, biotransformation and toxicology--Review focusing on seafood arsenic. *J Trace Elem Med Biol*, 31: 249-59.

- Naranmandura, H. et al., 2011. Comparative toxicity of arsenic metabolites in human bladder cancer EJ-1 cells. *Chem. Res. Toxicol.*, 24(9): 1586-96.
- Naranmandura, H., Ibata, K., Suzuki, K.T., 2007. Toxicity of dimethylmonothioarsinic acid toward human epidermoid carcinoma A431 cells. *Chem. Res. Toxicol.*, 20(8): 1120-5.
- Norton, G.J. et al., 2009. Identification of Low Inorganic and Total Grain Arsenic Rice Cultivars from Bangladesh. *Environmental Science & Technology*, 43(15): 6070-6075.
- Ona-Nguema, G., Morin, G., Juillot, F., Calas, G., Brown, G.E., Jr., 2005. EXAFS analysis of arsenite adsorption onto two-line ferrihydrite, hematite, goethite, and lepidocrocite. *Environ Sci Technol*, 39(23): 9147-55.
- Petrick, J.S., Ayala-Fierro, F., Cullen, W.R., Carter, D.E., Vasken Aposhian, H., 2000. Monomethylarsonous acid (MMA(III)) is more toxic than arsenite in Chang human hepatocytes. *Toxicol Appl Pharmacol*, 163(2): 203-7.
- Pickering, I.J. et al., 2000. Reduction and Coordination of Arsenic in Indian Mustard. *Plant Physiol.*, 122(4): 1171-1178.
- Planer-Friedrich, B. et al., 2015. Anaerobic Chemolithotrophic Growth of the Haloalkaliphilic Bacterium Strain MLMS-1 by Disproportionation of Monothioarsenate. *Environ. Sci. Technol.*, 49(11): 6554-63.
- Planer-Friedrich, B. et al., 2017. Thioarsenate Toxicity and Tolerance in the Model System *Arabidopsis thaliana*. *Environ. Sci. Technol.*, 51(12): 7187-7196.
- Planer-Friedrich, B., London, J., McCleskey, R.B., Nordstrom, D.K., Wallschläger, D., 2007. Thioarsenates in Geothermal Waters of Yellowstone National Park: Determination, Preservation, and Geochemical Importance. *Environmental Science & Technology*, 41(15): 5245-5251.
- Planer-Friedrich, B., Schaller, J., Wismeth, F., Mehlhorn, J., Hug, S.J., 2018. Monothioarsenate Occurrence in Bangladesh Groundwater and Its Removal by Ferrous and Zero-Valent Iron Technologies. *Environ Sci Technol*, 52(10): 5931-5939.
- Planer-Friedrich, B., Suess, E., Scheinost, A.C., Wallschläger, D., 2010. Arsenic speciation in sulfidic waters: reconciling contradictory spectroscopic and chromatographic evidence. *Anal. Chem.*, 82(24): 10228-35.
- Planer-Friedrich, B., Wallschläger, D., 2009. A Critical Investigation of Hydride Generation-Based Arsenic Speciation in Sulfidic Waters. *Environ. Sci. Technol.*, 43(13): 5007-5013.
- Raab, A., Meharg, A.A., Jaspars, M., Genney, D.R., Feldmann, J., 2004. Arsenic-glutathione complexes-their stability in solution and during separation by different HPLC modes. *Journal of Analytical Atomic Spectrometry*, 19(1): 183.
- Raab, A., Schat, H., Meharg, A.A., Feldmann, J., 2005. Uptake, translocation and transformation of arsenate and arsenite in sunflower (*Helianthus annuus*): formation of arsenic-phytochelatin complexes during exposure to high arsenic concentrations. *New Phytol.*, 168(3): 551-8.
- Raab, A., Williams, P.N., Meharg, A., Feldmann, J., 2007a. Uptake and translocation of inorganic and methylated arsenic species by plants. *Environ. Chem.*, 4(3): 197.
- Raab, A., Wright, S.H., Jaspars, M., Meharg, A.A., Feldmann, J., 2007b. Pentavalent Arsenic Can Bind to Biomolecules. *Angewandte Chemie*, 119(15): 2648-2651.
- Raml, R., Goessler, W., Francesconi, K.A., 2006. Improved chromatographic separation of thio-arsenic compounds by reversed-phase high performance liquid chromatography-inductively coupled plasma mass spectrometry. *J Chromatogr A*, 1128(1-2): 164-70.
- Raven, K.P., Jain, A., Loeppert, R.H., 1998. Arsenite and Arsenate Adsorption on Ferrihydrite: Kinetics, Equilibrium, and Adsorption Envelopes. *Environ. Sci. Technol.*, 32(3): 344-349.
- Saalfeld, S.L., Bostick, B.C., 2009. Changes in iron, sulfur, and arsenic speciation associated with bacterial sulfate reduction in ferrihydrite-rich systems. *Environ Sci Technol*, 43(23): 8787-93.

- Schmöger, M.E.V., Oven, M., Grill, E., 2000. Detoxification of Arsenic by Phytochelatins in Plants. *Plant Physiology*, 122(3): 793-801.
- Schütz, H., Holzapfel-Pschorn, A., Conrad, R., Rennenberg, H., Seiler, W., 1989. A 3-year continuous record on the influence of daytime, season, and fertilizer treatment on methane emission rates from an Italian rice paddy. *Journal of Geophysical Research*, 94(D13): 16405.
- Seyfferth, A.L. et al., 2016. Soil Incorporation of Silica-Rich Rice Husk Decreases Inorganic Arsenic in Rice Grain. *J Agric Food Chem*, 64(19): 3760-6.
- Seyfferth, A.L., Webb, S.M., Andrews, J.C., Fendorf, S., 2010. Arsenic localization, speciation, and co-occurrence with iron on rice (*Oryza sativa* L.) roots having variable Fe coatings. *Environ. Sci. Technol.*, 44(21): 8108-13.
- Seyfferth, A.L., Webb, S.M., Andrews, J.C., Fendorf, S., 2011. Defining the distribution of arsenic species and plant nutrients in rice (*Oryza sativa* L.) from the root to the grain. *Geochim. Cosmochim. Acta*, 75(21): 6655-6671.
- Shi, S. et al., 2016. OsHAC1;1 and OsHAC1;2 Function as Arsenate Reductases and Regulate Arsenic Accumulation. *Plant Physiol.*, 172(3): 1708-1719.
- Shimizu, M., Arai, Y., Sparks, D.L., 2011. Multiscale assessment of methylarsenic reactivity in soil. 1. Sorption and desorption on soils. *Environ. Sci. Technol.*, 45(10): 4293-9.
- Sigg, L., Stumm, W., 1994. *Aquatische Chemie: eine Einführung in die Chemie wässriger Lösungen und natürlicher Gewässer*. vdf, Zürich, 498 pp.
- Smieja, J.A., Wilkin, R.T., 2003. Preservation of sulfidic waters containing dissolved As(III). *Journal of Environmental Monitoring*, 5(6): 913.
- Somenahally, A.C., Hollister, E.B., Yan, W., Gentry, T.J., Loeppert, R.H., 2011. Water management impacts on arsenic speciation and iron-reducing bacteria in contrasting rice-rhizosphere compartments. *Environ Sci Technol*, 45(19): 8328-35.
- Song, W.Y. et al., 2014. A rice ABC transporter, OsABCC1, reduces arsenic accumulation in the grain. *Proc. Natl. Acad. Sci. U.S.A.*, 111(44): 15699-704.
- Stauder, S., Raue, B., Sacher, F., 2005. Thioarsenates in Sulfidic Waters. *Environ. Sci. Technol.*, 39(16): 5933-5939.
- Styblo, M., Del Razo, L., Vega, L., 2002. Comparative toxicity of trivalent and pentavalent inorganic and methylated arsenicals in rat and human cells. *Archives of toxicology*, 74(6): 289-99.
- Suess, E., Planer-Friedrich, B., 2012. Thioarsenate formation upon dissolution of orpiment and arsenopyrite. *Chemosphere*, 89(11): 1390-8.
- Sun, G.X. et al., 2008. Inorganic arsenic in rice bran and its products are an order of magnitude higher than in bulk grain. *Environ Sci Technol*, 42(19): 7542-6.
- Sun, S. et al., 2012. A constitutive expressed phosphate transporter, OsPht1;1, modulates phosphate uptake and translocation in phosphate-replete rice. *Plant Physiol.*, 159(4): 1571-81.
- Suzuki, N., Naranmandura, H., Hirano, S., Suzuki, K.T., 2008. Theoretical calculations and reaction analysis on the interaction of pentavalent thioarsenicals with biorelevant thiol compounds. *Chem. Res. Toxicol.*, 21(2): 550-3.
- Syu, C.H., Huang, C.C., Jiang, P.Y., Lee, C.H., Lee, D.Y., 2015. Arsenic accumulation and speciation in rice grains influenced by arsenic phytotoxicity and rice genotypes grown in arsenic-elevated paddy soils. *J Hazard Mater*, 286: 179-86.
- Takahashi, Y. et al., 2004. Arsenic behavior in paddy fields during the cycle of flooded and non-flooded periods. *Environ Sci Technol*, 38(4): 1038-44.
- Takamatsu, T., Aoki, H., Yoshida, T., 1982. Determination of Arsenate, Arsenite, Monomethylarsonate, and Dimethylarsinate in Soil Polluted with Arsenic. *Soil Science*, 133(4): 239-246.
- Teasley, W.A., Limmer, M.A., Seyfferth, A.L., 2017. How Rice (*Oryza sativa* L.) Responds to Elevated As under Different Si-Rich Soil Amendments. *Environ Sci Technol*, 51(18): 10335-10343.
- Tripathi, R.D. et al., 2014. Roles for root iron plaque in sequestration and uptake of heavy metals and metalloids in aquatic and wetland plants. *Metallomics*, 6(10): 1789-800.

- Van de Wiele, T. et al., 2010. Arsenic metabolism by human gut microbiota upon in vitro digestion of contaminated soils. *Environ. Health Perspect.*, 118(7): 1004-9.
- Verbruggen, N., Hermans, C., Schat, H., 2009. Mechanisms to cope with arsenic or cadmium excess in plants. *Curr. Opin. Plant Biol.*, 12(3): 364-72.
- Wallschläger, D., London, J., 2008. Determination of Methylated Arsenic-Sulfur Compounds in Groundwater. *Environ. Sci. Technol.*, 42(1): 228-234.
- Wang, P., Zhang, W., Mao, C., Xu, G., Zhao, F.J., 2016. The role of OsPT8 in arsenate uptake and varietal difference in arsenate tolerance in rice. *J. Exp. Bot.*, 67(21): 6051-6059.
- WHO, W.H.O., 2010. Exposure to Arsenic: a Major Public Health Concern In: Environment, P.H.a. (Editor). WHO Document Production Services, Geneva, Switzerland.
- Williams, P.N., Raab, A., Feldmann, J., Meharg, A.A., 2007a. Market Basket Survey Shows Elevated Levels of As in South Central U.S. Processed Rice Compared to California: Consequences for Human Dietary Exposure. *Environ. Sci. Technol.*, 41(7): 2178-2183.
- Williams, P.N. et al., 2007b. Greatly Enhanced Arsenic Shoot Assimilation in Rice Leads to Elevated Grain Levels Compared to Wheat and Barley. *Environ. Sci. Technol.*, 41(19): 6854-6859.
- Wind, T., Conrad, R., 1997. Localization of sulfate reduction in planted and unplanted rice field soil. *Biogeochemistry*, 37(3): 253-278.
- Wu, J., Zhang, R., Lilley, R.M., 2002. Methylation of arsenic in vitro by cell extracts from bentgrass (*Agrostis tenuis*): effect of acute exposure of plants to arsenate. *Functional Plant Biology*, 29(1): 73.
- Wu, Z., Ren, H., McGrath, S.P., Wu, P., Zhao, F.J., 2011. Investigating the contribution of the phosphate transport pathway to arsenic accumulation in rice. *Plant Physiol.*, 157(1): 498-508.
- Xu, J. et al., 2017. OsHAC4 is critical for arsenate tolerance and regulates arsenic accumulation in rice. *New Phytol.*, 215(3): 1090-1101.
- Xu, W. et al., 2015. Arabidopsis NIP3;1 Plays an Important Role in Arsenic Uptake and Root-to-Shoot Translocation under Arsenite Stress Conditions. *Mol Plant*, 8(5): 722-33.
- Xu, X.Y., McGrath, S.P., Zhao, F.J., 2007. Rapid reduction of arsenate in the medium mediated by plant roots. *New Phytol.*, 176(3): 590-9.
- Ye, Y. et al., 2017. OsPT4 Contributes to Arsenate Uptake and Transport in Rice. *Front. Plant Sci.*, 8: 2197.
- Zhang, J., Zhao, Q.-Z., Duan, G.-L., Huang, Y.-C., 2011. Influence of sulphur on arsenic accumulation and metabolism in rice seedlings. *Environ. Exp. Bot.*, 72(1): 34-40.
- Zhang, Y., Lin, X., Werner, W., 2003. The effect of soil flooding on the transformation of Fe oxides and the adsorption/desorption behavior of phosphate. *Journal of Plant Nutrition and Soil Science*, 166(1): 68-75.
- Zhao, F.J. et al., 2010. The role of the rice aquaporin Lsi1 in arsenite efflux from roots. *New Phytol.*, 186(2): 392-9.
- Zhao, F.J., Ma, J.F., Meharg, A.A., McGrath, S.P., 2009. Arsenic uptake and metabolism in plants. *New Phytol.*, 181(4): 777-94.
- Zhao, F.J., Zhu, Y.G., Meharg, A.A., 2013. Methylated arsenic species in rice: geographical variation, origin, and uptake mechanisms. *Environ. Sci. Technol.*, 47(9): 3957-66.
- Zheng, M.-Z., Li, G., Sun, G.-X., Shim, H., Cai, C., 2012. Differential toxicity and accumulation of inorganic and methylated arsenic in rice. *Plant and Soil*, 365(1-2): 227-238.
- Zheng, M.Z. et al., 2011. Spatial distribution of arsenic and temporal variation of its concentration in rice. *New Phytol.*, 189(1): 200-9.

Contribution to studies 1 to 4

Study 1: Thiolated arsenic species observed in rice paddy pore-waters

Jijia Wang	40%	initiated DTPA method development, conceived and performed all mesocosm and incubation experiments including analyses, evaluated the results and contributed to manuscript preparation
Carolin F. Kerl	20%	contributed to field survey, sample analyses, data evaluation, and manuscript preparation
Pengjie Hu	3%	initiated the Chinese soil survey and advised on incubation experiments, sampled and characterized the Chinese soils
Maria Martin	3%	contributed to field survey and data discussion, assisted in analyses of aqueous parameters from mesocosms
Tingting Mu	2%	sampled and characterized the Chinese soils
Lena Brüggewirth	2%	contributed to DTPA method development
Guangmei Wu	2%	sampled and characterized the Chinese soils
Daniel Said-Pullicino	3%	assisted in analyses of aqueous parameters from mesocosms
Marco Romani	2%	assisted in design, setup and operation of mesocosms and sample collection
Longhua Wu	3%	initiated the Chinese soil survey and advised on incubation experiments, sampled and characterized the Chinese soils
Britta Planer-Friedrich	20%	initiated and supervised the project, carried out the field survey, conceived experiments, and wrote the manuscript

Study 2: Monothioarsenate Uptake, Transformation, and Translocation in Rice Plants

Carolin F. Kerl	80%	development of research concept, laboratory work, analyses and data interpretation, preparation of manuscript
Colleen Rafferty	5%	assistance during plant growth and discussion of results
Stephan Clemens	5%	discussion of results, comments on manuscript
Britta Planer-Friedrich	10%	development of research concept, discussion of results, comments on manuscript

Study 3: Methylated thioarsenates and monothioarsenate differ in uptake, transformation, and contribution to total arsenic translocation in rice plants

Carolin F. Kerl	75%	development of research concept, laboratory work, analyses and data interpretation, preparation of manuscript
Alina R. Schindele	2.5%	assistance during laboratory work, discussion of results
Lena Brüggewirth	2.5%	assistance during laboratory work, discussion of results
Andrea E. Colina Blanco	2.5%	determination of root oxygen loss
Colleen Rafferty	2.5%	preparation of crude protein extracts
Stephan Clemens	5%	discussion of results, comments on manuscript
Britta Planer-Friedrich	10%	development of research concept, discussion of results, comments on manuscript

Study 4: Iron plaque of rice plants: no barrier for methylated thioarsenates

Carolin F. Kerl	85%	development of research concept, laboratory work, analyses and data interpretation, preparation of manuscript
Tiziana Boffa Balaran	5%	XRD analysis and data interpretation
Britta Planer-Friedrich	10%	development of research concept, discussion of Results comments on manuscript

Appendix: Studies 1-4

Study 1

Wang, J.; **Kerl, C. F.**; Hu, P.; Martin, M.; Mu, T.; Brüggewirth, L.; Wu, G.; Said-Pullicino, D.; Romani, M.; Wu, L.; Planer-Friedrich, B., Thiolated arsenic species observed in rice paddy pore-waters. *Nature Geoscience*. DOI: 10.1038/s41561-020-0533-1.

Study 2

Kerl, C. F.; Rafferty, C.; Clemens, S.; Planer-Friedrich, B., Monothioarsenate Uptake, Transformation, and Translocation in Rice Plants. *Environ. Sci. Technol.* **2018**, *52*, (16), 9154-9161. DOI: 10.1021/acs.est.8b02202

Study 3

Kerl, C. F.; Schindele, R. A.; Brüggewirth, L.; Colina Blanco, A. E.; Rafferty, C.; Clemens, S.; Planer-Friedrich, B., Methylated thioarsenates and monothioarsenate differ in uptake, transformation, and contribution to total arsenic translocation in rice plants. *Environ. Sci. Technol.* **2019**, *53*, (10): 5787-5796. DOI: 10.1021/acs.est.9b00592

Study 4

Kerl, C. F.; Boffa Balaran, T.; Planer-Friedrich, B., Iron plaque of rice plants: no barrier for methylated thioarsenates. *Environ. Sci. Technol.* **2019**, *53*, (23): 13666-13674. DOI: 10.1021/acs.est.9b04158

Study 1: Thiolated arsenic species observed in rice paddy pore-waters

Jiajia Wang; Carolin F. Kerl, Pengjie Hu, Maria Martin, Tingting Mu, Lena Brüggewirth, Guangmei Wu, Daniel Said-Pullicino, Marco Romani, Longhua Wu, Britta Planer-Friedrich

Nature Geoscience (DOI: 10.1038/s41561-020-0533-1)

Thiolated arsenic species observed in rice paddy pore-waters

Jiajia Wang¹, Carolin F. Kerl¹, Pengjie Hu², Maria Martin³, Tingting Mu², Lena Brüggewirth¹, Guangmei Wu², Daniel Said-Pullicino³, Marco Romani⁴, Longhua Wu² and Britta Planer-Friedrich^{1*}

¹ Department of Environmental Geochemistry, Bayreuth Center for Ecology and Environmental Research (BayCEER), University of Bayreuth, Universitaetsstrasse 30, 95440 Bayreuth, Germany

² Key Laboratory of Soil Environment and Pollution Remediation, Institute of Soil Science, Chinese Academy of Sciences, 210008 Nanjing, China

³ Department of Agriculture, Forest and Food Sciences, University of Turin, 10124 Turin, Italy

⁴ Rice Research Centre, Ente Nazionale Risi, 27030 Castello d'Agogna, Pavia, Italy

ABSTRACT: The accumulation of carcinogenic arsenic in rice, the main staple crop in the world, represents a health threat to millions of people. The speciation of arsenic controls its mobility and bioavailability, and therefore its entry into the food chain. Inorganic and methylated oxyarsenic species have been a focus of research, but arsenic characterization in the field has largely ignored thioarsenates, in which sulfur takes the place of oxygen. Here, based on field, mesocosm, and soil incubation studies across multiple paddy soils from rice cultivation areas in Italy, France, and China, we find that thioarsenates are important arsenic species in paddy-soil pore waters. We observed thioarsenates throughout the cropping season, with concentrations comparable to the much-better-investigated methylated oxyarsenates. Anaerobic soil incubations confirmed a large potential for thiolation across a wide diversity of paddy soil types in different climate zones and with different parent materials. In these incubations, inorganic thioarsenates occurred predominantly where soil pH exceeded 6.5 and in the presence of zero-valent sulfur. Methylated thioarsenates occurred predominantly at soil pH below 7 and in the presence of their precursors, methylated oxyarsenates. High concentrations of dissolved iron limited arsenic thiolation. Sulfate fertilization increased thioarsenate formation. It is currently unclear whether thiolation is good or bad for rice consumption safety. Nevertheless, we highlight thiolation as an important factor to arsenic biogeochemistry in rice paddies.

INTRODUCTION

Rice is the main staple crop for more than half of the World's population. At the same time, it represents a major dietary source of arsenic (As), a class I carcinogen¹. Premises for As accumulation in rice grains are its global occurrence in soils and efficient uptake by rice plants together with essential nutrients^{2, 3, 4}. Soil-derived As becomes plant-available under flooded conditions when the reductive dissolution of iron (Fe) (oxy)hydroxides and arsenate reduction release sorbed As⁵. Pore-water As speciation is dominated by inorganic As (arsenite and arsenate). Microbe-mediated As methylation leads to formation of mono- (MMA) and dimethylarsenate (DMA)⁶ which typically are minor species in pore-waters⁷, although DMA can contribute up to 90% of total As in the grain due to high root-shoot translocation⁸. Current research on As biogeochemistry in paddy soils mainly has been focusing on these four oxyarsenic species and it is well-accepted that As speciation is responsible for its mobility and bioavailability⁹.

Our objective was to reveal whether and to what extent thioarsenates contribute to As speciation in paddy soil pore-waters. Thioarsenates are pentavalent As species in which sulfur (S) replaces oxygen. They form upon reaction of arsenite with zero-valent S and sulfide (in case of inorganic thioarsenates)¹⁰, or MMA and DMA with sulfide (in case of methylated thioarsenates)^{11, 12} (Fig. 1). Thioarsenates typically occur in aquatic environments with excess dissolved sulfide¹³. Just very recently they

have also been detected in low sulfide environments where thiolation is probably controlled by reactions with reduced S bound to surfaces of minerals or organic matter^{10, 14}.

To date, occurrence of thioarsenates in paddy soils has never been addressed which is only partially a methodological problem. Routine sample preservation and many chromatographic separation methods use acids which transform thioarsenates to arsenite or oxyarsenates¹⁵ or lead to As loss by As-S precipitation¹⁶, so thioarsenates are plainly overlooked. However, the main reason for neglectance of thioarsenates is a conceptual limitation because flooded paddy soils are primarily regarded as methanogenic environments¹⁷. Sulfate reduction, though thermodynamically favored relative to methanogenesis, is often considered insignificant due to typically low (except for acid sulfate soils) sulfate contents¹⁸, and sulfide reactivity being limited by mackinawite (Fe^{II}S) precipitation¹⁹. There is, however, evidence for a "cryptic" S-cycle¹⁸, where sulfide re-oxidation to zero-valent S is coupled to reduction of Fe(III) (oxy)hydroxides and formation of mixed Fe^{II}Fe^{III} minerals or pyrite (Fe^{II}S₂) besides Fe²⁺²⁰. Further S oxidation to thiosulfate and sulfate is coupled to nitrate or oxygen reduction (Fig. 1). Such a S-cycle sustains high sulfate reduction rates in the bulk soil and especially the rhizosphere¹⁸. We hypothesized that low but continuously replenished sulfide and zero-valent S could promote thioarsenate formation besides or instead of As scavenging on newly formed Fe

minerals²¹. A similar observation was made in paddy soil incubation studies where initially sequestered As was remobilized under sulfidic conditions²². Thioarsenate formation was suspected, but no As-S speciation analysis was done. Sulfate fertilization, recently investigated for its potential benefits in improving nutrient uptake and rice growth²³, as well as mitigating methane emissions^{24,25} and rice As accumulation^{26,27}, might further contribute to thioarsenate formation.

During an initial field survey, we had discovered thioarsenates while sampling planted paddy fields covering the main rice cropping areas of the river Po plain in Italy (soil pH 5.0-6.1, As 5.1-16 mg/kg), and of the Camargue coastal plain in France (soil pH 7.5-7.6, As 10.4-20.2 mg/kg). Contribution of total thiolation to total As concentrations was 8.3% at maximum and 2.1% on average; numbers comparable to those observed for the much more-commonly-investigated methylated oxyarsenates (for details see supporting information section 1, Table S1, Fig. S1-S4).

Key to all further investigations was the development of a novel sampling and analytical method using diethylenetriamine-pentaacetic acid (DTPA, 10 mM) to complex excess dissolved Fe, followed by flash-freezing for sample preservation, sample dilution and the use of an adapted eluent for chromatographic separation to avoid negative effects of high DTPA concentrations such as retention time shifts, peak splitting, and poor species resolution. Detection limits of the optimized method were 0.03 µg/L As and recovery rates >80%, which is the currently by far best available stabilization and analysis method for detection of the up to 11 species of interest (see methods' section for details).

We then examined occurrence of inorganic and methylated thioarsenates in comparison to their oxyarsenic analogues over a range of scales moving from our initial field surveys to controlled mesocosm experiments and laboratory soil incubations.

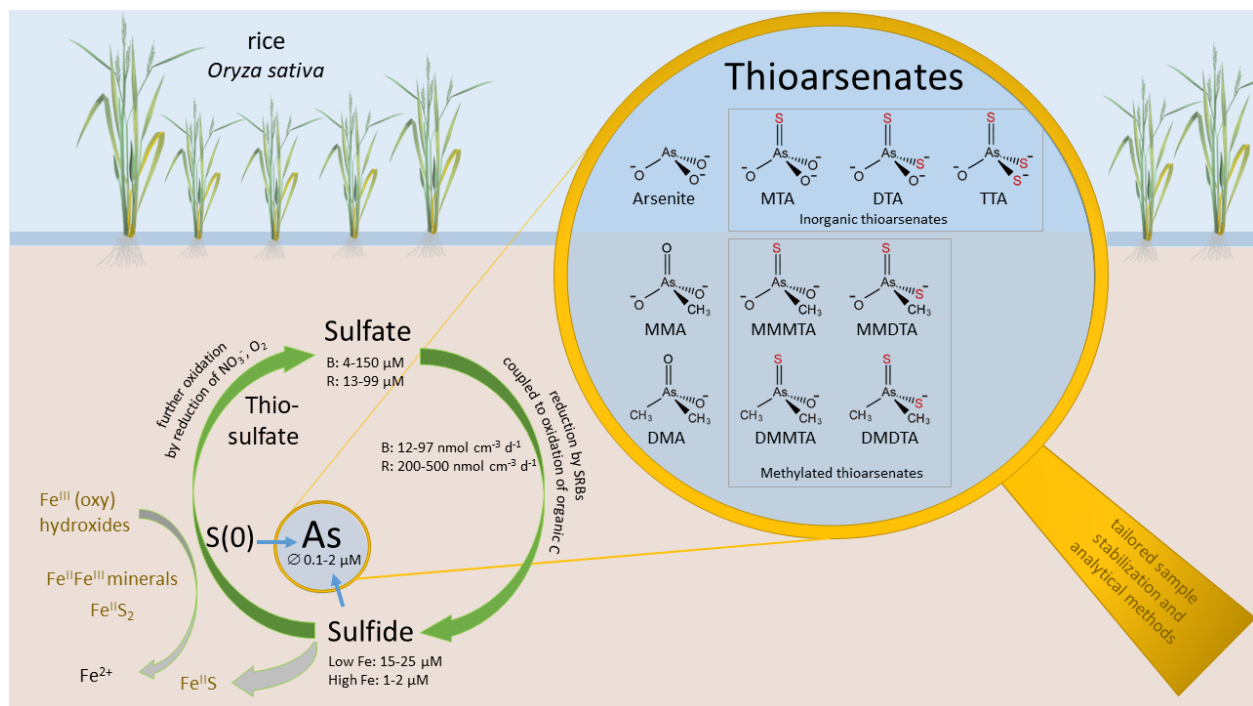


Figure 1 | Conceptual model for the formation of thioarsenates in paddy soils coupled to a cryptic S cycle. Low but continuously replenished concentrations of sulfide and zero-valent sulfur [S(0)] lead to As thiolation instead of or besides As scavenging by newly formed mixed Fe^{II}Fe^{III} minerals and pyrite (FeS₂) or, at excess sulfide, mackinawite (FeS) and AsS; concentrations and rate numbers (taken from references¹⁸ and³⁶) are displayed to present typical quantities and extents of sulfate reduction rates (B = bulk soil, R = rhizosphere, SRB = sulfate-reducing bacteria): MTA = monothioarsenate, DTA = dithioarsenate, TTA = trithioarsenate, MMA = monomethylarsenate, MMMTA = monomethylmonothioarsenate, MMDTA = monomethyldithioarsenate, DMA = dimethylarsenate, DMMTA = dimethylmonothioarsenate, DMDTA = dimethyldithioarsenate.

Thioarsenate formation in rice cultivation mesocosms.

Based on the field survey (Table S1), we selected two Italian paddy soils (an Eutric Gleysol from a paddy field near Cascina Veronica and an Umbric Gleysol from a paddy field near Cascina Fornazzo), characterized by highest proportions of thiolation, for mesocosm experiments (setup see Fig. S5). The two soils had the same total soil As contents (5.5 mg/kg) and were relatively similar in soil pH (5.6 and 5.8 for Veronica and Fornazzo, respectively), while in comparison to Fornazzo, Veronica had slightly lower contents of 0.5 M HCl-extractable Fe (52 vs. 71 mmol/kg), total C (2.0 vs. 4.7 %), and total S (2.6 vs. 3.2 g/kg) (Table S2). All mesocosms were planted

with the same rice variety (*Oryza sativa* L. cv. Selenio) and managed in a completely randomized factorial arrangement representing (i) treated with (S) or without sulfate (no S, control) fertilizers and (ii) water or dry seeded (Fig. S5, S6). In water seeded treatments soils were flooded from one day before seeding throughout the growing season, while in dry seeded treatments oxic soil conditions were maintained until tillering stage (20 days after seeding) after which the soils were flooded (Fig. S6). Consequently, dry seeded soils showed higher redox potentials and lower pore-water Fe(II) concentrations at tillering stage with respect to the water seeded treatments (Table S3).

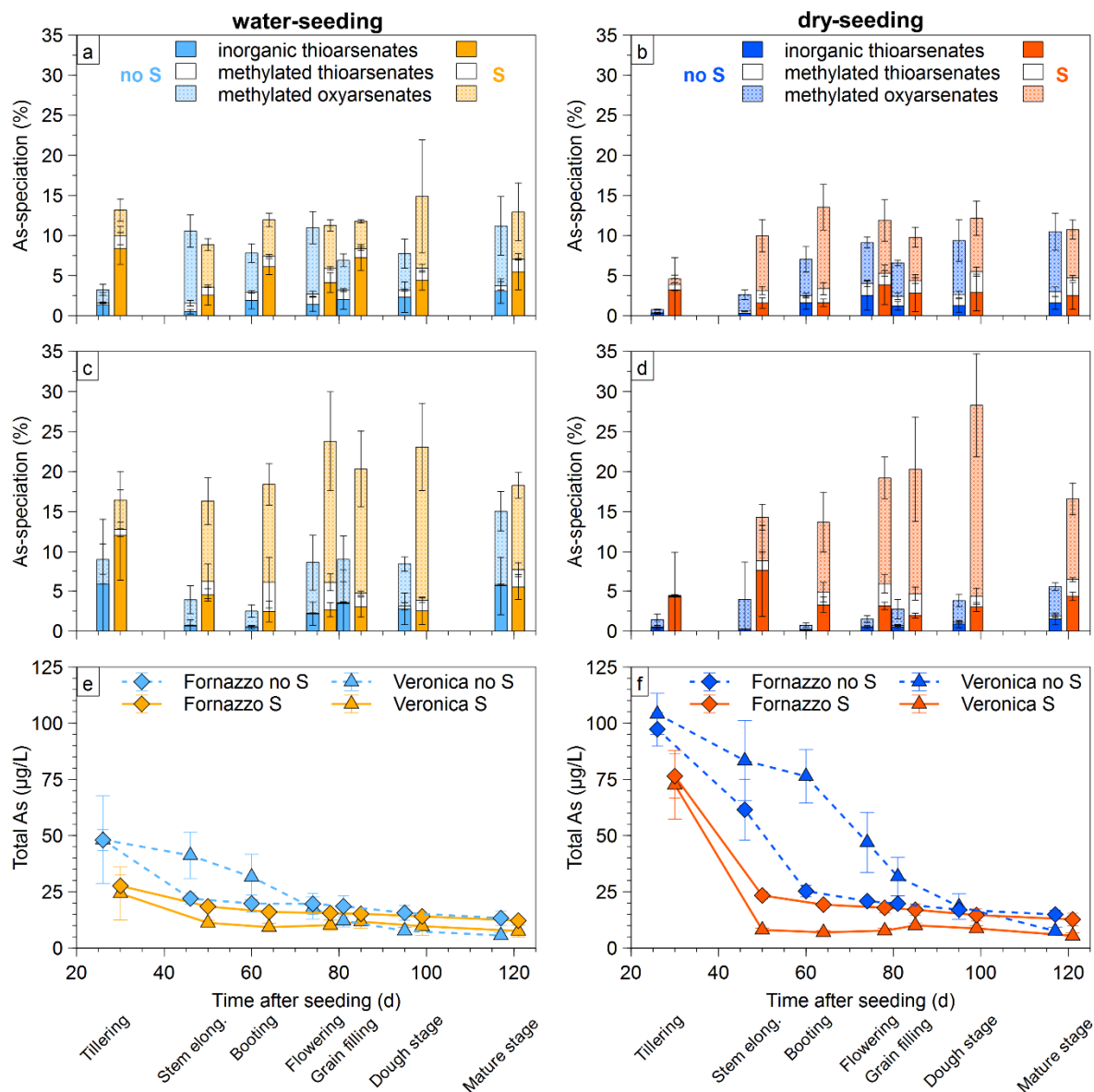


Figure 2 | Pore-water As thiolation, methylation, and total As concentrations over time during rice cultivation. a) Fornazzo soil, water seeded, b) Fornazzo soil, dry seeded, c) Veronica soil, water seeded, d) Veronica soil, dry seeded; blue colors refer to control treatments (no S), orange-red colors to sulfate addition (S); percentages refer to proportion of total As; e, f) total As concentrations for the two soils with and without sulfate addition; standard deviation reflects results from 3 mesocosms (n=3).

Thioarsenates were observed in all mesocosms of both soils at all seven sampling stages (tillering, stem

elongation, booting, flowering, grain filling, dough, and mature stage) under both water and dry seeded treatments

(Fig. 2a-d). The contribution of thioarsenates to total As ranged from 0.1% to 19%, on average 4.1%. For comparison, methylated oxyarsenates ranged from below detection limit to 33%, on average 6.5%. Concentrations of inorganic thioarsenates were generally higher (max. 6.4 $\mu\text{g/L}$ or 19% of total As) than those of methylated thioarsenates (max. 1.1 $\mu\text{g/L}$ or 8.2% of total As) in both soils. No clear trend in the proportion of inorganic or methylated thioarsenates was observed over time (Fig. 2a-d). For details on trends in total As pore-water concentrations over time see supporting information, section 2.

Sulfate fertilization significantly decreased total pore-water As concentrations (Fig. 2e, f). All S fertilized mesocosms, including dry seeded Veronica soil, had pore-water As concentrations at or below 20 $\mu\text{g/L}$ already at stem elongation stage. The same faster decrease in As concentrations upon addition of sulfate has been reported before due to stimulation of sulfate-reducing bacteria (SRB), increased sulfide production, and formation of new Fe minerals^{20, 28} (Fig. 1). A decrease due to re-adsorption was, however, mainly observed for inorganic oxyarsenic species, while proportions of inorganic and methylated thioarsenates, as well as methylated oxyarsenates, increased with sulfate fertilization (Fig. 3). Average total thiolation with sulfate addition was 5.9% compared to 2.2% in controls, average methylation was 8.8% compared to 4.3% in controls. Higher proportions of methylated As species upon sulfate addition are in line with previous observations²⁹. Similar to the control treatment, there were no significant trends in thiolation or methylation over time (Fig. 2a-d).

Seeding practices did not only impact total As concentrations (with higher concentrations in dry compared to water seeded treatments) but also As thiolation. Both without and with sulfate fertilization, higher percentages were observed in water compared to dry seeded mesocosms due to the longer duration of anaerobic conditions in the former (Fig. 3c, g).

Comparison between the two different soils showed that sulfate fertilization had a stronger impact in Veronica compared to Fornazzo soil. We observed both a stronger decrease in total As concentrations (Fig. 2e, f), as well as a stronger increase in average proportions of methylated oxy- and thioarsenates, in both water and dry seeded treatments, as well as inorganic thioarsenates in dry seeded treatments, for Veronica compared to Fornazzo soil (Fig. 3, Table S4). The exact redox chemistry, especially the role of organic C, remains to be investigated, but we propose that the lower soil C content caused less reducing conditions (reflected in higher redox potentials and less aqueous Fe^{II} ; Table S3) in Veronica soil compared to Fornazzo soil. Thereby, besides efficient removal of As on mixed $\text{Fe}^{\text{II}}\text{Fe}^{\text{III}}$ minerals, more recycling of SRB-produced sulfide to sulfate with formation of zero-valent S and As thiolation (see also below) was favored, compared to more removal on FeS minerals and less thiolation in Fornazzo soil.

Finally, multivariate regression tree analysis comparing the relative importance of the investigated effects on pore-water As speciation in our mesocosms showed the clearest separation between sulfate and non-sulfate treatments, followed by the differences of the two selected soil types. The different rice growing stages had the least effects on pore-water As speciation (Fig. S7).

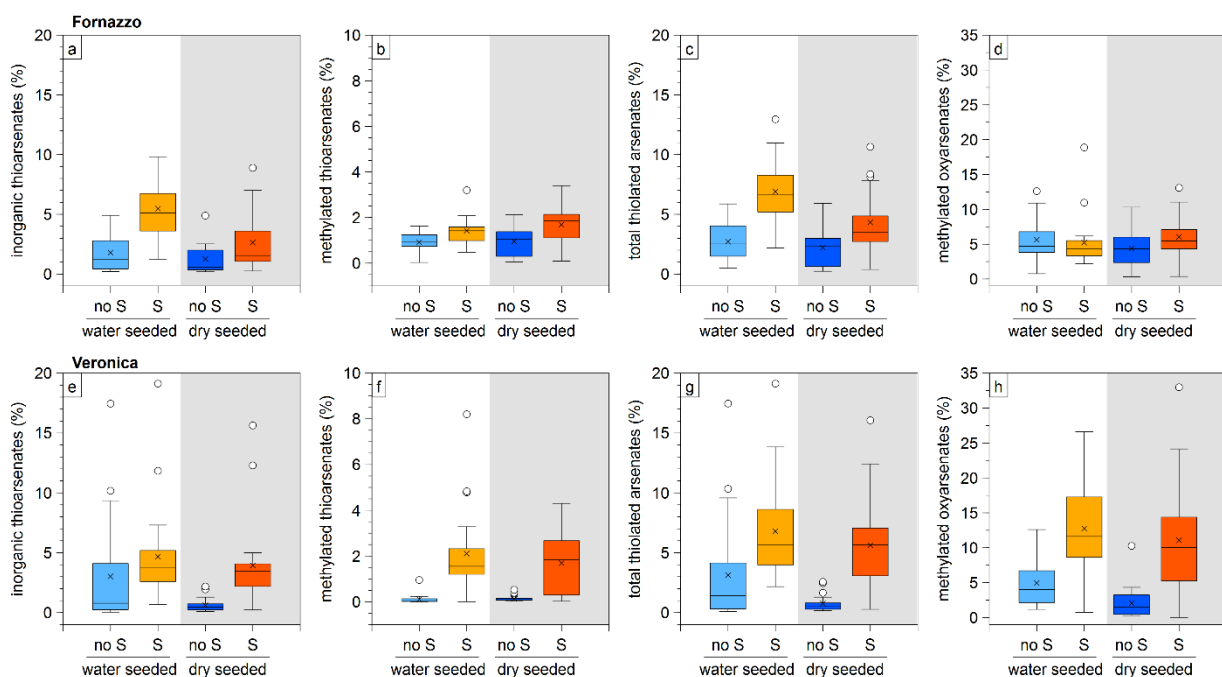


Figure 3 | Proportions of inorganic, methylated, and total thioarsenates as well as methylated oxyarsenates integrated over time. a, e) inorganic thioarsenates, b, f) methylated thioarsenates, c, g) total thioarsenates, d, h) methylated oxyarsenates integrated over all sampling times for Fornazzo and Veronica soils, respectively, water seeded (left side of each graph) and dry seeded (right, shaded side) treatment, blue colors refer to control treatments (no S), orange-red colors to sulfate addition (S); percentages refer to proportion of total As, boxplots: line: median; cross: mean; box: interquartile range; whiskers: 1.5 interquartile range; data from 3 mesocosms over 7 times (n=21).

Thioarsenate formation potential in soil incubations.

To estimate the potential for thioarsenate formation on a large scale, we conducted anaerobic soil incubation experiments with the two Italian soils plus 31 soils sampled from across China (for coordinates see Table S5a). China is one of the biggest rice cultivation countries. The selected soils cover all major rice production regions in China, with paddy soils located in different climate zones (Fig. S8), developed over different parent material, resulting in different soil types (Table S5a, Fig. S9), and at sites of different geology and geomorphology (Table S5b). The samples cover a wide range of soil pH (4.5 to 9.0), total As contents (2.6 to 38.8 mg/kg), 0.5 M HCl-

extractable Fe (30 to 184 mmol/kg), and SOM (14.0 to 104 g/kg) (Table S5c).

After two weeks of incubation, As thiolation was detected in all paddy soils with and without sulfate addition. The proportion of total thioarsenates ranged from 0.1% to 56%, with an average of 9.6% and a median of 4.8% (Fig. S10a). In comparison, the proportion of methylated oxyarsenates ranged from 0.5% to 17%, with an average of 3.1% and a median of 1.8% (Fig. S10e). The dominant individual As species were DTA (> trithioarsenate (TTA) > MTA) and DMDTA (> MMMTA ≥ MMDTA > DMMTA) for inorganic and methylated thioarsenates, respectively (Fig. S11), with different factors controlling their formation.

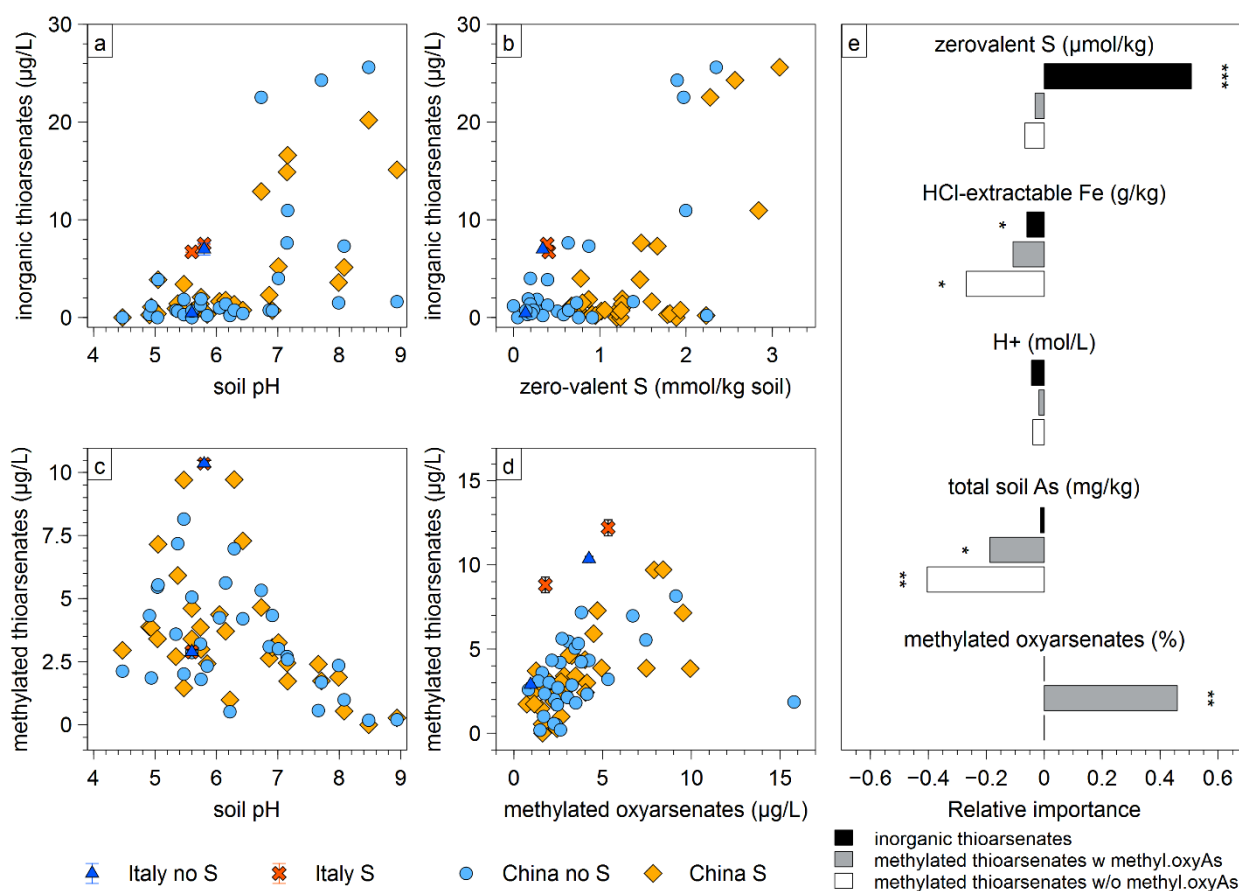


Figure 4 | Parameters that determine occurrence of inorganic and methylated thioarsenates in anaerobic soil incubations. Paddy soils were from Italy (2; experimental triplicates) and China (31, single experiments). a) concentrations of inorganic thioarsenates in relation to soil pH and b) solid phase zero-valent S, c) concentrations of methylated thioarsenates in relation to soil pH and d) methylated oxyarsenates; blue colors refer to control treatments (no S), orange-red colors to sulfate addition (S); standard deviation for samples from Italy reflect results from 3 incubations (n=3); e) linear regression analysis showing relative importance of selected soil parameters in control treatments on proportion of inorganic and methylated thioarsenates (with and without considering methylated oxyarsenates) (for complete list of soil parameters considered and data for sulfate addition see Table S7).

For inorganic thioarsenates, high absolute concentrations tended to occur at high soil pH and soil zero-valent S contents (Fig. 4a, b, confirmed by Spearman correlation (Table S6) and principal component analysis (Fig. S12)). The pH-dependency of inorganic thioarsenates formation is at first glance surprising. Inorganic thioarsenates are known to transform to oxyarsenic species at low pH^{15, 16}, but even though soil pH (when oxidic) ranged from 4.5 to 9.0, pore-water pH values of all incubations were near-neutral to slightly alkaline (6.9 to 7.9; Fig. S13a) and should not have influenced inorganic thioarsenate (trans)formation. Linear regression analysis showed that the most important predictor for inorganic thioarsenate formation potential in our incubations was soil zero-valent S (weight factor 51%, Fig. 4e, Table S7). Soil zero-valent S increased with soil pH (Fig. S13c), which explains the observed correlation of soil pH and inorganic thioarsenates as an indirect effect through zero-valent S. In most samples, we also detected aqueous zero-valent S (Fig. S13d), but absolute concentrations were more than one order of magnitude lower than those for solid phase zero-valent S, and even in the absence of detectable aqueous zero-valent S, inorganic thioarsenates were observed. The greater impact of solid phase zero-valent S is consistent with previous observations in low-sulfide terrestrial environments where inorganic thioarsenate formation was found to be controlled by reactions with S bound to surfaces of minerals or organic matter^{10, 14}. The concentrations of pedogenetic (0.5 M HCl-extractable) Fe had a negative, but relatively low impact on inorganic thioarsenate formation potential (weight factor -6%, Fig. 4e, Table S7), likely because little Fe dissolved at high pH (Fig. S13e).

Methylated thioarsenates showed a completely different behavior. The most important predictor for their formation was the proportion of methylated oxyarsenates (weight factor 46%, Fig. 4e, Table S7). Methylated thio- and oxyarsenates showed a strong positive correlation (Fig. 4d, Table S6). Negative correlation of methylated thioarsenates with soil pH (Fig. 4c, Table S6) suggests that their formation in nature proceeds by nucleophilic attack of reduced S to the As atom which is facilitated at low pH¹². The higher proportion of methylated oxyarsenates observed at low pH (Fig. S8e) is in line with previous observations in other environments of highest methylation rates at pH 3.5 to 5.5³⁰. An almost even contribution of thio- and oxyarsenates to total methylation (Fig. 4d), as well as the absence of a correlation with zero-valent S (Table S6), suggest that thiolation of methylated species proceeds rapidly and is typically not limited by S supply but mainly by the availability of methylated oxyarsenates (in contrast to inorganic thioarsenates where relatively large excess of S over arsenite is required for thiolation). Examining soil properties, low total soil As concentrations were the best predictor of the potential for a high (thio)methylation contribution to total As (weight factor -40%, Fig. 4e, Table S7). We found that high soil As concentrations only led to increased inorganic As release into pore-water while absolute concentrations

of methylated species did not change with increasing total soil As and therefore relative contributions decreased (Fig. S14). Finally, pedogenetic Fe had a stronger negative impact on methylated thioarsenates compared to inorganic thioarsenates (weight factor -27%, Fig. 4e, Table S7), likely because of the higher Fe solubility at low pH (Fig. S13e) where methylated thioarsenates prevailed.

Compared to the strong effects that the different soil properties had on thiolation in our incubation experiments, the effect of sulfate addition was less pronounced. It promoted total thiolation (Fig. S15a) by increasing zero-valent S contents (Fig. S13c, S15b) and decreasing pore-water Fe concentrations (Fig. S13e) and redox potential (Fig. S13b), but it did not generally change the relative differences in thioarsenate formation potential between different soils. An exception were soils that had very low initial soil zero-valent S contents. Here, sulfate addition led to a strong increase in zero-valent S and total thiolation (Fig. S15b, c). An example was Veronica soil where an increase of zero-valent S from 0.14 to 0.41 mmol/kg compared to a much smaller increase in Fornazzo soil (from 0.34 to 0.39 mmol/kg) might explain the observed stronger increase in total As thiolation in the soil incubations (inorganic thioarsenates from 3.9 to 24%, methylated thioarsenates from 25 to 32%) which is also in line with an observed stronger increase of total thiolation upon sulfate addition in the mesocosm studies (from 1.9 to 6.2%).

ENVIRONMENTAL IMPLICATIONS

Our combined results from field surveys, mesocosms, and soil incubations reveal thioarsenates as important but previously overlooked and unforeseen contributing species to As biogeochemistry in rice paddies. Thioarsenates form in various paddy soil types, throughout the cropping season, independent of seeding practice, and in quantities comparable to methylated oxyarsenates. Soil pH represented an easy-to-measure parameter indicative for thiolation potential. We suspect that in paddy soils where methylated oxyarsenates have been identified, methylated thioarsenates could have contributed comparable quantities that were, however, not distinguished from the methylated oxyarsenates due to analytical limitations in the current methodologies adopted. Sulfate fertilization promotes thiolation, especially in soils originally low in zero-valent S.

Comparison of our anaerobic soil incubations to mesocosm experiments shows lower proportions of inorganic and especially methylated thioarsenates in the presence of rice plants (Fig. S16). Higher order thiolated inorganic arsenates¹⁵ and MMMTA³¹ are known to be oxygen-sensitive, so that root radial oxygen loss might lead to (partial) transformation in the rhizosphere. However, MTA¹⁵ and DMMTA³² are not oxygen-sensitive. The differences in the proportion of thioarsenates between incubations and mesocosms might therefore point towards their preferential uptake. So far, uptake of thioarsenates and their efficient root-shoot translocation has only been shown in hydroponic

cultures using high concentrations of pure thioarsenate standards^{33, 34} and only one thioarsenate species (DMMTA) has been discovered in commercial rice grains by chance during an enzymatic extraction³⁵. Now that we deliver compelling support of the widespread presence of inorganic and methylated thioarsenates in paddy soil pore-waters, further transfer of methods and experiments from laboratory to field scale is required. Whether thiolation finally is boon or bane for rice safety remains to be investigated.

METHODS

Aqueous As species preservation and analysis

Arsenic speciation throughout the study was done using ion chromatography (IC, Dionex ICS-3000; AG/AS16 IonPac column, 4 mm, eluent gradient 2.5–100 mM NaOH at a flow rate of 1.2 mL/min) coupled to inductively coupled plasma-mass spectrometry (ICP-MS, XSeries2, Thermo-Fisher) at Bayreuth University. Retention times of the As species were verified by comparison with commercial standards (arsenite (NaAsO₂, Fluka), arsenate (Na₂HAsO₄ × 7H₂O, Fluka), MMA (CH₃AsNa₂O₃ × 6H₂O, Supelco), DMA (C₂H₆AsNaO₂ × 3H₂O, Sigma-Aldrich)), standards synthesized according to previously published methods (DMMTA (purity 67%; 28% DMDTA, 5% DMA) and MMMTA (purity 96%; 1% MMA, 3% MMDTA)¹, MTA (purity of 98.5%; 0.5% arsenite, 1% arsenate)²) or by comparison with previously published retention times (MMDTA, DMDTA, DTA, TTA)³.

For our initial field survey (see supporting information section 1) we used sample flash-freezing, a preservation method that we previously employed successfully in other aquatic environments^{4, 5, 6}. In contrast to sample acidification, this method revealed the occurrence of thioarsenates. However, we observed that As recoveries (calculated as the sum of all detected As species in flash-frozen samples versus total As measured in oxidized and HNO₃-acidified samples) were generally below 50%, in many cases even below 10% (Fig. S4), especially at Fe concentrations > 0.5 mM due to Fe (oxyhydr)oxide precipitation and As co-precipitation and sorption. The low recoveries prompted us to adapt the sample preservation and analysis method. Since acidification could not be used to keep Fe in solution because it changes thioarsenate speciation and could lead to AsS mineral precipitation⁷, we tested different Fe chelating agents. In pre-tests, paddy soil solutions derived from anaerobic incubations were preserved with different pH-neutralized chelating agents such as EDTA (ethylenediaminetetraacetic acid disodium salt solution, Sigma–Aldrich), deferoxamine mesylate salt (Sigma-Aldrich), and DTPA (diethylenetriamine-pentaacetic acid pentasodium salt, Sigma-Aldrich). Highest As species recoveries were observed when using DTPA, an octadentate ligand which can completely sequester Fe^{8, 9}. The better performance compared to EDTA, for which we previously reported accelerated oxidation of arsenite and some thioarsenate artefact formation¹⁰, might be attributed to the fact that

Fe^{II}-DTPA complexes are significantly less oxygen-sensitive than Fe^{II}-EDTA complexes¹¹. Based on expected high aqueous Fe concentrations in the sampled paddy soil pore-waters (measured values up to 6.9 mM in samples from China, see section 4), we used 10 mM DTPA, neutralized to pH 7.5, for Fe-complexation.

For a representative paddy soil pore-water matrix (“model pore-water”) for method development, we used pore-waters extracted from anaerobic incubations of paddy soil from Fornazzo (for details on soil properties see section 3, description of mesocosms). To address the effect of DTPA on As species retention times, peak shape, and species resolution, one week old model pore-water was spiked with 100 µg/L of different As species standards and 10 mM DTPA was added for sample preservation. DTPA had a significant effect on peak shapes and retention times, especially for the species with short retention times (Fig. S17). The DMA peak that eluted after 297 s in the absence of DTPA was shifted to the dead volume (142 s, Fig. S17a). DMMTA and DMDTA were partially retained at their original retention times (376 and 446 s) but peaks became wide and small and part of the As was lost in a high baseline background from 150 to 350 s (Fig. S17b). The same change in peak shape and total As loss was observed for arsenite (original retention time at 406 s; Fig. S17c). Mixes of arsenite, DMA, and DMMTA also showed that species resolution between arsenite and DMMTA was lost in the presence of DTPA (Fig. S17d). MMMTA and arsenate were less affected but peak splitting (Fig. S17e) and peak fronting (Fig. S17f), respectively, were observed in the presence of DTPA as well.

Since we could not reduce the DTPA concentration because of the expected Fe concentrations but needed to decrease the negative effects of DTPA on peak separation, we tested 10-fold dilution with deionized water of a fresh model pore-water sample without As spikes after addition of 10 mM DTPA (bringing DTPA concentrations down to 1 mM, but also diluting Fe, As, etc. 10-fold). The 1:10 sample dilution increased peak separation and largely avoided As elution in the dead volume (Fig. S18) but some peaks were close to or below detection limit. Adding 2.4% methanol to the 2.5-100 mM NaOH gradient eluent in the IC enhanced signal intensities of all peaks, except for arsenite, by a factor of 2 to 10 (Fig. S18). A slight decrease in retention times and some arsenate fronting was observed, but all peaks could be identified and little As was lost in the dead volume.

For a quantitative evaluation we spiked the fresh model pore-water sample with a mixed standard of 1 µg/L of DMA, DMMTA, arsenite, MMA, MMMTA, and arsenate. Comparing preservation in 10 mM DTPA in deionized water vs. model pore-water matrix (analyzed 1:5 and 1:10 diluted), showed that the pore-water matrix itself had a minor effect on peak shifting compared to the influence of DTPA (Fig. S19). A dilution of 1:5 resulted in peak broadening for DMA and DMMTA but no additional As loss. Quantitatively, the results of 1:10 or 1:5 dilution were comparable

(Table S8). Measured total As concentration in HNO₃ for that sample was 14.3 µg/L and recovery from speciation analysis for the 1:10 and 1:5 dilution with 76% and 77%, respectively, was good. Species with concentrations of 0.28 and 0.15 µg/L (equivalent to 2.5 and 1% of total As) could clearly be identified in the 1:10 and 1:5 dilutions, respectively.

Three commercial standards were routinely used for calibration (arsenate dibasic-heptahydrate, disodium methyl arsonate hexahydrate, dimethylarsinic acid in 2 mM DTPA). No significant differences were observed between using an average calibration of the three commercial standards or calibrating each species individually using the calibration standard which was closest in retention time. Arsenite was not used for calibration because in deionized water we observed transformation of arsenite in the presence of DTPA (Fig. S20). The arsenite transformation product eluted at the retention time of arsenate but with significant peak fronting. Whether the species really is arsenate (obtained from arsenite oxidation) or an As(III)- or As(V)-DTPA complex is currently unclear. In spiked natural samples, we did not observe this arsenite transformation.

The final protocol for As speciation that was applied for the mesocosm and incubation experiments described in the following is summarized as follows. Samples were filtered, preserved in 10 mM DTPA, flash-frozen on dry ice, and stored at -20 °C. Prior to analysis, frozen samples were thawed under anoxic atmosphere inside a glovebox (CO₂, N₂/H₂ 95/5% (v/v)) at room temperature. Samples were diluted 1:5 with deionized water and analyzed with a 2.5-100 mM NaOH gradient containing 2.4% methanol.

We are aware that sample dilution might transform higher thiolated As species such as DMDTA, MMDTA, DTA, or TTA as reported previously¹² and that we may therefore underestimate the extent of As thiolation. Further, recoveries generally were >80%, which is good considering that we calculate the sum of up to 11 species, but could still indicate a loss of As species by Fe scavenging. Therefore, where species proportions are reported in %, the reference is not the sum of species, but always total As from a sample preserved with 0.5% H₂O₂ and 0.8% HNO₃ as an independent measurement. The reported % values are therefore minimum values if a species is not affected at all by Fe scavenging. If thiolated species are scavenged by Fe similar to arsenite and arsenate we may further slightly underestimate their importance with the currently available analytical methods. Despite some remaining shortcomings, the developed DTPA-method is the current best compromise, given the complexity of the paddy soil pore-water samples which are rich in organic carbon, contain high Fe that is prone to oxidation (so mere flash-freezing does not work) and As-complexed sulfide that is prone to precipitation at low pH (so acidification does not work) plus relatively low concentrations of As. The method enabled us to provide the so far most complete aqueous As speciation data for paddy soil pore-waters.

Mesocosm rice cultivation

For mesocosm experiments, we selected two paddy soils characterized by highest proportions of thiolation in pore-water during our field survey in August 2016, Veronica (E 8°53'48", N 45°10'39"; Eutric Gleysol) and Fornazzo (E 8°57'50", N 45°13'54"; Umbric Gleysol) (Table S1, S2). A large batch of dry soil material was collected from the plow layer of the two fields in March 2017 and transported to the Rice Research Centre Ente Nazionale Risi (ENR) in Castello d'Agogna (Pavia, Italy) where we set up the mesocosms. For basic soil characterization, soil pH (measured in 2.5 mL 0.1 M CaCl₂ solution with 1 g soil), 0.5 M HCl-extractable Fe, total C and N (CHN analyzer), and total S (determination by ICP-MS after microwave digestion in aqua regia) were determined.

Twenty-four plastic containers (0.82 m²) were installed open air at the property of ENR. A nylon mesh roof top protected the setup from birds or hail. Each container was filled with approximately 30 cm of gravel with a size of 2-5 cm in diameter, overlaid by approximately 20 cm of soil. Twelve containers each were filled with the two different paddy soil types (Fig. S5). The soil layers were mixed with 5 t/ha equivalent rice straw according to the common rice straw returning practice in this region. The rice straw was cut into pieces of approximately 20 cm length before mixing it with the soil. Six containers of each paddy soil type were either dry or water seeded. Water seeded soils were first fertilized with 100 kg N/ha and flooded on May, 16th (Fig. S6) before sowing with pre-germinated rice seeds (*Oryza sativa* L. cv. *Selenio*) the following day. Dry seeded soils were fertilized with 100 kg N/ha and sown on May, 17th (Fig. S6). Planted seeds germinated within 10 days. Soils were kept moist until tillering stage (June, 6th) and subsequently flooded. All mesocosms were manually thinned to 340 rice plants per container. Irrigation water (characteristics see Table S9) was supplied with a garden hose for both dry and water seeded treatments, to maintain a standing water level of approximately 10 cm depth during the cropping season. In addition to basal fertilization, N-, P-, or K-fertilizers were applied in form of urea, triple superphosphate, and potassium chloride as solid salts at tillering, stem elongation and booting stages (Fig. S6). Three containers of each soil and seeding practice were additionally fertilized with sulfate fertilizer, the other three containers did not receive sulfate (control treatments). Sulfate was applied as ammonium sulfate and potassium sulfate, while equivalent amounts of urea and potassium chloride were used in the control treatment.

Sampling was done at seven rice growing stages, namely tillering stage (June, 14th), stem elongation stage (July, 4th), booting stage (July, 18th), flowering stage (August, 1th), grain filling stage (August, 8th), dough stage (August, 22th), and mature stage (September, 13th) (Fig. S6). Pore-water was extracted by micro rhizon samplers (Rhizon MOM, Rhizosphere Research Products, The Netherlands) inserted about 3-4 cm deep into the paddy soil and connected to 100 mL evacuated glass bottles. The bottles were prepared

prior to sampling by purging them with argon (purity > 99.9%) for 15 min, sealing them with a butyl rubber septum and then evacuating them to negative atmospheric pressure of ~900 mbar. Sampling took on average 40 minutes. An aliquot of pore-water was preserved in 10 mM DTPA, flash-frozen on dry ice, and stored at -20°C until analysis. Non-stable chemical parameters (pH, redox potential) were measured immediately on-site. Samples for dissolved organic carbon (DOC) and dissolved inorganic carbon (DIC) were kept anoxic, in the dark at 4°C, and analyzed the following day at the University of Turin (VarioTOC, Elementar, Hanau, Germany). Information on pH, EH, conductivity, DIC, DOC, Fe(II), and total As can be found in Table S3.

Soil sampling and anaerobic incubations

Paddy soil samples were collected from the cultivated horizon of 31 different paddy fields across China, which represent the main rice production regions in 18 different Chinese provinces. The geographic origins covered an area from 22.5° to 47.2° N and 98.4° to 131.6° E, spanning climate zones from sub-tropical monsoon climate (23 soils) to temperate continental climate (1 soil) and temperate monsoon climate (7 soils) (Fig. S8). Based on the Chinese soil taxonomic classification, all paddy soils are classified as Stagnic Anthrosols with both a hydric epipedon (including cultivated horizon and plowpan) and a hydric horizon. Those paddy soils represent three out of four key groups of Stagnic Anthrosols, namely Fe-accumuli- (15), Fe-leachi-(8), and Hapli- (8) Stagnic Anthrosols (Fig. S9). Detailed information regarding sampling site coordinates, soil classification, parent material, geology, geomorphology, and climate zone can be found in Table S5a, 5b. Twenty-nine out of the 31 paddy fields had As concentrations below the Chinese risk screening values for contamination of agricultural land (30 mg/kg when pH ≤ 6.5 13), and are thus considered to represent the natural background. Only two soils namely Guangxi-Nanning (CH2, 34.2 mg/kg) and Jiangxi-Ganzhou (CH6, 38.8 mg/kg) exceeded the Chinese risk screening values for paddy soil. We intentionally focused on non-contaminated paddy soils having background As concentrations because of the wider implications linked with human exposure, with respect to the less ubiquitous anthropogenically-contaminated sites (e.g. only 2.7% of paddy soils in China according to a recent survey¹⁴), that often have rather specific biogeochemistries that greatly depend on contamination source and type.

Selected soil properties, including pH, 0.5 M HCl-extractable Fe, SOM, CEC, clay content, total As and other chalcophile metals (Cd, Pb, Cu and Zn), and soil zero-valent S content were analyzed by standard methods^{15, 16, 17}. All soils were air-dried and sieved to < 2 mm before analysis and incubation.

For incubation, 10 g dry soil was suspended in 20 mL of 2.5 mM glucose solution without (control, no S) or with 1.5 mM K₂SO₄ (3 mmol/kg sulfate, S) in a glovebox (N₂/H₂ 95/5% (v/v)). The vials were incubated anaerobically, at room temperature and in

the dark for 14 days. This duration was assumed from pre-experiments and literature¹⁸ to be sufficient for microbial growth to reach a steady state. For sampling, soil suspensions were centrifuged and filtered (0.2 μm). Aqueous phase parameters (pH, redox potential, dissolved free sulfide and aqueous zero-valent S, total As) were measured as described above. Another aliquot was preserved in 10 mM DTPA, flash-frozen on dry-ice, and stored at -20 °C for As speciation analysis. Aqueous total Fe was measured immediately by the ferrozine test¹⁹. Soil for solid phase zero-valent S extraction was first freeze-dried (EDWARDS Modyla & Vacuum oven Heraeus), then extracted with chloroform (10 mg soil + 700 μL chloroform) and analyzed by HPLC²⁰. Thus, soil-bound zero-valent S in our study is operationally defined as chloroform-extractable, reduced inorganic S.

Statistical analyses

All statistical analyses were performed via R statistical computing environment. Spearman's correlation was calculated using the "Hmisc" package. Principal component analysis of As species (DMA, MMA, DMDTA, MMDTA, MMMTA, DMMTA, MTA, DTA, and TTA) in the batch incubations was calculated using the "vegan" package. Multiple linear regression (MLR) analysis between inorganic and methylated thioarsenates (%), respectively, and soil physical and chemical properties (soil pH, total zero-valent S, total soil As, 0.5 M HCl-extractable Fe, CEC, SOM, clay content, and soil chalcophile metals (sum of Cd, Pb, Cu, and Zn)) was done using "MASS" package (with default parameters). For methylated thioarsenates two models were calculated, one with, a second without considering methylated oxyarsenates. Relative importance of variables in multiple regression was calculated using the "relaimp" package (type = "Img")²¹. Residuals were checked for normal distribution, which is a prerequisite for multiple linear regression. Multivariate regression tree analyses were done using the "mvpart" package (with default parameters)²².

ACKNOWLEDGMENT

We acknowledge financial support for a Ph.D. stipend to Jijia Wang from the China Scholarship Council (CSC), mobility grants within the Bavarian Funding Programme for travels to France (BFHZ FK-40-15), Italy (BayIntAn2016), China (BayCHINA2018), as well as from the National Key Research and Development Project of China (2016YFE0106400) and the National Natural Science Foundation of China (41325003) for paddy soils survey, sampling and determination in China. We acknowledge data support from the Soil Data Center, National Earth System Science Data Sharing Service Infrastructure, National Science & Technology Infrastructure of China (<http://soil.geodata.cn>) and Ente Regionale per i Servizi all'Agricoltura e alle Foreste – Regione Lombardia of Italy (<https://www.ersaf.lombardia.it/>). We are indebted to the staff at the Rice Research Centre in Castello d'Agogna (Pavia, Italy) for help with soil sampling and mesocosm rice cultivation, including

Sergio Feccia, Fabio Mazza, Umberto Rolla, Eleonora Miniotti, Gianluca Beltarre, Angela Iuzzolino, Francesca Bonassi, Luca Pizzin, Daniele Tenni, Andrea Zanellato, Federico Massara, Edoardo Magnani, Gianluca Bertone, and Massimo Zini. We thank Cyrille Thomas and Arnaud Boissard from the Centre Français du Riz (Arles, Italy) for assistance with soil sampling in France. We are grateful to Michael T.F. Wagner, Cristina Lerda, Stefan Will, José Miguel Leon, Johannes Besold, Laura Wegner and Shuai Zhang for help with field sampling and laboratory assistance, to Yuying Yang for help with map design, and to Judith Mehlhorn for help with statistical analyses.

AUTHOR CONTRIBUTIONS

JW initiated DTPA method development, conceived and performed all mesocosm and incubation experiments including analyses, evaluated the results and contributed to manuscript preparation, CK contributed to field survey, sample analyses, data evaluation, and manuscript preparation, LB contributed to DTPA method development, PH & LW initiated the Chinese soil survey and advised on incubation experiments, PH, TM, GW & LW sampled and characterized the Chinese soils, MR assisted in design, setup and operation of mesocosms and sample collection, MM & DSP assisted in analyses of aqueous parameters from mesocosms, MM contributed to field survey and data discussion, BPF initiated and supervised the project, carried out the field survey, conceived experiments, and wrote the manuscript; all authors contributed to revising the manuscript.

ADDITIONAL INFORMATION

Supplementary information is available. Correspondence and requests for materials should be addressed to B.P.-F.

REFERENCES Paper

1. Stone R. Arsenic and paddy rice: A neglected cancer risk? *Science* 2008, 321(5886): 184-185.
2. Ma JF, Yamaji N, Mitani N, Xu X-Y, Su Y-H, McGrath SP, et al. Transporters of arsenite in rice and their role in arsenic accumulation in rice grain. *Proceedings of the National Academy of Sciences* 2008, 105(29): 9931-9935.
3. Wang P, Zhang W, Mao C, Xu G, Zhao F-J. The role of OsPT8 in arsenate uptake and varietal difference in arsenate tolerance in rice. *Journal of Experimental Botany* 2016, 67(21): 6051-6059.
4. Ye Y, Li P, Xu T, Zeng L, Cheng D, Yang M, et al. OsPT4 contributes to arsenate uptake and transport in rice. *Frontiers in Plant Science* 2017, 8(2197).
5. Xu XY, McGrath SP, Meharg AA, Zhao FJ. Growing rice aerobically markedly decreases arsenic accumulation. *Environmental Science & Technology* 2008, 42(15): 5574-5579.
6. Jia Y, Huang H, Zhong M, Wang F-H, Zhang L-M, Zhu Y-G. Microbial arsenic methylation in soil and rice rhizosphere. *Environmental Science & Technology* 2013, 47(7): 3141-3148.
7. Lomax C, Liu WJ, Wu LY, Xue K, Xiong JB, Zhou JZ, et al. Methylated arsenic species in plants originate from soil microorganisms. *New Phytologist* 2012, 193(3): 665-672.
8. Zhao F-J, Zhu Y-G, Meharg AA. Methylated arsenic species in rice: geographical variation, origin, and uptake mechanisms. *Environmental Science & Technology* 2013, 47(9): 3957-3966.
9. Meharg AA, Zhao F-J. *Biogeochemistry of arsenic in paddy environments*. Arsenic & Rice. Springer, 2012, pp 71-101.
10. Besold J, Biswas A, Suess E, Scheinost AC, Rossberg A, Mikutta C, et al. Monothioarsenate Transformation Kinetics Determining Arsenic Sequestration by Sulfhydryl Groups of Peat. *Environmental Science & Technology* 2018, 52(13): 7317-7326.
11. Wallschläger D, London J. Determination of methylated arsenic-sulfur compounds in groundwater. *Environmental Science & Technology* 2007, 42(1): 228-234.
12. Conklin SD, Fricke MW, Creed PA, Creed JT. Investigation of the pH effects on the formation of methylated thio-arsenicals, and the effects of pH and temperature on their stability. *J Anal Atom Spectrom* 2008, 23(5): 711-716.
13. Planer-Friedrich B, London J, McCleskey RB, Nordstrom DK, Wallschläger D. Thioarsenates in geothermal waters of Yellowstone National Park: determination, preservation, and geochemical importance. *Environmental Science & Technology* 2007, 41(15): 5245-5251.
14. Planer-Friedrich B, Schaller J, Wismeth F, Mehlhorn J, Hug SJ. Monothioarsenate Occurrence in Bangladesh Groundwater and Its Removal by Ferrous and Zero-Valent Iron Technologies. *Environmental Science & Technology* 2018, 52(10): 5931-5939.
15. Planer-Friedrich B, Wallschläger D. A critical investigation of hydride generation-based arsenic speciation in sulfidic waters. *Environmental Science & Technology* 2009, 43: 5007-5013.
16. Smieja JA, Wilkin RT. Preservation of sulfidic waters containing dissolved As(III). *J Environ Monitor* 2003, 5(6): 913-916.
17. Kogel-Knabner I, Amelung W, Cao ZH, Fiedler S, Frenzel P, Jahn R, et al. *Biogeochemistry of paddy soils*. *Geoderma* 2010, 157(1-2): 1-14.
18. Wind T, Conrad R. Localization of sulfate reduction in planted and unplanted rice field soil. *Biogeochemistry* 1997, 37(3): 253-278.
19. Ayotade KA. Kinetics and reactions of hydrogen sulphide in solution of flooded rice soils. *Plant and Soil* 1977, 46(2): 381-389.
20. Saalfield SL, Bostick BC. Changes in iron, sulfur, and arsenic speciation associated with bacterial sulfate reduction in ferrihydrite-rich systems. *Environmental Science & Technology* 2009, 43(23): 8787-8793.
21. Burton ED, Johnston SG, Kocar BD. Arsenic mobility during flooding of contaminated soil: the effect of microbial sulfate reduction. *Environmental Science & Technology* 2014, 48(23): 13660-13667.
22. Xu LY, Wu X, Wang SF, Yuan ZD, Xiao F, Ming Y, et al. Speciation change and redistribution of arsenic in

soil under anaerobic microbial activities. *Journal of Hazardous Materials* 2016, 301: 538-546.

23. Crusciol CAC, Nascente AS, Soratto RP, Rosolem CA. Upland rice growth and mineral nutrition as affected by cultivars and sulfur availability. *Soil Science Society of America Journal* 2013, 77(1): 328-335.

24. Schütz H, Holzapfel-Pschorn A, Conrad R, Rennenberg H, Seiler W. A 3-year continuous record on the influence of daytime, season, and fertilizer treatment on methane emission rates from an Italian rice paddy. *Journal of Geophysical Research: Atmospheres* 1989, 94(D13): 16405-16416.

25. Minamikawa K, Sakai N, Hayashi H. The effects of ammonium sulfate application on methane emission and soil carbon content of a paddy field in Japan. *Agriculture, Ecosystems & Environment* 2005, 107(4): 371-379.

26. Fan J, Xia X, Hu Z, Ziadi N, Liu C. Excessive sulfur supply reduces arsenic accumulation in brown rice. *Plant, Soil and Environment* 2013, 59(4): 169-174.

27. Zhang J, Zhao C-Y, Liu J, Song R, Du Y-X, Li J-Z, et al. Influence of sulfur on transcription of genes involved in arsenic accumulation in rice grains. *Plant Molecular Biology Reporter* 2016, 34(3): 556-565.

28. Jia Y, Bao P. Arsenic bioavailability to rice plant in paddy soil: influence of microbial sulfate reduction. *Journal of Soils and Sediments* 2015, 15(9): 1960-1967.

29. Zeng X, Jiang Y, Fan X, Chao S, Yang Y, Liu J, et al. Effects of sulfate application on inhibiting accumulation and alleviating toxicity of arsenic in panax notoginseng grown in arsenic-polluted soil. *Water, Air, & Soil Pollution* 2016, 227(5): 148.

30. Baker M, Inniss W, Mayfield C, Wong P, Chau Y. Effect of pH on the methylation of mercury and arsenic by sediment microorganisms. *Environmental Technology Letters* 1983, 4(2): 89-100.

31. Cullen WR, Liu Q, Lu X, McKnight-Whitford A, Peng H, Popowich A, et al. Methylated and thiolated arsenic species for environmental and health research — A review on synthesis and characterization. *Journal of Environmental Sciences* 2016, 49: 7-27.

32. Kim Y-T, Lee H, Yoon H-O, Woo NC. Kinetics of dimethylated thioarsenicals and the formation of highly toxic dimethylmonothioarsinic acid in environment. *Environmental Science & Technology* 2016.

33. Kerl CF, Rafferty C, Clemens S, Planer-Friedrich B. Monothioarsenate Uptake, Transformation, and Translocation in Rice Plants. *Environmental Science & Technology* 2018, 52(16): 9154-9161.

34. Kerl CF, Schindele RA, Brüggewirth L, Colina Blanco AE, Rafferty C, Clemens S, et al. Methylated thioarsenates and monothioarsenate differ in uptake, transformation, and contribution to total arsenic translocation in rice plants. *Environmental Science & Technology* 2019, 53(10): 5787-5796.

35. Ackerman AH, Creed PA, Parks AN, Fricke MW, Schwegel CA, Creed JT, et al. Comparison of a chemical and enzymatic extraction of arsenic from rice and an assessment of the arsenic absorption from contaminated water by cooked rice. *Environmental Science & Technology* 2005, 39(14): 5241-5246.

36. Ayotade KA. Kinetics and reactions of hydrogen-sulfide in solution of flooded rice soils. *Plant Soil* 1977, 46(2): 381-389.

REFERENCES Methods

1. Kerl CF, Schindele RA, Brüggewirth L, Colina Blanco AE, Rafferty C, Clemens S, et al. Methylated thioarsenates and monothioarsenate differ in uptake, transformation, and contribution to total arsenic translocation in rice plants. *Environmental Science & Technology* 2019, 53(10): 5787-5796.

2. Kerl CF, Rafferty C, Clemens S, Planer-Friedrich B. Monothioarsenate uptake, transformation, and translocation in rice plants. *Environmental Science & Technology* 2018, 52(16): 9154-9161.

3. Wallschläger D, London J. Determination of methylated arsenic-sulfur compounds in groundwater. *Environmental Science & Technology* 2007, 42(1): 228-234.

4. Planer-Friedrich B, London J, McCleskey RB, Nordstrom DK, Wallschläger D. Thioarsenates in geothermal waters of Yellowstone National Park: determination, preservation, and geochemical importance. *Environmental Science & Technology* 2007, 41(15): 5245-5251.

5. Besold J, Biswas A, Suess E, Scheinost AC, Rossberg A, Mikutta C, et al. Monothioarsenate Transformation Kinetics Determining Arsenic Sequestration by Sulfhydryl Groups of Peat. *Environmental Science & Technology* 2018, 52(13): 7317-7326.

6. Planer-Friedrich B, Schaller J, Wismeth F, Mehlhorn J, Hug SJ. Monothioarsenate occurrence in bangladesh groundwater and its removal by ferrous and zero-valent iron technologies. *Environmental Science & Technology* 2018, 52(10): 5931-5939.

7. Planer-Friedrich B, Wallschläger D. A critical investigation of hydride generation-based arsenic speciation in sulfidic waters. *Environmental Science & Technology* 2009, 43(13): 5007-5013.

8. Tang L, Yang J, Shen X. Effects of additional iron-chelators on Fe 2+-initiated lipid peroxidation: Evidence to support the Fe 2+... Fe 3+ complex as the initiator. *Journal of Inorganic Biochemistry* 1997, 68(4): 265-272.

9. Colman BP. Understanding and eliminating iron interference in colorimetric nitrate and nitrite analysis. *Environmental Monitoring and Assessment* 2010, 165(1-4): 633-641.

10. Suess E, Wallschläger D, Planer-Friedrich B. Stabilization of thioarsenates in iron-rich waters. *Chemosphere* 2011, 83(11): 1524-1531.

11. Zang V, Van Eldik R. Kinetics and mechanism of the autoxidation of iron (II) induced through chelation by ethylenediaminetetraacetate and related ligands. *Inorganic Chemistry* 1990, 29(9): 1705-1711.

12. Suess E, Scheinost AC, Bostick BC, Merkel BJ, Wallschläger D, Planer-Friedrich B. Discrimination of thioarsenites and thioarsenates by X-ray absorption spectroscopy. *Analytical Chemistry* 2009, 81(20): 8318-8326.

13. The Ministry of Ecology and Environment. Soil Environment Quality Risk Control Standard for Soil Contamination of Agriculture Land GB 15618-2018 2018.

14. Zhao F-J, Ma Y, Zhu Y-G, Tang Z, McGrath SP. Soil contamination in China: current status and mitigation strategies. *Environmental Science & Technology* 2014, 49(2): 750-759.

15. Ratering S, Schnell S. Localization of iron-reducing activity in paddy soil by profile studies. *Biogeochemistry* 2000, 48(3): 341-365.
16. Stroud JL, Khan MA, Norton GJ, Islam MR, Dasgupta T, Zhu Y-G, et al. Assessing the labile arsenic pool in contaminated paddy soils by isotopic dilution techniques and simple extractions. *Environmental Science & Technology* 2011, 45(10): 4262-4269.
17. Zhang S-Y, Zhao F-J, Sun G-X, Su J-Q, Yang X-R, Li H, et al. Diversity and abundance of arsenic biotransformation genes in paddy soils from Southern China. *Environmental Science & Technology* 2015, 49(7): 4138-4146.
18. Zhao F-J, Harris E, Yan J, Ma J, Wu L, Liu W, et al. Arsenic methylation in soils and its relationship with microbial *arsM* abundance and diversity, and As speciation in rice. *Environmental Science & Technology* 2013, 47(13): 7147-7154.
19. Stookey LL. Ferrozine - A new spectrophotometric reagent for iron. *Analytical chemistry* 1970, 42(7): 779-781.
20. Lohmayer R, Kappler A, Lösekann-Behrens T, Planer-Friedrich B. Role of sulfur species as redox partners and electron shuttles for ferrihydrite reduction by *Sulfurospirillum deleyianum*. *Applied and Environmental Microbiology* 2014: AEM. 04220-04213.
21. Grömping U. Relative importance for linear regression in R: the package relaimpo. *Journal of Statistical Software* 2006, 17(1): 1-27.
22. De'Ath G. Multivariate regression trees: a new technique for modeling species-environment relationships. *Ecology* 2002, 83(4): 1105-1117.

Supporting information

Thiolated arsenic species observed in rice paddy pore-waters

Jiajia Wang¹, Carolin F. Kerl¹, Pengjie Hu², Maria Martin³, Tingting Mu², Lena Brüggewirth¹, Guangmei Wu², Daniel Said-Pullicino³, Marco Romani⁴, Longhua Wu² and Britta Planer-Friedrich^{1*}

¹Environmental Geochemistry, Bayreuth Center for Ecology and Environmental Research (BayCEER), University of Bayreuth, 95440 Bayreuth, Germany.

²Key Laboratory of Soil Environment and Pollution Remediation, Institute of Soil Science, Chinese Academy of Sciences, 210008 Nanjing, China

³Department of Agriculture, Forest and Food Sciences, University of Turin, 10124 Turin, Italy

⁴Rice Research Centre, Ente Nazionale Risi, 27030 Castello d'Agogna, Pavia, Italy

*Phone: +49 921 55 3999. E-mail: b.planer-friedrich@uni-bayreuth.de.

Number of pages: 52

Number of figures: 20

Number of Tables: 9

1. Thioarsenates discovered in planted paddy fields in Italy and France

Methods. For an initial field survey, we sampled 23 different paddy fields in Italy (17 fields) and France (6 fields) (all located in the Mediterranean climate zone, for coordinates see Table S1) during the cropping season in August 2016 when the rice plants were in the flowering to grain filling stage. Sampling in Italy covered most of the rice cropping areas of the river Po plain, where the majority of the Italian rice is produced. The paddy fields were located in the alluvial plain, the river valley, and the lower river plain. All Italian soils developed on recent clastic deposits with mixed lithology (e.g., noncalcareous gravels, silty sands), and are mostly classified as luvisols, gleysols, and a few fluvisols and cambisols (Soil Atlas of Europe, <https://esdac.jrc.ec.europa.eu/content/soil-atlas-europe>). Paddy fields in France covered the whole extent of the only rice cultivation area in France which is located in the coastal plain of the Camargue region, in the delta of the river Rhone. The soils there developed on recent deposits of the Rhone river and are classified as gleyic fluvisols. In total, 35 pore-water samples were collected. At most paddy fields only one pore water sample was taken, at five paddy soils we took replicates. Pore-water was extracted by micro rhizon samplers (Rhizon MOM, Rhizosphere Research Products, The Netherlands) inserted about 3-4 cm deep into the paddy soil and connected to evacuated 100 mL glass bottles. The bottles were first sealed with a butyl rubber septum in an anoxic glovebox (N_2/H_2 95/5% (v/v)), then evacuated to negative atmospheric pressure of ~900 mbar. During sampling, glass bottles were shielded with aluminum foil to avoid potential photooxidation ¹. To retrieve enough volume (minimum 10 mL) for all analyses, minimum sampling time was 4 hours, maximum sampling time up to 24 hours. After retrieving the pore water samples, one soil sample from the plow layer was collected at each site.

After collection, pore-water samples were filtered through 0.2 μ m cellulose-acetate filters. Samples for As speciation analysis were immediately flash-frozen on dry ice, and stored at -20 °C before being analyzed by ion chromatography (IC, Dionex ICS-3000) coupled to inductively coupled plasma-mass spectrometry (ICP-MS, XSeries2, Thermo-Fisher) at Bayreuth University following a previously established method for analysis of inorganic and methylated thioarsenates ².

Retention times of the As species were verified by comparison with commercial standards (arsenite (NaAsO_2 , Fluka), arsenate ($\text{Na}_2\text{HAsO}_4 \times 7\text{H}_2\text{O}$, Fluka), MMA ($\text{CH}_3\text{AsNa}_2\text{O}_3 \times 6\text{H}_2\text{O}$, Supelco), DMA ($\text{C}_2\text{H}_6\text{AsNaO}_2 \times 3\text{H}_2\text{O}$, Sigma-Aldrich)), standards synthesized according to previously published methods (DMMTA (purity 67%; 28% DMDTA, 5% DMA) and MMMTA (purity 96%; 1% MMA, 3% MMDTA)³, MTA (purity of 98.5%; 0.5% arsenite, 1% arsenate)⁴ or by comparison with previously published⁵ retention times (MMDTA, DMDTA, DTA, TTA). Calibration standard solutions were made from arsenate dibasic-heptahydrate, sodium (meta)arsenite, disodium methyl arsonate hexahydrate, and dimethylarsinic acid. All other As species were quantified by peak area comparison to the standard closest in retention time. Validity of this method has been proven previously².

An example of the chromatographic separation of the different As species is reported in Fig. S1. Samples for total As and Fe were acidified in 0.5% H_2O_2 and 0.8% HNO_3 and kept at 4°C until analysis by ICP-MS. Samples for zero-valent S were stabilized with zinc acetate (25 μL of 200 g/L ZnAc + 725 μL sample), kept at 4°C until extraction by chloroform in the laboratory, then measured with high performance liquid chromatography (HPLC) (Merck Hitachi L-2130 pump, L-2200 autosampler, and L-2420 UV-VIS detector; C18 column, 100% methanol eluent at 0.2 mL/min) as described before⁶. Sulfide was measured photometrically on-site using the methylene blue method (HACH procedure No. 8131). Redox potential, pH, and conductivity were measured directly on-site by a WinLab redox micro-electrode, a WinLab 423 combination pH electrode, and a Mettler Toledo TetraCon 325 electrode.

Soil samples were analyzed for soil pH (measured in 2.5 mL 0.1 M CaCl_2 solution with 1 g soil), 0.5 M HCl-extractable Fe, total C and N (CHN analyzer), and total As and S (determination by ICP-MS after microwave digestion in aqua regia).

Results. Soil pH ranged from 5.0-6.1 and 7.5-7.6, total soil As contents from 5.2-16 and 10.4-20.2 mg/kg, HCl-extractable Soil Fe contents from 50-198 and 105-181 mmol/kg, and total C from 0.8-4.7 and 4.5-6.0 %, for the Italian and French paddy soils, respectively (Table S1a). Thioarsenates were determined in 23 out of 35 pore-water samples and in 14 out of 23 different fields (Table S1b). The contribution of total thiolation to total As concentrations was 8.3% at maximum and 2.1% on average. These numbers are comparable to those observed for the much more-commonly-investigated methylated oxyarsenates which we detected in 31 samples from 20 fields

(max. 10.4%, on average 1.3%). Inorganic thioarsenates (monothioarsenate (MTA) and dithioarsenate (DTA)) were detected in 11 samples (max. 7.4%, on average 3.2%) and methylated thioarsenates (monomethylmonothioarsenate (MMMTA), DMMTA, dimethyldithioarsenate (DMDTA)) in 18 samples (max. 2.9%, on average 0.7%). Seven samples taken within the same paddy field (Veronica, Table S1b) showed large heterogeneity in the proportion of thioarsenates (2.9-8.3%) without any obvious relation to pore-water chemistry, such as dissolved sulfide concentrations (Table S1b). Inorganic thioarsenates were observed in large quantities only at pore-water Fe concentrations < 0.5 mmol/L suggesting that Fe concentrations above a threshold value could limit their formation (Fig. S2a). Methylated thioarsenates, in contrast, occurred over a wider range of dissolved Fe concentrations (Fig. S2b) and Spearman's correlation test showed positive correlation with methylated oxyarsenates ($r = 0.60$, $P < 10^{-4}$; Fig. S2b, S2c, S3). There was no correlation between inorganic and methylated thioarsenates.

For these first field surveys, we used relatively long pore-water sampling times (4-24 hours) to obtain enough volume for analyses (minimum 10 mL) and, for species preservation, we used just flash-freezing, without adding stabilizing agents. Even though all As chromatographic peaks were clearly distinguishable (Fig. S1), high Fe concentrations (up to 2.3 mmol/L) caused Fe precipitation and, by co-precipitation and sorption, low As recoveries (calculated as the sum of all detected As species in flash-frozen samples versus total As measured in oxidized and acid-stabilized samples; Fig. S4).

All species proportions are reported with respect to total As (not the sum of species). As such, a partial precipitation or sorption of thiolated As species on any Fe (hydr)oxides ⁷ formed during sample storage could have contributed to an underestimation of the true proportions reported here.

For all later analyses, short sampling times (0.5-1 hour) and an optimized DTPA-sample stabilization and analysis were chosen. For details on the DTPA method development and evaluation see main manuscript and Fig. S15-S18.

Table S1a | Coordinates and basic soil chemistry from 17 Italian paddy fields (IT) and 6 French paddy fields (FR)

Paddy fields	Longitude	Latitude	Soil pH	HCl extractable soil Fe		total soil As		total soil S		total soil C	
				mmol/kg	mg/kg	mg/kg	g/kg	g/kg	%		
ITALY											
IT_Vignarello	8°44'42.82"	45°20'39.77"	5.5	62.6	8.9	3.4	2.0				
IT_Barbavara	8°47'09.49"	45°21'19.41"	5.5	67.6	10.5	3.2	2.7				
IT_Gambarana	8°46'30.88"	45°01'38.88"	5.8	197.7	16.0	6.0	1.4				
IT_Breme	8°37'06.19"	45°08'38.34"	5.8	177.0	13.8	5.4	1.3				
IT_Langosco	8°32'43.84"	45°12'34.24"	5.7	165.5	12.9	8.4	1.3				
IT_Vercelli	8°15'12.88"	45°18'36.59"	5.7	75.9	11.4	9.5	1.1				
IT_Cascina Oschiena	8°45'03.84"	45°18'36.58"	5.7	109.9	6.1	4.2	1.3				
IT_Fontanetto Po	8°11'59.46"	45°12'15.50"	6.0	144.9	9.1	4.8	3.4				
IT_Terranova	8°30'02.95"	45°11'53.56"	6.1	125.3	11.8	5.3	1.4				
IT_Rovasenda	8°16'40.00"	45°32'34.05"	5.8	97.2	14.3	4.3	1.0				
IT_Cascina Albera	8°56'48.18"	45°10'49.49"	5.8	52.0	5.9	2.7	1.4				
IT_Lomello	8°47'55.87"	45°07'26.71"	5.0	120.6	8.9	4.1	1.4				
			5.6	90.2	7.3	3.9	1.5				
IT_Cascina Fornazzo	8°57'49.97"	45°13'53.76"	5.8	71.7	5.6	3.2	4.7				
IT_Cascina Veronica	8°53'47.60"	45°10'39.30"	5.6	50.0	5.2	2.2	2.1				
			5.5	53.0	5.8	2.6	2.0				
			5.4	50.6	5.8	2.4	1.9				
IT_Castello d'Agogna (ENR) field 1	8°41'56.50"	45°14'51.30"	5.5	145.9	16.0	4.3	0.9				
			5.5	152.3	15.6	4.3	0.8				
IT_Castello d'Agogna (ENR) field 2			5.5	146.7	15.2	4.4	0.8				
			5.5	144.1	15.6	4.2	0.8				
IT_Castello d'Agogna (ENR) field 3			5.6	181.0	15.8	4.2	0.9				
			5.5	159.3	14.9	4.2	0.9				

FRANCE									
FR_Seyne	4°42'57.24"	43°34'23.63"	7.5	166.0	18.2	22.1	5.4		
FR_Vedeau	4°42'24.53"	43°26'04.63"	7.6	143.0	14.7	23.1	6.0		
FR_Adrien	4°33'40.93"	43°42'07.42"	7.5	109.5	10.4	18.0	4.9		
FR_Furane	4°31'06.35"	43°41'11.58"	7.5	134.1	20.2	19.8	4.9		
FR_Boismeaux	4°28'14.10"	43°35'54.44"	7.5	138.9	13.1	18.8	4.5		
FR_Signore	4°29'46.35"	43°37'10.51"	7.6	104.7	10.6	22.6	5.2		

Table S1b | Pore water chemistry including As speciation for samples from 17 Italian paddy fields (IT) and 6 French paddy fields (FR)

Paddy fields	pore water pH		E _H mV	Conductivity µS/cm	Sulfide µmol/L	Zerovalent sulfur mmol/L	Fe mmol/L	DMA	DMMTA _a	Arsenite	DMDTA ^b	MMA	MMMTA ^c	Arsenate	MTA ^d	DTA ^e	Total Thiolated As	Sum As species	Total As
ITALY																			
IT_Vignarello	6.1	194	310	<0.3	4.6	0.3	0.2	2.8	1.0									3.9	38.1
IT_Barbavara	6.6	184	305	<0.3	2.4	0.2	0.04	0.5	0.2									0.7	10.6
IT_Gambarana	6.9	71	1154	<0.3	<1	0.3	0.1	3.1	2.5			0.3						6.1	86.2
IT_Breme	6.6	-21	1340	<0.3	4.3	2.6	0.4	1.1	0.2	0.3		0.4					0.2	2.4	82.0
IT_Langosco	6.4	145	575	<0.3	5.4	0.9	0.2	0.5	0.2	0.2		0.1					0.3	1.3	37.3
IT_Vercelli	6.3	339	209	<0.3	<1	0.0		1.9	1.6									3.4	7.8
IT_Cascina Oschiena	6.5	72	1092	1.2	<1	1.5		0.1	0.5								0.1	0.9	68.2
IT_Fontanetto Po	7.0	377	1831	1.2	<1	<0.1	0.1	2.7	1.0			0.1						3.9	9.0
IT_Terranova	7.0	68	2490	1.3	5.8	0.2	1.5	11.8	2.3								0.1	15.8	84.2
IT_Rovasenda	6.6	116	370	1.2	<1	0.1	0.6	0.1	0.4								0.1	1.4	6.0
IT_Cascina Albera	6.7	93	315	1.8	1.2	0.6	0.1	1.4	0.3								0.04	1.8	31.3
IT_Lomello	6.8	92	280	0.9	2.7	0.1		1.4	0.4									1.8	25.9
	7.0	97	362	<0.3	5.2	0.0	0.2	2.6	2.3			0.1					0.2	5.5	15.2
IT_Cascina Fornazzo	7.1	98	673	<0.3	5.2	0.3	0.5	1.3	0.5	0.1		0.2					0.8	3.3	14.9
IT_Cascina Veronica	6.4	90	541	<0.3	<1	0.5	0.6	1.8	0.4	0.4		0.1					1.2	4.4	28.2
	6.2	122	341	<0.3	<1	0.3		0.9	0.1								0.5	2.1	9.1
	6.4	83	n.a	3.0	<1	0.3		1.6	3.8			0.04					0.8	6.2	17.7

Paddy fields	pore water pH		E _H mV	Conductivity µS/cm	Sulfide		Zerivalent sulfur	Fe mmol/L	DMA	DMMTAa	Arsenite	DMDTA ^b	MMA	MMMTA ^c	Arsenate	MTA ^d	DTA ^e	Total Thiolated As	Sum As species	Total As
	µmol/L	µmol/L			µmol/L	mmol/L														
IT_Cascina Veronica	6.3	117	285	1.1	<1	0.3					2.8		0.2	0.1	1.8	0.3	0.6	1.0	5.8	11.9
	n.a.	n.a.	n.a.	<0.3	<1	0.3					2.3		0.1		6.9	0.5	0.2	0.8	10.1	20.6
	6.5	169	n.a.	<0.3	1.8	0.3					0.7		0.05		1.2	0.2	0.3	0.5	2.4	8.0
	6.2	105	400	<0.3	<1	0.3	0.03				0.4		0.1		0.7	0.1	0.1	0.2	1.5	7.1
IT_Castello d'Agogna (ENR) field 1	6.8	-13	1183	1.0	1.5	1.8	0.1	0.3	0.6	0.6	0.6		0.5		0.1			0.3	1.6	105.4
	6.6	85	723	<0.3	<1	0.8	0.1		0.6	0.6	0.6				0.3				1.0	44.4
IT_Castello d'Agogna (ENR) field 2	6.7	83	n.a.	1.1	2.4	0.6	0.1	0.03	0.7	0.7	0.7				0.2			0.03	1.0	30.0
	6.8	1	1346	1.0	<1	1.8	0.1	0.1	0.5	0.5	0.5		0.3	0.1	0.1			0.2	1.2	58.5
	6.8	44	1181	<0.3	<1	0.8	0.2	0.1	0.5	0.5	0.5		0.5	0.2	0.1			0.3	1.6	24.8
	6.7	70	890	<0.3	<1	1.2	0.1	0.1	0.4	0.4	0.4		0.2		0.1			0.1	0.9	36.7
IT_Castello d'Agogna (ENR) field 3	6.7	83	792	<0.3	3.8	0.7	0.1		1.2	1.2	1.2		0.1		0.2				1.6	45.4
	6.8	117	364	<0.3	2.8	0.3	0.1		2.0	2.0	2.0				0.6				2.6	47.1
FRANCE																				
FR_Seyne	7.2	37	1030	<0.3		0.5			1.9		1.9				0.2				2.1	72.8
FR_Vedeau	6.8	32	2200	<0.3		0.7	1.4		6.7		6.7				0.5				8.6	165.2
FR_Adrien	7.3	91	1340	<0.3		0.2	0.2	0.1	21.9		21.9		0.04		2.8	0.2	0.1	0.4	25.3	86.7
FR_Furane	7.2	-16	1854	<0.3		1.4	1.0	0.1	11.7		11.7				2.5			0.1	15.3	335.2
FR_Boisemeaux	7.3	16	2010	<0.3		1.2	1.1	0.4	16.8		16.8	0.1	0.9	0.2	2.5	0.1		0.8	22.2	268.3
FR_Signore	7.5	37	1509	<0.3		0.6	0.3		4.4		4.4		0.1		0.4				5.3	69.5

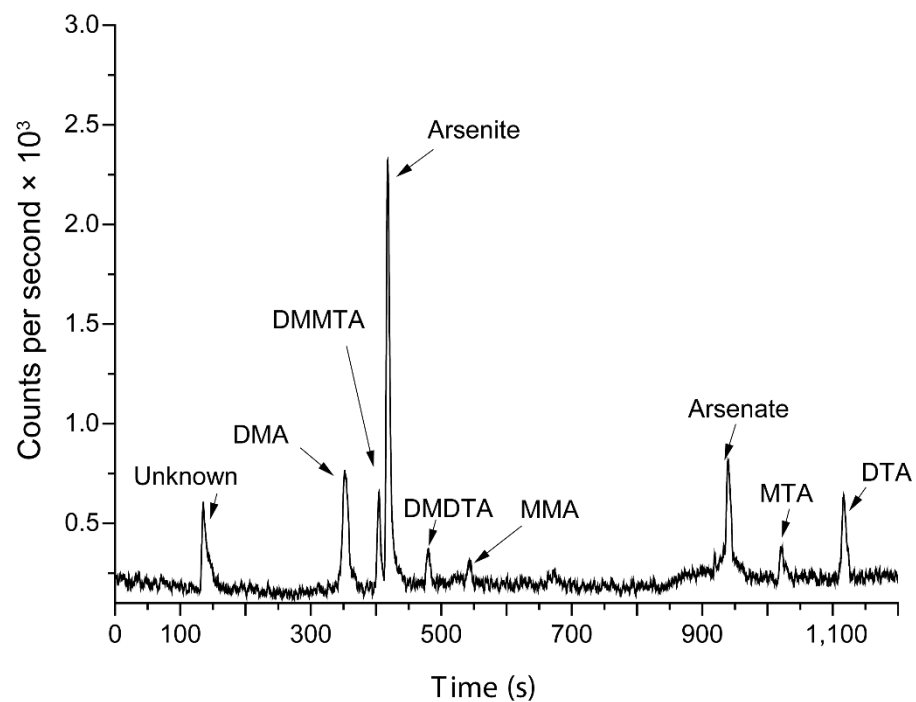


Figure S1 | Example chromatogram for determination of inorganic and methylated thio and oxy As species in paddy field pore-water by IC-ICP-MS. The presented sample is IT_Cascina Veronica (pH 6.36, Table S1).

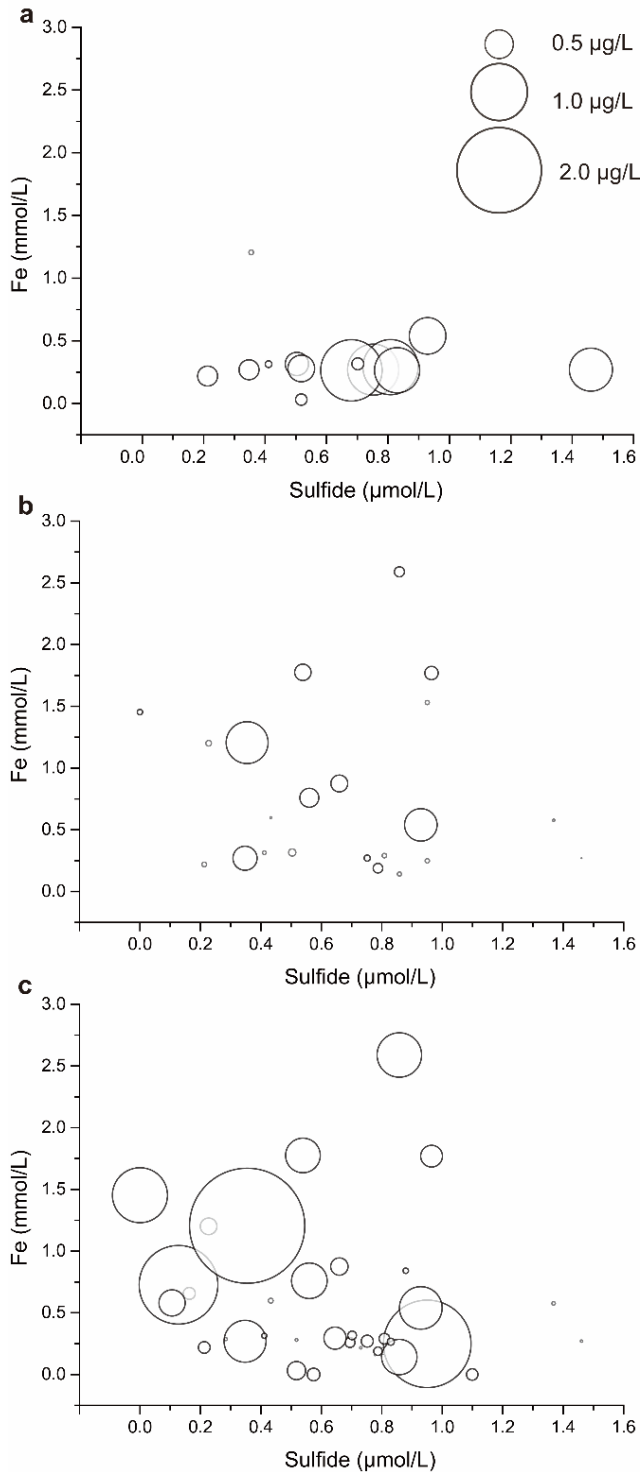


Figure S2 | Arsenic speciation in paddy field pore-waters from Italy and France in relation to aqueous Fe and sulfide. Contribution of a) inorganic thioarsenates, b) methylated thioarsenates and c) methylated oxyarsenates to total As; bubble size represents concentration of As species; bubbles are only displayed where concentrations of As species were above detection limit.

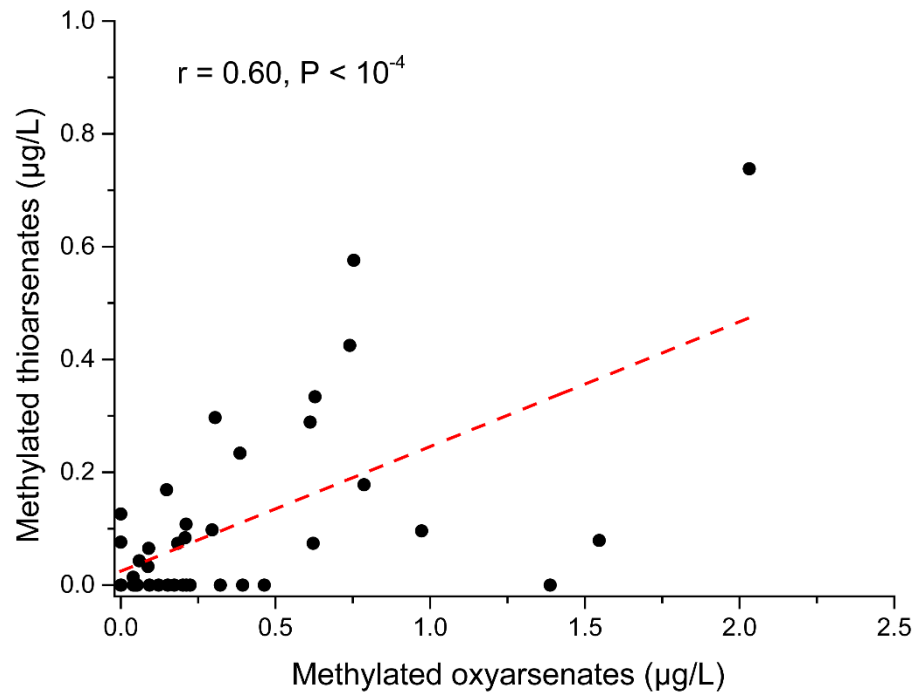


Figure S3 | Correlation of methylated thioarsenates with methylated oxyarsenates in paddy field pore-waters from Italy and France.

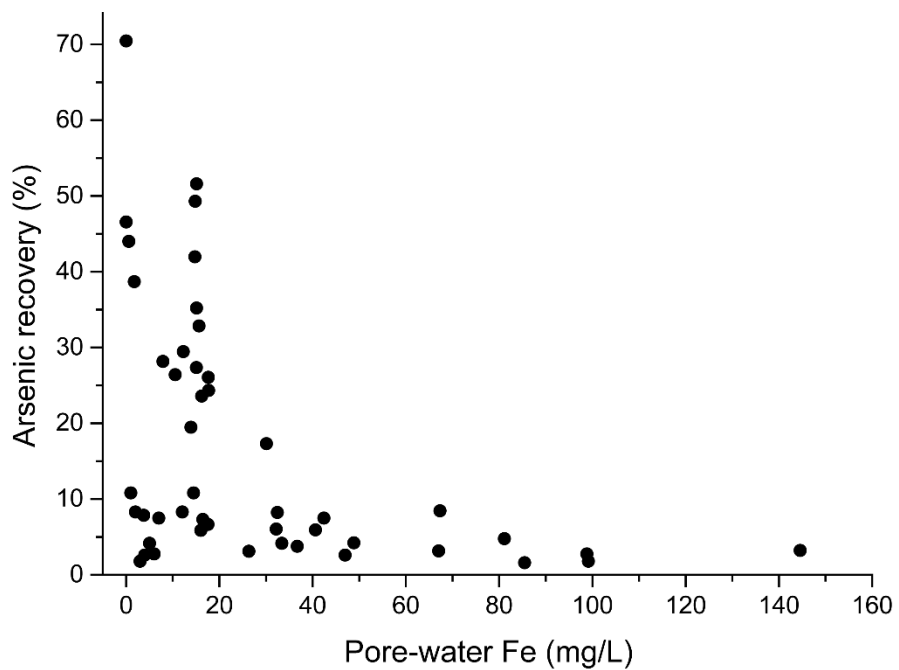


Figure S4 | Effect of Fe on As recovery for samples from paddy fields in Italy and France. Arsenic recovery is calculated as sum of As species from flash-frozen samples versus total As in H₂O₂-HNO₃-stabilized samples.

2. Mesocosm rice cultivation experiments – effects of sulfate-fertilization, seeding-practice, and soil type on thioarsenate formation

Looking at the pore-water total As concentrations during rice cultivation in the mesocosm experiments (Fig 2), one can see that over time, pore-water total As concentrations in control treatments decreased from approximately 100 and 50 $\mu\text{g/L}$ at tillering stage in the dry and water seeded mesocosms, respectively, to $<20 \mu\text{g/L}$ around flowering stage (except for the dry seeded Veronica soil where concentrations only dropped after the dough stage, Fig. 2e, f). Highest pore-water As concentrations occurred within days after flooding due to rapid As mobilization by reductive dissolution of Fe(III)-(oxy)hydroxides, and then decreased due to As re-adsorption on or precipitation with newly formed Fe minerals in line with previous reports ^{8,9}. The higher As concentrations in dry vs. water seeded treatments at the same sampling date could be explained by an overall less As mobilization in water seeded treatments because they are flooded in May when microbially catalyzed As mobilization is still partially limited by lower temperatures while flooding of dry seeded treatments in June leads to higher As mobilization due to enhanced microbial activity. In addition, the difference could reflect the time it takes for As concentrations after flooding and initial mobilization to drop again due to re-adsorption and precipitation reactions (4 weeks later in dry than in water seeded treatments). No clear trend in the proportion of inorganic or methylated thioarsenates was observed over time (Fig. 2a-d).

Table S2 | Soil classification and basic chemical parameters for Veronica and Fornazzo soil

Parameters	Veronica	Fornazzo
Geology/geomorphology	Lower river plain	Valley of the Ticino river
Parent material	Pleistocene alluvium	Olocene alluvium
Soil classification		
	Aeric Endoaquepts coarse-loamy over sandy, mixed, mesic	Histic Humaquepts coarse- loamy, mixed, mesic
USDA		
FAO	Eutric Gleysoil	Umbric Gleysoil
Texture		
gravel (%weight)	nd	23.9
clay %	2.1	1.4
fine silt %	11.5	6.2
coarse silt %	8.8	6.8
fine sand %	18.2	23.7
coarse sand %	59.3	61.8
Cation exchange capacity (cmol /kg)	9.52	14.39
Base saturation (%)	0.24	0.24
Effective base saturation (%)	0.84	0.91
soil pH	5.6	5.8
0.5 M HCl-extractable Fe (mmol/kg)	52	71
Oxalate-extracted Fe (mmol/kg)	9.9	19.2
C (%)	2.0	4.7
N (%)	0.6	0.5
Total As (mg/kg)	5.8	5.6
Oxalate-extracted As (mg/kg)	1.4	1.5
S (g/kg)	2.6	3.2

Table S3 | Pore water chemistry at different rice growing stages in the mesocosm experiments (2017) separated by soil type, fertilization (non-sulfate/sulfate), and seeding practice (dry-seeding/wet-seeding) (n=3)

Pore water parameters	Soil type & Seeding practice	Fertilization	Jun 14 th	Jul 4 th	Jul 18 th	Aug 1 th	Aug 8 th	Aug 22 th	Sep 13 th
			Tillering	Stem elongation	Booting	Flowering	Grain filling	Dough	Mature
pH	Veronica	non-sulfate	6.9 ± 0.1	6.8 ± 0.1	6.7 ± 0.2	6.5 ± 0.1	6.5 ± 0.1	6.8 ± 0.1	6.8 ± 0.1
			6.9 ± 0.1	6.9 ± 0.2	6.6 ± 0.1	6.8 ± 0.1	6.7 ± 0.1	7.1 ± 0.1	6.8 ± 0.2
	dry-seeding	non-sulfate	6.8 ± 0.3	6.5 ± 0.4	6.5 ± 0.1	6.4 ± 0.1	6.5 ± 0.1	6.8 ± 0.3	6.6 ± 0.1
			6.8 ± 0.2	6.9 ± 0.1	6.7 ± 0.1	6.7 ± 0.1	6.8 ± 0.2	7.0 ± 0.1	6.8 ± 0.1
	Fornazzo	non-sulfate	7.2 ± 0.2	7.3 ± 0.1	7.2 ± 0.1	7.1 ± 0.1	7.2 ± 0.1	7.2 ± 0.2	7.3 ± 0.2
			7.0 ± 0.1	7.1 ± 0.1	6.9 ± 0.1	7.1 ± 0.1	7.1 ± 0.1	7.5 ± 0.1	7.1 ± 0.1
	dry-seeding	non-sulfate	7.0 ± 0.1	7.0 ± 0.3	7.2 ± 0.1	7.0 ± 0.1	7.1 ± 0.1	7.2 ± 0.1	7.4 ± 0.1
			7.2 ± 0.1	7.2 ± 0.2	7.3 ± 0.1	7.0 ± 0.04	7.1 ± 0.1	7.3 ± 0.1	7.4 ± 0.1

E_H (mV)	Veronica									
	water-seeding	non-sulfate	181 ± 85	168 ± 62	185 ± 56	122 ± 5	161 ± 9	179 ± 19	160 ± 26	
		sulfate	123 ± 25	131 ± 36	159 ± 24	92 ± 16	121 ± 11	149 ± 18	126 ± 16	
	dry-seeding	non-sulfate	212 ± 44	163 ± 9	162 ± 11	180 ± 98	163 ± 5	165 ± 11	167 ± 24	
		sulfate	207 ± 59	135 ± 30	127 ± 47	89 ± 30	130 ± 17	131 ± 31	129 ± 16	
	Fornazzo									
	water-seeding	non-sulfate	181 ± 81	163 ± 15	148 ± 59	116 ± 19	103 ± 19	130 ± 36	118 ± 26	
		sulfate	96 ± 2	112 ± 50	87 ± 7	69 ± 10	77 ± 20	80 ± 11	84 ± 13	
	dry-seeding	non-sulfate	287 ± 6	211 ± 4	132 ± 43	111 ± 37	126 ± 11	135 ± 5	130 ± 29	
		sulfate	163 ± 61	143 ± 37	193 ± 75	109 ± 75	119 ± 35	146 ± 20	143 ± 51	
Conductivity (µS/cm)										
Veronica										
water-seeding	non-sulfate	533 ± 92	325 ± 30	504 ± 83	580 ± 54	777 ± 13	667 ± 263	601 ± 170		
	sulfate	745 ± 374	382 ± 165	455 ± 51	412 ± 34	493 ± 111	386 ± 59	567 ± 21		
dry-seeding	non-sulfate	805 ± 184	324 ± 41	554 ± 153	630 ± 52	835 ± 89	693 ± 38	651 ± 76		
	sulfate	614 ± 52	335 ± 72	434 ± 59	631 ± 424	414 ± 64	345 ± 37	478 ± 66		

Fornazzo										
	water-seeding	non-sulfate	956 ± 54	932 ± 94	1128 ± 95	1171 ± 118	1362 ± 120	1392 ± 211	1469 ± 223	
		sulfate	1026 ± 116	781 ± 32	922 ± 60	1038 ± 208	955 ± 64	1051 ± 147	1188 ± 10	
	dry-seeding	non-sulfate	723 ± 113	909 ± 63	1102 ± 24	1133 ± 49	1281 ± 37	1397 ± 125	1416 ± 130	
		sulfate	988 ± 124	846 ± 79	1483 ± 731	876 ± 119	841 ± 65	866 ± 69	1016 ± 102	
TIC (mg/L)^a										
Veronica										
	water-seeding	non-sulfate	14.16 ± 2.79	19.46 ± 1.75	15.65 ± 0.96	16.7 ± 2.62	10.42 ± 1.14	15.81 ± 5.37	20.44 ± 6.69	
		sulfate	15.78 ± 4.27	15.41 ± 4.62	20.33 ± 7.46	25.44 ± 5.94	33.57 ± 10.36	28.73 ± 3.37	31.52 ± 3.61	
	dry-seeding	non-sulfate	21.86 ± 8.47	18.01 ± 0.8	14.13 ± 0.9	12.77 ± 1.39	13.28 ± 9.72	10.48 ± 1.57	15.12 ± 0.65	
		sulfate	19.2 ± 1.69	22.34 ± 7.27	23.76 ± 6.24	25.16 ± 5.07	23.51 ± 5.28	24.81 ± 3.58	25.67 ± 3.73	
Fornazzo										
	water-seeding	non-sulfate	43.14 ± 12.93	88.92 ± 7.44	90.41 ± 8.63	100.94 ± 12.11	82.72 ± 7.89	96.99 ± 17.99	108.12 ± 22.39	
		sulfate	50.36 ± 10.5	76.07 ± 3.13	77.13 ± 0.79	89.25 ± 0.76	84.85 ± 9.04	99.84 ± 5.25	107.10 ± 5.75	
	dry-seeding	non-sulfate	66.67 ± 24.6	79.01 ± 6.86	75.84 ± 6.10	81.57 ± 12.66	61.97 ± 38.60	77.89 ± 1.59	85.61 ± 1.77	
		sulfate	86.25 ± 10.75	85.05 ± 9.16	79.54 ± 6.38	83.88 ± 6.11	98.32 ± 14.63	85.61 ± 6.21	89.12 ± 7.56	

TOC (mg/L)^b	Veronica										
	water-seeding	non-sulfate	23.03 ± 2.46	94.27 ± 25.89	101.71 ± 63.16	91.58 ± 60.92	73.44 ± 50.96	64.89 ± 41.32	59.91 ± 32.46		
		sulfate	30.63 ± 5.57	85.81 ± 32.97	93.45 ± 44.74	95.54 ± 47.79	91.58 ± 50.61	94.95 ± 53.44	92.03 ± 49.37		
	dry-seeding	non-sulfate	59.09 ± 21.00	58.73 ± 3.22	64.16 ± 6.93	61.25 ± 1.29	49.09 ± 5.30	46.03 ± 3.51	47.33 ± 3.09		
		sulfate	47.92 ± 6.44	57.30 ± 6.04	57.80 ± 6.06	57.92 ± 15.69	65.77 ± 12.15	57.25 ± 25.19	51.22 ± 25.59		
	Fornazzo										
	water-seeding	non-sulfate	73.85 ± 44.24	135.92 ± 21.00	147.04 ± 48.47	131.41 ± 49.74	102.8 ± 24.21	96.37 ± 35.54	94.20 ± 34.24		
		sulfate	56.46 ± 11.03	116.33 ± 26.03	110.91 ± 21.76	105.03 ± 10.82	95.76 ± 3.61	104.26 ± 10.07	99.93 ± 18.22		
	dry-seeding	non-sulfate	96.47 ± 17.48	105.86 ± 6.54	121.54 ± 9.10	118.47 ± 17.25	103.63 ± 7.21	80.97 ± 5.29	81.18 ± 10.63		
		sulfate	96.73 ± 10.32	108.26 ± 2.00	113.3 ± 20.63	109.97 ± 28.59	138.61 ± 38.75	106.29 ± 36.38	107.84 ± 42.60		
Fe^{II} (mmol/L)^c	Veronica										
	water-seeding	non-sulfate	0.23 ± 0.02	0.25 ± 0.01	0.29 ± 0.04	0.31 ± 0.07	0.45 ± 0.03	0.34 ± 0.14	0.28 ± 0.07		
		sulfate	0.22 ± 0.03	0.27 ± 0.02	0.25 ± 0.06	0.28 ± 0.07	0.34 ± 0.06	0.29 ± 0.07	0.25 ± 0.06		
	dry-seeding	non-sulfate	0.07 ± 0.04	0.20 ± 0.01	0.29 ± 0.03	0.35 ± 0.03	0.48 ± 0.04	0.43 ± 0.01	0.33 ± 0.00		
		sulfate	0.08 ± 0.02	0.25 ± 0.02	0.26 ± 0.01	0.26 ± 0.04	0.31 ± 0.04	0.30 ± 0.04	0.24 ± 0.04		

Fornazzo										
	water-seeding	non-sulfate	0.32 ± 0.07	0.43 ± 0.04	0.43 ± 0.03	0.43 ± 0.04	0.48 ± 0.03	0.41 ± 0.06	0.40 ± 0.03	
		sulfate	0.34 ± 0.05	0.40 ± 0.08	0.36 ± 0.05	0.37 ± 0.06	0.40 ± 0.03	0.39 ± 0.03	0.35 ± 0.04	
	dry-seeding	non-sulfate	0.11 ± 0.04	0.34 ± 0.01	0.40 ± 0.01	0.42 ± 0.04	0.49 ± 0.04	0.47 ± 0.03	0.42 ± 0.04	
		sulfate	0.14 ± 0.09	0.37 ± 0.05	0.37 ± 0.04	0.37 ± 0.07	0.44 ± 0.08	0.40 ± 0.08	0.37 ± 0.05	
Veronica										
	water-seeding	non-sulfate	48.18 ± 19.47	41.19 ± 10.28	31.62 ± 10.10	17.81 ± 4.89	12.12 ± 2.74	7.67 ± 1.55	5.57 ± 1.30	
		sulfate	24.24 ± 11.77	11.19 ± 1.07	9.26 ± 1.73	10.20 ± 2.27	11.71 ± 2.98	9.69 ± 4.03	7.58 ± 2.62	
	dry-seeding	non-sulfate	104.09 ± 9.14	83.34 ± 17.86	76.40 ± 11.97	46.93 ± 13.39	31.76 ± 8.53	18.40 ± 5.70	7.57 ± 1.73	
		sulfate	72.61 ± 15.21	8.04 ± 0.84	6.97 ± 0.86	7.69 ± 1.05	10.04 ± 1.10	8.71 ± 1.27	5.41 ± 1.25	
Fornazzo										
	water-seeding	non-sulfate	48.02 ± 4.66	22.02 ± 2.44	19.80 ± 3.80	19.65 ± 4.60	18.58 ± 4.58	15.63 ± 3.34	13.30 ± 3.22	
		sulfate	27.64 ± 4.80	18.45 ± 1.07	16.04 ± 1.38	15.51 ± 0.75	15.21 ± 0.55	14.05 ± 0.41	12.19 ± 0.74	
	dry-seeding	non-sulfate	97.32 ± 7.49	61.53 ± 13.53	25.32 ± 2.57	20.85 ± 0.66	19.72 ± 1.27	17.00 ± 1.62	14.91 ± 1.82	
		sulfate	76.46 ± 9.82	23.37 ± 1.56	19.29 ± 1.46	17.89 ± 2.19	16.99 ± 2.51	14.65 ± 2.69	12.71 ± 2.78	

^a Total inorganic carbon; ^b Total organic carbon; ^cFe^{II} was spectrophotometrically determined via 1,10-phenanthroline method.

Table S4 | Mean values for thiolation and methylation (integrated over the seven sampling times) for comparison of factors of increases by sulfate-addition (ratio S/no S) for the two different soil types (Veronica/Fornazzo) and water- vs. dry-seeding

	water-seeding		dry-seeding	
	Veronica	Fornazzo	Veronica	Fornazzo
Inorganic thioarsenates				
contribution to As speciation - no S [%]	3.0	1.8	0.6	1.3
contribution to As speciation - S [%]	4.7	5.5	3.9	2.6
ratio S/noS	1.5	3.1	6.4	2.1
Methylated thioarsenates				
contribution to As speciation - no S [%]	0.1	0.9	0.2	1.0
contribution to As speciation - S [%]	2.1	1.4	1.7	1.7
ratio S/noS	19.8	1.6	11.6	1.8
Total Thiolation				
contribution to As speciation - no S [%]	3.1	2.7	0.8	2.2
contribution to As speciation - S [%]	6.8	6.9	5.6	4.3
ratio S/noS	2.2	2.5	7.4	2
Methylated oxyarsenates				
contribution to As speciation - no S [%]	5.0	5.6	2.1	4.4
contribution to As speciation - S [%]	12.7	5.2	11.1	6.1
ratio S/noS	2.6	0.9	5.3	1.4

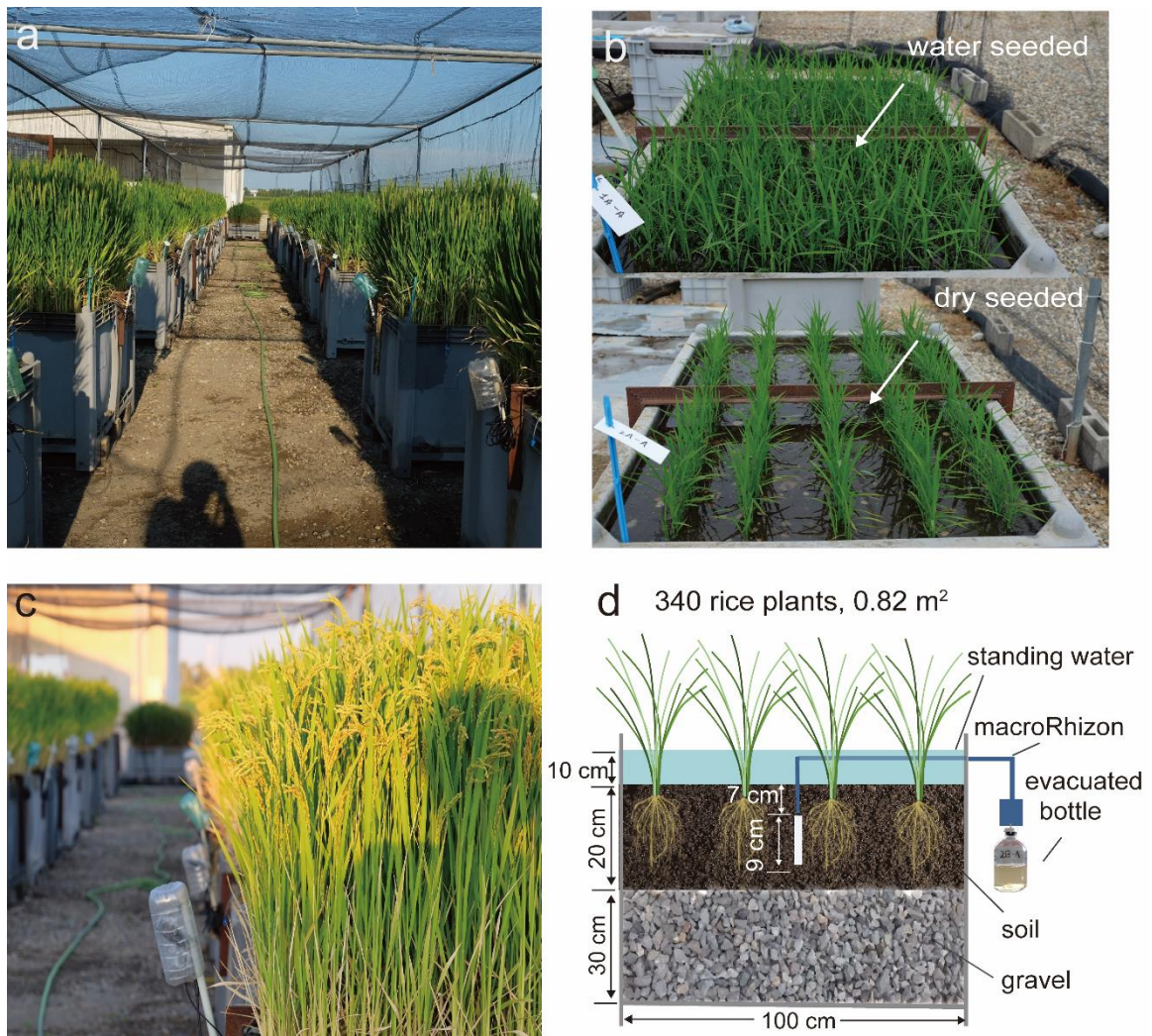


Figure S5 | Photos and schematic design of the mesocosm rice cultivation experiments. A total of 24 mesocosms with 2 different soil types, water and dry seeded, with and without sulfate fertilization (each setup conducted in triplicates) were installed at the Rice Research Centre Ente Nazionale Risi in Castello d'Agogna (Pavia, Italy); a) flowering stage; b) seeding practices; c) mature stage; d) scheme of the setup.

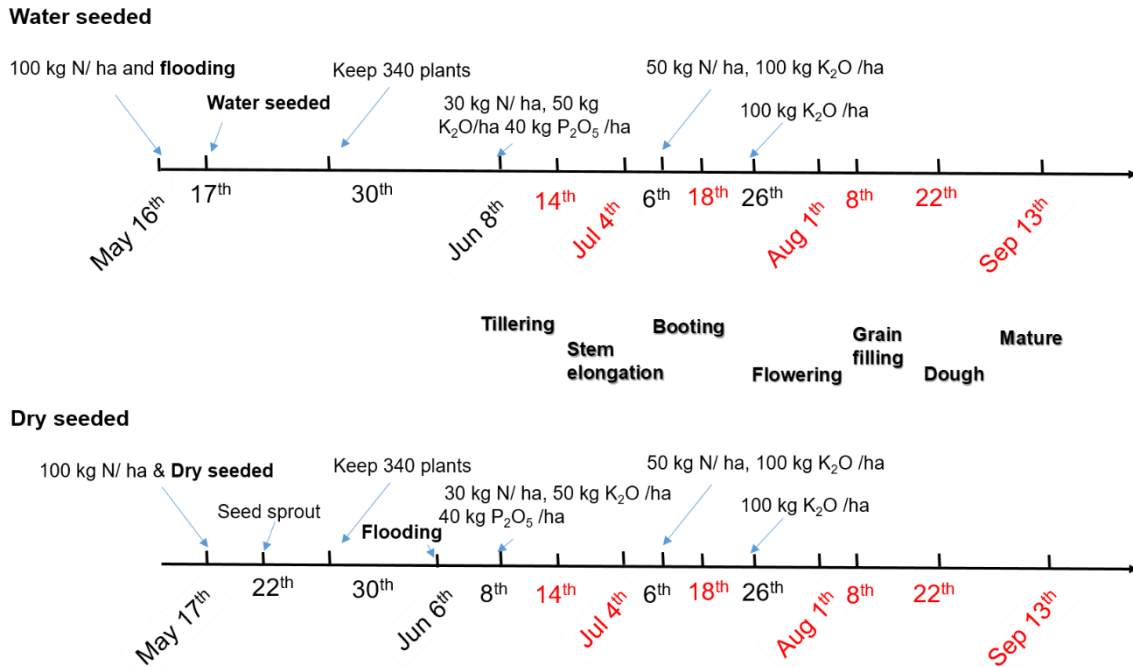


Figure S6 | Agronomic management of water and dry seeded mesocosm rice cultivation experiments in 2017. For sulfate treatments, ammonium sulfate and potassium sulfate were applied, while urea and potassium chloride were used equivalent in N and K for control treatments. Dates in red indicate pore-water sampling dates.

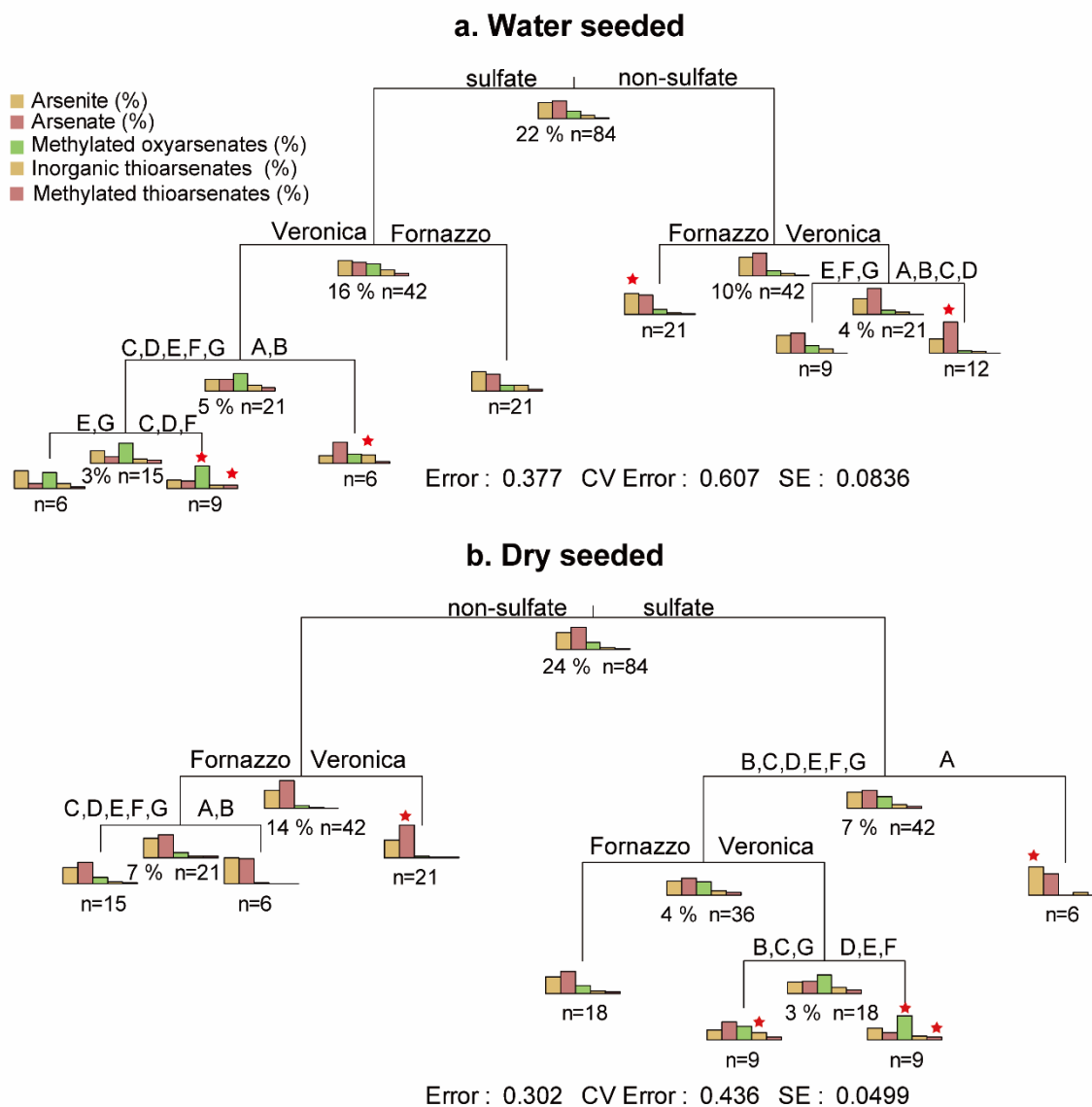


Figure S7 | Multivariate regression tree for pore-water As speciation in the mesocosm experiments for a) water seeded and b) dry seeded treatments. Multivariate regression tree analyses were done following previously published methods¹⁰. Capital letters A-G on the node represent the seven rice growth stages from tillering stage to maturity. Indicator species, based on relative abundance and relative frequency of occurrence of As species, are denoted by stars. Pre-separation in water and dry seeded was done because different redox regimes lead to an offset of growth stages in dry seeded compared to water seeded treatments by about 7-10 days.

3. Incubation experiments revealing soil properties that determine the potential for thioarsenate formation

Table S5a | Location, parent material, and soil classification of 31 paddy soils sampled in China.

No.	Location	Longitude	Latitude	Parent material	Soil classification (within the suborder Stagnic Anthrosols ^a)
CH1	Jiangmen, Guangdong	112°31'09.2"	22°30'33.9"	river alluvium	Fe-accumuli-
CH2	Nanning 2, Guangxi	108°17'12.6"	23°06'22.4"	limestone	Fe-accumuli-
CH3	Nanning1, Guangxi	108°16'52.0"	23°06'27.6"	limestone	Fe-accumuli-
CH4	Dehong, Yunnan	98°25'55.1"	24°26'31.1"	river alluvium	Fe-accumuli-
CH5	Chuxiong, Yunnan	102°03'5.71"	25°11'01.3"	river alluvium (sandy)	Fe-leachi-
CH6	Ganzhou, Jiangxi	114°27'11.8"	25°26'31.8"	river alluvium	Fe-accumuli-
CH7	Guiyang, Guizhou	106°40'17.6"	26°20'12.7"	limestone	Fe-leachi-
CH8	Qiandongnan, Guizhou	108°03'43.19"	26°36'46.71"	limestone	Fe-leachi-
CH9	Sanming, Fujian	117°10'30.44"	26°50'56.14"	river alluvium	Fe-accumuli-
CH10	Ji'an, Jiangxi	114°54'36.0"	26°58'21.4"	river alluvium	Fe-accumuli-
CH11	Zunyi, Guizhou	106°48'14.5"	27°30'13.15"	limestone	Hapli-
CH12	Yingtian, Jiangxi	117°15'21.1"	28°20'31.1"	river alluvium	Fe-accumuli-
CH13	Yueyang, Hunan	113°5'43.8"	29°14'23.0"	lacustrine deposits	Fe-accumuli-
CH14	Jinhua, Zhejiang	119°20'34.1"	29°01'04.9"	river alluvium	Hapli-
CH15	Jingzhou, Hubei	112° 31'49.03"	30° 5'53.10"	river alluvium	Fe-accumuli-
CH16	Hangzhou, Zhejiang	120°05'13.3"	30°28'05.6"	river alluvium	Fe-accumuli-
CH17	Jiaxing, Zhejiang	121°07'01.26"	30°48'06.3"	marine sediment	Fe-leachi-
CH18	Zhenjiang, Jiangsu	119°18'15.47"	31°57'58.38"	river alluvium	Fe-leachi-
CH19	Xuancheng, Anhui	118°29'55.7"	31°00'02.6"	river alluvium	Hapli-

CH20	Hefei, Anhui	117°13'28.1"	31°35'54.1"	lacustrine deposits	Fe-accumuli-
CH21	Xinyang, Henan	114°59'03"	31°54'13"	river alluvium (loess)	Fe-accumuli-
CH22	Hanzhong, Shaanxi	106°54'36.15"	33°09'37.77"	loess	Fe-leachi-
CH23	Yancheng, Jingsu	120°04'10.6"	33°16'12.5"	marine sediment	Fe-accumuli-
CH24	Xuzhou, Jiangsu	117°24'38.49"	34°17'46.59"	river alluvium	Fe-leachi-
CH25	Lianyungang, Jiangsu	119°20'06.1"	34°32'58.0"	river alluvium	Fe-leachi-
CH26	Jining, Shandong	116°33'32.5"	35°18'47.7"	river alluvium	Fe-accumuli-
CH27	Yinchuan, Ningxia	106°16'0.97"	38°10'04.78"	river alluvium	Hapli-
CH28	Panjin, Liaoning	122°13'46.6"	40°58'26.09"	marine sediment	Hapli-
CH29	Siping, Jilin	124°42'29.1"	43°28'47.8"	river alluvium	Hapli-
CH30	Wuchang, Heilongjiang	127°02'12.9"	45°03'42.1"	river alluvium	Hapli-
CH31	Jiamusi, Heilongjiang	131°36'34.2"	47°11'12.8"	river alluvium	Hapli-

^a Based on the Chinese Soil Taxonomic Classification (adopted by WRB in 1998) all paddy soils used here are classified as Stagnic Anthrosols. Stagnic Anthrosols are anthrosols that have an anthrostagnic moisture regime, and both a hydragric epipedon (including a cultivated horizon and a plowpan) and a hydragric horizon.

Table S5b | Geology/geomorphology and climate zones of the 31 paddy fields sampled in China.

No.	Geology/Geomorphology	Climate Zone
CH1	The lower hilly and wide valley basin of Jiangmen	Sub-tropical Monsoon
CH2	The valley plain area of Wuming Basin	Sub-tropical Monsoon
CH3	The valley plain area of Wuming Basin	Sub-tropical Monsoon
CH4	The lower hilly and wide valley basin of Dehong	Sub-tropical Monsoon
CH5	The low mountain and hilly area in Lufeng Basin	Sub-tropical Monsoon
CH6	The lower hilly and wide valley basin of Ganzhou	Sub-tropical Monsoon
CH7	The lower hilly and wide valley basin of Guiyang	Sub-tropical Monsoon
CH8	The lower hilly and wide valley basin of Qiandongnan	Sub-tropical Monsoon
CH9	The lower hilly and wide valley basin of Sanming	Sub-tropical Monsoon
CH10	The lower hilly and wide valley basin of Ji'an	Sub-tropical Monsoon
CH11	The lower hilly and wide valley basin of Zunyi	Sub-tropical Monsoon
CH12	The valley plain area of Xinjiang Basin	Sub-tropical Monsoon
CH13	The low-lying land of lakeshore plain of Dongting Lake	Sub-tropical Monsoon
CH14	The first grade terrace of Xinlixi River in the valley plain area of Jinqu Basin, Eastern China	Sub-tropical Monsoon
CH15	The alluvial and lacustrine plain area of Jiangnan Plain, Central China	Sub-tropical Monsoon
CH16	The alluvial-marine plain area in North Zhejiang Plain, Eastern China	Sub-tropical Monsoon
CH17	The alluvial-marine plain area of the Yangtze River Delt	Sub-tropical Monsoon
CH18	The hilly and low-lying area of Zhenjiang in Jiangsu Province, Eastern China	Sub-tropical Monsoon
CH19	The first grade terrace in the valley plain of QingYijiang River	Sub-tropical Monsoon
CH20	The low-lying land of lakeshore plain of Chaohu Lake in Anhui Province, Eastern China	Sub-tropical Monsoon
CH21	The low foothill area of Xinyang in southern margin of North China Plain	Sub-tropical Monsoon

CH22	The first grade terrace of Bao River in alluvial and lacustrine plain area of the Hanzhong Basin, in southern Shaanxi Province, China	Sub-tropical Monsoon
CH23	The alluvial-marine plain area of Yancheng in North Jiangsu Plain, Eastern China	Sub-tropical Monsoon
CH24	The alluvial and lacustrine plain area of Xuzhou in North China Plain	Temperate Monsoon
CH25	The coastal plain area in North Jiangsu Plain, Eastern China	Temperate Monsoon
CH26	The low-lying land of lakeshore plain of Weishan Lake in North China Plain	Temperate Monsoon
CH27	The first grade terrace of the Yellow River in Yinchuan Plain, Northwest China	Temperate Continental
CH28	The coastal plain area in Liaohai Plain, Northeast China	Temperate Monsoon
CH29	The first grade terrace of East Liao River in Liaohai Plain, Northeast China	Temperate Monsoon
CH30	The interchannel zone between Lalin River and Mangniu River in Song Nen Plain, Northeast China	Temperate Monsoon
CH31	The first grade terrace of Songhua River in Sanjiang Plain, Northeast China	Temperate Monsoon

Table S5c | Basic soil chemistry of the 31 paddy soils sampled in China.

No.	soil pH	CEC ^a cmol/kg	Clay %	SOC ^b g/kg	Total As	Chalcophile metals				HCl-extractable Fe mmol/kg	Total zerovalent sulfur ^c	
						Cd	Pb	Cu	Zn		control	3 mmol/kg sulfate
CH1	5.1	4.0	16.5	27.9	6.7	0.1	9.9	3.3	35.3	31.9	0.4	1.5
CH2	5.6	9.2	20.3	56.5	34.2	0.3	33.3	15.7	82.3	74.7	0.9	1.9
CH3	6.1	8.2	24.4	36.7	15.5	0.6	23.2	28.5	108.4	94.6	0.2	0.7
CH4	6.2	9.2	33.0	25.9	5.9	0.1	24.6	11.7	87.3	84.1	2.2	2.2
CH5	6.9	20.0	29.8	61.6	8.2	0.7	25.3	74.4	103.4	113.3	0.6	1.9
CH6	4.9	5.5	14.7	20.7	38.8	0.4	53.9	36.7	111.3	78.1	0.0	0.7
CH7	6.9	15.7	13.2	104.4	15.5	0.5	26.6	31.0	142.8	69.7	0.1	1.2
CH8	5.8	8.2	37.5	39.7	10.3	0.2	21.1	17.5	83.7	30.0	0.2	1.3
CH9	5.3	4.2	9.6	42.9	2.6	0.2	31.7	20.0	126.4	41.5	0.3	0.7
CH10	4.9	5.6	17.0	25.5	8.4	0.1	19.1	14.0	63.8	106.3	0.2	0.9
CH11	8.0	16.6	28.6	46.8	11.1	0.6	23.0	25.3	100.1	99.4	0.7	0.8
CH12	4.5	4.2	18.5	39.3	7.5	0.6	19.7	74.3	52.8	60.4	0.1	1.2
CH13	5.6	9.8	17.0	14.0	15.9	0.3	29.9	21.3	89.3	129.1	0.2	1.0
CH14	5.5	10.9	16.9	21.4	8.0	0.2	23.2	7.9	57.4	57.2	0.3	0.9
CH15	8.1	11.8	11.4	25.7	12.4	0.3	22.3	30.9	110.2	130.2	0.9	1.7
CH16	6.4	16.6	43.2	35.8	6.1	0.2	24.6	24.4	79.7	98.1	0.2	1.8
CH17	7.0	18.3	31.1	33.7	11.0	0.2	22.8	26.6	110.5	110.7	0.2	0.8
CH18	7.2	9.7	16.6	28.2	7.9	0.1	18.7	16.9	58.9	110.3	0.6	1.5
CH19	5.0	10.7	24.8	34.5	9.9	0.2	23.6	14.3	62.0	90.3	0.8	1.2
CH20	5.7	15.7	20.6	27.6	7.0	0.1	14.8	12.5	44.1	99.5	0.4	1.3
CH21	5.4	10.4	18.3	34.3	5.8	0.1	16.3	12.7	55.4	132.1	0.5	1.2

CH22	5.5	12.9	21.0	38.8	9.5	0.3	20.4	19.5	77.6	142.3	0.6	1.8
CH23	6.2	6.4	25.1	33.3	5.9	0.1	15.0	13.5	67.4	105.7	0.2	1.3
CH24	7.7	15.6	13.1	32.5	11.8	0.2	16.9	19.5	76.2	115.1	1.3	2.3
CH25	8.9	16.3	28.3	27.2	16.5	0.2	27.9	27.1	119.6	120.4	1.4	1.6
CH26	7.7	17.9	28.7	42.7	13.0	0.3	35.0	23.3	83.1	113.9	1.9	2.6
CH27	8.5	4.7	10.6	17.9	11.3	0.2	12.4	15.8	61.9	79.2	2.4	3.1
CH28	7.2	20.6	15.8	28.4	7.9	0.1	17.9	18.1	71.4	69.5	2.0	2.8
CH29	6.7	16.6	13.8	30.4	8.6	0.1	15.4	16.9	67.2	130.5	2.0	2.3
CH30	6.3	18.8	25.1	45.1	9.6	0.1	17.3	19.9	68.3	146.3	0.2	1.1
CH31	5.9	19.0	25.3	39.5	10.0	0.1	14.9	14.0	44.8	184.7	0.3	1.0

^a Cation exchange capacity; ^b Soil organic carbon; ^c Total zerovalent sulfur formation after 14 days of soil incubation as described in section 4, which was calculated as sum of aqueous and solid phase zerovalent sulfur for control treatments and 3 mmol/kg sulfate addition treatments, respectively.

Table S6 | Spearman's correlation analyses for soil and pore water parameters for anaerobic soil incubations of 31 paddy soils from China and 2 paddy soils from Italy; marked in green are R values with a P-value < 0.05

R (control, no S)	methyalted thioarsenates [%]	total thiolation [%]	soil pH	soil-bound zerovalent S [μmol/kg]	HCl-extractable Fe [g/kg]	soil total As [mg/kg]	soil organic carbon [g/kg]	CEC [cmol/kg]	Clay [%]	Total chalcophile metals [mmol/kg]	porewater pH	methyalted oxyarsenates [%]	porewater S zerovalent S [μmol/l]	porewater As [μg/L]	porewater Fe [mg/L]
inorganic thioarsenates [%]	0.22	0.85	0.58	0.46	-0.10	-0.18	-0.10	0.17	-0.25	-0.04	0.44	-0.01	0.25	-0.48	-0.89
methyalted thioarsenates [%]		0.54	-0.31	-0.21	-0.36	-0.63	0.19	-0.01	0.00	-0.17	-0.46	0.69	0.03	-0.63	-0.04
total thiolation [%]			0.28	0.30	-0.21	-0.34	0.02	0.06	-0.33	-0.16	0.16	0.29	0.26	-0.58	-0.66
soil pH				0.54	0.33	0.32	0.06	0.54	0.08	0.21	0.87	-0.54	-0.03	-0.12	-0.79
soil-bound zerovalent S [μmol/kg]					0.28	0.10	-0.04	0.30	-0.09	-0.16	0.69	-0.19	0.31	-0.24	-0.51
HCl-extractable Fe [g/kg]						0.27	0.00	0.54	0.16	-0.09	0.37	-0.31	-0.09	0.24	0.02
soil total As [mg/kg]							0.00	0.12	-0.07	0.46	0.37	-0.56	-0.33	0.45	0.02
soil organic carbon [g/kg]								0.30	0.36	0.32	0.04	0.12	-0.02	-0.24	0.06
CEC [cmol/kg]									0.37	0.08	0.57	-0.17	0.08	0.00	-0.33
Clay [%]										0.10	0.05	0.22	-0.16	-0.09	0.13
Total chalcophile metals [mmol/kg]											0.23	-0.27	-0.26	-0.15	-0.16
porewater pH												-0.59	0.17	-0.02	-0.71
methyalted oxyarsenates [%]													0.07	-0.41	0.23
porewater zerovalent S [μmol/L]														0.06	-0.20
porewater As [μg/L]															0.33

P-Value (control, no S)	methylated thioarsenates [%]	total thiolation [%]	soil pH	soil-bound zerovalent S [µmol/kg]	HCl-extractable Fe [g/kg]	soil total As [g/kg]	soil organic carbon [g/kg]	CEC [cmol/kg]	Clay [%]	Total chalcophile metals [mmol/kg]	porewater pH	methylated oxyarsenates [%]	porewater zerovalent S [µmol/l]	porewater As [µg/L]	porewater Fe [mg/L]
inorganic thioarsenates [%]	0.22	0.00	0.00	0.01	0.57	0.32	0.58	0.35	0.17	0.85	0.01	0.97	0.17	0.01	0.00
methylated thioarsenates [%]		0.00	0.08	0.23	0.04	0.00	0.30	0.95	1.00	0.36	0.01	0.00	0.86	0.00	0.85
total thiolation [%]			0.11	0.09	0.24	0.05	0.93	0.75	0.07	0.39	0.38	0.10	0.15	0.00	0.00
soil pH				0.00	0.06	0.07	0.74	0.00	0.69	0.26	0.00	0.00	0.89	0.52	0.00
soil-bound zerovalent S [µmol/kg]					0.12	0.56	0.82	0.10	0.64	0.38	0.00	0.29	0.08	0.20	0.00
HCl-extractable Fe [g/kg]						0.14	0.98	0.00	0.40	0.64	0.04	0.07	0.62	0.19	0.91
soil total As [mg/kg]							1.00	0.52	0.72	0.01	0.04	0.00	0.06	0.01	0.90
soil organic carbon [g/kg]								0.10	0.05	0.08	0.85	0.50	0.93	0.20	0.75
CEC [cmol/kg]									0.04	0.65	0.00	0.37	0.68	1.00	0.07
Clay [%]										0.60	0.79	0.23	0.38	0.61	0.49
Total chalcophile metals [mmol/kg]											0.22	0.15	0.16	0.42	0.40
porewater pH												0.00	0.36	0.92	0.00
methylated oxyarsenates [%]													0.69	0.02	0.19
porewater zerovalent S [µmol/L]														0.74	0.25
porewater As [µg/L]															0.07

R (Sulfate Treatment)	methylated thioarsenates [%]	total thiolation [%]	soil pH	soil-bound zerovalent S [μmol/kg]	HCl-extractable Fe [g/kg]	soil total As [mg/kg]	soil organic carbon [g/kg]	CEC [cmol/kg]	Clay [%]	Total chalcophile metals [mmol/kg]	porewater pH	methylated oxyarsenates [%]	porewater zerovalent S [μmol/l]	porewater As [μg/L]	porewater Fe [mg/L]
inorganic thioarsenates [%]	0.08	0.91	0.59	0.35	-0.07	-0.14	-0.16	0.18	-0.17	-0.03	0.63	-0.06	-0.19	-0.39	-0.86
methylated thioarsenates [%]		0.40	-0.41	-0.33	-0.35	-0.67	0.21	-0.02	0.02	-0.21	-0.34	0.72	-0.13	-0.46	0.27
total thiolation [%]			0.38	0.21	-0.22	-0.34	-0.06	0.11	-0.20	-0.11	0.52	0.18	-0.23	-0.50	-0.73
soil pH				0.49	0.33	0.32	0.06	0.54	0.08	0.21	0.66	-0.47	-0.07	-0.05	-0.90
soil-bound zerovalent S [μmol/kg]					0.21	0.12	-0.04	0.25	-0.04	-0.15	0.44	-0.30	0.25	-0.26	-0.54
HCl-extractable Fe [g/kg]						0.26	0.00	0.54	0.15	-0.09	0.39	-0.38	0.07	0.29	-0.07
soil total As [mg/kg]							0.00	0.12	-0.07	0.46	0.09	-0.67	-0.17	0.47	-0.08
soil organic carbon [g/kg]								0.30	0.36	0.32	-0.15	0.09	0.05	-0.21	-0.01
CEC [cmol/kg]									0.37	0.08	0.38	-0.26	0.11	0.07	-0.39
Clay [%]										0.10	-0.18	0.17	0.25	-0.09	0.11
Total chalcophile metals [mmol/kg]											-0.02	-0.22	-0.12	-0.14	-0.16
porewater pH												-0.36	-0.03	-0.04	-0.69
methylated oxyarsenates [%]													-0.14	-0.46	0.34
porewater zerovalent S [μmol/L]														-0.04	0.03
porewater As [μg/L]															0.34

P-Value (Sulfate Treatment)	methylated thioarsenates [%]	total thiolation [%]	soil pH	soil-bound zerovalent S [µmol/kg]	HCl-extractable Fe [g/kg]	soil total As [mg/kg]	[g/kg]	CEC [cmol/kg]	Clay [%]	Total chalcophile metals [mmol/kg]	porewater pH	methylated oxyarsenates [%]	porewater zerovalent S [µmol/l]	porewater As [µg/L]	porewater Fe [mg/L]
inorganic thioarsenates [%]	0.65	0.00	0.00	0.04	0.68	0.44	0.37	0.34	0.35	0.86	0.00	0.74	0.28	0.03	0.00
methylated thioarsenates [%]		0.02	0.02	0.06	0.05	0.00	0.25	0.90	0.90	0.26	0.06	0.00	0.46	0.01	0.16
total thiolation [%]		0.03	0.03	0.23	0.22	0.05	0.73	0.56	0.27	0.56	0.00	0.32	0.20	0.00	0.00
soil pH				0.00	0.06	0.07	0.74	0.00	0.69	0.26	0.00	0.01	0.68	0.79	0.00
soil-bound zerovalent S [µmol/kg]					0.25	0.49	0.81	0.18	0.82	0.41	0.01	0.09	0.16	0.15	0.00
HCl-extractable Fe [g/kg]						0.14	0.99	0.00	0.41	0.62	0.03	0.03	0.71	0.12	0.72
soil total As [mg/kg]							1.00	0.52	0.72	0.01	0.65	0.00	0.33	0.01	0.69
soil organic carbon [g/kg]								0.10	0.05	0.08	0.41	0.63	0.77	0.27	0.95
CEC [cmol/kg]									0.04	0.65	0.03	0.16	0.56	0.71	0.04
Clay [%]										0.60	0.33	0.36	0.17	0.64	0.57
Total chalcophile metals [mmol/kg]											0.89	0.23	0.51	0.46	0.41
porewater pH												0.05	0.87	0.82	0.00
methylated oxyarsenates [%]													0.42	0.01	0.08
porewater zerovalent S [µmol/L]														0.81	0.88
porewater As [µg/L]															0.07

Table S7 | Relative importance of predictor values for the occurrence of inorganic and methylated thioarsenates (%) using multiple linear regression analysis with soil physical and chemical properties separated by control (no S) and sulfate-addition (S) incubations; for methylated thioarsenates two models were used, one including the share of methylated oxyarsenates in the pore water and one only using soil parameters; significance levels (sig. level) are indicated as *** (0-0.001), ** (0.001-0.01), * (0.01-0.05), and . (0.1-1)

Control (no S)	weight factor %	lower 95% range [%]	upper 95% range [%]	sig. level
inorganic thioarsenates				
CEC [cmol/kg]	13.6	1.7	30.2	**
Clay [%]	-18.3	-3.3	-40.6	**
HCl-extractable Fe [g/kg]	-6	-1.1	-16.6	*
{H+} [mol/L]	-4.4	-2.8	-14.5	
zerovalent S [μmol/kg]	50.8	17.8	74.9	***
SOC [g/kg]	-4.5	-0.9	-11.2	
total soil As [mg/kg]	-1.3	-0.4	-8.1	
Total chalcophile metals [mmol/kg]	-1.1	-0.5	-8.2	
$r^2 = 0.7352, p = 7.1 \cdot 10^{-5}$				
methylated thioarsenates + oxyarsenates				
CEC [cmol/kg]	3.2	1.6	24.5	
Clay [%]	-9.8	-1.1	-21.6	*
HCl-extractable Fe [g/kg]	-10.8	-3.3	-29.1	
{H+} [mol/L]	-1.8	-0.9	-10.9	
zerovalent S [μmol /kg]	-3.2	-0.8	-20.4	
SOC [g/kg]	-0.8	-0.7	-9.4	
total soil As [mg/kg]	-18.8	-8.8	-30.3	*
Total chalcophile metals [mmol/kg]	5.7	2.3	23	*
methylated oxyarsenates [%]	45.9	8.2	55.7	**
$r^2 = 0.6902, p = 8.9 \cdot 10^{-4}$				

methylated thioarsenates - oxyarsenates				
CEC [cmol/kg]	-6	-1.6	-25.7	
Clay [%]	-10.1	-1	-23.8	.
HCl-extractable Fe [g/kg]	-26.9	-3.9	-45.4	*
{H+} [mol/L]	-4	-1.3	-19.6	
zerovalent S [μ mol /kg]	-6.7	-0.9	-30.3	
SOC [g/kg]	-1	-0.8	-15.6	
total soil As [mg/kg]	-40.4	-12.3	-49.1	**
Total chalcophile metals [mmol/kg]	4.9	2.6	37.1	
$r^2 = 0.5022, p = 2.8 \cdot 10^{-2}$				

Sulfate treatment	weight factor %	lower 95% range [%]	upper 95% range [%]	sig. level
inorganic thioarsenates				
CEC [cmol/kg]	20.6	3	30.6	**
Clay [%]	-12.6	-1.6	-31.5	*
HCl-extractable Fe [g/kg]	-8.8	-1.8	-19.4	*
{H+} [mol/L]	-4.2	-2.7	-17.3	
zerovalent S [μ mol /kg]	46.1	21	68.6	**
SOC [g/kg]	-6.3	-1.1	-15.5	*
total soil As [mg/kg]	-0.8	-0.4	-10.4	
Total chalcophile metals [mmol/kg]	-0.8	-0.5	-7.7	
$r^2 = 0.674, p = 5.6 \cdot 10^{-4}$				

methylated thioarsenates + oxyarsenates				
CEC [cmol/kg]	4.3	1.5	14.6	
Clay [%]	-1.5	-0.5	-17.5	
HCl-extractable Fe [g/kg]	-12.9	-3.2	-21	
{H+} [mol/L]	-0.8	-0.5	-15.4	
zerovalent S [μ mol /kg]	-3.7	-0.6	-13.6	
SOC [g/kg]	-0.3	-0.4	-8.2	
total soil As [mg/kg]	-11.2	-4.7	-23.6	
Total chalcophile metals [mmol/kg]	1.5	0.6	19.9	
methylated oxyarsenates [%]	63.8	21.2	65.8	***
$r^2 = 0.8304, p = 2.8 \cdot 10^{-6}$				

methylated thioarsenates - oxyarsenates				
CEC [cmol/kg]	-8.3	-1.8	-19.6	
Clay [%]	-1.9	-0.6	-29.4	
HCl-extractable Fe [g/kg]	-39.1	-3.6	-47.3	*
{H+} [mol/L]	-1.7	-1.2	-27.5	
zerovalent S [μ mol /kg]	-10.9	-0.9	-28	.
SOC [g/kg]	-0.8	-0.8	-14.9	
total soil As [mg/kg]	-33.1	-9.3	-49.7	*
Total chalcophile metals [mmol/kg]	4.1	1.1	40.9	
$r^2 = 0.5151, p = 2.2 \cdot 10^{-2}$				

Note: Implications of HCl-extractable Fe, pH, zerovalent S, total soil As, and methylated oxyarsenates are discussed in the main manuscript; the reasons for the sig. negative impact of clay on both inorganic and methylated thioarsenates and the sig. positive impact of CEC (Cation Exchange Capacity) on inorganic thioarsenates are currently unclear. The correlation with CEC might be in line with previous observations of high ionic strengths increasing the kinetics of inorganic thioarsenate formation from arsenite and reduced sulfur in solution. ^{11, 12}

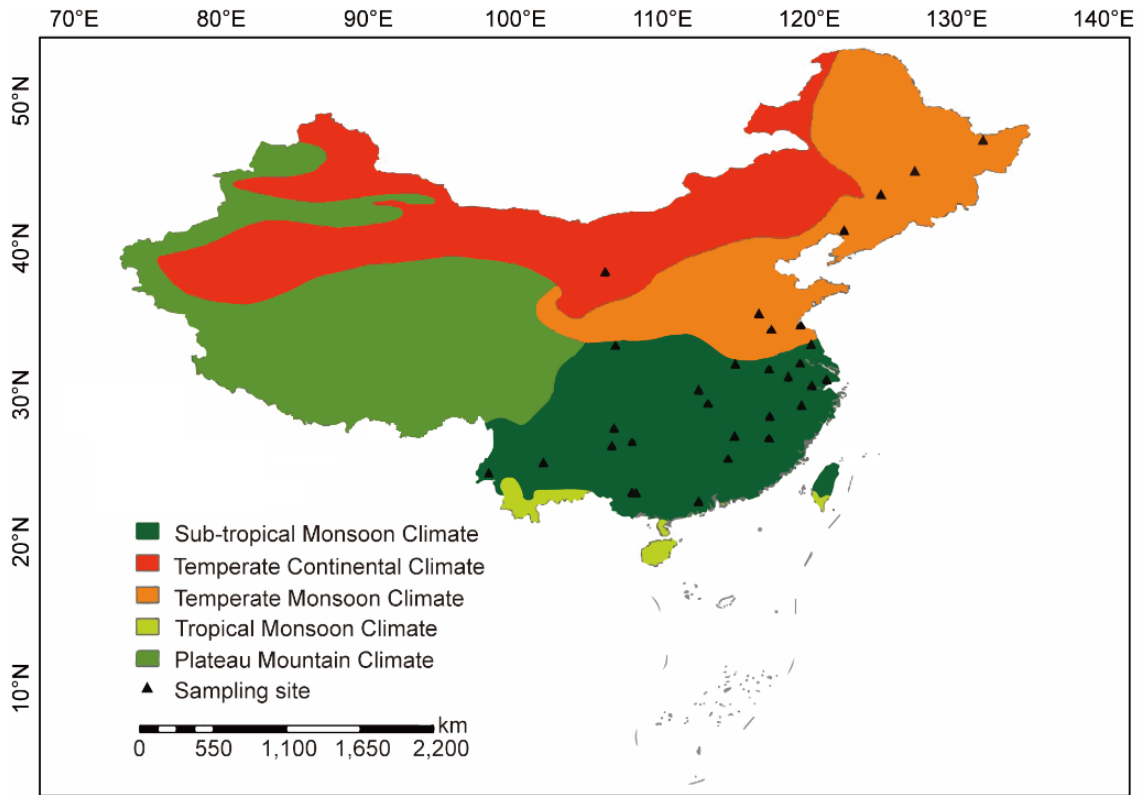


Figure S8 | Sampling sites of 31 paddy fields in different climate zones over China. The geographic origins covered an area from 22.5° to 47.2° N and 98.4° to 131.6° E, spanning climate zones from sub-tropical monsoon climate (23 fields) to temperate continental climate (1 fields) and temperate monsoon climate (7 fields). The base map used is from the National Fundamental Geographic Information System of China.

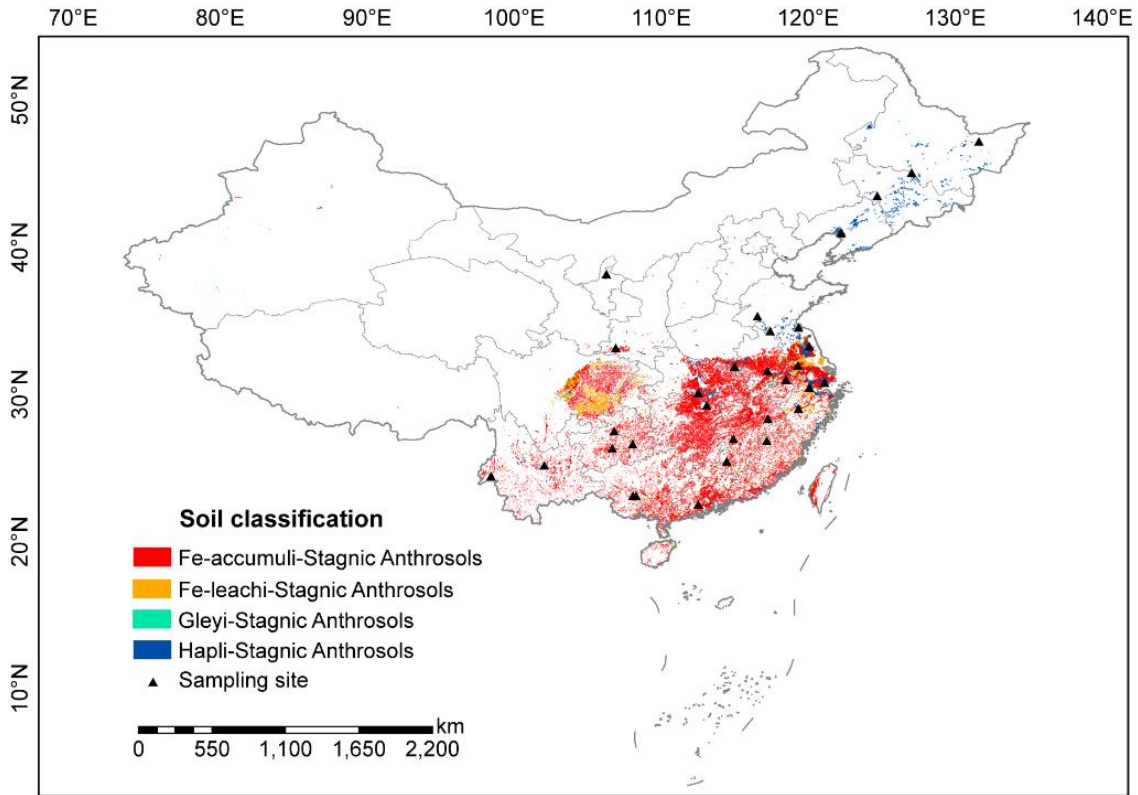


Figure S9 | Sampling sites of 31 paddy fields based on soil classification over China. The colored background indicates the distribution of Stagnic Anthrosols in China. Based on Chinese Soil Taxonomic Classification (adopted by WRB in 1998), all paddy soils used here are classified as Stagnic Anthrosols, including Fe-accumuli- (15 soils), Fe-leachi-(8 soils), Hapli- (8 soils) Stagnic Anthrosols. Stagnic Anthrosols are anthrosols that have an anthrostagnic moisture regime and have both a hydragic epipedon (including a ultivated horizon and a plowpan) and a hydragic horizon. The base map used is from the National Fundamental Geographic Information System of China.

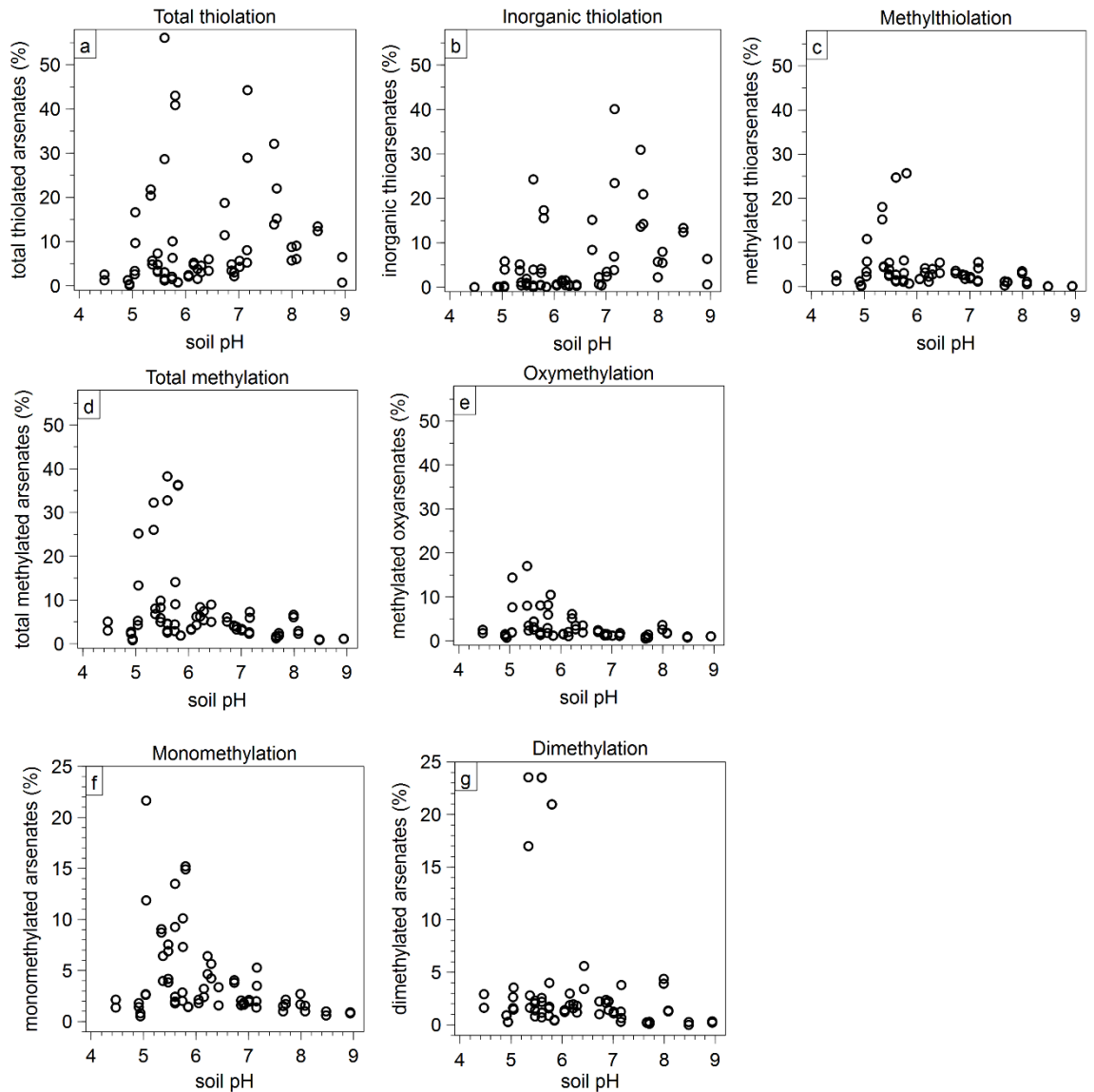


Figure S10 | Summarized As speciation determined in anaerobic soil incubations in relation to soil pH. Data from control and sulfate addition for 31 paddy soils from China and 2 paddy soils from Italy were combined. a) total thiolation which is the sum of b) inorganic thiolation and c) methylthiolation; d) total methylation which is the sum of e) oxymethylation and c) methylthiolation; f) all mono- and g) all dimethylated arsenates (integrating oxy and thio species).

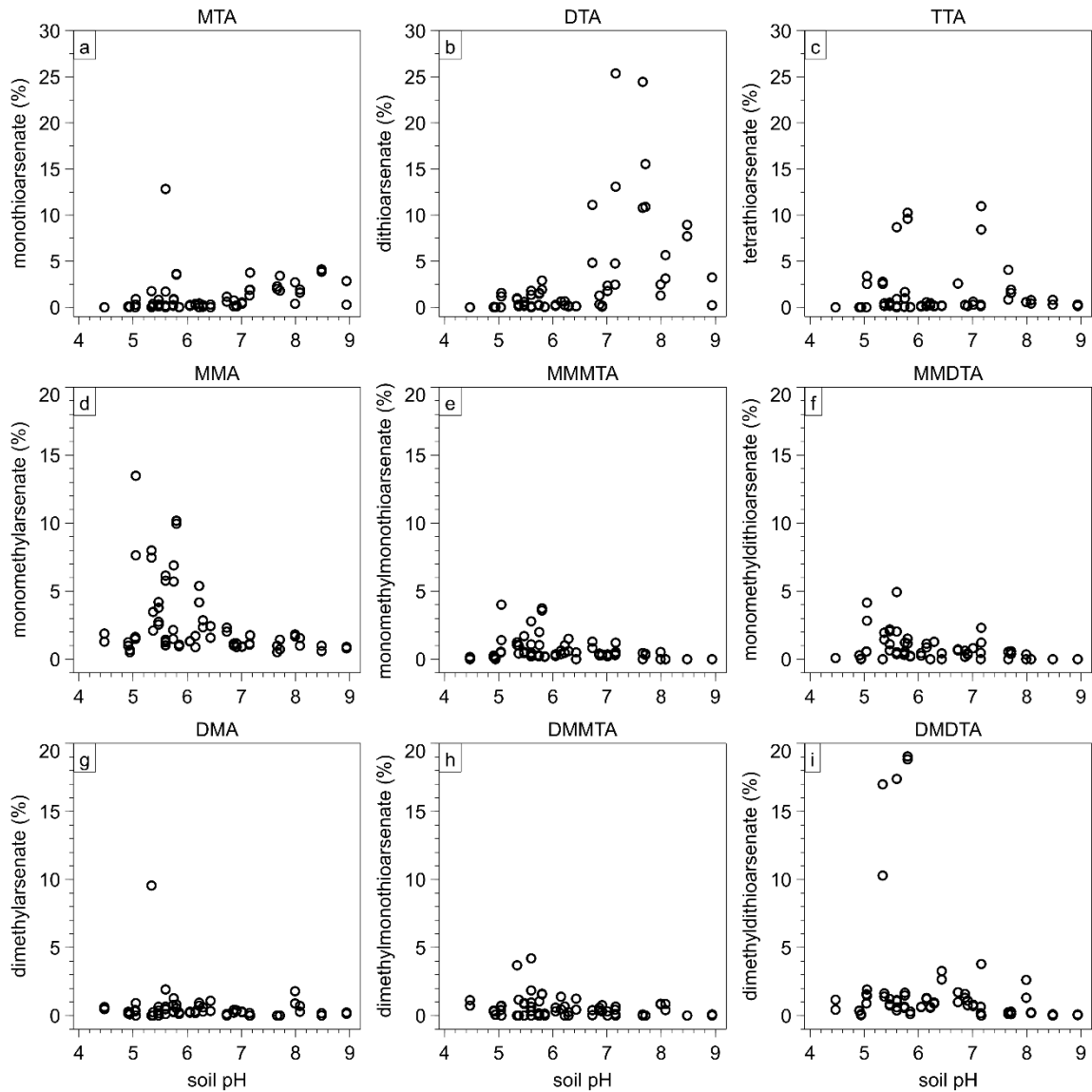


Figure S11 | Individual As speciation of inorganic thioarsenates in anaerobic soil incubations in relation to soil pH. a) MTA, b) DTA, c) TTA, d) monomethylated oxy- (MMA) and thioarsenates e) MMMTA, f) MMDTA) and g) dimethylated oxy- (DMA), and thioarsenates h) DMMTA, i) DMDTA. Data from control and sulfate addition for 31 paddy soils from China and 2 paddy soils from Italy were combined.

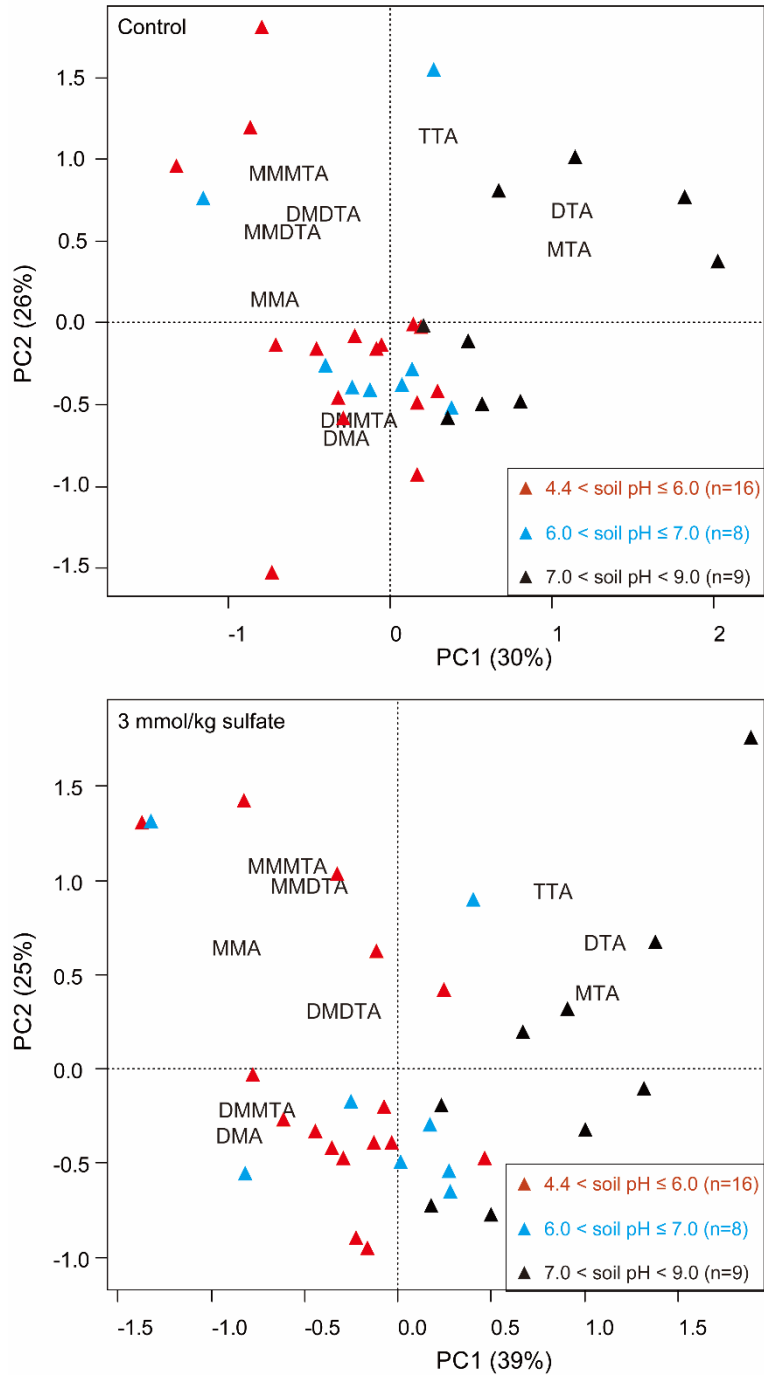


Figure S12 | Principal component analysis of As speciation in anaerobic soil incubations. Site distribution reveals clustering of methylated oxyarsenates (DMA and MMA) and methylated thioarsenates (DMDTA, MMDTA, MMMTA, DMMTA) with low pH soils and inorganic thioarsenates (MTA, DTA, and TTA) with high pH soils during anaerobic incubation of 31 paddy soils from China and 2 paddy soils from Italy; a) control treatment and b) sulfate addition.

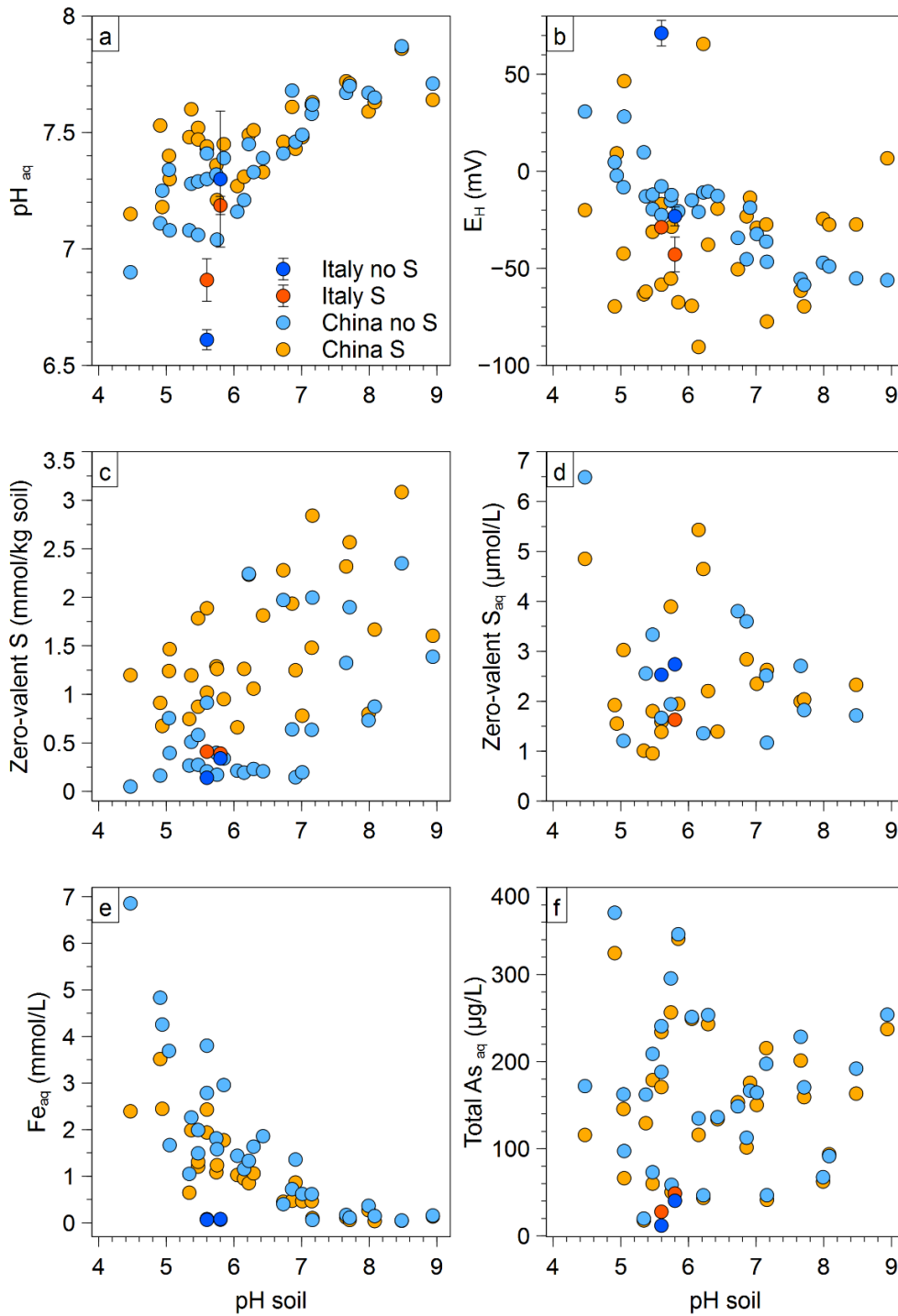


Figure S13 | Pore-water chemistry for anaerobic soil incubations as a function of soil pH. a) pore-water pH, b) E_H , c) solid phase zero-valent S, d) aqueous zero-valent S, e) total dissolved Fe, and f) total dissolved As for anaerobic soil incubations of 31 paddy soils from China and 2 paddy soils from Italy (experimental triplicates); blue colors refer to control treatments (no S), orange-red colors to sulfate addition (S).

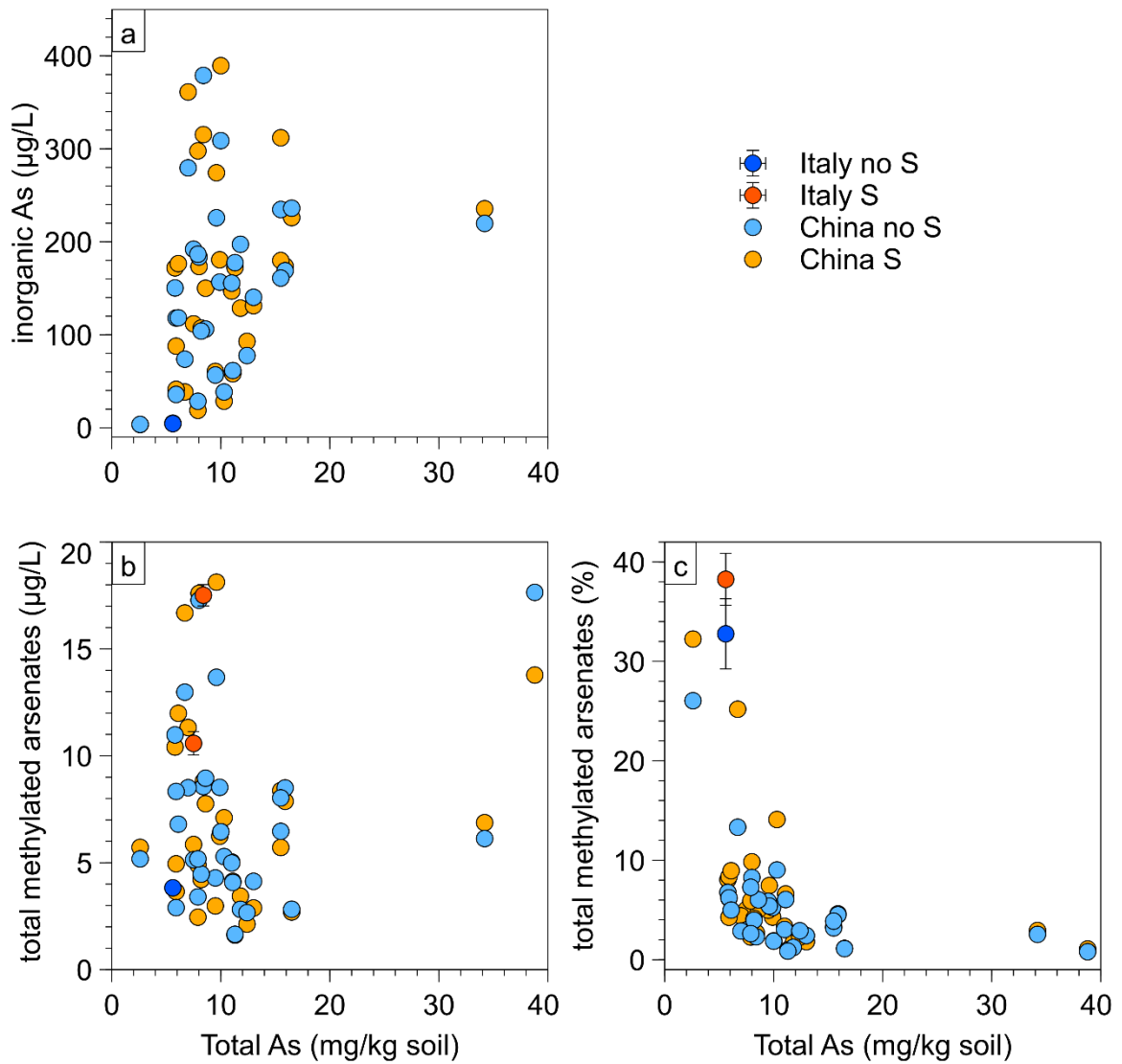


Figure S14 | Absolute and relative concentrations of inorganic As (a, b) and methylated oxyarsenates (c, d) in relation to total soil As. Anaerobic soil incubations were conducted with 31 paddy soils from China and 2 paddy soils from Italy (experimental triplicates); blue colors refer to control treatments (no S), orange-red colors to sulfate addition (S).

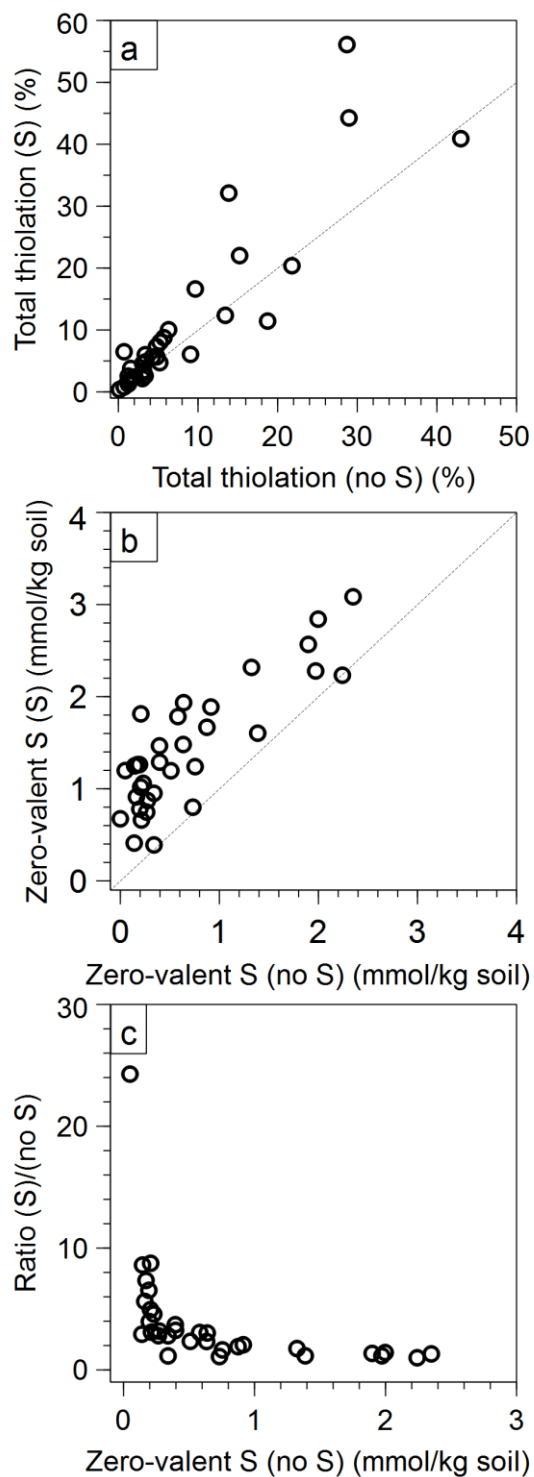


Figure S15 | Effects of sulfate addition on arsenic thiolation and zero-valent S formation. Comparison of a) total thiolation (%) and b) solid phase zero-valent S with and without sulfate addition; c) ratio of zero-valent S increase from control to sulfate-treatment versus original zero-valent S concentrations in control for anaerobic soil incubations of 31 paddy soils from China and 2 paddy soils from Italy.

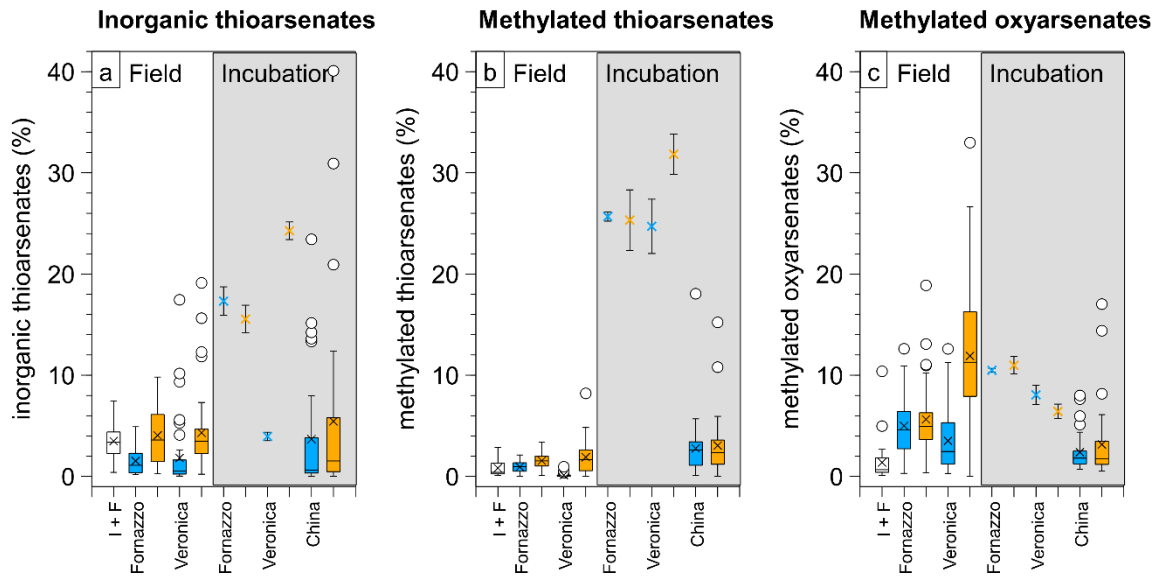


Figure S16 | Comparison of arsenic speciation in anaerobic soil incubations to mesocosm experiments and field survey. a) occurrence of inorganic thioarsenates, b) methylated thioarsenates, and c) methylated oxyarsenates in the field with plants (one-time survey Italy/France at late plant growth stage (I+F); n = 35; mesocosms with Veronica and Fornazzo soil integrated over whole rice cultivation period of 4 months; n = 42 each) and in anaerobic soil incubations (with Veronica and Fornazzo soils (n=3 each) and paddy soils over a pH-gradient in China (n=31 each); blue colors refer to control treatments (no S), orange colors to sulfate addition (S))

4. Methods

Table S8 | Quantitative Recovery of As species in a fresh model pore water sample spiked with 1 µg/L of DMA, DMMTA, arsenite, MMA, MMMTA, and arsenate, stabilized with 10 mM DTPA, and analyzed 1:5 and 1:10 diluted with deionized water using 2.4 % methanol in the eluent and either individual or averaged calibration

	Counts per second										Sum of As species	
	DMA	DMMTA ^a	Arsenite	DMDTA ^b	MMA	MMMTA ^c	MMDTA ^d	Arsenate	MTA ^e	DTA ^f		
DMA 1 µg/L Standard	1001699											
MMA 1 µg/L Standard					815446							
Arsenate 1 µg/L Standard							876310					
sample 1:10 dilution	151318	164191	37415	14160	114871	62514	87301	252602	19856	13196		
sample 1:5 dilution	309624	400192	104872	36697	247134	153063	185058	415801	23790	13544		
sample 1:10 dilution (measured concentration)	0.15	0.16	0.04	0.02	0.14	0.08	0.10	0.29	0.02	0.02		
sample 1:5 dilution (measured concentration)	0.31	0.40	0.11	0.05	0.30	0.19	0.21	0.47	0.03	0.02		
sample 1:10 dilution x 10 (final concentration by individual calibration)	1.51	1.64	0.37	0.17	1.41	0.77	1.00	2.88	0.23	0.15		10.85 ^g

	DMA	DMMTA ^a	Arsenite	DMDTA ^b	MMA	MMMTA ^c	MMDTA ^d	Arsenate	MTA ^e	DTA ^f	Sum of As species
sample 1:5 dilution x 5 (final concentration by individual calibration)	1.55	2.00	0.52	0.23	1.52	0.94	1.06	2.37	0.14	0.08	10.94 ^g
sample 1:10 dilution x 10 (final concentration by averaged calibration)	1.69	1.83	0.42	0.16	1.28	0.70	0.97	2.81	0.22	0.15	11.02 ^g
sample 1:5 dilution x 5 (final concentration by averaged calibration)	1.72	2.23	0.58	0.20	1.38	0.85	1.03	2.32	0.13	0.08	11.14 ^g
sample 1:10 dilution	13.9%	15.1%	3.4%	1.6%	13.0%	7.1%	9.2%	26.6%	2.1%	1.4%	>2.5% well detectable
sample 1:5 dilution	14.1%	18.3%	4.8%	2.1%	13.9%	8.6%	9.7%	21.7%	1.2%	0.7%	>1% well detectable
(%) of total As											

Table S9 | Characteristics of irrigation water for mesocosm rice cultivation experiments.

Parameters	Irrigation water
pH	7.7
Conductivity ($\mu\text{S}/\text{cm}$)	508
TIC (mg/L) ^a	17.5
TOC (mg/L) ^b	1.2
Cl^- (mg/L)	11.4
NO_3^- (mg/L)	1.11
NO_2^- (mg/L)	1.05
PO_4^{3-} (mg/L)	1.01
SO_4^{2-} (mg/L)	11.1
Si (mg/L)	8.9
Mn ($\mu\text{g}/\text{L}$)	1.5
Cu ($\mu\text{g}/\text{L}$)	2.6
Zn ($\mu\text{g}/\text{L}$)	16.5
As ($\mu\text{g}/\text{L}$)	6.4

^a Total inorganic carbon; ^b Total organic carbon

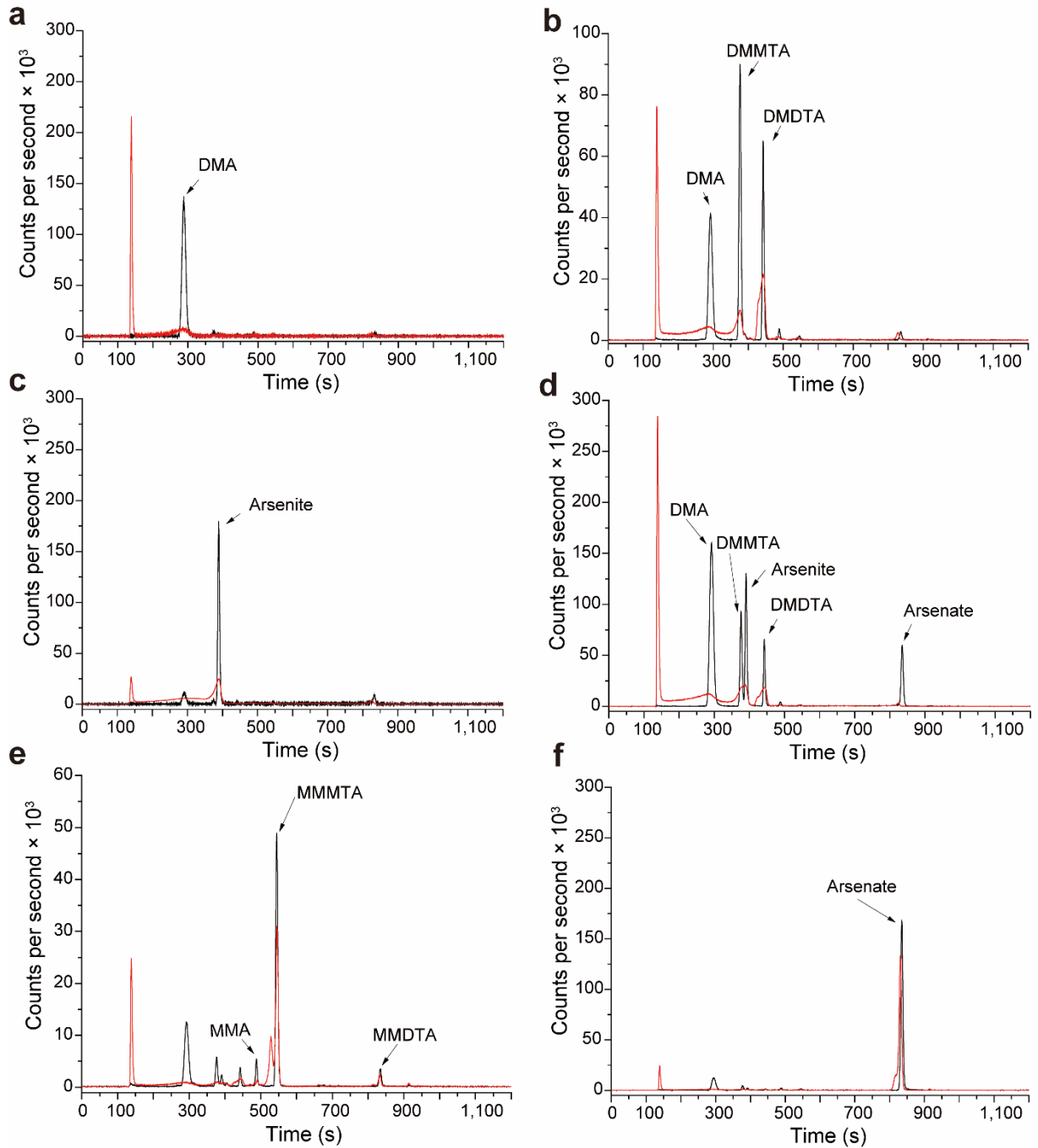


Figure S17 | Effect of 10 mM DTPA on retention time, peak shape, and resolution of As speciation. Tested model pore-water was spiked with 100 $\mu\text{g/L}$ standards of a) DMA; b) DMMTA; c) arsenite; d) a mix of arsenite, DMA, DMMTA; e) MMMTA; f) arsenate; black lines = without DTPA, red lines = with 10 mM DTPA.

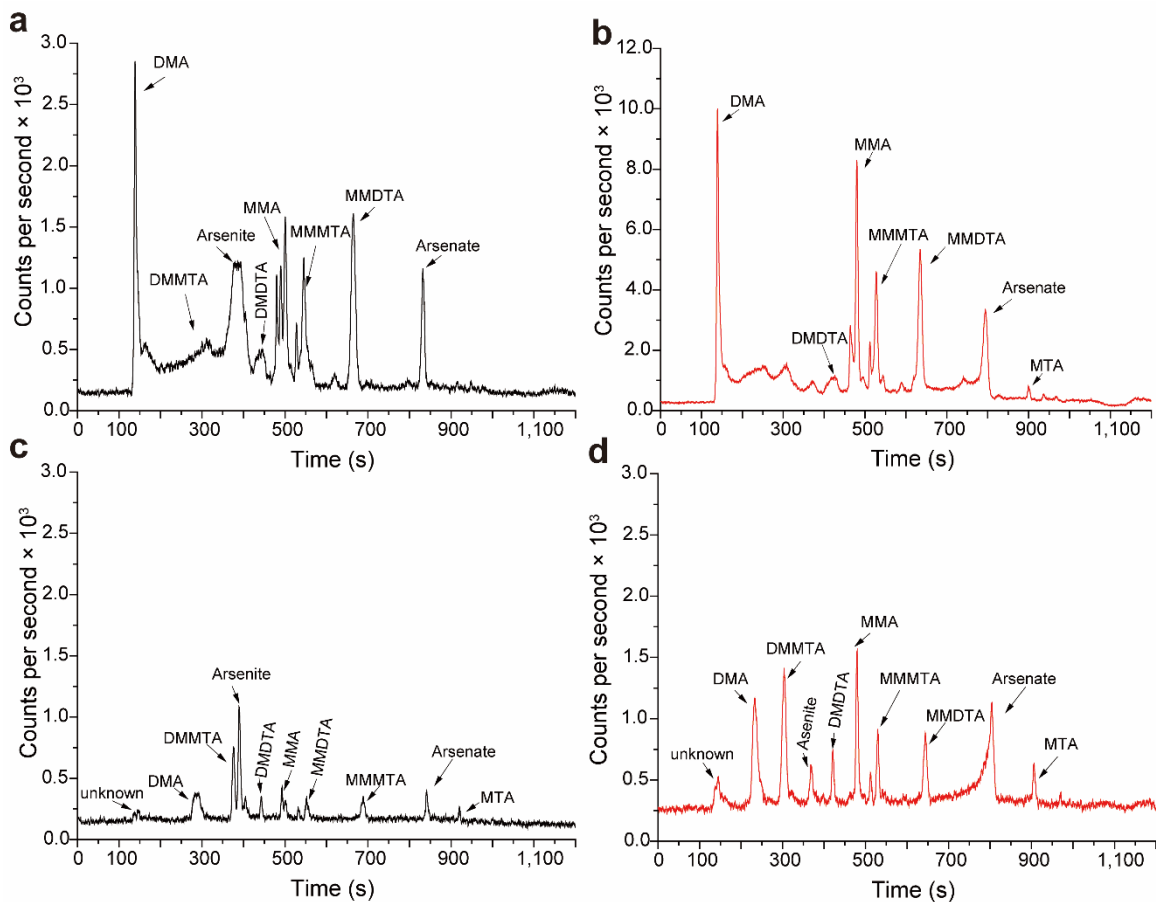


Figure S18 | Effect of sample dilution and use of methanol in the eluent on retention time, peak shape, and resolution of As speciation. Fresh, non-spiked model pore-water samples stabilized with 10 mM DTPA were a) analyzed without dilution and without 2.4% methanol; b) analyzed without dilution with 2.4% methanol; c) diluted 1:10 with deionized water before analysis and analyzed without 2.4% methanol; d) diluted 1:10 with deionized water before analysis and analyzed with 2.4% methanol. All samples were analyzed with a 2.5-100 mM NaOH gradient eluent.

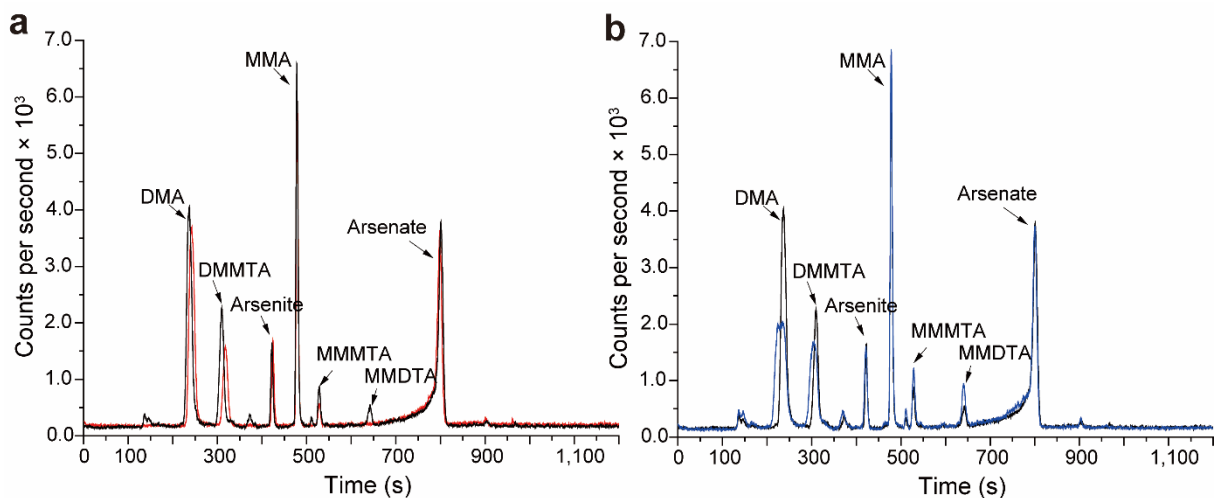


Figure S19 | Effect of pore-water matrix and different DTPA dilution on retention time, peak shape, and resolution of As speciation. Fresh model pore-water samples were spiked with 1 $\mu\text{g/L}$ of DMA, DMMTA, arsenite, MMA, MMMTA, and arsenate, stabilized with 10 mM DTPA (all analyzed with 2.4% methanol in the eluent). a) comparison deionized water (red) and pore-water matrix 1:10 diluted (black), b) comparison 1:5 (blue) vs. 1:10 (black) dilution of pore-water matrix sample.

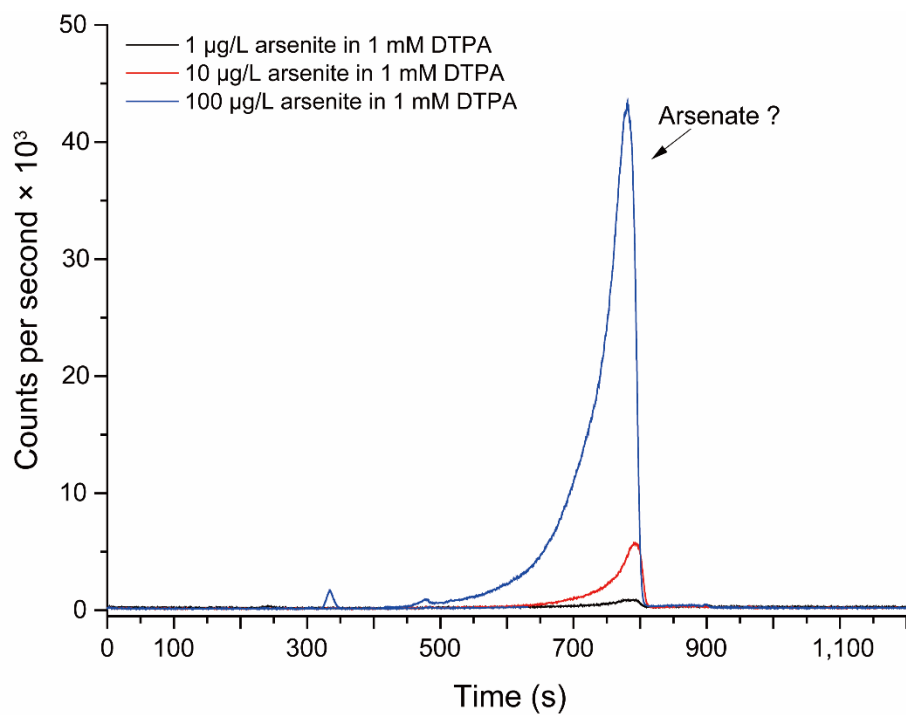


Figure S20 | Effect of 1 mM DTPA on arsenite standards in deionized water. The question mark behind the arsenate label indicates that the observed transformation product elutes at the retention time of arsenate but might also be an unidentified As-DTPA complex.

References

1. Samanta G, Clifford DA. Preservation of inorganic arsenic species in groundwater. *Environmental Science & Technology* 2005, **39**(22): 8877-8882.
2. Planer-Friedrich B, London J, McCleskey RB, Nordstrom DK, Wallschläger D. Thioarsenates in geothermal waters of Yellowstone National Park: determination, preservation, and geochemical importance. *Environmental Science & Technology* 2007, **41**(15): 5245-5251.
3. Kerl CF, Schindele RA, Brüggewirth L, Colina Blanco AE, Rafferty C, Clemens S, *et al.* Methylated thioarsenates and monothioarsenate differ in uptake, transformation, and contribution to total arsenic translocation in rice plants. *Environmental Science & Technology* 2019, **53**(10): 5787-5796.
4. Kerl CF, Rafferty C, Clemens S, Planer-Friedrich B. Monothioarsenate uptake, transformation, and translocation in rice plants. *Environmental Science & Technology* 2018, **52**(16): 9154-9161.
5. Wallschläger D, London J. Determination of methylated arsenic-sulfur compounds in ground water. *Environmental Science & Technology* 2008, **42**(1): 228–234.
6. Lohmayer R, Kappler A, Lösekann-Behrens T, Planer-Friedrich B. Role of sulfur species as redox partners and electron shuttles for ferrihydrite reduction by *Sulfurospirillum deleyianum*. *Applied and Environmental Microbiology* 2014: AEM. 04220-04213.
7. Couture RM, Rose J, Kumar N, Mitchell K, Wallschläger D, Van Cappellen P. Sorption of arsenite, arsenate, and thioarsenates to iron oxides and iron sulfides: a kinetic and spectroscopic investigation. *Environmental Science & Technology* 2013, **47**(11): 5652-5659.
8. Saalfield SL, Bostick BC. Changes in iron, sulfur, and arsenic speciation associated with bacterial sulfate reduction in ferrihydrite-rich systems. *Environmental Science & Technology* 2009, **43**(23): 8787-8793.
9. Jia Y, Bao P, Zhu Y-G. Arsenic bioavailability to rice plant in paddy soil: influence of microbial sulfate reduction. *Journal of Soils and Sediments* 2015, **15**(9): 1960-1967.
10. De'Ath G. Multivariate regression trees: a new technique for modeling species-environment relationships. *Ecology* 2002, **83**(4): 1105-1117.
11. Planer-Friedrich B, Franke D, Merkel B, Wallschläger D. Acute toxicity of thioarsenates to *Vibrio fischeri*. *Environmental Toxicology and Chemistry* 2008, **27**(10): 2027-2035.
12. Suess E, Mehlhorn J, Planer-Friedrich B. Anoxic, ethanolic, and cool – An improved method for thioarsenate preservation in iron-rich waters. *Applied Geochemistry* 2015, **62**: 224-233.

Study 2: Monothioarsenate Uptake, Transformation, and Translocation in Rice Plants

Carolin F. Kerl, Colleen Rafferty, Stephan Clemens, Britta Planer-Friedrich

Reprinted with permission from

Environmental Science & Technology (52, pp. 9154-9161)

Copyright 2018 American Chemical Society

Monothioarsenate Uptake, Transformation, and Translocation in Rice Plants

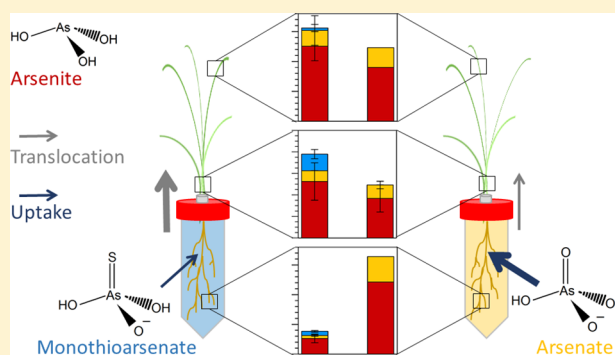
Carolin F. Kerl,[†] Colleen Rafferty,[‡] Stephan Clemens,[‡] and Britta Planer-Friedrich^{*,†,‡}

[†]Environmental Geochemistry, Bayreuth Center for Ecology and Environmental Research (BayCEER), University of Bayreuth, D-95440 Bayreuth, Germany

[‡]Plant Physiology, Bayreuth Center for Ecology and Environmental Research (BayCEER), University of Bayreuth, D-95440 Bayreuth, Germany

Supporting Information

ABSTRACT: Thioarsenates form under sulfur-reducing conditions in paddy soil pore waters. Sulfur fertilization, recently promoted for decreasing total arsenic (As) grain concentrations, could enhance their formation. Yet, to date, thioarsenate toxicity, uptake, transformation, and translocation in rice are unknown. Our growth inhibition experiments showed that the toxicity of monothioarsenate (MTA) was similar to that of arsenate but lower than that of arsenite. Higher toxicity of MTA with lower phosphate availability might imply uptake through phosphate transporters similar to arsenate. To demonstrate direct uptake of MTA by rice plants, a species-preserving extraction method for plant samples was developed. When plants were exposed to 10 μ M MTA for 72 h, up to 19% and 4% of total As accumulated in roots and shoots, respectively, was MTA. Monothioarsenate was detected in xylem sap and root exudates, and its reduction to arsenite in rice roots and shoots was shown. Total As uptake was lower upon exposure to MTA compared to arsenate, but root to shoot translocation was higher, resulting in comparable As shoot concentrations. Thus, before promoting sulfur fertilization, uptake and detoxifying mechanisms of thioarsenates as well as potential contribution to grain As accumulation need to be better understood.



INTRODUCTION

Human arsenic (As) exposure from rice consumption is a well-known problem. Rice takes up approximately 10 times more As than other crops^{1,2} and is a major staple food for half of the world's population.^{3,4} Inorganic As (arsenate and arsenite) is a class 1 carcinogen, and there is no safe intake limit for humans.⁴ In soils, As is ubiquitously present with an average global geogenic background ranging from 5 to 7.5 mg/kg.⁵ During rice cultivation on flooded paddy soils, As is mobilized due to reducing conditions with arsenite being the dominant species. Arsenate might form, e.g. in the rhizosphere due to rice plant root oxygen loss.^{6–8}

Arsenate (pK_{a1} 2.2, pK_{a2} 6.9) is a structural analog to phosphate (pK_{a1} 2.1, pK_{a2} 7.1) and is taken up inadvertently in rice plants via phosphate transporters such as OsPht1;1,⁹ OsPht1;4,^{10,11} or OsPht1;8.¹² Arsenite (pK_{a1} 9.2) is uncharged (H_3AsO_3) in paddy soil pore water and passively taken up via nodulin 26-like intrinsic protein (NIP) aquaglyceroporins Lsi1 (OsNIP2),^{13–16} a transporter for silicic acid. If As is in its oxidized state, it will, after uptake, first be reduced to arsenite by arsenate reductase, for example HAC1;1, HAC1;2, and HAC4.^{17,18} Arsenite is then either effluxed from the roots^{15,19} or complexed by phytochelatin (PC)^{20–23} and stored as arsenite-PC complexes in root vacuoles after transport by

OsABCC1.²⁴ Both processes decrease As toxicity in the plant. Part of the arsenite might also be loaded into the xylem, presumably by NIP proteins.^{19,25,26} Further transfer from xylem to phloem in node I is required to transport As into the grains via long-distance phloem transport.¹⁹

Until now, only the uptake of inorganic and methylated (mono- and dimethyl As acid) As species has been studied in rice plants. No information about the uptake of thioarsenates ($HAsS_nO_{4-n}^{2-}$, $n = 1–4$) is available. Thioarsenates are structural analogues to arsenate and form under sulfur-reducing conditions from arsenite by OH^-/SH^- -ligand exchange and oxidative addition of zerovalent sulfur.^{27–29} Sulfur-reducing conditions can occur in flooded rice paddy fields,^{30,31} especially when sulfur (S) is applied as fertilizer. This has recently been suggested to lower grain As concentrations^{30,32–36} with the beneficial side effect that emissions of methane are significantly decreased.³⁷ No conclusive data about the effects of S fertilization have been obtained so far. Enhanced formation of PCs and arsenite-PC

Received: April 25, 2018

Revised: July 12, 2018

Accepted: July 19, 2018

Published: July 19, 2018

complexes^{32,33,35} or iron plaque^{34,35} were proposed as the dominant mechanisms. However, thiolation could also be a significant process depending on the S(-II)/As(III) and S(0)/As(III) ratios, pH, and micro-oxic conditions in the soil. First data from recent studies in our group show that thioarsenates can contribute up to 10% to total As in natural paddy soils without sulfate fertilization and up to 60% in microcosms with sulfate spikes.³⁸ Monothioarsenate (MTA) is the most stable of all thioarsenate species³⁹ and can occur over the whole pH range typically found in paddy fields (pH 2.5–8).^{31,40}

The toxicity and uptake of MTA has to date only been studied in the model plant *Arabidopsis thaliana*.⁴¹ Monothioarsenate was found to be more toxic than arsenate but less toxic than arsenite, and root to shoot translocation was higher for MTA compared to arsenate. Additional experiments with PC-synthesis and transport mutants showed that the PC detoxification pathway is important for MTA as well as for arsenate. However, in the absence of species-preserving extraction protocols, As speciation in *A. thaliana* roots and shoots could not be investigated, and therefore no direct evidence for uptake of intact MTA by plants could be obtained.

The aim of this study was to develop an extraction method for MTA in rice roots and shoots and to generate information about toxicity, uptake, transformation, and translocation of MTA in rice plants. Growth inhibition by arsenite, arsenate, and MTA was compared for 20 days exposure in hydroponic culture. Reduction of arsenate and MTA to arsenite and efflux of arsenate and MTA to the nutrient solution were investigated. Uptake, transformation, and translocation were studied in short-term hydroponic experiments.

METHODS AND MATERIALS

Growth Conditions for Rice. All experiments were conducted with a European rice variety (*Oryza sativa* L. cv. Arelate), and seedlings were grown under the following conditions unless specified otherwise. Rice grains were germinated inside a plastic box on wet paper towels at 33 °C for 7 days (d). Seedlings were transferred into polymerase chain reaction (PCR) tubes (Biozym) and placed in 50 mL tubes (Sarstedt) containing nutrient solution (Table SI 1). The plants were grown inside a growth cabinet under long day conditions (16 h of light/8 h of darkness) at 23 °C and 110 μE for 20 d, and the nutrient solution was changed twice a week to ensure sufficient supply of nutrients.

Method Development for MTA Extraction from Plant Tissues. *Stability of MTA in MQ Extracts of Plant Tissues.* Monothioarsenate stability was tested in the presence of rice roots and shoots to determine whether plant tissues affect As speciation. Therefore, rice plants were grown hydroponically without As for 20 d. Shoots and roots were flash-frozen and ground in liquid nitrogen (N_2) or dried for 2 days at 110 °C to destroy enzymes and other proteins. Microreaction tubes (Sarstedt) were filled with 0.4 g of glass beads (Retsch), 0.7 g of shoot material, or 0.4 g of root material, respectively, and 1.5 mL of 0.66 μM MTA in ultrapure water (MQ). Because of a lack of a commercially available standard, MTA was synthesized as $\text{Na}_3\text{AsO}_3\cdot\text{S}\cdot 2\text{H}_2\text{O}$ in our laboratory as described in detail previously.^{42,43} The purity was 98.5% MTA, the remainder being 0.5% arsenite and 1% arsenate (analyzed by IC-ICP-MS). Stability tests of 0.66 μM MTA were performed under N_2 -atmosphere using a glovebox (COY, N_2/H_2 95/5% (v/v)). Samples were vortexed at room temperature (RT) for

10–240 min. An extra subset of flash-frozen roots and shoots was heated in a boiling water bath for 5 min and then cooled back to RT in an ice bath for 2 min followed by 53 min vortexing at RT to destroy enzymes and other proteins. The two methods are termed “RT” and “5 min boiling” in the following. All samples were filtered with 0.2 μm cellulose acetate (CA) filters (Machery-Nagel), and As speciation was analyzed within 30 min using ion-chromatography coupled to inductively coupled plasma mass spectrometry (IC-ICP-MS).

Stability of MTA in Different Extractants in the Absence of Plant Tissues. To date, there is no method for the extraction of thioarsenates from plant tissues. We tested the stability of arsenite and MTA (0.66 μM each) in different potential extractants in the absence of plants. The extractants were phosphate-buffer (PBS; 2 mM NaH_2PO_4 (Grüssing) + 0.2 mM $\text{Na}_2\text{-EDTA}$ (Grüssing); pH 6.0),⁴⁴ MQ, 0.1 and 0.01 M NaOH (Merck), 10% ethanol (EtOH, VWR), 1% formic acid (FAc, Fluka), and 0.28 M HNO_3 (Kraft). These extractants were selected because arsenite and arsenate are commonly extracted using PBS,^{6,44–46} whereas earlier publications tested MQ, NaOH, and MQ:methanol mixtures.^{47–49} For the extraction of As phytochelatin complexes, 1% formic acid was used in earlier studies,⁵⁰ and for As speciation analysis rice grains are often extracted using 0.28 M HNO_3 .^{51,52} For all extractants, the two different extraction procedures, RT and 5 min boiling, were tested for 60 min.

Evaluation of Extraction Efficiency in Different Extractants in the Presence of Plant Tissues. Extraction was then tested using 20 d old plants which were exposed to P-free nutrient solution containing 50 μM MTA for 24 h. The nutrient solution was changed every 6 and 12 h during day- and nighttime, respectively, to maintain As speciation (3 replicates for MTA and 1 for arsenate exposure). After exposure, rice roots were washed for 10 min using 1 mM KH_2PO_4 (Grüssing), 0.5 mM $\text{Ca}(\text{NO}_3)_2$ (Grüssing), and 5 mM MES (Roth),^{44,53} flash-frozen, and ground in liquid N_2 . Between 0.03 and 0.05 g of shoot or root material was extracted under N_2 -atmosphere in ultrapure water, 10% EtOH, or PBS using both extraction procedures described above (RT and 5 min boiling), and As speciation was analyzed immediately by IC-ICP-MS. In addition to that, total As concentrations in roots and shoots were determined by ICP-MS after microwave digestion.

Toxicity Experiment. In order to obtain growth inhibition curves, arsenite (NaAsO_2 ; Fluka), arsenate ($\text{Na}_2\text{HAsO}_4\cdot 7\text{H}_2\text{O}$; Fluka), or MTA were added to the nutrient solution (5–225 μM ; Table SI 2) for the whole growth period of 20 d (4 replicates for each treatment). The same experiment was also performed with only 50% of the initial phosphate concentration in the nutrient solution (–50% P; 5–150 μM As; Table SI 2) to investigate whether MTA might be taken up via phosphate transporters like arsenate. After 20 d, the primary root and shoot lengths, as well as the seedling fresh weights, were determined. The stability of arsenite, arsenate, or MTA was tested by incubating the nutrient solution without plants for 4 d in the growth cabinet and analyzing the As speciation with IC-ICP-MS (4 d was the maximum time before changing the nutrient solution). Dose response curves were derived from these data using a three-parameter-log–logistic dose–response model in the program Sigma plot and the IC_{50} values were obtained graphically.

MTA and Arsenate Influx/Efflux Experiments. For quantifying species transformation of arsenate and MTA in the

nutrient solution, 20 d old plants were exposed to 10 μM arsenate or MTA for 24 h in a 100 mL P-free nutrient solution. For analysis of As speciation in the nutrient solution, samples were taken after 0, 3, 5, 7.5, 12, and 24 h, filtered through 0.2 μm CA filters, and flash-frozen until analysis by IC-ICP-MS (Influx-experiment, 4 replicates per treatment). The nutrient solution, containing 10 μM arsenate or MTA, was changed after 6 and 12 h during day- and nighttime, respectively, for all further experiments to maintain As speciation. For quantifying the As efflux into the nutrient solution after arsenate or MTA exposure for 24 h, roots were washed as described before and placed into a 15 mL As-free solution containing tap water with P- and Ca-concentrations like in the original nutrient solution. This solution was selected because pretests with different growth media compositions (MQ/tap water, \pm Ca, \pm P, and \pm Fe) showed best MTA stability at low concentrations (10 ppb). Arsenic speciation samples were taken after 3, 9, and 24 h, filtered through 0.2 μm CA filters, and flash-frozen until analysis by IC-ICP-MS (Efflux-experiment, 4 replicates).

Sampling of Xylem Sap. To obtain xylem sap, plants exposed to 10 μM arsenate or MTA for 24 h were cut 2 cm above the roots with a sharp blade. Xylem was collected over 1.5 h using a 2 μL pipet. Samples were diluted in 750 μL of ice-cold PBS, and As speciation was analyzed immediately by IC-ICP-MS (9 replicates). Xylem sap collected from three plants was pooled into one sample.

MTA and Arsenate Uptake and Translocation. To follow uptake and translocation of arsenate and MTA, rice plants were exposed to 10 μM arsenate or MTA for 3, 6, 24, 48, and 72 h. Sampled roots were washed as described before (3 replicates for MTA, 1 replicate for arsenate). After the fresh weights of roots and shoots were determined, plants were flash-frozen and ground in liquid N_2 . Plant material (0.01–0.06 g) was extracted in 1.5 mL of PBS. Samples were boiled for 5 min and vortexed for an additional 55 min as described above (“5 min boiling” method). Arsenic speciation was analyzed immediately, and additional samples were microwave-digested to obtain total As concentrations. Translocation factors were calculated (As-shoot/As-root).

As-Measurements. Arsenic speciation was analyzed by IC (Dionex ICS-3000) using a PRP-X100 column (Hamilton, 10 mM NH_4NO_3 , 10 mM $\text{NH}_4\text{H}_2\text{PO}_4$, and 500 mg/L $\text{Na}_2\text{-EDTA}$ at a flow rate of 1.0 mL/min and 50 μL injection volume)⁵⁴ coupled to ICP-MS (XSeries2, Thermo-Fisher) using oxygen as reaction cell gas (AsO^+ , m/z 91). Retention times of arsenite, arsenate, and MTA were determined using individual standards. For total As concentrations, 0.01–0.08 g of plant material was digested in concentrated HNO_3 (Kraft) and 30% H_2O_2 (VWR) (ratio 1.5:1) in a CEM Mars 5 microwave digestion system (CEM Corp., Matthews, NC) and analyzed by ICP-MS.

RESULTS AND DISCUSSION

Evaluation of the Species-Preserving Extraction Method. First tests of MTA stability in shoot and root matrices showed significant reduction of MTA to arsenite (38 and 83% MTA remained after 240 min, respectively). No reduction to arsenite was observed in controls without plants over 240 min (98% MTA, Figure 1) as well as in experiments where plants were dried at 110 $^\circ\text{C}$ for 2 days, destroying all enzymes and other proteins. No kinetic information can be obtained from this experiment, because the amount of proteins present in the roots and shoots was not quantified. Never-

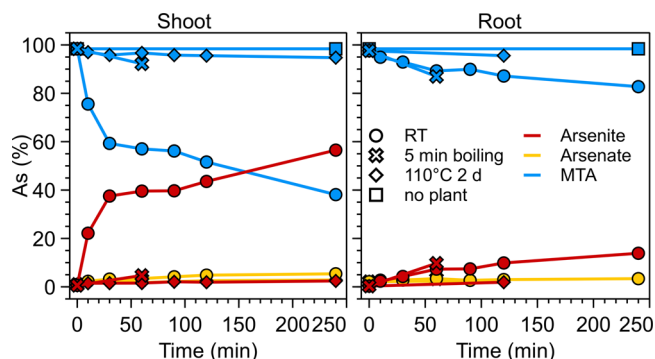


Figure 1. Test of 0.66 μM MTA stability in the presence of shoot (left) and root extracts (right) from 20 d old rice seedlings grown without As exposure. Test conditions were as follows: powders of flash frozen roots and shoots extracted in MQ for 10–240 min at RT (circles) or boiled for 5 min and then extracted for 55 min at RT (crosses); powder of roots and shoots dried at 110 $^\circ\text{C}$ for 2 d and extracted in MQ for 10–240 min at RT (diamonds), all in comparison to controls without plants (squares). As speciation of the initial MTA solution was determined by IC-ICP-MS for different treatments of plant samples; legend in the right panel applies to both graphs.

theless, the tests clearly showed that MTA reduction to arsenite was an enzymatic process. For speciation analyses of root and shoot samples, drying samples at 110 $^\circ\text{C}$ for 2 days was not an option because it may alter As speciation. Previous experiments at 80 $^\circ\text{C}$ had shown no speciation changes for MTA over 2 h⁵⁵ but a transformation of about 60% MTA to arsenite after 2 d.⁵⁶ We therefore tested boiling samples for a very short time (5 min) and vortexing them for 55 min afterward. Using this “5 min boiling” method, MTA transformation was limited to less than 8% and 13% in shoots and roots, respectively.

Testing the stability of arsenite and MTA in different potential extractants in the absence of plants, we found that MTA was stable in all extractants (95–99%; Figure SI 1) at RT, while arsenite was only stable in PBS, MQ, and 10% EtOH over 60 min (94–100%; Figure SI 2). Therefore, NaOH, HNO_3 , and formic acid are excluded from the following discussion. Results can be found in Figures SI 1 and 2 (62–80% arsenite recovery). In the absence of plants, arsenite and MTA were stable in PBS, MQ, and 10% EtOH when samples were boiled before (“5 min boiling”; Figure SI 2). Testing the stability of MTA in different potential extractants in the presence of rice shoot and root material, MTA was partially reduced to arsenite in all extractants (57–84 and 87–91% MTA remained in shoots and roots after 60 min, respectively) at RT. Boiling the samples for 5 min limited the reduction of MTA to arsenite to less than 10% (91–92 and 87–93% MTA) in shoots and roots.

The extraction efficiency was tested with rice seedlings exposed to 50 μM MTA for 24 h (Figure 2). Extraction at RT using PBS, MQ, and 10% EtOH showed large variations between the extractants (27–37 and 101–247 $\mu\text{mol}/\text{kg}$ in shoots and roots) and poor recovery (76–102 and 70–172%) especially for root samples. After boiling the samples for 5 min no or minor differences were observed between MQ, PBS, and 10% EtOH in shoots and roots (31–33 and 190 $\mu\text{mol}/\text{kg}$). Comparing the results for As concentrations from total As analysis by ICP-MS versus the sum of species analyzed by IC-ICP-MS (arsenite, arsenate, MTA) we found an overall

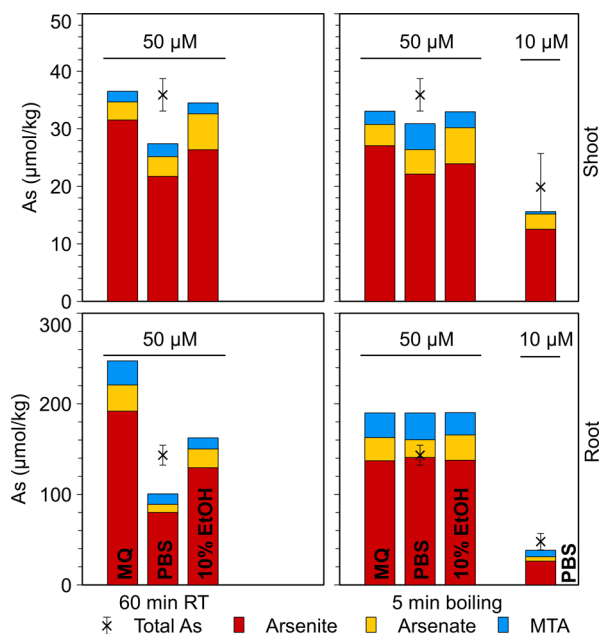


Figure 2. Comparison of As extraction in shoots (top panel) and roots (bottom panel) using MQ, PBS, and 10% EtOH at RT for 60 min (left) or after 5 min boiling and 55 min at RT (right). Rice seedlings were grown for 20 d without As and exposed to 50 µM and 10 µM MTA for 24 h. Nutrient solution was exchanged frequently during influx to minimize reduction to arsenite (every 6 h during daytime and after 12 h during nighttime). Total As concentrations were determined after microwave digestion (cross) ($n = 3$).

good agreement for the shoot samples (sum of species slightly lower than totals; 86–92%, $n = 3$, Figure 2 upper right panel). For the roots, samples exposed to 10 µM MTA for 24 h showed comparable values (sum of species 72–83% of totals, $n = 3$), but in plants exposed to 50 µM MTA for 24 h the sum of species was consistently higher than totals (132%; $n = 3$, Figure 2 lower right panel). Whether this difference was due to underestimation of totals or overestimation of species concentrations could not be determined. However, considering all samples that were analyzed for this study, no systematic error was found for comparison of sum of species to total As concentration ($94 \pm 32\%$, $n = 52$). Higher uncertainties were especially found in plants after short-term exposure (3 or 6 h) where total As concentrations as low as 2.6 nM were measured which are close to the limit of quantification of 1.5 nM for our ICP-MS.

Monothioarsenate Toxicity to Rice. Exposing rice seedlings to increasing arsenite, arsenate, and MTA concentrations resulted in lower relative shoot lengths and weights (Figure 3). Growth inhibition was strongest for arsenite (IC_{50} of shoot weight: 4 µM; Figures SI 3, 4) followed by MTA (IC_{50} : 50 µM) and arsenate (IC_{50} : 190 µM). When the phosphate concentration in the nutrient solution was lowered by 50%, IC_{50} values for arsenate (IC_{50} : 25 µM; Figures SI 3, 5) and MTA (IC_{50} : 7.5 µM) were decreased by a factor of 6.7 and 7.6, respectively, whereas arsenite (IC_{50} : 3.1 µM) decreased only by a factor of 1.4 (Table SI 3). The results from this toxicity experiment clearly showed that MTA was toxic for rice plants. The higher toxicity of MTA in nutrient solution with lower phosphate availability could be indirect evidence for MTA uptake through phosphate transporters similar to arsenate^{10,57} (detailed discussion see below). The same order

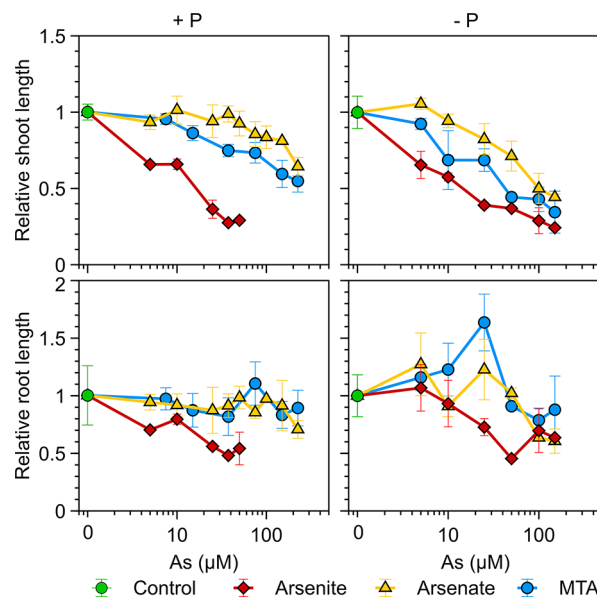


Figure 3. Relative root and shoot lengths for 20 d old rice seedlings exposed to increasing concentrations (logarithmic scale) of arsenite, arsenate, and MTA ($n = 4$) in original nutrient solution (+ P; left panel) and with 50% reduction of phosphate (– P; right panel) in the nutrient solution.

of toxicity (arsenite > MTA > arsenate) was observed in experiments with *A. thaliana*⁴¹ and human cells⁵⁸ before.

Arsenic Speciation Changes in Nutrient Solution of Hydroponic MTA Influx and Efflux Experiments. In the nutrient solution (control without plants), arsenite, arsenate, and MTA stability was confirmed over 4 days. Less than 10% oxidation to arsenate was found for arsenite and MTA. Arsenate was completely stable (Figure SI 6). In contrast to the control without plants, significant reduction of MTA to arsenite was observed in hydroponic cultures with rice seedlings (Figure 4; Influx experiment). Within 6 h, 50% of

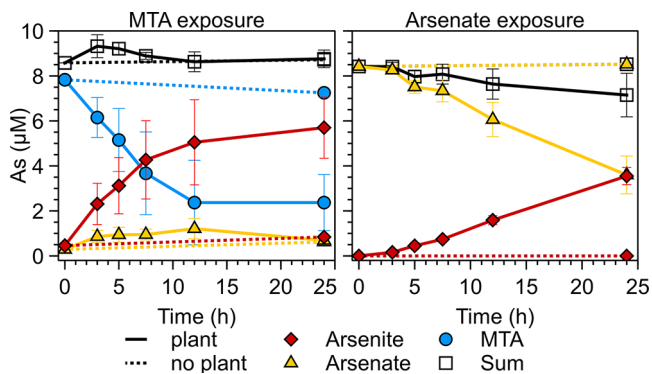


Figure 4. Arsenic speciation in growth media monitored over 24 h with rice seedlings exposed to 10 µM MTA (left) or arsenate (right) and control without plants in dashed lines (Influx experiment, $n = 4$). Sum of species and totals are used as synonyms in the text.

MTA was reduced to arsenite, whereas arsenate reduction was slower (50% reduced to arsenite after 24 h). For arsenate, reduction to arsenite and efflux of arsenite is a known part of the detoxification process.^{44,59} The reduction of MTA to arsenite by plants has not been observed so far, while microbes are known to transform MTA to arsenite^{27,55,56,60} or arsenate.⁶¹

Total As concentrations did not change in the hydroponic cultures over 24 h during MTA exposure, but during arsenate exposure, total As started to decrease after 12 h ($1.3 \pm 1.0 \mu\text{M}$ loss after 24 h). The loss of As in the nutrient solution is already a first indication toward higher uptake of arsenate into the rice roots, which is later also mirrored in higher As concentrations detected in arsenate-exposed roots (see discussion below). After the observed rapid reduction of MTA to arsenite by rice seedlings in these experiments, we renewed the nutrient solution in all further experiments every 6 h during daytime and every 12 h during nighttime to minimize arsenite uptake.

The reduction of MTA to arsenite in the nutrient solution gave indirect evidence that MTA is actively taken up by rice plants and reduced inside the plant to arsenite and that this arsenite is then effluxed from the roots. However, reduction on the root surface could not be excluded. We therefore investigated the root efflux in As-free media after 24 h exposure to arsenate or MTA (Figure SI 7, Efflux experiment). Total effluxed As concentrations were 4-times higher in plants exposed to arsenate ($82 \pm 3 \mu\text{mol/kg}$ root) than in plants exposed to MTA ($21 \pm 3 \mu\text{mol/kg}$ root). In plants exposed to MTA, we detected up to 3% MTA in the efflux medium, which supports the assumption that MTA was taken up intact into the plant. Surprisingly, the dominant As species detected in the efflux medium after both exposure to arsenate and MTA was arsenate (84–97%), not arsenite. This dominance of arsenate might be due to oxidation or preferential release of non-PC-complexed As (Note that total concentrations in the efflux experiment are 10–20 times lower than in the influx experiment; for a detailed discussion on the possible reasons for arsenate dominance in the efflux also refer to Figure SI 7.).

Detection of Monothioarsenate in the Xylem Sap.

Both the influx and the efflux experiments provided indirect evidence that MTA can be taken up by rice plants, yet direct detection in plant material was still missing. By sampling xylem sap from plants exposed to arsenate or MTA for 24 h, we were able to directly detect MTA ($20 \pm 5\%$) in the xylem of rice seedlings (Figure 5). This clearly showed that MTA was taken up intact by rice roots and at least partially transported into shoots. Comparing the total amount of As in the xylem, slightly more As was found in the MTA-exposed plants (0.08 ± 0.02

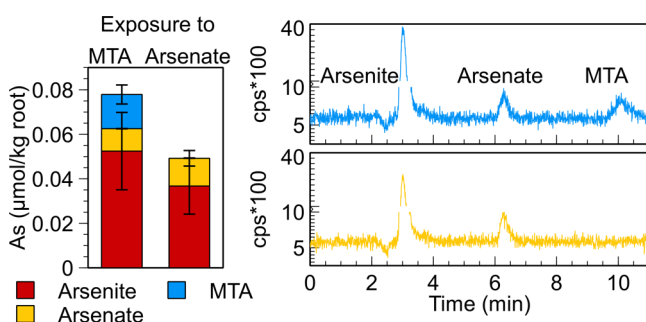


Figure 5. Left side: As speciation in xylem sap of rice seedlings which had been exposed to $10 \mu\text{M}$ MTA (left) or arsenate (right) for 24 h. Sum of species was $0.08 \pm 0.02 \mu\text{mol/kg}$ root for MTA exposure and $0.05 \pm 0.01 \mu\text{mol/kg}$ root for arsenate exposure. Growth media were changed every 6 h (daytime) and after 12 h (nighttime) during influx to minimize reduction to arsenite ($n = 3$). Right side: Exemplary chromatograms for As speciation in xylem analyzed with IC-ICP-MS (MTA exposure: top panel; arsenate exposure: bottom panel).

$\mu\text{mol/kg}$ root) than in arsenate-exposed plants ($0.05 \pm 0.01 \mu\text{mol/kg}$ root), although the difference was not significant.

Analysis of Monothioarsenate Uptake and Translocation Time Courses by Species-Preserving Plant Tissue Extractions. The uptake and translocation of MTA in comparison to arsenate was studied over 72 h in 20 d old rice seedlings. The dominant As species in the roots was arsenite in both treatments (67–77% in MTA-exposed and 63–81% in arsenate-exposed plants, respectively) with minor contributions of arsenate (11–14% and 18–37%, respectively). In MTA-exposed plants, between 12–19% MTA was found in the roots. In shoots, arsenite was the dominant species (71–86%) except for plants exposed to arsenate for more than 48 h (up to 54% arsenate). A maximum of 4% MTA was also detected in shoots. The absolute arsenite concentrations in shoots of the MTA-exposed plants were higher than in the arsenate-exposed plants (ranging from 1.1 to $28.4 \mu\text{mol/kg}$ for MTA and from 0.7 to $20.0 \mu\text{mol/kg}$ for arsenate throughout the 3 to 72 h exposure).

Total As uptake after 72 h was lower in plants exposed to MTA compared to arsenate ($34 \mu\text{mol/kg}$ for MTA exposure compared to $50 \mu\text{mol/kg}$ for arsenate exposure in shoots and $61 \mu\text{mol/kg}$ compared to $360 \mu\text{mol/kg}$ in roots, Figure 6). The higher As uptake, especially in roots, during the arsenate exposure is in line with the higher loss of As found in the arsenate influx experiment (Figure 2). The same trend was observed in *A. thaliana* plants exposed to arsenate and MTA for 4 d, where root uptake was 4–5 times lower for MTA-exposed plants⁴¹ (here 5 times lower after 3 d). No uptake

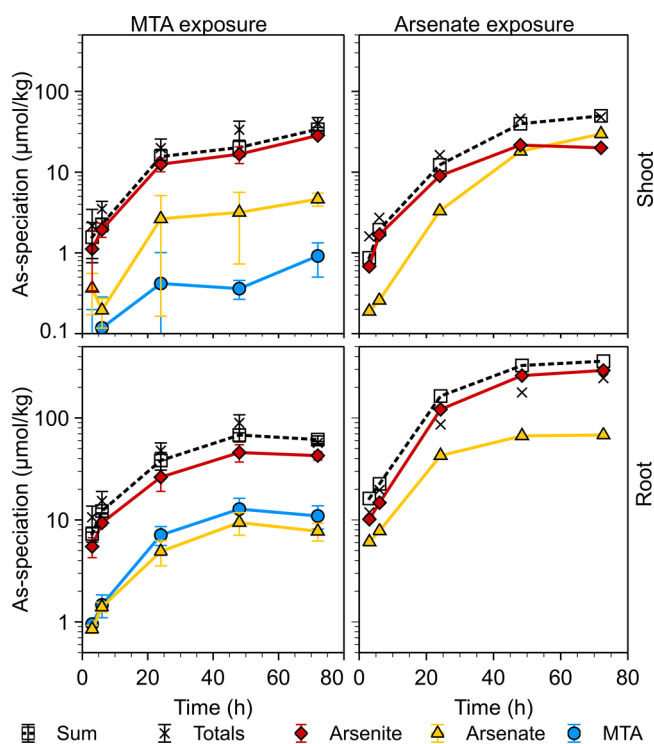


Figure 6. Arsenic uptake kinetics for rice seedlings grown for 20 d without As following exposure to $10 \mu\text{M}$ MTA (left) and arsenate (right) for 3, 6, 26, 48, and 72 h. Arsenic speciation (logarithmic scale) in shoots (top panel) and roots (bottom panel) was determined using PBS-extraction (5 min boiling and 55 min at RT). Total As concentrations were determined after microwave digestion (cross) ($n = 3$ for MTA and $n = 1$ for arsenate).

transporter is known for MTA in plants, yet. However, the increased arsenate and MTA toxicity when plants were grown in the presence of 50% lower phosphate concentration (Figures SI 4, 5) may be interpreted as first evidence that MTA, like arsenate, is taken up inadvertently via phosphate transporters.^{10,19,57} Arsenate [$\text{MW}(\text{HAsO}_4^{2-}) = 140 \text{ g/mol}$; $\text{p}K_{\text{a}2} = 6.9$] and phosphate [$\text{MW}(\text{HPO}_4^{2-}) = 96 \text{ g/mol}$; $\text{p}K_{\text{a}2} = 7.2$] are structural analogues but are slightly different in molecular weight and $\text{p}K_{\text{a}}$ -values. Comparing MTA [$\text{MW}(\text{HAsSO}_4^{2-}) = 156 \text{ g/mol}$; $\text{p}K_{\text{a}2} = 7.3$] to arsenate and phosphate the molecular weight is similar to arsenate, whereas the $\text{p}K_{\text{a}2}$ is similar to phosphate. All three ions have a tetrahedral structure, but the double bonds $\text{As}=\text{O}$ (1.69–1.71 Å^{62,63}), $\text{As}=\text{S}$ (2.14–2.15 Å⁶⁴), and $\text{P}=\text{O}$ (1.56 Å⁶⁵) have different lengths, slightly changing the molecule geometry. Therefore, the chemical parameters of MTA, arsenate, and phosphate might be similar enough to enable uptake through the same phosphate transporters.

The root to shoot translocation factor determined for arsenate in the present study (0.14; Figure SI 8) is comparable to that determined in a previous study (0.1).⁶⁶ In comparison to arsenate, the root to shoot translocation factor for MTA-exposed plants was higher (0.55 ± 0.04 after 72 h). This observation is also in line with the higher As concentrations found in the xylem of MTA-exposed plants in the present study and the reported higher translocation of MTA relative to arsenate in *A. thaliana*.⁴¹ The reason for higher MTA translocation is unclear, yet. One important limitation for As translocation from roots to shoots is detoxification of As by phytochelatins (PC)^{20–23} and storage of arsenite-PC complexes in root vacuoles mediated by OsABCC1.²⁴ The first step in the detoxification process is the reduction of arsenate to arsenite by arsenate reductase.^{17,18} Rapid reduction of MTA to arsenite observed in the present experiments and synthesis of PCs after MTA exposure observed in previous experiments with *A. thaliana*⁴¹ suggest that detoxification of MTA could proceed similar to detoxification of arsenate. Furthermore, in case no reduction or PC-complexation occurs at all, translocation factors should be higher and comparable to those of DMA^V (translocation factor up to 4.9⁶⁷), for which no corresponding DMA-PC complexes⁶⁸ are known. MTA translocation could be comparable to MMA^V (translocation factor up to 0.2^{66,67}) for which relatively high transport to shoots is known despite an efficient reduction to MMA(III) and complexation with PCs in rice roots.^{50,67} Whether MTA can be directly complexed by PCs (e.g., as MTA^{III}-PC) is not known, yet. Differences in identity and localization of the enzymes responsible for MTA reduction to arsenite (or MTA^{III}) compared to those for arsenate reduction to arsenite could result in lower rates of As complexation and storage in roots and more efficient transport to the xylem.

Implications. Improved strategies to decrease As accumulation in rice grains are currently investigated to comply with the As threshold levels in China⁶⁹ and those just recently (2016) introduced in the European Union.⁷⁰ Besides different water-management strategies and selection of low As accumulation rice varieties, fertilization of paddy soils with sulfur is being tested, with the beneficial side effect that emission of the greenhouse gas methane is significantly reduced. However, the effects of S fertilization in soils and plants are not fully understood, yet. One aspect of S fertilization is the formation of thioarsenates, but only limited information about the behavior of thioarsenates in plants

(obtained with the model organism *A. thaliana*⁴¹) was available until now.

Taking the results from the present study into consideration, focusing only on the uptake of arsenate, arsenite, and methylated As from paddy soils into rice might not be sufficient to explain As accumulation in rice grains, because we could show that MTA was taken up by rice plants intact and transported into the xylem. Monothioarsenate reduction to arsenite inside the rice plant was observed. Its role for As metabolism, however, is not understood, yet. Higher rates of As translocation from roots to shoots, when rice was exposed to MTA compared to arsenate, were also observed for *A. thaliana* in a previous study.⁴¹ This observation requires further detailed investigations on passage to the grain in order to determine whether MTA contributes to As accumulation in grains. The mechanisms for the high MTA translocation are not clear, yet. Different uptake and translocation rates for MTA and arsenate might indicate that as yet unknown enzymes play an important part in the MTA-metabolism. Hence, the transporters for MTA uptake and translocation as well as the MTA-reductases need to be identified to gain a better mechanistic understanding.

■ ASSOCIATED CONTENT

📄 Supporting Information

The Supporting Information is available free of charge on the ACS Publications website at DOI: 10.1021/acs.est.8b02202.

Composition of nutrient solutions, As concentrations applied in the toxicity experiment, stability test of MTA and arsenite in different extractants, relative root and shoot weights, dose response curves for toxicity experiment and experiment with 50% less phosphate, comparison of IC₅₀ values, speciation of nutrient solution without plants, As speciation during efflux experiment, and translocation factors for MTA and arsenate exposure (PDF)

■ AUTHOR INFORMATION

Corresponding Author

*Phone: +49 921 55 3999. E-mail: b.planer-friedrich@uni-bayreuth.de.

ORCID

Britta Planer-Friedrich: 0000-0002-0656-4283

Notes

The authors declare no competing financial interest.

■ ACKNOWLEDGMENTS

We acknowledge financial support for a Ph.D. stipend to Carolin Kerl from the German Academic Scholarship Foundation. We thank Sonja Pinzer and Andrea Colina Blanco for assistance with plant growth and Stefan Will for help with IC-ICP-MS measurements.

■ REFERENCES

- (1) Williams, P. N.; Villada, A.; Deacon, C.; Raab, A.; Figuerola, J.; Green, A. J.; Feldmann, J.; Meharg, A. A. Greatly Enhanced Arsenic Shoot Assimilation in Rice Leads to Elevated Grain Levels Compared to Wheat and Barley. *Environ. Sci. Technol.* **2007**, *41* (19), 6854–6859.
- (2) Williams, P. N.; Raab, A.; Feldmann, J.; Meharg, A. A. Market Basket Survey Shows Elevated Levels of As in South Central U.S.

Processed Rice Compared to California: Consequences for Human Dietary Exposure. *Environ. Sci. Technol.* **2007**, *41* (7), 2178–2183.

(3) Chen, Y.; Han, Y. H.; Cao, Y.; Zhu, Y. G.; Rathinasabapathi, B.; Ma, L. Q. Arsenic Transport in Rice and Biological Solutions to Reduce Arsenic Risk from Rice. *Front. Plant Sci.* **2017**, *8*, 268.

(4) Meharg, A. A.; Williams, P. N.; Adomako, E.; Lawgali, Y. Y.; Deacon, C.; Villada, A.; Cambell, R. C. J.; Sun, G.; Zhu, Y.-G.; Feldmann, J.; Raab, A.; Zhao, F.-J.; Islam, R.; Hossain, S.; Yanai, J. Geographical Variation in Total and Inorganic Arsenic Content of Polished (White) Rice. *Environ. Sci. Technol.* **2009**, *43* (5), 1612–1617.

(5) Matschullat, J. Arsenic in the geosphere — a review. *Sci. Total Environ.* **2000**, *249* (1–3), 297–312.

(6) Zhao, F. J.; McGrath, S. P.; Meharg, A. A. Arsenic as a food chain contaminant: mechanisms of plant uptake and metabolism and mitigation strategies. *Annu. Rev. Plant Biol.* **2010**, *61*, 535–59.

(7) Armstrong, W. The Use of Polarography in the Assay of Oxygen Diffusing from Roots in Anaerobic Media. *Physiol. Plant.* **1967**, *20* (3), 540–553.

(8) Ando, T.; Yoshida, S.; Nishiyama, I. Nature of oxidizing power of rice roots. *Plant Soil* **1983**, *72* (1), 57–71.

(9) Sun, S.; Gu, M.; Cao, Y.; Huang, X.; Zhang, X.; Ai, P.; Zhao, J.; Fan, X.; Xu, G. A constitutive expressed phosphate transporter, OsPht1;1, modulates phosphate uptake and translocation in phosphate-replete rice. *Plant Physiol.* **2012**, *159* (4), 1571–81.

(10) Cao, Y.; Sun, D.; Ai, H.; Mei, H.; Liu, X.; Sun, S.; Xu, G.; Liu, Y.; Chen, Y.; Ma, L. Q. Knocking Out OsPT4 Gene Decreases Arsenate Uptake by Rice Plants and Inorganic Arsenic Accumulation in Rice Grains. *Environ. Sci. Technol.* **2017**, *51* (21), 12131–12138.

(11) Ye, Y.; Li, P.; Xu, T.; Zeng, L.; Cheng, D.; Yang, M.; Luo, J.; Lian, X. OsPT4 Contributes to Arsenate Uptake and Transport in Rice. *Front. Plant Sci.* **2017**, *8*, 2197.

(12) Wang, P.; Zhang, W.; Mao, C.; Xu, G.; Zhao, F. J. The role of OsPT8 in arsenate uptake and varietal difference in arsenate tolerance in rice. *J. Exp. Bot.* **2016**, *67* (21), 6051–6059.

(13) Ma, J. F.; Yamaji, N.; Mitani, N.; Xu, X. Y.; Su, Y. H.; McGrath, S. P.; Zhao, F. J. Transporters of arsenite in rice and their role in arsenic accumulation in rice grain. *Proc. Natl. Acad. Sci. U. S. A.* **2008**, *105* (29), 9931–5.

(14) Li, R. Y.; Ago, Y.; Liu, W. J.; Mitani, N.; Feldmann, J.; McGrath, S. P.; Ma, J. F.; Zhao, F. J. The rice aquaporin Lsi1 mediates uptake of methylated arsenic species. *Plant Physiol.* **2009**, *150* (4), 2071–80.

(15) Zhao, F. J.; Ago, Y.; Mitani, N.; Li, R. Y.; Su, Y. H.; Yamaji, N.; McGrath, S. P.; Ma, J. F. The role of the rice aquaporin Lsi1 in arsenite efflux from roots. *New Phytol.* **2010**, *186* (2), 392–9.

(16) Ma, J. F.; Yamaji, N. A cooperative system of silicon transport in plants. *Trends Plant Sci.* **2015**, *20* (7), 435–42.

(17) Shi, S.; Wang, T.; Chen, Z.; Tang, Z.; Wu, Z.; Salt, D. E.; Chao, D. Y.; Zhao, F. J. OsHAC1;1 and OsHAC1;2 Function as Arsenate Reductases and Regulate Arsenic Accumulation. *Plant Physiol.* **2016**, *172* (3), 1708–1719.

(18) Xu, J.; Shi, S.; Wang, L.; Tang, Z.; Lv, T.; Zhu, X.; Ding, X.; Wang, Y.; Zhao, F. J.; Wu, Z. OsHAC4 is critical for arsenate tolerance and regulates arsenic accumulation in rice. *New Phytol.* **2017**, *215* (3), 1090–1101.

(19) Clemens, S.; Ma, J. F. Toxic Heavy Metal and Metalloid Accumulation in Crop Plants and Foods. *Annu. Rev. Plant Biol.* **2016**, *67*, 489–512.

(20) Clemens, S. Toxic metal accumulation, responses to exposure and mechanisms of tolerance in plants. *Biochimie* **2006**, *88* (11), 1707–19.

(21) Mendoza-Cozatl, D. G.; Jobe, T. O.; Hauser, F.; Schroeder, J. I. Long-distance transport, vacuolar sequestration, tolerance, and transcriptional responses induced by cadmium and arsenic. *Curr. Opin. Plant Biol.* **2011**, *14* (5), 554–62.

(22) Verbruggen, N.; Hermans, C.; Schat, H. Mechanisms to cope with arsenic or cadmium excess in plants. *Curr. Opin. Plant Biol.* **2009**, *12* (3), 364–72.

(23) Pickering, I. J.; Prince, R. C.; George, M. J.; Smith, R. D.; George, G. N.; Salt, D. E. Reduction and Coordination of Arsenic in Indian Mustard. *Plant Physiol.* **2000**, *122* (4), 1171–1178.

(24) Song, W. Y.; Yamaki, T.; Yamaji, N.; Ko, D.; Jung, K. H.; Fujii-Kashino, M.; An, G.; Martinoia, E.; Lee, Y.; Ma, J. F. A rice ABC transporter, OsABCC1, reduces arsenic accumulation in the grain. *Proc. Natl. Acad. Sci. U. S. A.* **2014**, *111* (44), 15699–704.

(25) Xu, W.; Dai, W.; Yan, H.; Li, S.; Shen, H.; Chen, Y.; Xu, H.; Sun, Y.; He, Z.; Ma, M. Arabidopsis NIP3;1 Plays an Important Role in Arsenic Uptake and Root-to-Shoot Translocation under Arsenite Stress Conditions. *Mol. Plant* **2015**, *8* (5), 722–33.

(26) Lindsay, E. R.; Maathuis, F. J. Arabidopsis thaliana NIP7;1 is involved in tissue arsenic distribution and tolerance in response to arsenate. *FEBS Lett.* **2016**, *590* (6), 779–86.

(27) Planer-Friedrich, B.; Hartig, C.; Lohmayer, R.; Suess, E.; McCann, S. H.; Oremland, R. Anaerobic Chemolithotrophic Growth of the Haloalkaliphilic Bacterium Strain MLMS-1 by Disproportionation of Monothioarsenate. *Environ. Sci. Technol.* **2015**, *49* (11), 6554–63.

(28) Stauder, S.; Raue, B.; Sacher, F. Thioarsenates in Sulfidic Waters. *Environ. Sci. Technol.* **2005**, *39* (16), 5933–5939.

(29) Planer-Friedrich, B.; Suess, E.; Scheinost, A. C.; Wallschläger, D. Arsenic speciation in sulfidic waters: reconciling contradictory spectroscopic and chromatographic evidence. *Anal. Chem.* **2010**, *82* (24), 10228–35.

(30) Jia, Y.; Bao, P.; Zhu, Y. G. Arsenic bioavailability to rice plant in paddy soil: influence of microbial sulfate reduction. *J. Soils Sediments* **2015**, *15* (9), 1960–1967.

(31) Ayotade, K. A. Kinetics and reactions of hydrogen sulphide in solution of flooded rice soils. *Plant Soil* **1977**, *46* (2), 381–389.

(32) Dixit, G.; Singh, A. P.; Kumar, A.; Singh, P. K.; Kumar, S.; Dwivedi, S.; Trivedi, P. K.; Pandey, V.; Norton, G. J.; Dhankher, O. P.; Tripathi, R. D. Sulfur mediated reduction of arsenic toxicity involves efficient thiol metabolism and the antioxidant defense system in rice. *J. Hazard. Mater.* **2015**, *298*, 241–51.

(33) Zhang, J.; Zhao, Q.-Z.; Duan, G.-L.; Huang, Y.-C. Influence of sulphur on arsenic accumulation and metabolism in rice seedlings. *Environ. Exp. Bot.* **2011**, *72* (1), 34–40.

(34) Hu, Z. Y.; Zhu, Y. G.; Li, M.; Zhang, L. G.; Cao, Z. H.; Smith, F. A. Sulfur (S)-induced enhancement of iron plaque formation in the rhizosphere reduces arsenic accumulation in rice (*Oryza sativa* L.) seedlings. *Environ. Pollut.* **2007**, *147* (2), 387–93.

(35) Fan, J.; Xia, X.; Hu, Z.; Ziadi, N.; Liu, C. Excessive sulfur supply reduces arsenic accumulation in brown rice. *Plant, Soil Environ.* **2013**, *59* (4), 169–174.

(36) Boye, K.; Lezama-Pacheco, J.; Fendorf, S. Relevance of Reactive Fe:S Ratios for Sulfur Impacts on Arsenic Uptake by Rice. *Soils* **2017**, *1* (1), 1.

(37) Ro, S.; Seanjan, P.; Tulaphitak, T.; Inubushi, K. Sulfate content influencing methane production and emission from incubated soil and rice-planted soil in Northeast Thailand. *Soil Sci. Plant Nutr.* **2011**, *57* (6), 833–842.

(38) Planer-Friedrich, B.; Halder, D.; Kerl, C. F.; Schaller, J.; Wang, J.; Martin, M.; Romani, M. Thioarsenates — so Far Unrecognized Arsenic Species in Paddy Soils. *Goldschmidt Abstracts, Paris* **2017**, 3176.

(39) Planer-Friedrich, B.; Wallschläger, D. A Critical Investigation of Hydride Generation-Based Arsenic Speciation in Sulfidic Waters. *Environ. Sci. Technol.* **2009**, *43* (13), 5007–5013.

(40) Zeng, F.; Ali, S.; Zhang, H.; Ouyang, Y.; Qiu, B.; Wu, F.; Zhang, G. The influence of pH and organic matter content in paddy soil on heavy metal availability and their uptake by rice plants. *Environ. Pollut.* **2011**, *159* (1), 84–91.

(41) Planer-Friedrich, B.; Kuhnlenz, T.; Halder, D.; Lohmayer, R.; Wilson, N.; Rafferty, C.; Clemens, S. Thioarsenate Toxicity and Tolerance in the Model System Arabidopsis thaliana. *Environ. Sci. Technol.* **2017**, *51* (12), 7187–7196.

- (42) Schwedt, G.; Rieckhoff, M. Separation of thio- and oxothioarsenates by capillary zone electrophoresis and ion chromatography. *J. Chromatogr., A* **1996**, *736* (1–2), 341–350.
- (43) Suess, E.; Scheinost, A. C.; Bostick, B. C.; Merkel, B. J.; Wallschlaeger, D.; Planer-Friedrich, B. Discrimination of thioarsenites and thioarsenates by X-ray absorption spectroscopy. *Anal. Chem.* **2009**, *81* (20), 8318–26.
- (44) Xu, X. Y.; McGrath, S. P.; Zhao, F. J. Rapid reduction of arsenate in the medium mediated by plant roots. *New Phytol.* **2007**, *176* (3), 590–9.
- (45) Lomax, C.; Liu, W. J.; Wu, L.; Xue, K.; Xiong, J.; Zhou, J.; McGrath, S. P.; Meharg, A. A.; Miller, A. J.; Zhao, F. J. Methylated arsenic species in plants originate from soil microorganisms. *New Phytol.* **2012**, *193* (3), 665–72.
- (46) Zhang, M.; Zhao, Q.; Xue, P.; Zhang, S.; Li, B.; Liu, W. Do Si/As ratios in growth medium affect arsenic uptake, arsenite efflux and translocation of arsenite in rice (*Oryza sativa*)? *Environ. Pollut.* **2017**, *229*, 647–654.
- (47) Maher, W. A.; Ellwood, M. J.; Krikowa, F.; Raber, G.; Foster, S. Measurement of arsenic species in environmental, biological fluids and food samples by HPLC-ICPMS and HPLC-HG-AFS. *J. Anal. At. Spectrom.* **2015**, *30* (10), 2129–2183.
- (48) Mir, K. A.; Rutter, A.; Koch, I.; Smith, P.; Reimer, K. J.; Poland, J. S. Extraction and speciation of arsenic in plants grown on arsenic contaminated soils. *Talanta* **2007**, *72* (4), 1507–18.
- (49) Yuan, C.-g.; Jiang, G.-b.; He, B. Evaluation of the extraction methods for arsenic speciation in rice straw, *Oryza sativa* L., and analysis by HPLC-HG-AFS. *J. Anal. At. Spectrom.* **2005**, *20* (2), 103.
- (50) Raab, A.; Schat, H.; Meharg, A. A.; Feldmann, J. Uptake, translocation and transformation of arsenate and arsenite in sunflower (*Helianthus annuus*): formation of arsenic-phytochelatin complexes during exposure to high arsenic concentrations. *New Phytol.* **2005**, *168* (3), 551–8.
- (51) Huang, J.-H.; Ilgen, G.; Fecher, P. Quantitative chemical extraction for arsenic speciation in rice grains. *J. Anal. At. Spectrom.* **2010**, *25* (6), 800–802.
- (52) Huang, J. H.; Fecher, P.; Ilgen, G.; Hu, K. N.; Yang, J. Speciation of arsenite and arsenate in rice grain – Verification of nitric acid based extraction method and mass sample survey. *Food Chem.* **2012**, *130* (2), 453–459.
- (53) Abedin, M. J.; Feldmann, J.; Meharg, A. A. Uptake kinetics of arsenic species in rice plants. *Plant Physiol.* **2002**, *128* (3), 1120–8.
- (54) Van de Wiele, T.; Gallawa, C. M.; Kubachka, K. M.; Creed, J. T.; Basta, N.; Dayton, E. A.; Whitacre, S.; Du Laing, G.; Bradham, K. Arsenic metabolism by human gut microbiota upon in vitro digestion of contaminated soils. *Environ. Health Perspect.* **2010**, *118* (7), 1004–9.
- (55) Planer-Friedrich, B.; Fisher, J. C.; Hollibaugh, J. T.; Süß, E.; Wallschläger, D. Oxidative Transformation of Trithioarsenate Along Alkaline Geothermal Drainages—Abiotic versus Microbially Mediated Processes. *Geomicrobiol. J.* **2009**, *26* (5), 339–350.
- (56) Hartig, C.; Lohmayer, R.; Kolb, S.; Horn, M. A.; Inskeep, W. P.; Planer-Friedrich, B. Chemolithotrophic growth of the aerobic hyperthermophilic bacterium *Thermocrinis ruber* OC 14/7/2 on monothioarsenate and arsenite. *FEMS Microbiol. Ecol.* **2014**, *90* (3), 747–60.
- (57) Wu, Z.; Ren, H.; McGrath, S. P.; Wu, P.; Zhao, F. J. Investigating the contribution of the phosphate transport pathway to arsenic accumulation in rice. *Plant Physiol.* **2011**, *157* (1), 498–508.
- (58) Hinrichsen, S.; Lohmayer, R.; Zdrenka, R.; Dopp, E.; Planer-Friedrich, B. Effect of sulfide on the cytotoxicity of arsenite and arsenate in human hepatocytes (HepG2) and human urothelial cells (UROtsa). *Environ. Sci. Pollut. Res.* **2014**, *21* (17), 10151–62.
- (59) Zhao, F. J.; Ma, J. F.; Meharg, A. A.; McGrath, S. P. Arsenic uptake and metabolism in plants. *New Phytol.* **2009**, *181* (4), 777–94.
- (60) Hartig, C.; Planer-Friedrich, B. Thioarsenate transformation by filamentous microbial mats thriving in an alkaline, sulfidic hot spring. *Environ. Sci. Technol.* **2012**, *46* (8), 4348–56.
- (61) Edwardson, C. F.; Planer-Friedrich, B.; Hollibaugh, J. T. Transformation of monothioarsenate by haloalkaliphilic, anoxygenic photosynthetic purple sulfur bacteria. *FEMS Microbiol. Ecol.* **2014**, *90* (3), 858–68.
- (62) Mikutta, C.; Frommer, J.; Voegelin, A.; Kaegi, R.; Kretzschmar, R. Effect of citrate on the local Fe coordination in ferrihydrite, arsenate binding, and ternary arsenate complex formation. *Geochim. Cosmochim. Acta* **2010**, *74* (19), 5574–5592.
- (63) Paktunc, D.; Foster, A.; Laflamme, G. Speciation and Characterization of Arsenic in Ketz River Mine Tailings Using X-ray Absorption Spectroscopy. *Environ. Sci. Technol.* **2003**, *37* (10), 2067–2074.
- (64) Suess, E.; Scheinost, A. C.; Bostick, B. C.; Merkel, B. J.; Wallschlaeger, D.; Planer-Friedrich, B. Discrimination of Thioarsenites and Thioarsenates by X-ray Absorption Spectroscopy. *Anal. Chem.* **2009**, *81* (20), 8318–8326.
- (65) Holleman, A.; Wiberg, N.; Krieger-Hauwede, M. *Band 1 Grundlagen und Hauptgruppenelemente*, 103 ed.; De Gruyter: Boston, 2016; Vol. 1.
- (66) Raab, A.; Williams, P. N.; Meharg, A.; Feldmann, J. Uptake and translocation of inorganic and methylated arsenic species by plants. *Environ. Chem.* **2007**, *4* (3), 197.
- (67) Mishra, S.; Mattusch, J.; Wennrich, R. Accumulation and transformation of inorganic and organic arsenic in rice and role of thiol-complexation to restrict their translocation to shoot. *Sci. Rep.* **2017**, *7*, 40522.
- (68) Zhao, F. J.; Zhu, Y. G.; Meharg, A. A. Methylated arsenic species in rice: geographical variation, origin, and uptake mechanisms. *Environ. Sci. Technol.* **2013**, *47* (9), 3957–66.
- (69) Stone, R. Food safety. Arsenic and paddy rice: a neglected cancer risk? *Science* **2008**, *321* (5886), 184–5.
- (70) European Commission, amending Regulation (EC) No 1881/2006 as regards maximum levels of inorganic arsenic in foodstuffs. In *Commission, E., Ed.* 2015.

Supporting Information

Environmental Science & Technology

Monothioarsenate uptake, transformation, and translocation in rice plants

Carolin F. Kerl,[†] Colleen Rafferty,[‡] Stephan Clemens,[‡] Britta Planer-Friedrich,[†]*

[†]Environmental Geochemistry, Bayreuth Center for Ecology and Environmental Research (BayCEER), University of Bayreuth, D-95440 Bayreuth, Germany

[‡]Plant Physiology, Bayreuth Center for Ecology and Environmental Research (BayCEER), University of Bayreuth, D-95440 Bayreuth, Germany

* Corresponding author phone: +49 921 55 3999, E-mail: b.planer-friedrich@uni-bayreuth.de

(12 pages, 8 figures, 3 tables)

CONTENTS

Table SI 1. Nutrient solution	page S1
Table SI 2. Arsenic concentration for toxicity experiment	page S2
Table SI 3. Comparison of IC50 values	page S3
Figure SI 1. Test of 0.66 μ M MTA stability in different extractants	page S4
Figure SI 2. Test of 0.66 μ M arsenite stability in different extractants	page S5
Figure SI 3. Relative root and shoot weights	page S6
Figure SI 4. Dose response curves	page S7
Figure SI 5. Dose response curves with 50% phosphate reduction	page S8
Figure SI 6. Abiotic control of nutrient solution	page S9
Figure SI 7. As speciation during efflux experiment	page S10
Figure SI 8. Translocation factors from root to shoot	page S11
References	page S12

Table SI 1. Composition of nutrient solution used for plant growth.

Nr.	Macronutrients	Concentration (mg/L)	Vendor
1	Ca(NO ₃) ₂ *4H ₂ O	1000	Grüssing
2	KCl	120	Grüssing
3*	KH ₂ PO ₄	250	Grüssing
4	MgSO ₄ *7H ₂ O	250	Merck
5	Fe-EDDAH (5.7% Fe)	20	Duchefa Biochemie

Nr.	Micronutrients	Concentration (µg/L)	Vendor
1	KJ	27	Grüssing
2	LiCl	27	Fluka
3	CuSO ₄ *5H ₂ O	55	Grüssing
4	ZnSO ₄ *7H ₂ O	111	Roth
5	H ₃ BO ₃	55	Merck
6	Al ₂ (SO ₄) ₃	55	Alfa Aesar
7	MnCl ₂ *4H ₂ O	388	AppliChem
8	NiSO ₄ *7H ₂ O	55	Aldrich
9	Co(NO ₃) ₂ *6H ₂ O	55	Fluka
10	KBr	27	Merck
11	(NH ₄) ₆ Mo ₇ O ₂₄	55	Fluka

* -50% P: 125 mg/L KH₂PO₄

Table SI 2. Arsenic concentration for toxicity experiment in original nutrient solution or with -50% P.

Experiment	Arsenite (μM)	Arsenate (μM)	MTA (μM)
original	5	5	
	-	-	7.5
	10	10	-
	-	-	15
	25	25	-
	37.5	37.5	37.5
	50	50	-
	-	75	75
	100	100	-
		150	150
	225	225	
-50% P	5	5	5
	10	10	10
	25	25	25
	50	50	50
	100	100	100
	150	150	150

Table SI 3. Comparison of IC₅₀ values from rice seedlings grown in original nutrient solution (Table 1) and seedlings grown in nutrient solution with -50% phosphate. Factors were calculated as (IC₅₀ (original) / IC₅₀(-50% P)).

		Arsenite	MTA	Arsenate
		IC₅₀ (μM)	IC₅₀ (μM)	IC₅₀ (μM)
Shoot length	original	15	>225	>225
	-50% P	14	52	110
	Factor	<i>1.1</i>	<i>>4.3</i>	<i>>2.0</i>
Shoot weight	original	4.2	50	190
	-50% P	3.1	7.5	25
	Factor	<i>1.4</i>	<i>6.7</i>	<i>7.6</i>

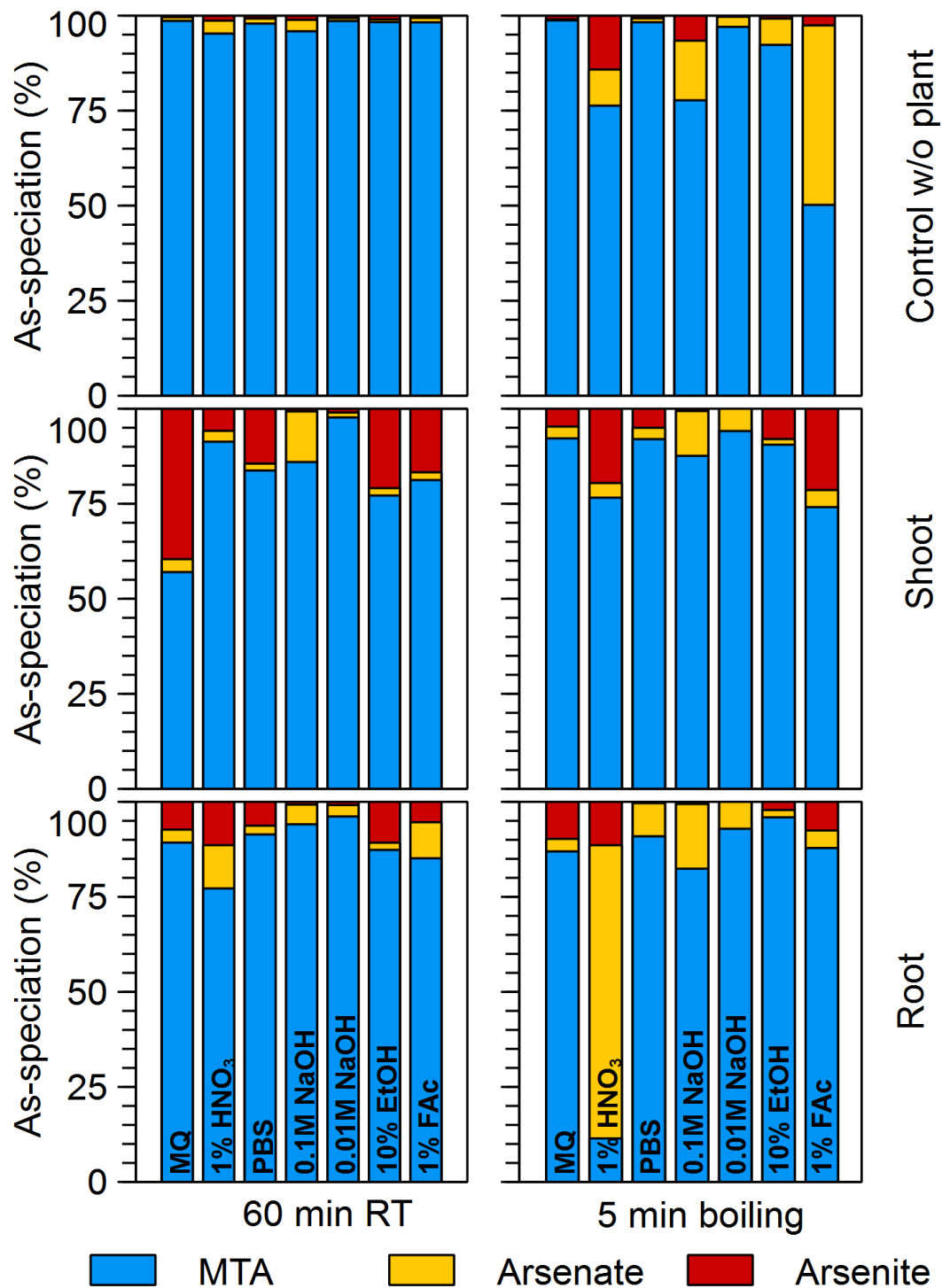


Figure SI 1. Test of 0.66 μ M MTA stability in different extractants for 60 min as abiotic control (top panel), for shoot (middle panel) and roots (bottom panel). All samples were extracted at RT for 60 min, as well as with 5 min boiling and 55 min at RT afterwards

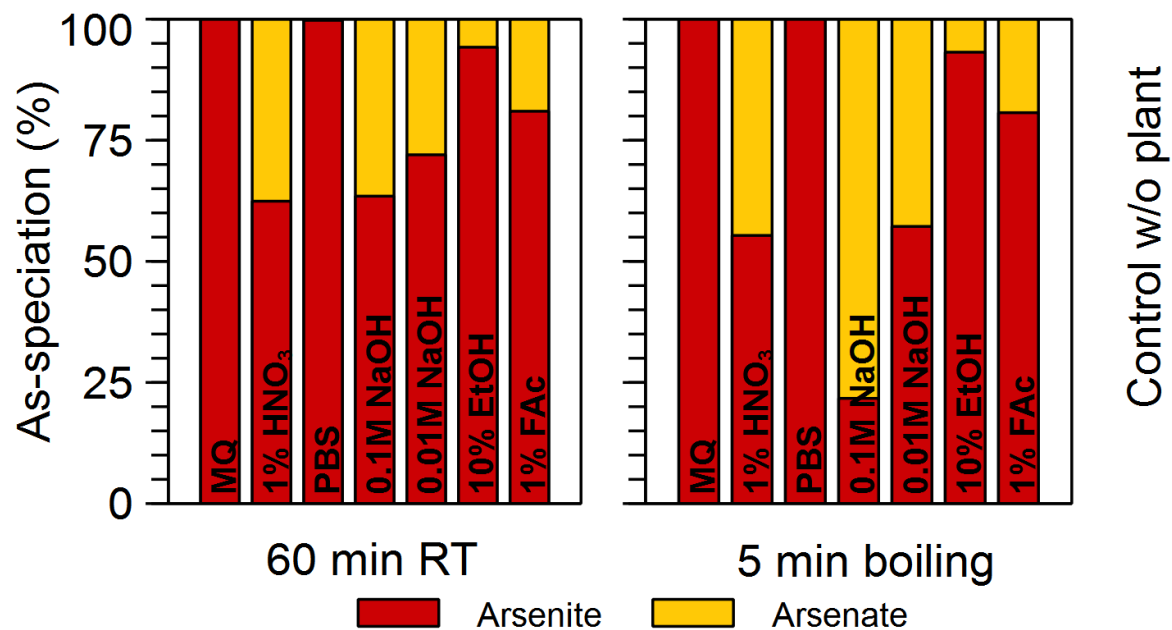


Figure SI 2. Test of 0.66 μM arsenite stability in different extractants for 60 min as abiotic. All samples were extracted at RT for 60 min, as well as with 5 min boiling and 55 min at RT afterwards.

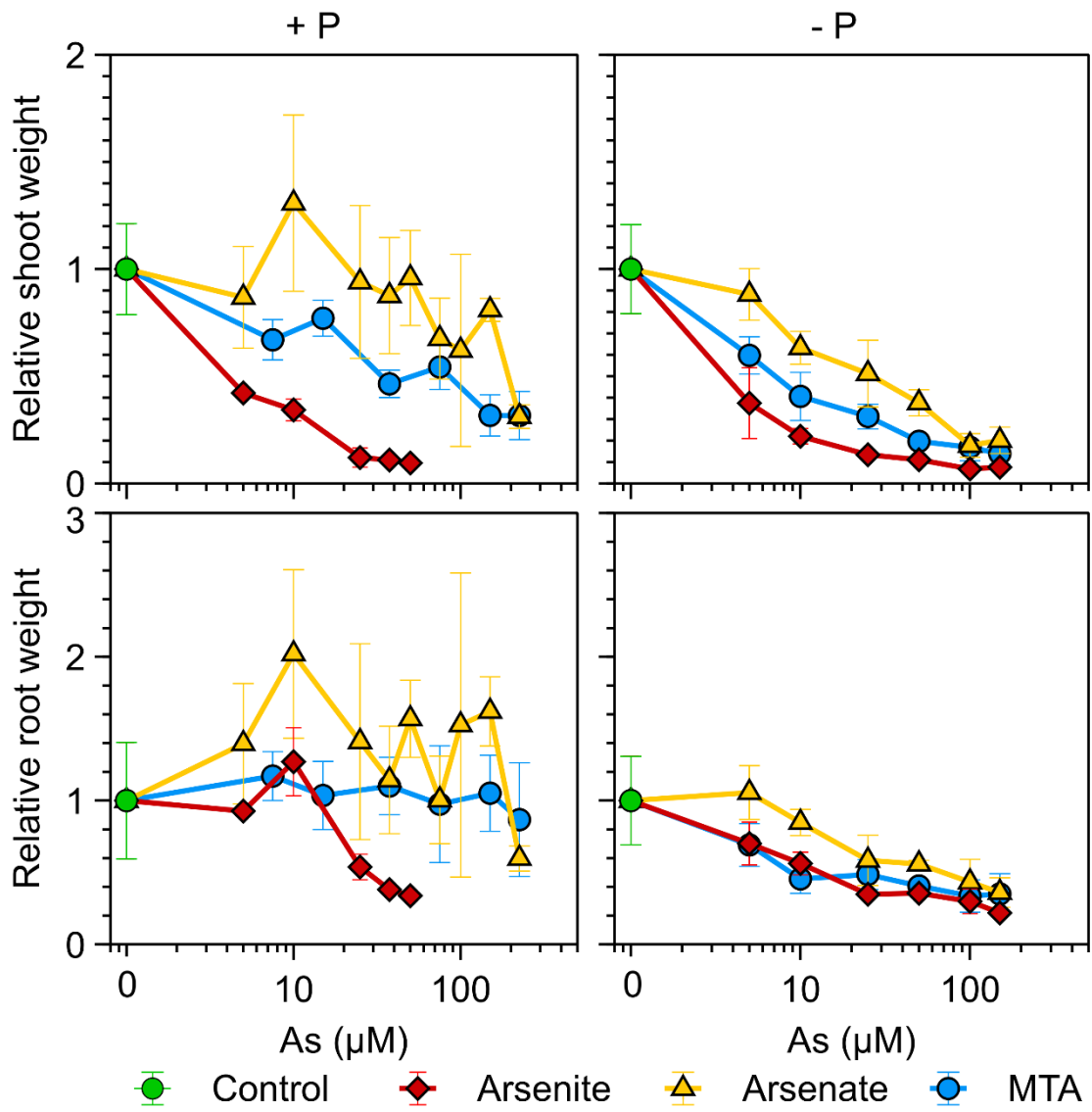


Figure SI 3. Relative shoot and root weights for 20 d old rice seedlings exposed to increasing concentrations (logarithmic scale) of arsenite, arsenate, and MTA (n=4) in original nutrient solution (+ P; on the left panel) and with 50% reduction of phosphate in nutrient solution (- P; on right panel).

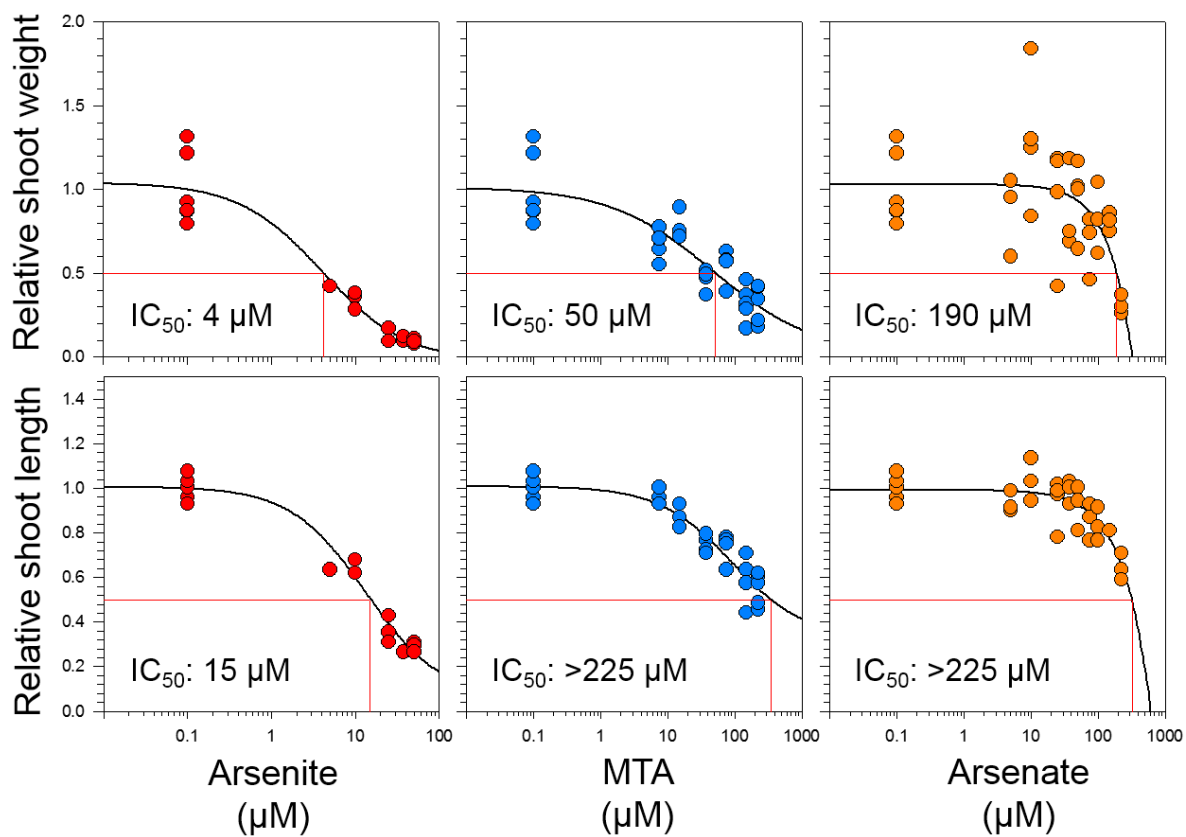


Figure SI 4. Dose response curves of relative shoot weights and lengths versus individual As species concentration (logarithmic scale) after exposure to arsenite, arsenate and MTA (n=4). IC_{50} values (marked by red lines) were derived from these curves using a three parameter log-logistic dose-response model in the program Sigma plot.

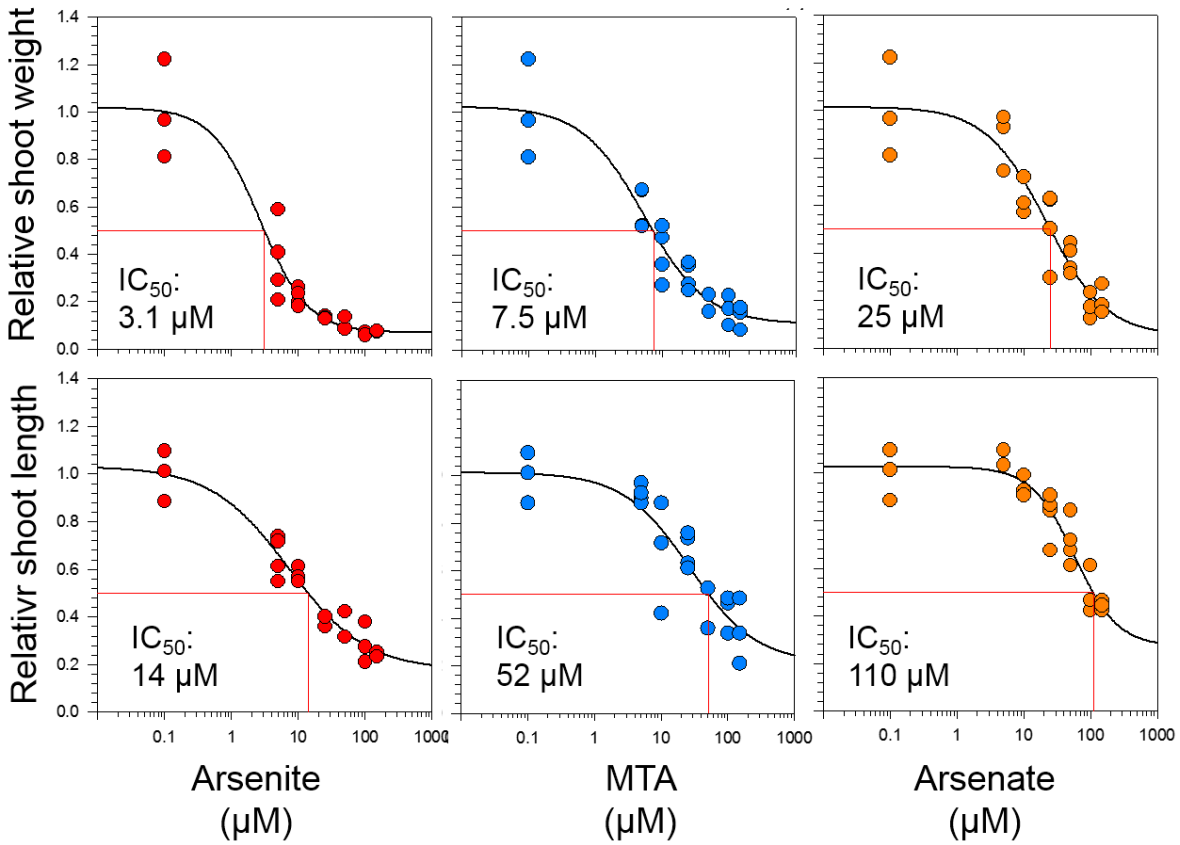


Figure SI 5. Dose response curves of relative shoot weights and lengths versus individual As species concentration (logarithmic scale) after exposure to arsenite, arsenate and MTA and 50% reduction of phosphate in nutrient solution (n=4). IC_{50} values (marked by red lines) were derived from these curves using a three parameter log-logistic dose-response model in the program Sigma plot.

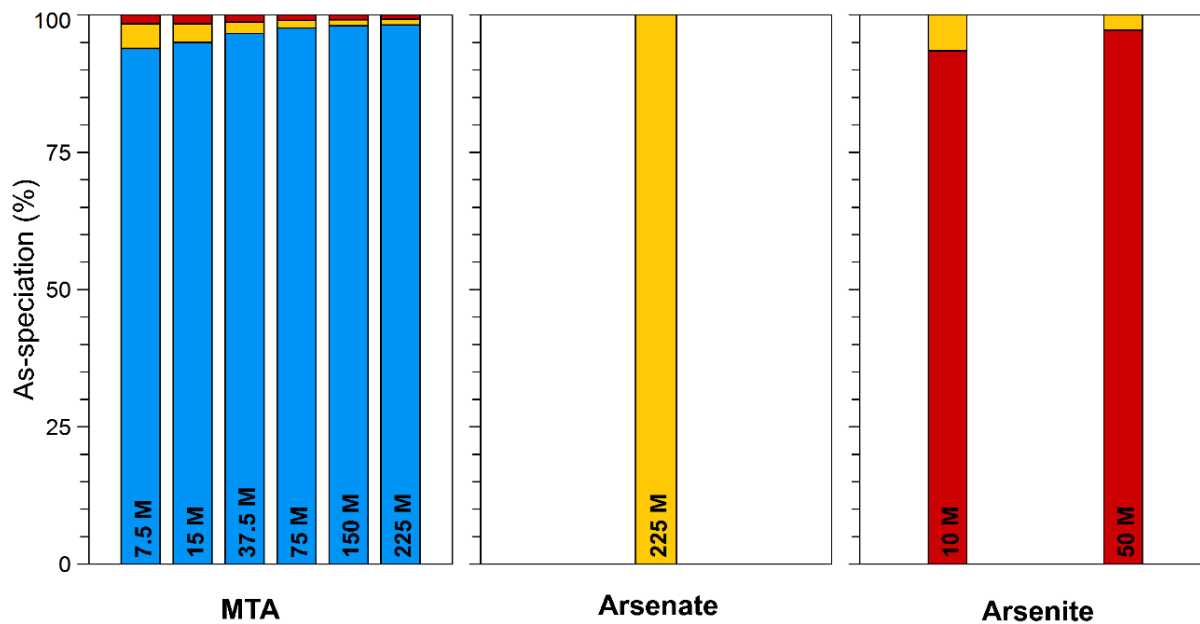


Figure SI 6. Abiotic control of nutrient solution after 4 days in growth cabinet under the same conditions as plants. As speciation for nutrient solution amended with MTA, arsenate, and arsenite.

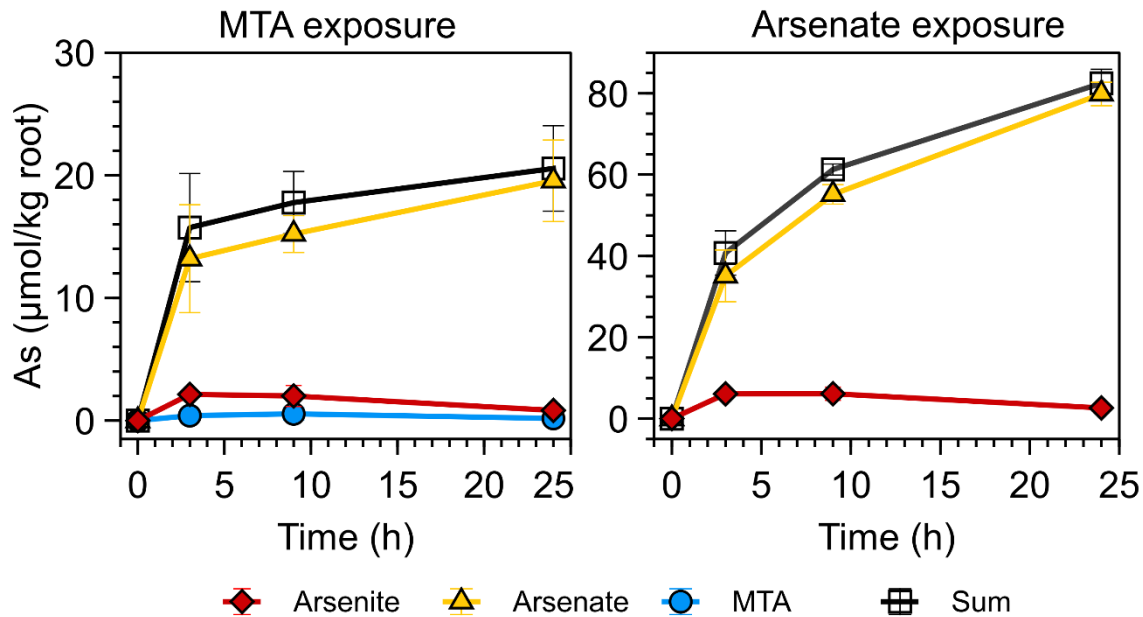


Figure SI 7. Efflux of arsenite, arsenate, and MTA after rice seedlings had been exposed to 10 μM MTA (left) or arsenate (right) for 24 h. Growth media was changed every 6 h during daytime and after 12 h during nighttime during influx to minimize reduction to arsenite (Efflux experiment, $n=4$). Sum of species and totals are used as synonyms in the text.

Based on the results from the influx experiment, mostly arsenite should be effluxed by the rice plants, but arsenate was the dominant species found. One explanation could be that arsenite is effluxed continuously at trace amounts (maximum As concentration measured in efflux media 0.9 μM in 24 h compared to 10 μM in the influx experiment) that are quickly abiotically oxidized. Even though abiotic oxidation rates of up to 0.8 $\mu\text{M}/\text{h}$ have been reported before ¹, our abiotic controls of 0.06 and 0.13 μM arsenite in efflux media were not oxidized to arsenate within 24 h, showing that the arsenate in our experiments is no abiotic oxidation artefact. An alternative, and here probably more likely, explanation could be that root oxygen loss (ROL) is the main driver for arsenite oxidation. Rice roots are known to release oxygen ^{2,3} into the rhizosphere creating oxidizing microenvironments where, for example, iron plaque is formed ⁴. Oxidation of arsenite to arsenate is very likely under these conditions as arsenate is the dominant As species found in iron plaque ^{5,6}. Compared to the arsenite release during the influx experiment (Figure 4), the As concentrations were much lower during the efflux experiment and therefore, the effluxed arsenate could be the remaining arsenate that was not reduced to arsenite yet.

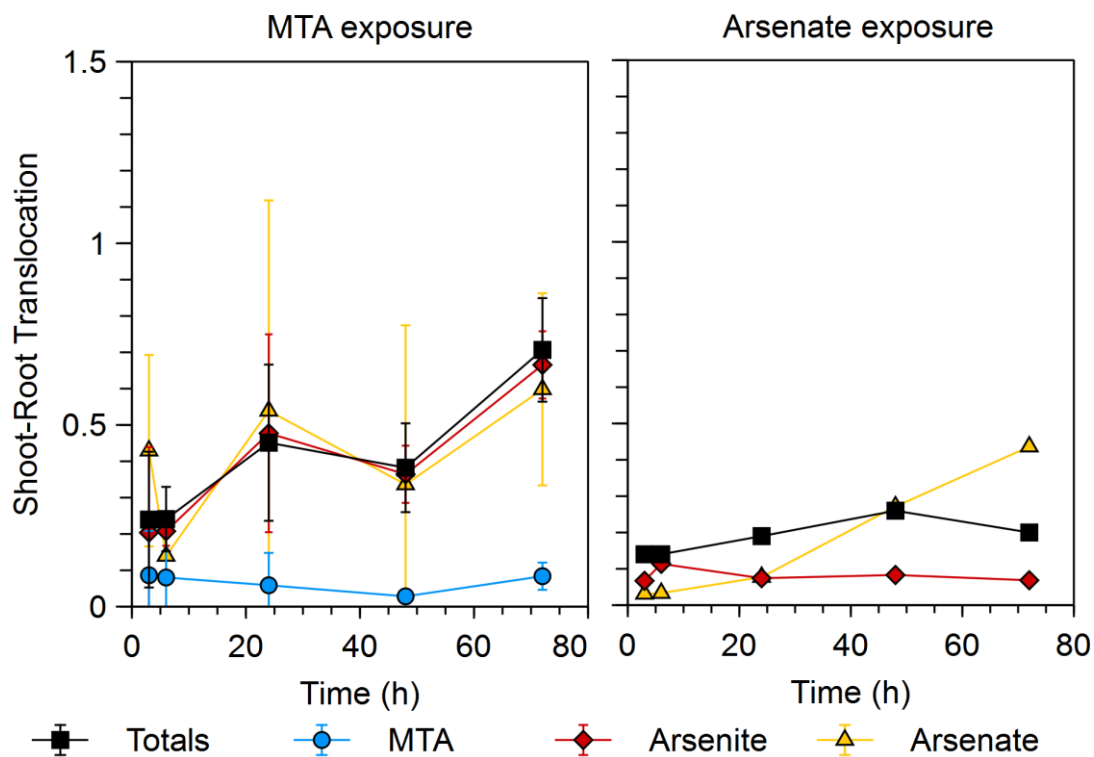


Figure SI 8. Translocation factors from root to shoot for rice seedlings grown for 20 d without As following exposure to 10 μ M MTA (left) and arsenate (right) for 3, 6, 24, 48, and 72 h. Factors were calculated for As species in seedlings, as well as for total As (n=3 for MTA and n=1 for arsenate).

References

1. Gihring, T. M.; Druschel, G. K.; McCleskey, R. B.; Hamers, R. J.; Banfield, J. F., Rapid Arsenite Oxidation by *Thermus aquaticus* and *Thermus thermophilus*: Field and Laboratory Investigations. *Environ. Sci. Technol.* **2001**, *35*, (19), 3857-3862.
2. Armstrong, W., The Use of Polarography in the Assay of Oxygen Diffusing from Roots in Anaerobic Media. *Physiol. Plant.* **1967**, *20*, (3), 540-553.
3. Ando, T.; Yoshida, S.; Nishiyama, I., Nature of oxidizing power of rice roots. *Plant Soil* **1983**, *72*, (1), 57-71.
4. Chen, C. C.; Dixon, J. B.; Turner, F. T., Iron Coatings on Rice Roots: Morphology and Models of Development I. *Soil Sci. Soc. Am. J.* **1980**, *44*, (5), 1113.
5. Liu, W. J.; Zhu, Y. G.; Hu, Y.; Williams, P. N.; Gault, A. G.; Meharg, A. A.; Charnock, J. M.; Smith, F. A., Arsenic Sequestration in Iron Plaque, Its Accumulation and Speciation in Mature Rice Plants (*Oryza Sativa* L.). *Environ. Sci. Technol.* **2006**, *40*, (18), 5730-5736.
6. Voegelin, A.; Weber, F.-A.; Kretzschmar, R., Distribution and speciation of arsenic around roots in a contaminated riparian floodplain soil: Micro-XRF element mapping and EXAFS spectroscopy. *Geochim. Cosmochim. Acta* **2007**, *71*, (23), 5804-5820.

Study 3: Methylated thioarsenates and monothioarsenate differ in uptake, transformation, and contribution to total arsenic translocation in rice plants

Carolin F. Kerl, R. Alina Schindele, Lena Brüggewirth, Andrea E. Colina Blanco, Colleen Rafferty, Stephan Clemens, Britta Planer-Friedrich

Reprinted with permission from

Environmental Science & Technology (53, pp. 5787-5796)

Copyright 2019 American Chemical Society

Methylated Thioarsenates and Monothioarsenate Differ in Uptake, Transformation, and Contribution to Total Arsenic Translocation in Rice Plants

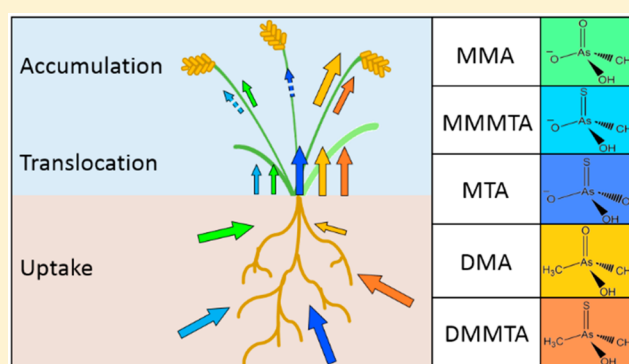
Carolin F. Kerl,[†] Ruth Alina Schindele,[†] Lena Brüggewirth,[†] Andrea E. Colina Blanco,[†] Colleen Rafferty,[‡] Stephan Clemens,[‡] and Britta Planer-Friedrich^{*,†,‡}

[†]Environmental Geochemistry, Bayreuth Center for Ecology and Environmental Research (BayCEER), University of Bayreuth, D-95440 Bayreuth, Germany

[‡]Plant Physiology, Bayreuth Center for Ecology and Environmental Research (BayCEER), University of Bayreuth, D-95440 Bayreuth, Germany

Supporting Information

ABSTRACT: Methylated and inorganic thioarsenates have recently been reported from paddy fields besides the better-known oxyarsenates. Methylated thioarsenates are highly toxic for humans, yet their uptake, transformation, and translocation in rice plants is unknown. Here, hydroponic experiments with 20 day old rice plants showed that monomethylmonothioarsenate (MMMTA), dimethylmonothioarsenate (DMMTA), and monothioarsenate (MTA) were taken up by rice roots and could be detected in the xylem. Total arsenic (As) translocation from roots to shoots was higher for plants exposed to DMMTA, MTA, and dimethylarsenate (DMA^{V}) compared to MMMTA and monomethylarsenate (MMA^{V}). All thioarsenates were partially transformed in the presence of rice roots, but processes and extents differed. MMMTA was subject to abiotic oxidation and largely dethiolated to MMA^{V} already outside the plant, probably due to root oxygen loss. DMMTA and MTA were not oxidized abiotically. Crude protein extracts showed rapid enzymatic reduction for MTA but not for DMMTA. Our study implies that DMMTA has the highest potential to contribute to total As accumulation in grains either as DMA^{V} or partially as DMMTA. DMMTA has once been detected in rice grains using enzymatic extraction. By routine acid extraction, DMMTA is determined as DMA^{V} and thus escapes regulation despite its toxicity.



INTRODUCTION

Rice, being a staple food for half of the world's population,^{1,2} takes up approximately 10 times more arsenic (As) than other cereals^{3,4} and contributes to human As exposure.⁵ Arsenic is ubiquitously present in soils and mobilized during rice cultivation on flooded paddy soils by reductive dissolution of iron (Fe) minerals.^{6,7} While arsenite is the most abundant As species under reducing conditions, minor amounts of arsenate, monomethylarsenate (MMA^{V}), and dimethylarsenate (DMA^{V}) were reported in pore water of paddy soils.^{5,8} Methylated oxyarsenates originate from soil microorganisms or algae that are able to biomethylate inorganic As by the enzyme As(III) S-adenosylmethionine (SAM) methyltransferase prior to uptake by plants.^{9,10} Uptake of inorganic arsenite (by nodulin 26-like intrinsic protein (NIP) aquaglyceroporins such as Lsi1 (OsNIP2;1)^{11–13}) and arsenate (by phosphate transporters such as OsPht1;1,¹⁴ OsPht1;4,^{15,16} or OsPht1;8¹⁷) is well-studied. Less is known about methylated As which is microbially produced in the rhizosphere.¹⁰ Similar to arsenite, nondissociated MMA^{V} ($(\text{CH}_3)\text{AsO}(\text{OH})_2$, $\text{pK}_{\text{a}1}$ 4.2) and

DMA^{V} ($(\text{CH}_3)_2\text{AsO}(\text{OH})$, $\text{pK}_{\text{a}1}$ 6.1) are taken up via OsNIP2;1.¹⁸ However, additional, so far unknown transporters are hypothesized to account for the uptake of dissociated MMA^{V} and DMA^{V} .⁵ Further transport of As to xylem and phloem is limited by As sequestration in root cell vacuoles via phytochelatin (PC) complexation. Inorganic As is stored as $\text{As}^{\text{III}}\text{-PC}$ complexes^{19–22} and MMA^{V} is stored as $\text{MMA}^{\text{III}}\text{-PC}$ complexes after reduction of MMA^{V} to MMA^{III} .^{23,24} No $\text{DMA}^{\text{III}}\text{-PC}$ complexes have been found in rice roots so far.²³ Lack of DMA^{III} complexation explains the strong differences in root-to-shoot translocation rates which follow the order arsenite < MMA^{V} < DMA^{V} .^{24,25} In consequence, DMA^{V} concentrations in rice grains can reach up to 90% of total As,²⁶ while in soils it typically contributes only a few percent (maximum 20%) to total As.¹⁰

Received: January 28, 2019

Revised: April 23, 2019

Accepted: April 29, 2019

Published: April 29, 2019

In addition to the better-known oxyarsenates, paddy soil pore waters can also contain inorganic and methylated thioarsenates.²⁷ Even though to date there is still little analytical evidence for thioarsenate occurrence in paddy soils, because routine sample stabilization and analytical techniques do not preserve thioarsenates, their formation is highly plausible from a geochemical point of view. Paddy fields are well-known methane emitters^{28,29} and sulfate reduction to sulfide precedes methane formation (standard redox potential for sulfide formation (−221 mV) vs methane formation (−243 mV)).^{5,30} Even though rice fields typically have low dissolved free sulfide concentrations,³¹ peatland studies have just recently shown that thiolation is largely controlled by As–S surface reactions and proceeds even when there is little to no detectable dissolved sulfide.³² Inorganic thioarsenates are structural analogues to arsenate and form under sulfur-reducing, alkaline conditions from arsenite via OH[−]/SH[−] ligand exchange and addition of zerovalent sulfur.^{33,34} Methylated thioarsenates form, in contrast to inorganic thioarsenates, after nucleophilic attack under acidic pH via ligand exchange of OH[−]/SH[−] in MMA^V or DMA^V molecules.³⁵ One driver for the occurrence of thiolation is sulfur (S) addition, even though naturally occurring S concentrations are already sufficient for As thiolation in paddy soils.²⁷ Sulfur fertilization has recently been suggested to lower grain As concentration;^{36–41} however, no conclusive data have been obtained so far.

While MMA^V and DMA^V are considered less toxic than inorganic As, monomethylmonothioarsenate (MMMTA^V; (CH₃)AsS(OH)₂) and dimethylmonothioarsenate (DMMTA^V; (CH₃)₂AsS(OH)) are considered highly toxic with LD₅₀ values in the same range as those for trivalent As in arsenite, MMA^{III}, or DMA^{III}.⁴² Despite their toxicity, however, knowledge about (methyl)thiolated As species in plants is very limited, in contrast to well-studied metabolism in other organisms.⁹ Recently, rice plants were found to take up monothioarsenate (MTA; AsS(OH)₃), to partly reduce MTA to arsenite, and to transport it in the xylem.⁴³ However, uptake transporters or enzymes catalyzing the reduction are not yet identified for MTA. In *Arabidopsis thaliana*, it was shown that PC-dependent detoxification confers MTA tolerance.⁴⁴ In contrast, no data are available about uptake, transformation, or translocation of methylated thioarsenates in plants, even though DMMTA was detected in rice grains more than 10 years ago.⁴⁵ One reason for the lack of studies about DMMTA in rice grains might be that the widely used acid based As species extraction converts DMMTA into DMA^V during sample preparation.⁴⁶ Only enzymatic extraction as used by Ackerman et al.⁴⁵ appears to preserve DMMTA, at least partly. Considering food guidelines for rice grains in Europe and China [0.2 mg of inorganic As/(kg of dry weight (d.w.))],^{47,48} this is problematic since methylated As is excluded from threshold values due to lower toxicity compared to inorganic As even though measured DMA^V is the sum of actual DMA^V and transformed DMMTA. The occurrence of methylated thioarsenates in paddy soils and the detection of DMMTA in rice grains indicate that methylated thioarsenates have the potential to contribute to As accumulation in rice grains.

The purpose of this study was to obtain first insights into uptake, transformation, and contribution to total As translocation of methylated thioarsenates in rice plants and to compare the behavior of methylated thioarsenates to that of inorganic MTA. Transformation of (methylated) thioarsenate

speciation was studied in nutrient solution and in the presence of crude protein extracts derived from three different rice cultivars grown hydroponically. Uptake, speciation of As in xylem sap, and translocation of total As was studied for one cultivar by exposing rice seedlings to methylated thioarsenates for 6–72 h and measuring accumulation of total As in plant tissues.

METHODS AND MATERIALS

Growth Conditions for Rice. Experiments were conducted with a European rice variety (*Oryza sativa* (*O. sativa*) L. cv. Arelate) and two Chinese rice varieties (*O. sativa* L. cv. Yangdao 6 “YD” and Nongken 57 “NK”). Arelate was chosen for comparison because we used it previously to study MTA uptake in rice.⁴³ The other two rice varieties were added because of reported differences in root oxygen loss (ROL).⁴⁹ Our determinations of ROL, quantifying titanium^{III} citrate oxidation from all three cultivars under experimental conditions, showed the highest ROL for NK, less for YD, and significantly less for Arelate ($P < 0.05$; see [Supporting Information](#) Figure SI 1 for a detailed description). A similar pattern was found for ROL/(g of root), with significantly higher values for NK than for YD and Arelate ($P < 0.05$; [Figure SI 1](#)).

Growth conditions for plants were described in detail elsewhere.⁴³ Briefly, after germinating seeds for 7 days, seedlings were transferred to 50 mL tubes (Sarstedt) containing nutrient solution ([Table SI 1](#)), which was renewed twice a week to ensure sufficient nutrient supply. Seedlings were grown for 20 days under long day conditions (16 h of light/8 h of darkness) at 23 °C and 110 μE. Seedling weights for all experiments can be found in the [Supporting Information](#) ([Table SI 2](#)).

Synthesis of Methylated Thioarsenates. Monomethylmonothioarsenate ((CH₃)AsS(OH)₂) was synthesized as described before^{50,51} under anoxic atmosphere inside a glovebox (COY, 95/5% N₂/H₂ (v/v)). Briefly, MMA^V (CH₃AsNa₂O₃·6 H₂O, Supelco) and sulfide (Na₂S·9 H₂O, Sigma-Aldrich) solutions were mixed with molar As:S ratios of 1:2.66 and pH was adjusted to 3 by adding 0.1 M HCl (Kraft). After 30 min reaction time, pH was increased to 12.3 using 1 M NaOH (Merck) and reaction continued for another 60 min, before aliquots were flash-frozen on dry ice and stored at −20 °C until usage.

DMMTA ((CH₃)₂AsS(OH)) was synthesized following a slightly modified method by Cullen et al.³⁵ Briefly, DMA^V ((CH₃)₂AsNaO₂·3 H₂O, Sigma-Aldrich) and Na₂S·9 H₂O (As:S ratio, 1:1.6) were mixed in molar ratios of 1:1.6 As:S in anoxic atmosphere, and concentrated sulfuric acid (H₂SO₄, Sigma-Aldrich) was added dropwise to an As:H₂SO₄ ratio of 1:1.6. After 25 min reaction time, formed DMMTA was extracted using diethyl ether (C₄H₁₀O, VWR Chemicals) and separated from liquid phase. A constant stream of N₂ was used to evaporate the solvent and yellowish-white crystals formed. Synthesized DMMTA was stored anoxically and in darkness at 5 °C. For DMMTA stock solutions, crystals were dissolved in water and filtered using 0.2 μm cellulose–acetate (CA) filters (Machery-Nagel), before aliquots were flash-frozen on dry ice and stored at −20 °C until usage.

Monothioarsenate was synthesized as Na₃AsO₃S·2H₂O in our laboratory as described in detail previously.^{52,53}

MMMTA, DMMTA, and MTA were identified by ion chromatography coupled to inductively coupled mass spec-

trometry (IC-ICP-MS) using previously published retention times⁵⁰ (Figure SI 2 for chromatograms). The purity of the MMMTA was 96% containing 1% MMA^V and 3% DMDTA. The DMMTA stock contained 67% DMMTA, 28% DMDTA ((CH₃)₂AsS(SH)), and 5% DMA^V. The MTA stock contained 98.5% MTA, 0.5% arsenite, and 1% arsenate.

All experiments with hydroponically grown rice plants were conducted with nominal As concentrations of 10 μM, with the exception of one subset of MMMTA samples where, by mistake, only 3 μM As was applied. However, no difference in transformation kinetics of control treatments (without plants) with 3 and 10 μM MMMTA were found, so we included this data set. Data are displayed in percent for better comparability. Absolute As concentrations for all experiments can be found in the Supporting Information Tables SI 3–SI 7.

Stability of Methylated Thioarsenates. In order to maintain the highest stability of MMMTA and DMMTA during the experiments and meanwhile minimize the share of DMDTA from the synthesized standard, two nutrient solutions were tested: “original” nutrient solution and nutrient solution without Fe (– Fe). A 10 μM amount of MMMTA or DMMTA in the respective nutrient solution was filled in 50 mL tubes and shaded from light with aluminum foil, and samples were taken after 1, 3, 6, 12, and 24 h. Samples were filtered using 0.2 μm CA filters, flash-frozen on dry ice, and stored at –20 °C until analysis by IC-ICP-MS. MMMTA and DMMTA were stable in both nutrient solutions. However, 50% of the DMDTA was converted to DMMTA in the Fe-containing nutrient solution within 1 h (Figure SI 3). Transformation of DMDTA to DMMTA in the presence of Fe^{III} was reported before.⁵⁴ Therefore, all further experiments were conducted with Fe-containing nutrient solution to start experiments with a high share of DMMTA.

The different susceptibilities of thiolated As species to abiotic oxidation were tested by purging 50 mL of nominally 10 μM MTA, DMMTA, or MMMTA in original nutrient solution with pressurized air (≈40 mM O₂/h). Subsamples of 500 μL were taken after 0.25, 0.5, 1, 2, 4, 6, 12, and 24 h, filtered, and flash-frozen. Oxygen flow was about 1 order of magnitude higher than ROL in our experiments, but larger sized bubbles (less reactive surface area) during purging might have lowered oxidation rates. For interpretation, we therefore do not use quantitative comparison of oxidation rates between purging and ROL but only relative differences for the individual thiolated As species.

Methylated Thioarsenates Influx and Protein Extracts. Transformation of (methylated) thioarsenates by three different rice cultivars, Arelate, YD, and NK, was studied by exposing 20 day old plants for 24 h to 50 mL of nominally 10 μM MMA^V, MMMTA, DMA^V, DMMTA, or MTA in nutrient solution. Subsamples of 500 μL for analysis of As speciation were taken after 0, 3, 6, 12, and 24 h, filtered through 0.2 μm CA filters, and flash-frozen until analysis by IC-ICP-MS.

For a first approach to determine whether transformation of (methylated) thioarsenates could be enzymatically driven, we used crude protein extracts similar to earlier studies that tested enzyme-driven arsenate reduction.^{55–57} Twenty day old plant roots were washed, flash-frozen, and ground in liquid nitrogen (N₂). To extract intact root proteins, protein buffer (Table SI 8) and ground root material were mixed in a 7:1 ratio, incubated on ice for 15 min, and centrifuged twice for 10 min at 4000 rpm. The protein buffer was freshly prepared before analysis and stored on ice in the meantime. Transformations of

As species were studied by spiking 500 μL of root protein extract with 3.33 μM MMMTA, DMMTA, or MTA under anoxic atmosphere (glovebox) for 0, 10, 30, 60, and 120 min. Effects of plant or buffer matrix were tested by analyzing denatured root protein extracts (boiled for 2 min at 100 °C) and buffer solution without root material with respective As spike after 120 min. All samples were filtered using 0.2 μm CA filters, and As speciation was analyzed immediately by IC-ICP-MS.

Sampling of Xylem sap. All further experiments were conducted with 20 day old Arelate plants only. To maintain As speciation during exposure, nutrient solution containing 10 μM MMA^V, MMMTA, DMA^V, or DMMTA was changed after 6 and 12 h during day- and nighttime, respectively.

After exposure to 10 μM MMA^V, MMMTA, DMA^V, or DMMTA for 24 h, xylem sap was collected from rice plants cut 2 cm above roots with a sharp blade. Over 1.5 h xylem sap was collected using a 2 μL pipet and diluted in 750 μL of phosphate-buffered saline [PBS; 2 mM NaH₂PO₄ (Grüssing) + 0.2 mM Na₂-EDTA (Grüssing) (pH 6.0)]⁵⁸ chilled on ice. Xylem sap from three plants was pooled into one sample and As speciation was analyzed immediately after filtering with a 0.2 μm CA filter. Oxidation during xylem sap sampling cannot be entirely ruled out; therefore arsenite and arsenate are summarized as inorganic As and the measured methylated thioarsenates represent the minimum amount of methylated thiolated As in the xylem.

Uptake and Translocation of Methylated Thioarsenates. Uptake and translocation in rice roots and shoots was analyzed after exposure to 10 μM MMA^V, MMMTA, DMA^V, or DMMTA for 6, 24, 48, and 72 h. Roots were washed 10 min in 1 mM KH₂PO₄, 5 mM Ca(NO₃)₂, and 5 mM MES to remove As sorbed to the root surface.⁵⁸ The fresh weight for roots and shoots was determined, as well as dry weight after drying at 60 °C for 2 days. Total As concentrations were determined by ICP-MS after microwave digestion (Mars 5 microwave digestion system, CEM Corp., Matthews, NC, USA) of 0.1–0.2 g of plant material in concentrated HNO₃ (Kraft) and 30% H₂O₂ (VWR) (ratio, 1.5:1). Total As translocation factors (TFs) were calculated (As-shoot/As-root).

Arsenic Measurements. Arsenic speciation was analyzed by ion chromatography (Dionex ICS-3000) coupled to ICP-MS (XSeries2, Thermo-Fisher) using oxygen as the reaction cell gas (AsO⁺, *m/z* 91). Samples from experiments conducted with MMA^V, DMA^V, or MTA were separated using a PRP-X100 column (Hamilton, 10 mM NH₄NO₃, 10 mM NH₄H₂PO₄, and 500 mg/L Na₂-EDTA at a flow rate of 1.0 mL/min),^{43,59} and samples from experiments conducted with MMMTA or DMMTA, as well as protein extracts and xylem sap, were separated using an AS16 column (Dionex AG/AS16 IonPac column; 2.5–100 mM NaOH; flow rate, 1.2 mL/min).⁵⁰ Total As concentrations were determined by ICP-MS (AsO⁺, *m/z* 91) using rhodium (Rh⁺, *m/z* 103) as an internal standard.

Statistics. Two-way ANOVA with Tukey post hoc test was performed using Sigma Plot 11.

RESULTS AND DISCUSSION

Transformation or Stability of MMMTA, DMMTA, and MTA upon Aeration. The only species that transformed in experiments purging nutrient solutions with air was MMMTA. DMMTA and MTA showed no transformation over 24 h, which is in line with previous literature reports.^{54,60} For

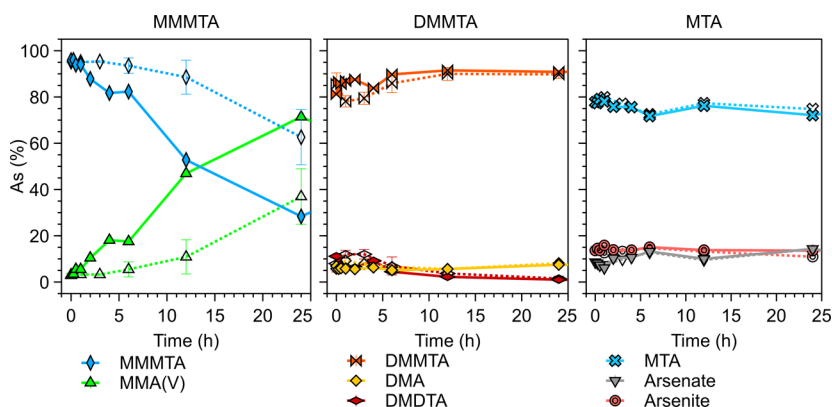


Figure 1. Abiotic air purging experiment (40 mM O₂/h) of 3 μM MMMTA and 10 μM DMMTA or MTA in nutrient solution for 24 h (air-purged (solid lines, *n* = 1); controls (dotted lines, *n* = 3)).

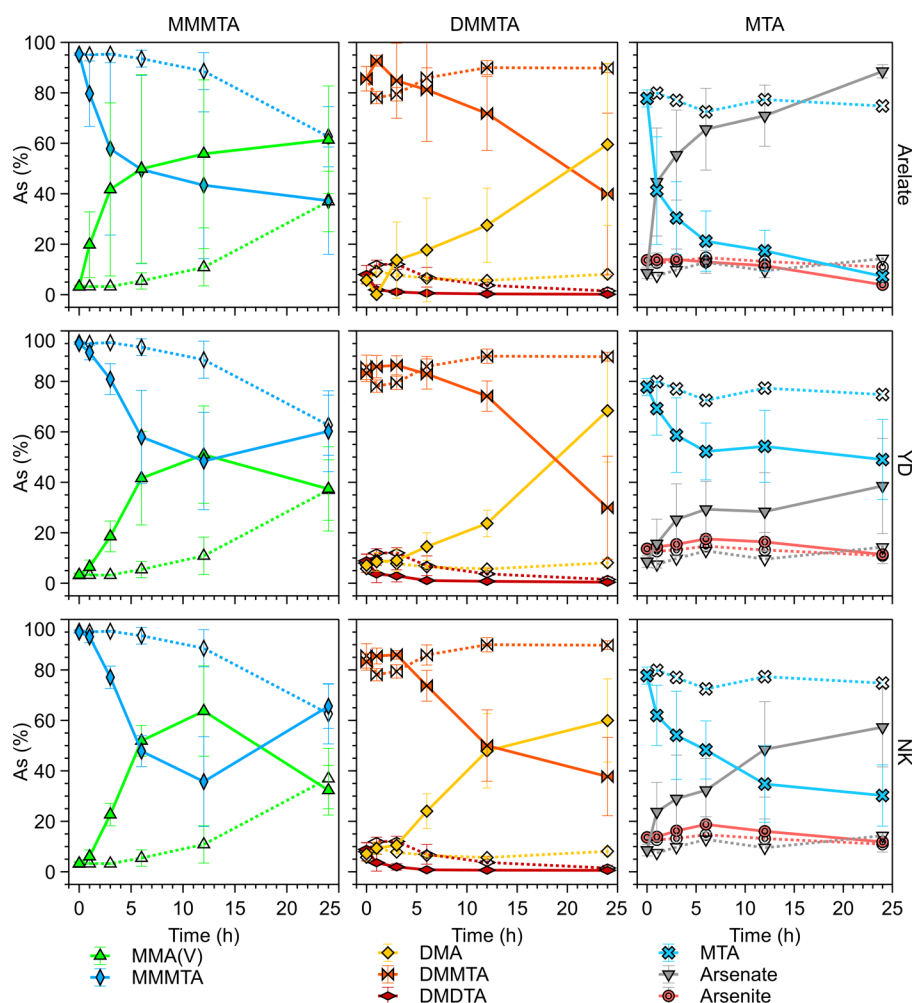


Figure 2. Arsenic speciation in nutrient solution monitored over 24 h with 20 day old rice seedlings (upper panel, Arelate; middle panel, YD; lower panel, NK) exposed to 10 μM MMMTA, DMMTA, or MTA (solid lines) and controls without plants (dotted lines; influx experiment; *n* = 3–7).

MMMTA, 71% was transformed to MMA after 24 h when purged with air, while no more than $37 \pm 12\%$ was transformed in control treatments, where only a small headspace was filled with air (Figure 1). Rapid conversion of MMMTA to MMA^V upon exposure to air has been observed before,³⁵ but the reason for this fast abiotic transformation of MMMTA currently remains unclear.

Arsenic Speciation Changes in Nutrient Solution of Hydroponic MMMTA, DMMTA, and MTA Influx Experiments and Protein Extracts. Speciation changes observed during influx experiments are discussed together with those observed in crude protein extracts, because the latter only shows enzymatic transformations in the plant while the former integrates transformations in solution by ROL and abiotic or enzymatic transformations in the plant after uptake, followed

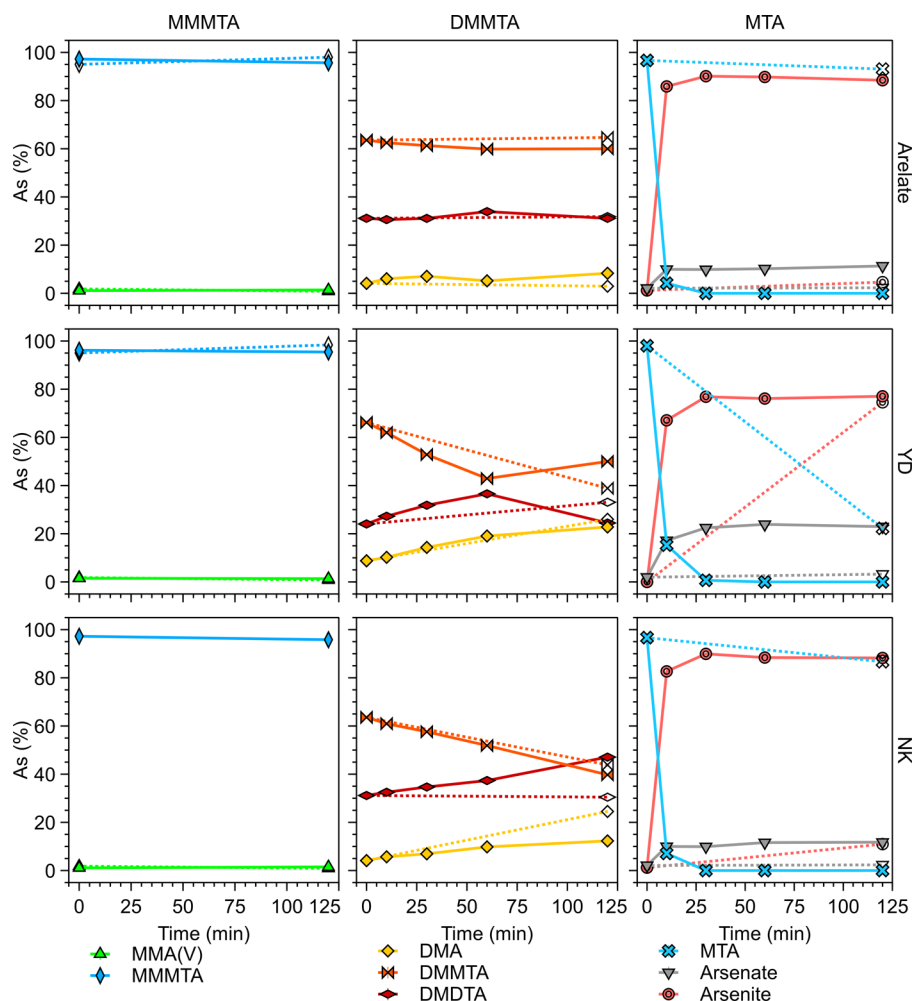


Figure 3. Arsenic speciation in protein extracts (upper panel, Arelate; middle panel, YD; lower panel, NK) spiked with 3.33 μM MMMTA, DMMTA, and MTA monitored over 120 min (protein extract (solid lines); controls denatured at 100 $^{\circ}\text{C}$ for 2 min (dotted lines); $n = 1$).

by efflux of transformation products. All three As species were transformed during the influx experiments, but only MTA showed significant and fast transformation in crude protein extracts.

For MMMTA, transformation to MMA^{V} was observed in all three cultivars during the first 12 h of the influx experiment (Arelate, $56 \pm 29\%$; YD, $51 \pm 19\%$; NK, $64 \pm 18\%$ MMA^{V} , respectively) and transformation was faster than in control treatments ($11 \pm 7\%$ MMA^{V} ; Figure 2(left panel)). No significant differences were observed between the three cultivars over time and compared to controls after 24 h. MMA^{V} itself can be further reduced to MMA^{III} , as observed in nutrient solutions of plants initially exposed to MMA^{V} , but the extent was small (2% MMA^{III} after 24 h; Figure SI 4) and no MMA^{III} was observed during MMMTA exposures.

In contrast to the influx experiment, MMMTA was stable in the presence of crude root protein extracts, as well as denatured controls over 120 min (Figure 3(left panel)), indicating that enzymatic transformation of MMMTA to MMA^{V} is negligible, based on our crude protein extracts. We therefore assume that transformations during influx experiments were most likely caused by ROL, leading to the oxidation of sulfide bound in MMMTA and thereby transformation of MMMTA to MMA^{V} . This observation is also in

line with results from air purging that showed MMMTA was not stable in the presence of oxygen.

For DMMTA, transformation to DMA was observed for all three cultivars (Arelate, $60 \pm 32\%$; YD, $68 \pm 20\%$; NK, $60 \pm 17\%$ DMA, respectively; Figure 2(middle panel)). In control treatments, DMMTA remained stable after 24 h. No significant differences in transformation rates were found between cultivars. However, the remaining DMDTA was transformed significantly faster in the presence of plants than in controls without plants for the first 6 h ($P < 0.05$). When plants were exposed to DMA, no further species transformation occurred (data not shown), as reported in literature before.¹⁸ Since DMMTA was stable during air purging, we concluded that the observed transformation was not due to root oxygen loss but happened after DMMTA uptake by the plant.

In contrast to MMMTA and MTA, DMMTA was not stable in protein buffer without root proteins and transformed to DMA (31%) and DMDTA (57%), respectively (Figure SI 5). Abiotic complexation of DMMTA with glutathione (GSH) molecules via thiol groups of GSH and further disproportionation to DMA^{III} -GSH and DMDTA was reported under acidic conditions, whereas DMA^{III} and DMDTA were directly formed in the presence of GSH under neutral to basic conditions.^{61,62} The used protein buffer did not contain GSH but contained dithiothreitol (DTT) with a thiol group.

The capability of DTT to disproportionate DMMTA was confirmed by incubating DMMTA and DTT for 120 min and DMMTA was disproportionated in the presence of DTT to 35% DMA and 37% DMDTA after 120 min. DMMTA transformation to DMA in crude protein extracts showed no significant differences to the abiotic transformations observed in denatured controls (after 120 min for Arelate 60 and 65% DMMTA, respectively, YD 50 and 39%, respectively, and NK 40 and 44%, respectively; Figure 3(middle panel)). Also, in comparison to fast transformation of MTA during influx experiments and in protein extracts (see paragraph below), DMMTA transformation in both protein buffer and denatured protein buffer was slower and incomplete. We therefore conclude that DMMTA transformation in our crude protein extracts is negligible compared to abiotic transformation in the root matrix. A possible reaction is conversion of DMMTA to DMDTA and DMA^{III} in the presence of GSH under neutral and slightly alkaline conditions as they occur in cytoplasm (pH 7.5).⁶²

For MTA, transformation to arsenite has been previously reported for the Arelate cultivar in similar influx experiments.⁴³ Here, our influx experiments showed transformation of MTA to arsenate for all three cultivars within 24 h (Arelate, 89 ± 3%; YD, 39 ± 19%; NK, 57 ± 16% arsenate, respectively; Figure 2(right panel)), while control treatments remained stable. Comparing MTA transformation within the three cultivars, Arelate was significantly faster than NK and YD ($P < 0.05$, except for NK 6 h). Formation of arsenate instead of the expected arsenite might be due to different oxidizing potentials or compositions of the nutrient solutions. We were able to trace back that both phosphorus and Fe in the nutrient solution increased the share of arsenate slightly (Figure SI 6), but also in their absence arsenate formation was observed. Hence, there is still an unexplained influence of the nutrient solution composition on final product formation (arsenite or arsenate) from MTA.

In crude protein extracts, MTA transformed to arsenite rapidly and the order of cultivars was the same as in the influx experiments (share of arsenite after 10 min in Arelate, 86%; YD, 67%; NK, 83%; Figure 3(right panel)). No transformation was observed in denatured controls. ROL cannot explain transformation of MTA to arsenite, because MTA was stable in the presence of oxygen during the air-purging experiments and the fastest transformation was found for Arelate, the cultivar with the lowest ROL (Figure SI 1). We therefore conclude that transformation of MTA to arsenite was enzymatic, which would also explain the fast transformation rates compared to slower abiotic transformation in protein extracts for DMMTA. Up to now, no enzyme in plants is known to reduce MTA to arsenite. For its structural analogue, arsenate, reduction to arsenite by HAC-family enzymes has been described,^{63,64} but it is unclear to date whether MTA and arsenate are both accepted as substrates by the same reductases. The preliminary results from our crude protein extracts show a specific need to study the cellular stability of MTA in detail and to identify the enzymes responsible for its transformation.

In summary, the experiments showed that MMMTA is transformed to MMA already outside the roots, probably just by ROL, while both DMMTA and MTA are transformed inside the rice plants. For DMMTA transformation to DMA is probably a non-enzymatic reaction with SH-containing molecules and for MTA transformation to arsenite is probably enzymatically catalyzed.

Detection of Methylated Thioarsenates in Xylem. In order to evaluate whether methylated thioarsenates could be taken up intact into rice plants and transported to shoots, xylem sap of rice plants exposed to methylated thioarsenates was analyzed. After exposure to MMMTA, up to 18 ± 1% of all As species detected in the xylem was MMMTA; for DMMTA it was up to 7 ± 1% of all As species (Figure 4). The xylem

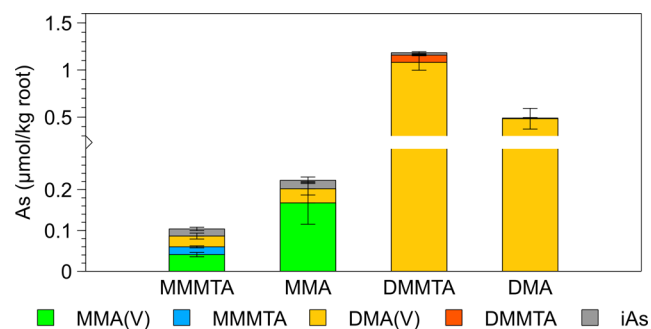


Figure 4. Arsenic speciation in xylem sap after 20 day old rice seedlings had been exposed to 10 μM MMA^V, MMMTA, DMA^V, or DMMTA for 24 h. Growth medium was changed every 6 h during daytime and after 12 h during nighttime to minimize transformation of As speciation ($n = 3$); As concentrations are normalized to root weights to account for small differences in seedling weights (Table SI 2).

data therefore show that both As species were taken up and transported. We assume that the detected amounts are minimum numbers, because some MMMTA or DMMTA might have transformed during sampling and handling for analysis where small amounts (1–2 μL) were taken over 1.5 h and diluted in an ice-cold phosphate buffer under oxic conditions. The dominant species in the xylem were the expected transformation products MMA^V from MMMTA and DMA^V from DMMTA. In DMMTA experiments, the only other species was traces of inorganic As (2 ± 1%), which is in line with previous studies.¹⁸ In MMMTA and MMA^V experiments, in addition to inorganic As (17 ± 3 and 10 ± 4%, respectively) also DMA^V (25 ± 4 and 15 ± 3%, respectively) was found. The presence of DMA^V could either be explained by further methylation of MMA^V to DMA^V in nonsterile hydroponic cultures^{10,26} or by traces of DMA^V in the nutrient solution that accumulated in the xylem due to high root-to-shoot translocation^{24,25} (Figure SI 7). No MMA^{III} was detected in xylem sap of MMMTA- and MMA^V-exposed plants, as could have been expected from root speciation^{10,18,24} and our influx experiment. This observation might be either explained by rapid oxidation of MMA^{III} to MMA^{V24} during xylem sap sampling when a few microliters of sample were transferred to phosphate buffer (see methods of xylem sampling for further details) or by sequestration as MMA^{III}-PC in root vacuoles (see discussion below for further details).¹⁸

Comparing the sum of As species for each treatment, most As was transported in xylem of DMMTA-exposed plants (1.18 ± 0.09 nmol/g root) followed by DMA^V (0.49 ± 0.11 nmol/g root), and similar amounts of As were transported in MMMTA and MMA^V treatment (0.10 ± 0.01 and 0.22 ± 0.07 nmol/g root). The implications of As transport in the xylem will be discussed in detail together with uptake and translocation below.

Uptake and Translocation of Methylated Thioarsenates over Time. In order to quantify differences in the total As uptake and translocation after exposure to methylated thioarsenates in comparison with methylated oxyarsenates and the inorganic MTA, 20 day old plants were exposed to MMA^V, DMA^V, MMMTA, and DMMTA for 6–72 h. Data for MTA were taken from our previous study for comparison.⁴³ After 72 h, total As uptake was highest for roots exposed to MMMTA ($220 \pm 27 \mu\text{mol/kg}$), followed by MMA^V ($146 \pm 5 \mu\text{mol/kg}$), and DMMTA-exposed roots ($130 \pm 22 \mu\text{mol/kg}$), then MTA ($57 \pm 2 \mu\text{mol/kg}$), and significantly lower for DMA^V-exposed roots ($14 \pm 1 \mu\text{mol/kg}$; Figure 5 (lower panel)). The pattern

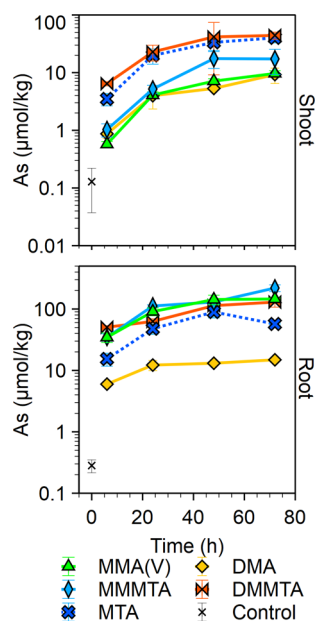


Figure 5. Arsenic uptake kinetics for rice seedlings grown for 20 days without As before exposure to $10 \mu\text{M}$ MMA^V, MMMTA, DMA^V, or DMMTA for 6, 24, 48, and 72 h. MTA data were added from our previous study.⁴³ Total As concentrations were determined after microwave digestion ($n = 3$) and contain error bars.

was different in shoots where the total As concentrations for DMA^V, MMA^V, and MMMTA-exposed plants were similar after 72 h (9 ± 3 , 10 ± 1 , and $17 \pm 8 \mu\text{mol/kg}$, respectively), but higher for MTA- ($40 \pm 7 \mu\text{mol/kg}$) and significantly higher for DMMTA-exposed plants ($44 \pm 6 \mu\text{mol/kg}$; $P < 0.001$; Figure 5(upper panel)). Calculation of shoot-to-root TFs for total As in plants exposed to one of the following As species for 72 h yielded the following order DMA^V (0.61 ± 0.15) = MTA (0.55 ± 0.14)⁴³ \approx DMMTA (0.34 ± 0.03) > MMMTA (0.08 ± 0.03) = MMA^V (0.07 ± 0.01 , Figure SI 7).

Results for the methylated oxyarsenates were in line with previous observations. The lower DMA^V compared to MMA^V root concentrations are probably largely due to higher translocation, not lower uptake. Typically, MMA^V (pK_{a1} , 4.2) and DMA^V (pK_{a1} , 6.1) are taken up as uncharged molecules by aquaporin channel OsNIP2;1.¹⁸ Even though it has been postulated that dissociated MMA^V and DMA^V can be taken up as well,⁵ no corresponding transporters have been identified to date and the general observation is that uptake decreases with increasing pH.¹⁸ The pH of our nutrient solutions was 5.0, so if there was a reduced uptake due to increasing dissociation, it should have affected MMA^V rather than DMA^V. On the other hand, rice roots are known to reduce MMA^V to MMA^{III} and

form an MMA^{III}–PC complex that is sequestered in root vacuoles.^{24,25} Low total As concentrations in shoots and xylem, as well as low TFs for MMA^V, are in line with MMA^V sequestration in roots, as reported before.^{24,25} DMA in contrast is not reduced by rice roots and does not form PC complexes,²⁵ explaining its low concentration in roots but high concentrations in shoots and xylem, as well as high TFs.

For the methylated thioarsenates, to the best of our knowledge, no pK_{a1} values have been determined experimentally, yet. Based on chromatographic behavior, pK_{a1} for DMMTA was assumed to be between 6 and 7.⁶⁵ With a pK_{a1} similar to that of DMA^V, uptake for DMMTA should not be limited. Whether uptake of MMMTA is similar to that of MMA^V is currently unknown. Reduction or complexation of MMMTA was not reported in plant roots so far. However, high total As concentrations in roots indicated that MMMTA was either sequestered in root cells, too, or MMMTA was transformed to MMA^V in the rhizosphere due to ROL and taken up as MMA^V. Taking into account that we found no indication for a transformation of MMMTA to MMA^V by root proteins (Figure 3(left panel)), storage as MMMTA–PC might be possible. This needs to be further investigated. Similar total As concentrations in shoots and xylem as well as similar total As TFs compared to MMA^V might represent further evidence for similar detoxification routes as documented for MMA^V.

Surprisingly, DMMTA concentrations in roots were about 10 times higher than for DMA^V, indicating high uptake and/or sequestration in roots. No direct evidence for DMMTA–PC complexation was reported in literature, but a DMMTA–GSH complex has been described in *Brassica oleracea* exposed to DMA^V.⁵⁴ Shoot concentrations of DMMTA-exposed plants were significantly higher than for other As species, which was in line with the highest As concentrations in xylem sap and high total As TFs. Xylem speciation showed that the high translocation was not only due to transformation of DMMTA to highly mobile DMA^V, but DMMTA itself contributed to shoot uptake. This might indicate that DMMTA is not quantitatively complexed by thiols.

A similar pattern of sequestration in roots with concurrent high total As TFs and shoot As concentrations was found for MTA before (Figure 5 and Figure SI 7; data from Kerl et al.⁴³). Arsenic speciation in protein extracts showed MTA was rapidly reduced to arsenite (Figure 3(right panel)), which can be complexed as As^{III}–PC in root vacuoles.^{19–22} High total As translocation to shoots was assumed to be due to efficient xylem loading that was faster than MTA–arsenite reduction and PC complexation.⁴³ Alternatively, reduction and PC complexation might be spatially separated in root tissue.

Implications for Grain Arsenic. To limit chronic exposure of humans and comply with threshold values for As in rice grains, different approaches, such as water management and selection of low As accumulation varieties or S-fertilization, are investigated. Sulfur fertilization seems to be a promising strategy for lowering As uptake in rice on the one hand;³⁶ on the other hand, S-fertilization promotes formation of methylated, thiolated, and methylthiolated arsenates that can be taken up and translocated by rice plants.⁴³ The important question is, could inorganic and methylated thioarsenates reach rice grains or increase total grain As?

MMMTA and MTA might be less critical with regard to accumulation in grain. Even though MMMTA is highly toxic and might not be transformed inside rice plants, it showed low

translocation to shoots similar to MMA^V. Overall, contribution to total grain As might be very minor because most MMTA seems to be transformed to MMA^V by ROL outside the rice roots and MMA^V concentrations in rice grains are usually only a few micrograms per kilogram.²⁶ For MTA, direct accumulation in grains might also be negligible, because MTA is transformed to arsenite rapidly. However, high total As translocation factors imply MTA exposure might increase total As concentrations in grains, instead of lowering grain As.

In contrast to MMTA and MTA, DMMTA could be much more critical from a food safety perspective because uptake and total As translocation are high. Although, in our experiments, a relatively large share of DMMTA was transformed to DMA^V, up to 20% DMMTA has been detected in enzymatic extracts of commercial rice samples before.^{45,46} In our own preliminary studies using the same extraction method, we also detected up to 11% DMMTA in 2 out of 11 randomly selected commercial samples (data not shown). DMMTA is highly toxic, comparable to inorganic As, but co-determined as DMA using common acid extraction for rice grains because the acid converts DMMTA to DMA^V.³⁷ This is especially problematic, because DMA^V is not considered toxic and exempt from food regulatory guidelines. Contribution of DMMTA and total As in rice grains especially after S-fertilization needs to be further investigated, and potentially both standard extraction methods and guidelines need to be adapted.

■ ASSOCIATED CONTENT

Supporting Information

The Supporting Information is available free of charge on the ACS Publications website at DOI: [10.1021/acs.est.9b00592](https://doi.org/10.1021/acs.est.9b00592).

Root oxygen loss method description and results; compositions; retention times; stability test of DMMTA; results of influx experiment; stabilities in protein buffer; influence of nutrient solution composition; translocation factors; seedling weights; absolute As values for all experiments (PDF)

■ AUTHOR INFORMATION

Corresponding Author

*Phone: +49 921 55 3999; email: b.planer-friedrich@uni-bayreuth.de.

ORCID

Britta Planer-Friedrich: [0000-0002-0656-4283](https://orcid.org/0000-0002-0656-4283)

Notes

The authors declare no competing financial interest.

■ ACKNOWLEDGMENTS

We acknowledge financial support for a Ph.D. stipend to C.F.K. from the German Academic Scholarship Foundation and funding by the German Research Foundation (DFG) Grants PL 302/25 and CL 152/11. We thank Stefan Will for help with IC-ICP-MS measurements as well as Jijia Wang and Prof. Dr. Xinbin Feng (State Key Laboratory of Environmental Geochemistry, Institute of Geochemistry, Chinese Academy of Sciences, Guiyang, China) for providing YD and NK seeds.

■ REFERENCES

(1) Meharg, A. A.; Williams, P. N.; Adomako, E.; Lawgali, Y. Y.; Deacon, C.; Villada, A.; Cambell, R. C. J.; Sun, G.; Zhu, Y.-G.; Feldmann, J.; Raab, A.; Zhao, F.-J.; Islam, R.; Hossain, S.; Yanai, J.

Geographical Variation in Total and Inorganic Arsenic Content of Polished (White) Rice. *Environ. Sci. Technol.* **2009**, *43* (5), 1612–1617.

(2) Chen, Y.; Han, Y. H.; Cao, Y.; Zhu, Y. G.; Rathinasabapathi, B.; Ma, L. Q. Arsenic Transport in Rice and Biological Solutions to Reduce Arsenic Risk from Rice. *Front. Plant Sci.* **2017**, *8*, 268.

(3) Williams, P. N.; Villada, A.; Deacon, C.; Raab, A.; Figuerola, J.; Green, A. J.; Feldmann, J.; Meharg, A. A. Greatly Enhanced Arsenic Shoot Assimilation in Rice Leads to Elevated Grain Levels Compared to Wheat and Barley. *Environ. Sci. Technol.* **2007**, *41* (19), 6854–6859.

(4) Williams, P. N.; Raab, A.; Feldmann, J.; Meharg, A. A. Market Basket Survey Shows Elevated Levels of As in South Central U.S. Processed Rice Compared to California: Consequences for Human Dietary Exposure. *Environ. Sci. Technol.* **2007**, *41* (7), 2178–2183.

(5) Meharg, A. A.; Zhao, F.-J. *Arsenic & Rice*. In Springer: Dordrecht, The Netherlands, 2012; Vol. 1, p 172.

(6) Marin, A. R.; Masscheleyn, P. H.; Patrick, W. H. Soil Redox-Ph Stability of Arsenic Species and Its Influence on Arsenic Uptake by Rice. *Plant Soil* **1993**, *152* (2), 245–253.

(7) Masscheleyn, P. H.; Delaune, R. D.; Patrick, W. H. Effect of Redox Potential and Ph on Arsenic Speciation and Solubility in a Contaminated Soil. *Environ. Sci. Technol.* **1991**, *25* (8), 1414–1419.

(8) Zhao, F. J.; McGrath, S. P.; Meharg, A. A. Arsenic as a food chain contaminant: mechanisms of plant uptake and metabolism and mitigation strategies. *Annu. Rev. Plant Biol.* **2010**, *61*, 535–59.

(9) Fan, C.; Liu, G.; Long, Y.; Rosen, B.; Cai, Y. Thiolation in arsenic metabolism: a chemical perspective. *Metallomics* **2018**, *10* (10), 1368–1382.

(10) Lomax, C.; Liu, W. J.; Wu, L.; Xue, K.; Xiong, J.; Zhou, J.; McGrath, S. P.; Meharg, A. A.; Miller, A. J.; Zhao, F. J. Methylated arsenic species in plants originate from soil microorganisms. *New Phytol.* **2012**, *193* (3), 665–72.

(11) Ma, J. F.; Yamaji, N.; Mitani, N.; Xu, X. Y.; Su, Y. H.; McGrath, S. P.; Zhao, F. J. Transporters of arsenite in rice and their role in arsenic accumulation in rice grain. *Proc. Natl. Acad. Sci. U. S. A.* **2008**, *105* (29), 9931–5.

(12) Zhao, F. J.; Ago, Y.; Mitani, N.; Li, R. Y.; Su, Y. H.; Yamaji, N.; McGrath, S. P.; Ma, J. F. The role of the rice aquaporin Lsi1 in arsenite efflux from roots. *New Phytol.* **2010**, *186* (2), 392–9.

(13) Ma, J. F.; Yamaji, N. A cooperative system of silicon transport in plants. *Trends Plant Sci.* **2015**, *20* (7), 435–42.

(14) Sun, S.; Gu, M.; Cao, Y.; Huang, X.; Zhang, X.; Ai, P.; Zhao, J.; Fan, X.; Xu, G. A constitutive expressed phosphate transporter, OsPht1;1, modulates phosphate uptake and translocation in phosphate-replete rice. *Plant Physiol.* **2012**, *159* (4), 1571–81.

(15) Cao, Y.; Sun, D.; Ai, H.; Mei, H.; Liu, X.; Sun, S.; Xu, G.; Liu, Y.; Chen, Y.; Ma, L. Q. Knocking Out OsPT4 Gene Decreases Arsenate Uptake by Rice Plants and Inorganic Arsenic Accumulation in Rice Grains. *Environ. Sci. Technol.* **2017**, *51* (21), 12131–12138.

(16) Ye, Y.; Li, P.; Xu, T.; Zeng, L.; Cheng, D.; Yang, M.; Luo, J.; Lian, X. OsPT4 Contributes to Arsenate Uptake and Transport in Rice. *Front. Plant Sci.* **2017**, *8*, 2197.

(17) Wang, P.; Zhang, W.; Mao, C.; Xu, G.; Zhao, F. J. The role of OsPT8 in arsenate uptake and varietal difference in arsenate tolerance in rice. *J. Exp. Bot.* **2016**, *67* (21), 6051–6059.

(18) Li, R. Y.; Ago, Y.; Liu, W. J.; Mitani, N.; Feldmann, J.; McGrath, S. P.; Ma, J. F.; Zhao, F. J. The rice aquaporin Lsi1 mediates uptake of methylated arsenic species. *Plant Physiol.* **2009**, *150* (4), 2071–80.

(19) Clemens, S. Toxic metal accumulation, responses to exposure and mechanisms of tolerance in plants. *Biochimie* **2006**, *88* (11), 1707–19.

(20) Mendoza-Cozatl, D. G.; Jobe, T. O.; Hauser, F.; Schroeder, J. I. Long-distance transport, vacuolar sequestration, tolerance, and transcriptional responses induced by cadmium and arsenic. *Curr. Opin. Plant Biol.* **2011**, *14* (5), 554–62.

- (21) Verbruggen, N.; Hermans, C.; Schat, H. Mechanisms to cope with arsenic or cadmium excess in plants. *Curr. Opin. Plant Biol.* **2009**, *12* (3), 364–72.
- (22) Pickering, I. J.; Prince, R. C.; George, M. J.; Smith, R. D.; George, G. N.; Salt, D. E. Reduction and Coordination of Arsenic in Indian Mustard. *Plant Physiol.* **2000**, *122* (4), 1171–1178.
- (23) Raab, A.; Schat, H.; Meharg, A. A.; Feldmann, J. Uptake, translocation and transformation of arsenate and arsenite in sunflower (*Helianthus annuus*): formation of arsenic-phytochelatin complexes during exposure to high arsenic concentrations. *New Phytol.* **2005**, *168* (3), 551–8.
- (24) Mishra, S.; Mattusch, J.; Wennrich, R. Accumulation and transformation of inorganic and organic arsenic in rice and role of thiol-complexation to restrict their translocation to shoot. *Sci. Rep.* **2017**, *7*, 40522.
- (25) Raab, A.; Williams, P. N.; Meharg, A.; Feldmann, J. Uptake and translocation of inorganic and methylated arsenic species by plants. *Environ. Chem.* **2007**, *4* (3), 197.
- (26) Zhao, F. J.; Zhu, Y. G.; Meharg, A. A. Methylated arsenic species in rice: geographical variation, origin, and uptake mechanisms. *Environ. Sci. Technol.* **2013**, *47* (9), 3957–66.
- (27) Planer-Friedrich, B.; Halder, D.; Kerl, C. F.; Schaller, J.; Wang, J.; Martin, M.; Romani, M. *Thioarsenates—So Far Unrecognized Arsenic Species in Paddy Soils*; Goldschmidt Abstracts: Paris, 2017; p 3176.
- (28) Naser, H. M.; Nagata, O.; Tamura, S.; Hatano, R. Methane emissions from five paddy fields with different amounts of rice straw application in central Hokkaido, Japan. *Soil Sci. Plant Nutr.* **2007**, *53* (1), 95–101.
- (29) Shiratori, Y.; Watanabe, H.; Furukawa, Y.; Tsuruta, H.; Inubushi, K. Effectiveness of a subsurface drainage system in poorly drained paddy fields on reduction of methane emissions. *Soil Sci. Plant Nutr.* **2007**, *53* (4), 387–400.
- (30) Sigg, L.; Stumm, W. *Aquatische Chemie: eine Einführung in die Chemie wässriger Lösungen und natürlicher Gewässer*. vdf: Zürich, 1994; p 498.
- (31) Ayotade, K. A. Kinetics and reactions of hydrogen sulphide in solution of flooded rice soils. *Plant Soil* **1977**, *46* (2), 381–389.
- (32) Besold, J.; Biswas, A.; Suess, E.; Scheinost, A. C.; Rossberg, A.; Mikutta, C.; Kretzschmar, R.; Gustafsson, J. P.; Planer-Friedrich, B. Monothioarsenate Transformation Kinetics Determining Arsenic Sequestration by Sulfhydryl Groups of Peat. *Environ. Sci. Technol.* **2018**, *52* (13), 7317–7326.
- (33) Stauder, S.; Raue, B.; Sacher, F. Thioarsenates in Sulfidic Waters. *Environ. Sci. Technol.* **2005**, *39* (16), 5933–5939.
- (34) Planer-Friedrich, B.; Suess, E.; Scheinost, A. C.; Wallschläger, D. Arsenic speciation in sulfidic waters: reconciling contradictory spectroscopic and chromatographic evidence. *Anal. Chem.* **2010**, *82* (24), 10228–35.
- (35) Cullen, W. R.; Liu, Q.; Lu, X.; McKnight-Whitford, A.; Peng, H.; Popowich, A.; Yan, X.; Zhang, Q.; Fricke, M.; Sun, H.; Le, X. C. Methylated and thiolated arsenic species for environmental and health research - A review on synthesis and characterization. *J. Environ. Sci. (Beijing, China)* **2016**, *49*, 7–27.
- (36) Jia, Y.; Bao, P.; Zhu, Y. G. Arsenic bioavailability to rice plant in paddy soil: influence of microbial sulfate reduction. *J. Soils Sediments* **2015**, *15* (9), 1960–1967.
- (37) Dixit, G.; Singh, A. P.; Kumar, A.; Singh, P. K.; Kumar, S.; Dwivedi, S.; Trivedi, P. K.; Pandey, V.; Norton, G. J.; Dhankher, O. P.; Tripathi, R. D. Sulfur mediated reduction of arsenic toxicity involves efficient thiol metabolism and the antioxidant defense system in rice. *J. Hazard. Mater.* **2015**, *298*, 241–51.
- (38) Zhang, J.; Zhao, Q.-Z.; Duan, G.-L.; Huang, Y.-C. Influence of sulphur on arsenic accumulation and metabolism in rice seedlings. *Environ. Exp. Bot.* **2011**, *72* (1), 34–40.
- (39) Hu, Z. Y.; Zhu, Y. G.; Li, M.; Zhang, L. G.; Cao, Z. H.; Smith, F. A. Sulfur (S)-induced enhancement of iron plaque formation in the rhizosphere reduces arsenic accumulation in rice (*Oryza sativa* L.) seedlings. *Environ. Pollut.* **2007**, *147* (2), 387–93.
- (40) Fan, J.; Xia, X.; Hu, Z.; Ziadi, N.; Liu, C. Excessive sulfur supply reduces arsenic accumulation in brown rice. *Plant, Soil Environ.* **2013**, *59* (4), 169–174.
- (41) Boye, K.; Lezama-Pacheco, J.; Fendorf, S. Relevance of Reactive Fe:S Ratios for Sulfur Impacts on Arsenic Uptake by Rice. *Soils* **2017**, *1* (1), 1.
- (42) Naranmandura, H.; Ibata, K.; Suzuki, K. T. Toxicity of dimethylmonothioarsinic acid toward human epidermoid carcinoma A431 cells. *Chem. Res. Toxicol.* **2007**, *20* (8), 1120–5.
- (43) Kerl, C. F.; Rafferty, C.; Clemens, S.; Planer-Friedrich, B. Monothioarsenate Uptake, Transformation, and Translocation in Rice Plants. *Environ. Sci. Technol.* **2018**, *52* (16), 9154–9161.
- (44) Planer-Friedrich, B.; Kuhnlenz, T.; Halder, D.; Lohmayer, R.; Wilson, N.; Rafferty, C.; Clemens, S. Thioarsenate Toxicity and Tolerance in the Model System *Arabidopsis thaliana*. *Environ. Sci. Technol.* **2017**, *51* (12), 7187–7196.
- (45) Ackerman, A. H.; Creed, P. A.; Parks, A. N.; Fricke, M. W.; Schwegel, C. A.; Creed, J. T.; Heitkemper, D. T.; Vela, N. P. Comparison of a Chemical and Enzymatic Extraction of Arsenic from Rice and an Assessment of the Arsenic Absorption from Contaminated Water by Cooked Rice. *Environ. Sci. Technol.* **2005**, *39* (14), 5241–5246.
- (46) Mantha, M.; Yearly, E.; Trent, J.; Creed, P. A.; Kubachka, K.; Hanley, T.; Shockey, N.; Heitkemper, D.; Caruso, J.; Xue, J.; Rice, G.; Wymer, L.; Creed, J. T. Estimating Inorganic Arsenic Exposure from U.S. Rice and Total Water Intakes. *Environ. Health Perspect.* **2017**, *125* (5), No. 057005.
- (47) *Commission Regulation (EU) 2015/1006 of 25 June 2015 amending Regulation (EC) No 1881/2006 as regards maximum levels of inorganic arsenic in foodstuffs*; European Commission: Brussels, Belgium, 2015.
- (48) Chen, H.; Tang, Z.; Wang, P.; Zhao, F. J. Geographical variations of cadmium and arsenic concentrations and arsenic speciation in Chinese rice. *Environ. Pollut.* **2018**, *238*, 482–490.
- (49) Li, Y. L.; Fan, X. R.; Shen, Q. R. The relationship between rhizosphere nitrification and nitrogen-use efficiency in rice plants. *Plant, Cell Environ.* **2007**, *31* (1), 73–85.
- (50) Wallschläger, D.; London, J. Determination of Methylated Arsenic-Sulfur Compounds in Groundwater. *Environ. Sci. Technol.* **2008**, *42* (1), 228–234.
- (51) Hinrichsen, S.; Geist, F.; Planer-Friedrich, B. Inorganic and methylated thioarsenates pass the gastrointestinal barrier. *Chem. Res. Toxicol.* **2015**, *28* (9), 1678–80.
- (52) Schwedt, G.; Rieckhoff, M. Separation of thio- and oxothioarsenates by capillary zone electrophoresis and ion chromatography. *J. Chromatogr. A* **1996**, *736* (1–2), 341–350.
- (53) Suess, E.; Scheinost, A. C.; Bostick, B. C.; Merkel, B. J.; Wallschläger, D.; Planer-Friedrich, B. Discrimination of thioarsenites and thioarsenates by X-ray absorption spectroscopy. *Anal. Chem.* **2009**, *81* (20), 8318–26.
- (54) Kim, Y. T.; Lee, H.; Yoon, H. O.; Woo, N. C. Kinetics of Dimethylated Thioarsenicals and the Formation of Highly Toxic Dimethylmonothioarsinic Acid in Environment. *Environ. Sci. Technol.* **2016**, *50* (21), 11637–11645.
- (55) Bleeker, P. M.; Hakvoort, H. W.; Bliet, M.; Souer, E.; Schat, H. Enhanced arsenate reduction by a CDC25-like tyrosine phosphatase explains increased phytochelatin accumulation in arsenate-tolerant *Holcus lanatus*. *Plant J.* **2006**, *45* (6), 917–29.
- (56) Duan, G. L.; Zhu, Y. G.; Tong, Y. P.; Cai, C.; Kneer, R. Characterization of arsenate reductase in the extract of roots and fronds of Chinese brake fern, an arsenic hyperaccumulator. *Plant Physiol.* **2005**, *138* (1), 461–9.
- (57) Wu, J.; Zhang, R.; Lilley, R. M. Methylation of arsenic in vitro by cell extracts from bentgrass (*Agrostis tenuis*): effect of acute exposure of plants to arsenate. *Functional Plant Biology* **2002**, *29* (1), 73.
- (58) Xu, X. Y.; McGrath, S. P.; Zhao, F. J. Rapid reduction of arsenate in the medium mediated by plant roots. *New Phytol.* **2007**, *176* (3), 590–9.

(59) Van de Wiele, T.; Gallawa, C. M.; Kubachka, K. M.; Creed, J. T.; Basta, N.; Dayton, E. A.; Whitacre, S.; Du Laing, G.; Bradham, K. Arsenic metabolism by human gut microbiota upon in vitro digestion of contaminated soils. *Environ. Health Perspect.* **2010**, *118* (7), 1004–1009.

(60) Planer-Friedrich, B.; Fisher, J. C.; Hollibaugh, J. T.; Süß, E.; Wallschläger, D. Oxidative Transformation of Trithioarsenate Along Alkaline Geothermal Drainages—Abiotic versus Microbially Mediated Processes. *Geomicrobiol. J.* **2009**, *26* (5), 339–350.

(61) Raab, A.; Wright, S. H.; Jaspars, M.; Meharg, A. A.; Feldmann, J. Pentavalent Arsenic Can Bind to Biomolecules. *Angew. Chem.* **2007**, *119* (15), 2648–2651.

(62) Suzuki, N.; Naranmandura, H.; Hirano, S.; Suzuki, K. T. Theoretical calculations and reaction analysis on the interaction of pentavalent thioarsenicals with biorelevant thiol compounds. *Chem. Res. Toxicol.* **2008**, *21* (2), 550–3.

(63) Shi, S.; Wang, T.; Chen, Z.; Tang, Z.; Wu, Z.; Salt, D. E.; Chao, D. Y.; Zhao, F. J. OsHAC1;1 and OsHAC1;2 Function as Arsenate Reductases and Regulate Arsenic Accumulation. *Plant Physiol.* **2016**, *172* (3), 1708–1719.

(64) Xu, J.; Shi, S.; Wang, L.; Tang, Z.; Lv, T.; Zhu, X.; Ding, X.; Wang, Y.; Zhao, F. J.; Wu, Z. OsHAC4 is critical for arsenate tolerance and regulates arsenic accumulation in rice. *New Phytol.* **2017**, *215* (3), 1090–1101.

(65) Raml, R.; Goessler, W.; Francesconi, K. A. Improved chromatographic separation of thio-arsenic compounds by reversed-phase high performance liquid chromatography-inductively coupled plasma mass spectrometry. *J. Chromatogr A* **2006**, *1128* (1–2), 164–70.

Supporting Information

Environmental Science & Technology

Methylated thioarsenates and monothioarsenate differ in uptake, transformation, and contribution to total arsenic translocation in rice plants

Carolin F. Kerl[†], Ruth Alina Schindele[†], Lena Brüggewirth[†], Andrea E. Colina Blanco[†], Colleen Rafferty[‡], Stephan Clemens[‡], Britta Planer-Friedrich^{†}*

[†]Environmental Geochemistry, Bayreuth Center for Ecology and Environmental Research (BayCEER), University of Bayreuth, D-95440 Bayreuth, Germany

[‡] Plant Physiology, Bayreuth Center for Ecology and Environmental Research (BayCEER), University of Bayreuth, D-95440 Bayreuth, Germany

* Corresponding author phone: +49 921 55 3999, E-mail: b.planer-friedrich@uni-bayreuth.de

(S17 pages, 7 figures, 8 tables)

CONTENTS

Figure SI 1 Root oxygen loss.....	1
Figure SI 2 Retention times for As species	3
Figure SI 3 DMMTA stability with and without Fe	4
Figure SI 4 Influx-experiment for MMA ^V with sample chromatogram.....	5
Figure SI 5 MMMTA, DMMTA, & MTA stability in protein buffer.....	6
Figure SI 6 Influence of nutrient solution composition in arsenite oxidation	7
Figure SI 7 Translocation factors	9
Table SI 1 Nutrient solution	10
Table SI 2 Seedling fresh weights for all experiments	11
Table SI 3 Absolute values of DMMTA stability with and without Fe	12
Table SI 4 Absolute values of air purging	13
Table SI 5 Absolute values of influx experiment	14
Table SI 6 Absolute values of protein extracts	15
Table SI 7 Absolute values of protein buffer.....	16
Table SI 8 Protein extract	17

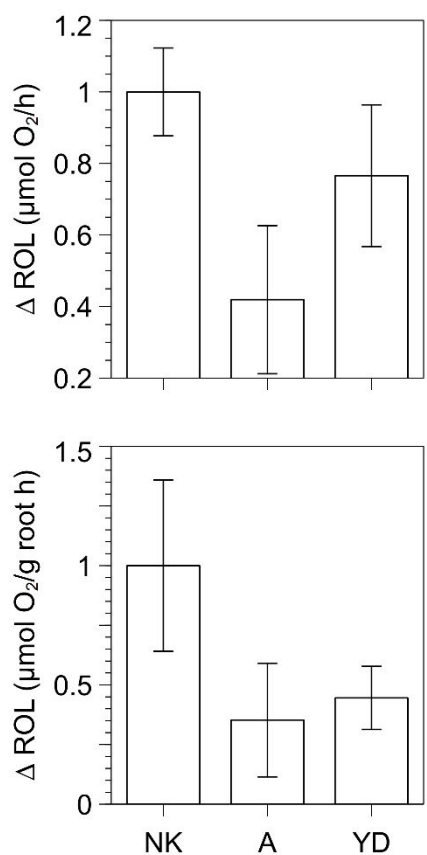


Figure SI 1. Differences in root oxygen loss of 20 day-old plants under experimental conditions (n=9). Differences between cultivars were calculated and cultivar with highest ROL was normalized to 1.

The root oxygen loss (ROL) was determined according to Kludze, et al. ¹. Briefly, 0.2 M sodium citrate solution (Sigma-Aldrich) was prepared under anoxic atmosphere in a glovebox (COY, N₂/H₂ 95/5% (v/v)) to prevent oxidation ² and 15% titanium(III)-chloride solution (Sigma-Aldrich) was added to form titanium(III)-citrate. The pH of the titanium(III)-citrate solution was adjusted to 5.6 by adding saturated sodium carbonate (Roth).

The nutrient solution was purged with N₂ for 1 h to remove oxygen. Twenty day old rice plants were coated with parafilm and placed into 40 mL nutrient solution. The test tubes were layered with paraffin immediately after 5 mL of titanium(III)-citrate were spiked into the nutrient solution. After 6 h, aliquots of the nutrient solution were taken with a needle and syringe and absorbance of the titanium(III)-citrate solution was measured photometrically at 527 nm (LKB B).

The released oxygen was quantified by obtaining a standard absorbance curve for a titanium(III)-citrate dilution series of 0.27 – 15 mmol/L and extrapolating the measured absorbance of samples.

$$ROL = \frac{c(y - z)}{6};(1) \quad ROL_w = \frac{c(y - z)}{6 \cdot w};(2)$$

ROL= radial oxygen loss in $\mu\text{mol O}_2 \text{ plant}^{-1} \text{ h}^{-1}$;

c = initial volume of Ti(III)-citrate added to each test tube in L;

y = concentration of Ti(III) in solution of control (without plants) in $\mu\text{mol Ti(III) L}^{-1}$;

z = concentration of Ti(III) in solution after 6 h treatment with plants in $\mu\text{mol Ti(III) in solution plant}^{-1} \text{ L}^{-1}$

w = dry weight of root in g

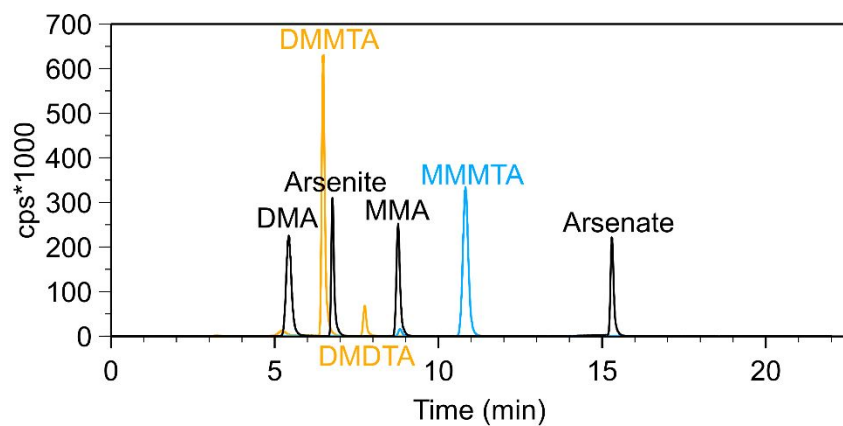


Figure SI 2. Example chromatogram for retention times of different As species on AS16 column (Dionex AG/AS16 IonPac column, 2.5–100 mM NaOH, flow rate 1.2 mL/min)³: in black calibration standard with 500 ppb DMA^V, arsenite, MMA^V and arsenate; in yellow 960 ppb DMMTA stock solution with traces of 50 ppb DMA^V, and 100 ppb DMDTA, and in blue 850 ppb MMMTA stock solution with traces of 30 ppb MMA^V.

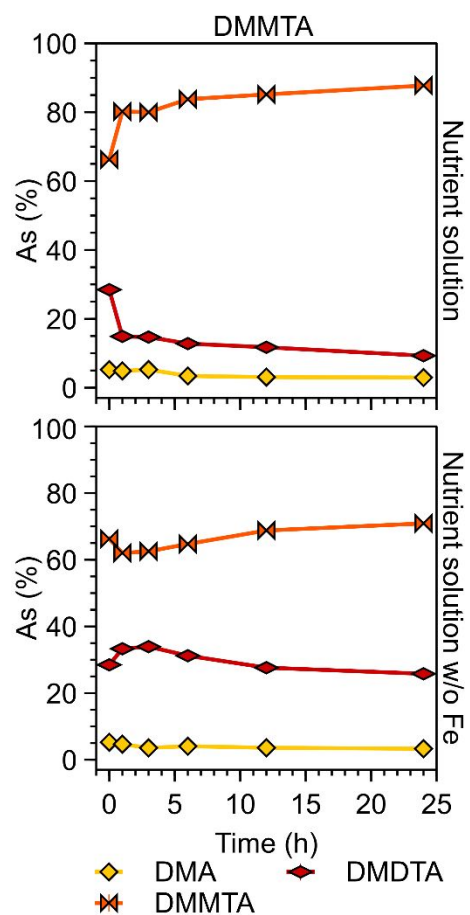


Figure SI 3. Stability test of 10 μM DMMTA in nutrient solution with and without Fe. As speciation of the initial DMMTA solution was determined by IC-ICP-MS for different treatments (n=1).

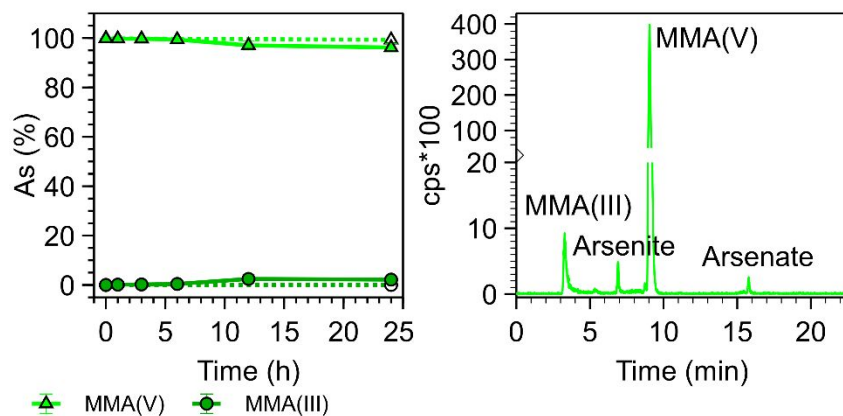


Figure SI 4. As-speciation in nutrient solution monitored over 24 h with rice seedlings exposed to 10 μM MMA^V (–) and control without plants (···). As speciation of the initial MMA^V solution was determined by IC-ICP-MS as shown in an example chromatogram on the right side (Influx experiment; n=3).

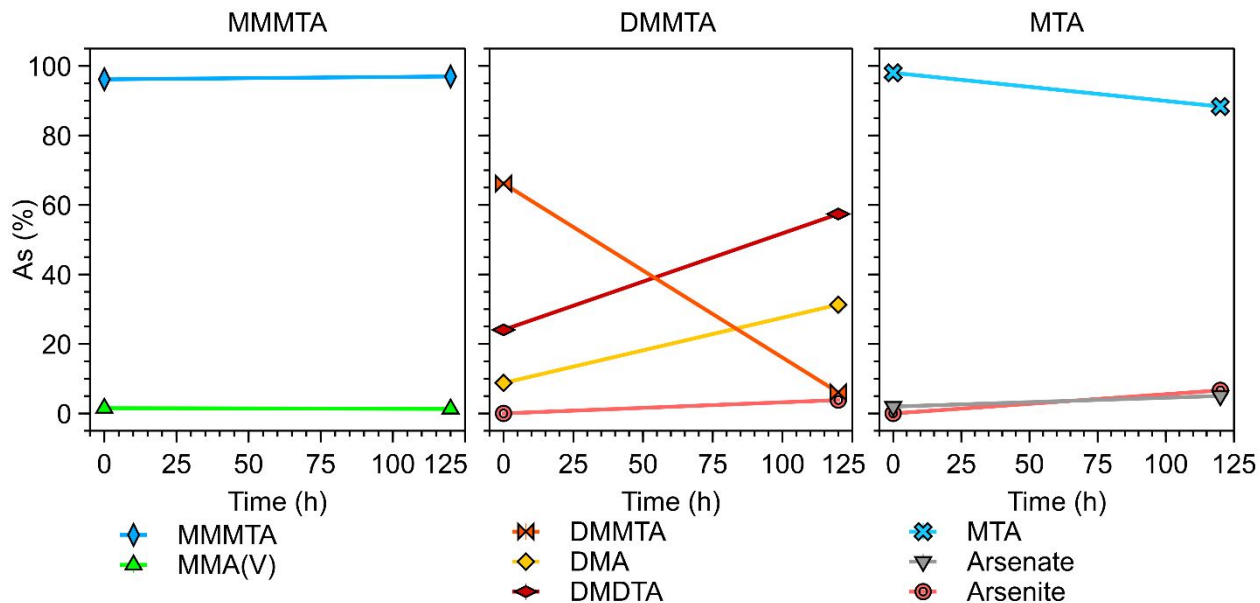


Figure SI 5. As-speciation in protein buffer without roots spiked with 3.33 μM MMMTA, DMMTA, and MTA monitored over 120 min. As speciation of the initial MMMTA, DMMTA and MTA solution was determined by IC-ICP-MS for different treatments (n=1).

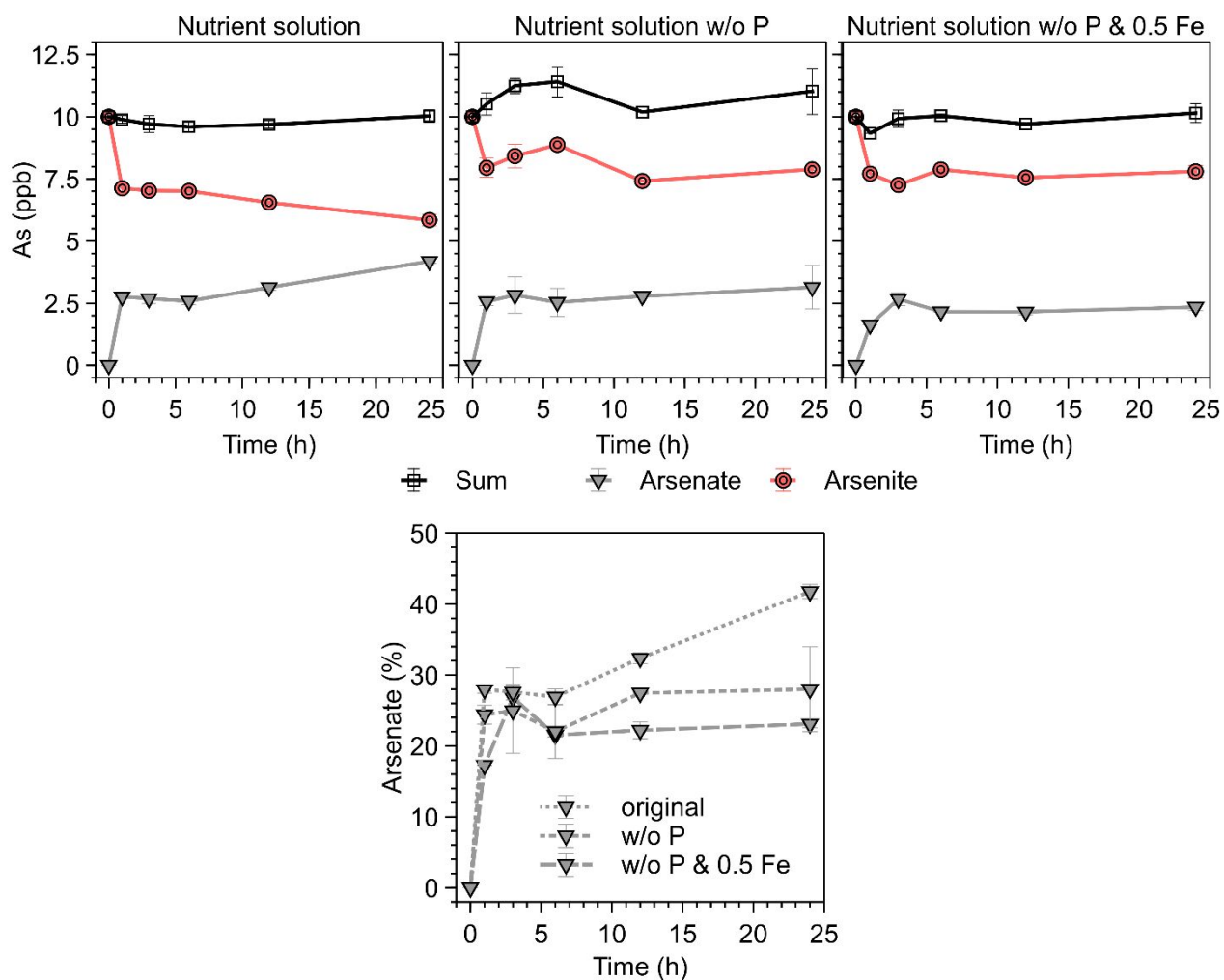


Figure SI 6. As-speciation in original nutrient solution, nutrient solution without P, and without P & 0.5 Fe (-50% Fe compared to original nutrient solution) as used in Kerl, et al. ⁴ spiked with 10 ppb arsenite monitored over 24 h. Share of arsenate is displayed in % for better comparison of three nutrient solutions. As speciation of the initial arsenite solution was determined by IC-ICP-MS (n=3).

Same experimental setup was used as for influx experiments except that a 10 ppb arsenite spike instead of MTA was used. The ‘original’ nutrient solution compared to the nutrient solution without P and without P & 0.5 Fe was tested to see influence of nutrient solution composition on abiotic arsenite oxidation. All nutrient solutions oxidize arsenite initially to arsenate, however, the ‘original’ nutrient solution oxidized more arsenite to arsenate over time (42±1 ppb compared to 34±2 ppb (w/o P) 23±1 ppb (w/o P & Fe) after 24 h). Abiotic transformation of arsenite to arsenate

during influx experiment using the ‘original’ nutrient solution is in line with results shown in Figure 2 in the main manuscript.

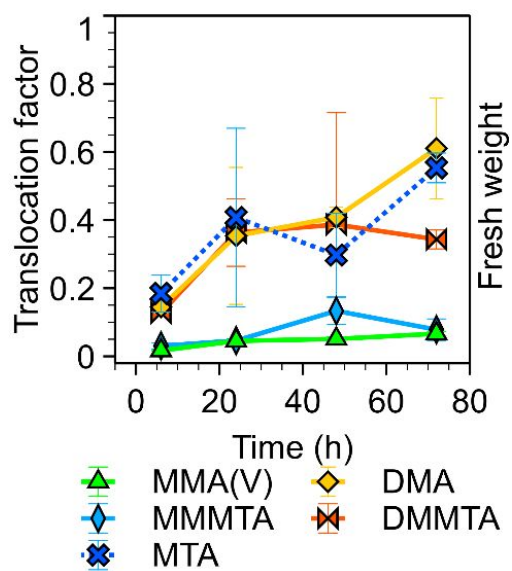


Figure SI 7. Translocation factors from root to shoot for rice seedlings grown for 20 d without As following exposure to 10 μM MMA^V, MMMTA, DMA^V, or DMMTA for 6, 26, 48, and 72 h (n=3). Data for MTA from Kerl, et al. ⁴

Table SI 1. Composition of nutrient solution used for plant growth.

Nr.	Macronutrients	Concentration (mg/L)	Vendor
1	Ca(NO ₃) ₂ *4H ₂ O	1000	Grüssing
2	KCl	120	Grüssing
3	KH ₂ PO ₄	250	Grüssing
4	MgSO ₄ *7H ₂ O	250	Merck
5	Fe-EDDAH (5.7% Fe)	20	Duchefa Biochemie
Nr.	Micronutrients	Concentration (µg/L)	Vendor
1	KI	27	Grüssing
2	LiCl	27	Fluka
3	CuSO ₄ *5H ₂ O	55	Grüssing
4	ZnSO ₄ *7H ₂ O	111	Roth
5	H ₃ BO ₃	55	Merck
6	Al ₂ (SO ₄) ₃	55	Alfa Aesar
7	MnCl ₂ *4H ₂ O	388	AppliChem
8	NiSO ₄ *7H ₂ O	55	Aldrich
9	Co(NO ₃) ₂ *6H ₂ O	55	Fluka
10	KBr	27	Merck
11	(NH ₄) ₆ Mo ₇ O ₂₄	55	Fluka

Table SI 2. Table SI 2 Seedling fresh weights for all experiments.

		Influx				Xylem			
		root fresh weight in (g)		shoot fresh weight in (g)		root fresh weight in (g)			
Arelate	MMA^V	0.1739	± 0.0966	0.2136	± 0.0229	0.1978	± 0.0461		
	MMMTA	0.5783	± 0.1207	0.5490	± 0.1603	0.2495	± 0.0793		
	DMA^V	0.2173	± 0.0472	0.2283	± 0.0336	0.2090	± 0.1372		
	DMMTA	0.3948	± 0.0612	0.4493	± 0.0681	0.2987	± 0.0531		
	MTA	0.4053	± 0.1785	0.5111	± 0.1494				
YD	MMMTA	0.5753	± 0.0705	0.6515	± 0.0493				
	DMMTA	0.6098	± 0.0702	0.6558	± 0.0721				
	MTA	0.4694	± 0.1266	0.7032	± 0.1299				
NK	MMMTA	0.4060	± 0.0795	0.4048	± 0.0534				
	DMMTA	0.2975	± 0.0180	0.3800	± 0.0381				
	MTA	0.3688	± 0.0903	0.5308	± 0.1683				

		Uptake			
		root fresh weight in (g)		shoot fresh weight in (g)	
MMA^V	0 h	0.3524	± 0.0782	0.5519	± 0.1195
	6 h	0.4281	± 0.0674	0.7006	± 0.0778
	24 h	0.3227	± 0.0658	0.5248	± 0.0493
	48 h	0.3182	± 0.0379	0.6258	± 0.0853
	72 h	0.3984	± 0.0702	0.7705	± 0.0828
MMMTA	0 h	0.3524	± 0.0782	0.5519	± 0.1195
	6 h	0.3692	± 0.0229	0.6653	± 0.0268
	24 h	0.2870	± 0.0447	0.5830	± 0.1299
	48 h	0.2835	± 0.1063	0.4775	± 0.2234
	72 h	0.4093	± 0.0168	0.9060	± 0.1303
DMA^V	0 h	0.3524	± 0.0782	0.5519	± 0.1195
	6 h	0.2718	± 0.0847	0.4607	± 0.0953
	24 h	0.2547	± 0.1066	0.4491	± 0.2160
	48 h	0.3910	± 0.0603	0.8004	± 0.0671
	72 h	0.4817	± 0.0484	0.9273	± 0.1366
DMMTA	0 h	0.3524	± 0.0782	0.5519	± 0.1195
	6 h	0.2855	± 0.0849	0.4189	± 0.0676
	24 h	0.3771	± 0.1071	0.6061	± 0.1393
	48 h	0.3201	± 0.0394	0.8374	± 0.1139
	72 h	0.3115	± 0.0590	0.5555	± 0.1113

Table SI 3. Absolute values of DMMTA stability with and without Fe.

	Time (h)	DMMTA (μM)		
		DMA ^V	DMMTA	DMDTA
Nutrient solution	0	0.59	7.43	3.19
	1	0.63	10.30	1.91
	3	0.67	10.18	1.87
	6	0.45	11.19	1.71
	12	0.39	10.62	1.46
	24	0.37	11.08	1.17
Nutrient solution w/o Fe	0	0.59	7.43	3.19
	1	0.44	5.78	3.10
	3	0.34	5.91	3.21
	6	0.37	5.91	2.85
	12	0.33	6.28	2.52
	24	0.31	6.59	2.40

Table SI 4. Absolute values of air purging.

Time (h)	MMMTA (μM)		DMMTA (μM)			MTA (μM)		
	MMA^V	MMMTA	DMA^V	DMMTA	DMDTA	Arsenite	Arsenate	MTA
0	0.07	2.26	0.69	8.19	1.12	1.07	0.67	6.08
0.25	0.08	2.31	0.56	8.52	0.70	1.16	0.65	6.20
0.5	0.13	2.28	0.64	9.19	0.82	1.08	0.57	6.25
1	0.13	2.29	0.56	8.44	0.64	1.15	0.44	5.64
2	0.26	2.21	0.56	8.91	0.63	1.13	0.84	6.14
4	0.45	2.03	0.65	8.64	0.95	1.11	0.85	6.07
6	0.43	2.04	0.53	9.31	0.46	1.22	1.07	5.80
12	1.19	1.34	0.71	11.50	0.28	1.19	0.86	6.57
24	1.92	0.76	0.95	11.55	0.13	1.31	1.38	6.96

Table SI 5. Absolute values of influx experiment.

Time (h)	MMMTA (μM)		DMA ^V	DMMTA (μM)		Arsenite	MTA (μM)	
	MMA ^V	MMMTA		DMMTA	MTA		Arsenate	MTA
0	0.2 ± 0.1	5.5 ± 3.5	0.8 ± 0.2	11.6 ± 2.4	1.1 ± 0.5	1.1 ± 0.1	0.7 ± 0.2	6.1 ± 0.3
1	0.9 ± 0.3	5.5 ± 3.6	0.7 ± 0.1	13.0 ± 0.9	0.3 ± 0.3	1.1 ± 0.2	3.6 ± 1.8	3.2 ± 1.6
3	1.7 ± 1.1	5.7 ± 4.7	1.7 ± 1.6	12.5 ± 3.5	0.2 ± 0.2	1.2 ± 0.4	4.8 ± 1.5	2.6 ± 1.2
6	2.5 ± 2.7	4.9 ± 4.7	2.0 ± 1.7	11.5 ± 4.4	0.1 ± 0.1	1.1 ± 0.3	5.9 ± 2.0	1.8 ± 0.9
12	3.0 ± 1.5	4.2 ± 3.7	3.6 ± 1.3	10.7 ± 4.1	0.0 ± 0.0	1.1 ± 0.6	6.3 ± 1.3	1.6 ± 1.0
24	3.7 ± 1.8	3.3 ± 2.8	7.7 ± 2.8	6.8 ± 5.8	0.0 ± 0.0	0.4 ± 0.2	8.8 ± 1.6	0.7 ± 0.3
0	0.1 ± 0.0	3.2 ± 0.2	0.9 ± 0.2	10.8 ± 1.0	1.2 ± 0.5	1.1 ± 0.1	0.7 ± 0.2	6.1 ± 0.3
1	0.2 ± 0.1	2.5 ± 0.1	0.8 ± 0.3	7.7 ± 0.3	0.3 ± 0.3	1.1 ± 0.1	1.2 ± 0.8	5.3 ± 0.9
3	0.5 ± 0.2	2.3 ± 0.1	0.8 ± 0.4	7.7 ± 0.3	0.3 ± 0.2	1.2 ± 0.1	2.0 ± 1.2	4.6 ± 1.1
6	1.2 ± 0.5	1.6 ± 0.4	1.3 ± 0.5	7.5 ± 0.7	0.1 ± 0.0	1.4 ± 0.2	2.3 ± 1.0	4.1 ± 0.9
12	1.5 ± 0.7	1.3 ± 0.4	2.2 ± 0.5	6.9 ± 0.7	0.1 ± 0.0	1.3 ± 0.2	2.3 ± 1.5	4.3 ± 1.1
24	1.1 ± 0.5	1.7 ± 0.4	6.9 ± 2.2	3.0 ± 2.0	0.0 ± 0.0	1.0 ± 0.3	3.5 ± 1.8	4.3 ± 1.4
0	0.1 ± 0.0	3.2 ± 0.2	0.9 ± 0.2	10.8 ± 1.0	1.2 ± 0.5	1.1 ± 0.1	0.7 ± 0.2	6.1 ± 0.3
1	0.2 ± 0.1	2.7 ± 0.3	0.8 ± 0.2	7.6 ± 0.3	0.3 ± 0.3	1.1 ± 0.1	1.9 ± 1.0	4.8 ± 0.7
3	0.6 ± 0.1	2.3 ± 0.4	0.9 ± 0.2	7.6 ± 0.3	0.2 ± 0.1	1.2 ± 0.1	2.3 ± 1.5	4.1 ± 1.3
6	1.5 ± 0.2	1.3 ± 0.2	2.2 ± 0.7	6.6 ± 0.4	0.1 ± 0.0	1.5 ± 0.2	2.6 ± 1.2	3.8 ± 1.0
12	1.8 ± 0.6	0.9 ± 0.4	4.4 ± 1.3	4.6 ± 1.3	0.1 ± 0.0	1.3 ± 0.4	3.9 ± 1.4	2.8 ± 1.3
24	1.0 ± 0.4	1.9 ± 0.0	5.6 ± 1.5	3.5 ± 1.5	0.1 ± 0.0	1.0 ± 0.3	4.8 ± 1.5	2.5 ± 1.0
0	0.2 ± 0.1	5.5 ± 3.5	0.8 ± 0.2	11.6 ± 2.4	1.1 ± 0.5	1.1	0.7	6.1
1	0.1 ± 0.0	2.7 ± 0.1	1.2 ± 0.4	10.1 ± 0.4	1.6 ± 0.2	1.0	0.6	6.3
3	0.1 ± 0.0	2.9 ± 0.1	1.0 ± 0.1	9.9 ± 0.2	1.5 ± 0.3	1.1	0.8	6.2
6	0.4 ± 0.5	4.6 ± 2.8	0.8 ± 0.2	11.0 ± 1.8	0.8 ± 0.5	1.1	1.0	5.6
12	0.7 ± 0.9	4.0 ± 2.1	0.8 ± 0.1	12.6 ± 0.7	0.5 ± 0.3	0.9	0.7	5.6
24	2.2 ± 2.3	2.6 ± 1.1	1.0 ± 0.1	11.8 ± 1.6	0.2 ± 0.1	0.9	1.2	6.2

Table SI 6. Absolute values of protein extracts.

	Time (min)	MMMTA (nmol/g root protein)			DMMTA (nmol/g root protein)			MTA (nmol/g root protein)		
		MMA ^v	MMMTA	DMA ^v	DMMTA	DMDTA	Arsenite	Arsenite	Arsenate	MTA
Arelate Root	0	29	2480	68	1042	510	14	24	1098	
	10			101	1042	510	1518	176	74	
	30			128	1109	563	1595	175	0	
	60			98	1135	643	1548	176	0	
	120	35	2400	128	926	480	1441	185	0	
YD Dena- tured Root	0	29	2480	68	1042	510	14	24	1098	
	120	25	2868	48	1064	523	58	29	1164	
	0	41	2584	161	1213	441	0	22	1078	
	10			169	1025	451	1111	285	253	
	30			208	768	462	1391	407	12	
NK Dena- tured Root	60			227	510	435	1411	443	0	
	120	36	2509	196	430	210	1374	409	0	
	0	41	2584	161	1213	441	0	22	1078	
	120	21	2562	334	500	426	1062	46	317	
	0	29	2480	68	1042	510	14	24	1098	
Dena- tured Root	10			94	1005	536	1392	168	120	
	30			107	888	534	1470	162	0	
	60			137	722	520	1522	200	0	
	120	37	2356	163	528	626	916	122	0	
	0	29	2480	68	1042	510	14	24	1098	
Dena- tured Root	120	21	2323	390	697	484	133	28	1049	

Table SI 7. Absolute values of protein buffer.

	Time (min)	MMMTA (nM)		DMMTA (nM)			MTA (nM)		
		MMA ^V	MMMTA	DMA ^V	DMMTA	DMDTA	Arsenite	Arsenate	MTA
Buffer	0	71	4496	280	2111	767	0	38	1875
	120	66	4879	435	84	797	167	126	2216

Table SI 8. Composition of protein extract.

Nr.	Chemicals	Concentration	Vendor
1	Tris-HCl, pH 7 (2-Amino-2-(hydroxymethyl)propane-1,3-diol Hydrochloride)	50 mM	Roth
2	DTT ((2 <i>S</i> ,3 <i>S</i>)-1,4-Bis(sulfanyl)butane-2,3-diol)	3 mM	Roth
3	EDTA (2,2',2'',2'''-(Ethane-1,2-diyl)dinitrilo)tetraacetic acid)	1 mM	Grüssing
4	complete EDTA-free protease inhibitor	1 x conc.	Sigma-Aldrich
5	Triton X-100 (Polyethylene glycol <i>p</i> -(1,1,3,3-tetramethylbutyl)-phenyl ether)	0.5%	Sigma-Aldrich

The protein concentration was measured using the Bradford protein assay.⁵

References

1. Kludze, H. K.; DeLaune, R. D.; Patrick, W. H., A Colorimetric Method for Assaying Dissolved Oxygen Loss from Container-Grown Rice Roots. *Agronomy Journal* **1994**, *86*, (3), 483.
2. Zehnder, A.; Wuhrmann, K., Titanium (III) citrate as a nontoxic oxidation-reduction buffering system for the culture of obligate anaerobes. *Science* **1976**, *194*, (4270), 1165-1166.
3. Wallschläger, D.; London, J., Determination of Methylated Arsenic-Sulfur Compounds in Groundwater. *Environ. Sci. Technol.* **2008**, *42*, (1), 228-234.
4. Kerl, C. F.; Rafferty, C.; Clemens, S.; Planer-Friedrich, B., Monothioarsenate Uptake, Transformation, and Translocation in Rice Plants. *Environ. Sci. Technol.* **2018**, *52*, (16), 9154-9161.
5. Bradford, M. M., A rapid and sensitive method for the quantitation of microgram quantities of protein utilizing the principle of protein-dye binding. *Analytical Biochemistry* **1976**, *72*, (1-2), 248-254.

Study 4: Iron plaque of rice plants: no barrier for methylated thioarsenates

Carolin F. Kerl, Tiziana Boffa Balaran, Britta Planer-Friedrich

Reprinted with permission from

Environmental Science & Technology (53, pp. 13666-13674)

Copyright 2019 American Chemical Society

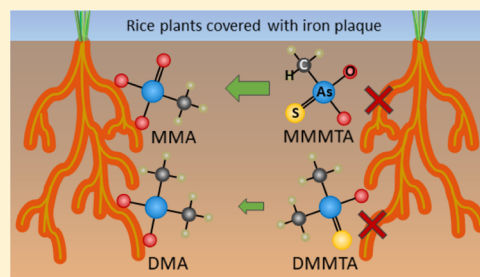
Iron Plaque at Rice Roots: No Barrier for Methylated Thioarsenates

Carolin F. Kerl,[†] Tiziana Boffa Ballaran,[‡] and Britta Planer-Friedrich^{*,†}

[†]Environmental Geochemistry, Bayreuth Center for Ecology and Environmental Research (BayCEER), and [‡]Bayerisches Geoinstitut BGI, University of Bayreuth, D-95440 Bayreuth, Northern Bavaria, Germany

Supporting Information

ABSTRACT: Iron (hydr)oxide coating at rice roots, so-called iron plaque (IP), is often an important barrier for uptake of inorganic oxyarsenic species and their accumulation in rice grains. Sorption of methylated thioarsenates, which can co-exist with inorganic and methylated oxyarsenates in paddy soils, was not studied yet, even though these toxic species were detected in xylem and grains of rice plants before. Hydroponic experiments at pH 6.5 with 20 day-old rice plants showed lower net arsenic enrichment in IP for plants exposed to monomethylthioarsenate (MMMTA) compared to monomethylarsenate (MMA) and no enrichment for dimethylmonothioarsenate (DMMTA). Goethite was the dominant mineral phase in our IP. Sorption experiments with synthesized goethite and ferrihydrite revealed a 30-times-higher sorption capacity for MMMTA to amorphous ferrihydrite than to crystalline goethite, comparable to methylated oxyarsenates. No evidence for direct MMMTA binding was found. Instead, we postulate that MMMTA transformation to MMA is a prerequisite for removal. DMMTA showed very little sorption, even to amorphous ferrihydrite, which is in line with a lack of direct binding and reported slow transformation to dimethylarsenate. Our study implies that IP is no effective barrier for methylated thioarsenates and that especially DMMTA is very mobile with a high risk of uptake in rice plants.



INTRODUCTION

Arsenic (As) accumulation in rice grains is a well-known health concern in regions where rice is a major staple food.^{1,2} Several countries, including the European Union, China, and the USA, have introduced threshold values for inorganic As (arsenite and arsenate) in rice (200 $\mu\text{g}/\text{kg}$ for polished rice) and especially low limits for baby food (100 $\mu\text{g}/\text{kg}$).^{3,4} High As grain accumulation is caused by rice cultivation under flooded conditions, which induce reductive dissolution of soil iron (Fe) minerals with concurrent release of sequestered As.^{5,6} Arsenic released to the pore water is mostly reduced to arsenite, which is highly mobile, while arsenate concentrations are typically low.^{7,8} Soil microorganisms or algae are able to biomethylate inorganic As by the enzyme As^{III}-S-adenosylmethionine methyltransferase to organic As (monomethylarsenate; MMA and dimethylarsenate; DMA).^{9,10} The methylated oxyarsenates are considered less toxic and therefore exempt from threshold values.^{3,4}

Mitigation strategies to reduce As accumulation in rice typically address As immobilization in soil (e.g., by dedicated water management with drainage periods during cultivation¹¹) or decrease of uptake by the plant (e.g., by supplying silicon which competes with arsenite, MMA, and DMA for uptake through aquaglyceroporin channels¹²). A very efficient barrier for As uptake can, however, also be iron plaque (IP). IP is formed by oxidation of Fe^{II}, which is mobile under reducing soil conditions, along the surface of rice roots when plants release oxygen. IP typically contains varying amounts of Fe(oxyhydr)oxide minerals such as ferrihydrite, goethite, lepidocrocite, or siderite, depending on pore-water chem-

istry.^{13–18} These freshly formed minerals can offer sorption sites to nutrients or toxic metal(oid)s such as phosphate or As. The sorption of inorganic and organic As on IP and Fe minerals has been studied in great detail during the past decades, revealing that sorption is strongly dependent on mineral crystallinity, pH, As speciation, and competitive ions.^{19–21} Differences in IP crystallinity and mineralogy due to soil or hydroponic culture composition determine the capacity of IP to sorb inorganic As, generally lowering the As uptake in rice plants;^{22–25} however, for example, in the presence of high phosphate concentrations,²³ desorption of previously sorbed arsenate from IP can even increase net As uptake in rice plants.²⁶

Just very recently, we have shown that As speciation in paddy soil pore waters comprises more than just the four oxyarsenic species typically considered.²⁷ Even though dissolved free sulfide concentrations in paddy soils typically are low, arsenic–sulfur species, so-called thioarsenates, can form. Inorganic thioarsenates hereby form under sulfur-reducing, pH neutral to alkaline conditions from arsenite via OH[−]/SH[−]-ligand exchange and addition of zerovalent sulfur.^{28,29} Methylated thioarsenates form under acidic pH from the methylated oxyarsenates MMA or DMA via ligand exchange of OH[−] by SH[−] after nucleophilic attack.³⁰ Although methylated thioarsenates, namely, monomethylmonothioarsen-

Received: July 12, 2019

Revised: September 27, 2019

Accepted: November 1, 2019

Published: November 1, 2019

ate (MMMTA; $(\text{CH}_3)_2\text{AsS}(\text{OH})_2$) and dimethylmonothioarsenate [DMMTA; $(\text{CH}_3)_2\text{AsS}(\text{OH})$], are considered to be more toxic than MMA and DMA,^{31,32} their existence, fate, and mobility in paddy soils are relatively unknown, yet. We have previously shown that methylated thioarsenates can be taken up by rice plants and that hydroponically grown rice plants accumulated most total As in shoots after exposure to DMMTA.³³ An earlier market survey even detected DMMTA in commercially available rice grains.^{2,34}

Whether IP could contribute anything to decrease uptake of methylated thioarsenates in rice grains was unknown to date. To the best of our knowledge, not even information about the sorption behavior of methylated thioarsenates to synthetic Fe minerals was available so far. Previous studies with inorganic thioarsenates revealed that thiolation increased the mobility of As species in Fe-rich systems. Mono- and trithioarsenate (MTA and TTA) sorbed less on goethite, ferrihydrite, and mackinawite compared to inorganic As.^{35,36} If, similarly, thiolation decreases sorption affinity for methylated arsenates, their mobility in paddy soils and risk for uptake might be higher than that of methylated oxyarsenates which combined with their higher toxicity poses a serious health concern.

The aim of our study was to determine whether IP can decrease the uptake of methylated thioarsenates to the same extent as that of methylated oxyarsenates by comparing total As in shoots and roots of rice plants with and without IP after exposure to the respective individual species. Additionally, we compared the sorption of methylated thioarsenates and methylated oxyarsenates to goethite and ferrihydrite as two endmembers of IP minerals in terms of sorption kinetics, nonequilibrium isotherms, and pH dependency to understand the potential for mineral sorption and species transformation at IPs.

METHODS AND MATERIALS

Synthesis of Methylated Thioarsenates and Fe Minerals. MMMTA [$(\text{CH}_3)_2\text{AsS}(\text{OH})_2$] was synthesized as described before.^{37,38} Briefly, MMA (disodium methyl arsonate hexahydrate, $\text{CH}_3\text{AsNa}_2\text{O}_3 \cdot 6\text{H}_2\text{O}$, Supelco) and sulfide (sodium sulfide nonahydrate, $\text{Na}_2\text{S} \cdot 9\text{H}_2\text{O}$, Sigma-Aldrich) solutions were mixed with molar As/S ratios of 1:10 and pH was adjusted to 3 by adding 1 M HCl (Kraft) in an anoxic atmosphere inside a glovebox [COY , N_2/H_2 95/5% (v/v)]. After 30 min reaction time, pH was increased to 12.3 using 1 M NaOH (Merck) and reaction continued for another 60 min, before aliquots were flash-frozen on dry ice and stored at -20 °C until usage.

DMMTA [$(\text{CH}_3)_2\text{AsS}(\text{OH})$] was synthesized slightly modifying a method by Cullen et al.³⁰ Briefly, DMA [dimethyl arsenic acid, $(\text{CH}_3)_2\text{AsNaO}_2 \cdot 3\text{H}_2\text{O}$, Sigma-Aldrich] and sulfide (As/S^{-II} ratio 1:1.6) were mixed and concentrated sulfuric acid (H_2SO_4 , Sigma-Aldrich) was added to an As/S^{+VI} ratio of 1:1.6. After 25 min of reaction time, the formed DMMTA was extracted using diethyl ether ($\text{C}_4\text{H}_{10}\text{O}$, VWR Chemicals) and yellowish-white crystals formed after evaporation of solvent. Synthesized DMMTA was stored anoxically and in darkness at 5 °C. For DMMTA stock solutions, crystals were dissolved in water and filtered using 0.2 μm cellulose-acetate (CA) filters (Machery-Nagel), before aliquots were flash-frozen on dry ice and stored at -20 °C until usage.

MMMTA and DMMTA were identified by ion chromatography coupled to inductively coupled mass spectrometry (IC-ICP-MS) using previously published retention times³⁷ and

example chromatograms.³³ Purity of the MMMTA was 84% containing 3% MMA and 13% monomethyldithioarsenate [MMDTA; $(\text{CH}_3)_2\text{AsS}(\text{SH})(\text{OH})$]. The DMMTA stock contained 67% DMMTA, 28% dimethyldithioarsenate [DMDTA; $(\text{CH}_3)_2\text{AsS}(\text{SH})$] and 5% DMA.

Commercially available goethite (α -FeOOH, Bayferrox 920Z, Lanxess) used for all experiments was purified as described before.³⁶ Briefly, 75 g of α -FeOOH was suspended in 900 mL of 0.1 M NaNO_3 and pH was adjusted to 10 using NaOH for 24 h to remove impurities. The suspension was centrifuged and washed five times with 0.1 M NaNO_3 , following several washing steps with ultrapure water until conductivity was <5 $\mu\text{S}/\text{cm}$. After washing, the material was freeze-dried.

2-line ferrihydrite (called ferrihydrite hereafter) was synthesized as described before.^{21,39} Briefly, 20 g of iron^{III} nitrate nonahydrate [$\text{Fe}(\text{NO}_3)_3 \cdot 9\text{H}_2\text{O}$; Acros Organics] was dissolved in ultrapure water and pH was adjusted to 7.3 using 1 M KOH (Aldrich). After aging for 2 h, the precipitated mineral was centrifuged and washed with ultrapure water four times and was finally suspended in artificial rhizosphere pore water (ARPW, see below) to a final concentration of 0.5 M ferric iron (Fe^{III}). The suspension was stored cooled (4 °C) under nitrogen atmosphere and in darkness. All experiments with ferrihydrite were performed within one week after synthesis.

Hydroponic Culture. Growth conditions for plants were described in detail elsewhere.⁴⁰ Briefly, after germinating rice seeds (*Oryza sativa* L. cv. Arelate) for 7 days, seedlings were transferred to 50 mL tubes (Sarstedt) containing nutrient solution (Table S1), which was renewed twice a week to ensure sufficient nutrient supply. Seedlings were grown for 20 days under long day conditions (16 h of light/8 h of darkness) at 23 °C and 110 μE .

IP Formation. IP formation was induced when rice seedlings were 12 days old by growing them on phosphate-free nutrient solution for one day to remove excess P and limit the precipitation of Fe–P minerals. For the following 7 days, half of the plants were grown with 1/20 of the initial P concentration and Fe-EDDAH (Duchefa Biochemie) was replaced by 100 mg/L $\text{Fe}^{\text{II}}\text{Cl}_2$ (Sigma-Aldrich) to form IP along rice roots (treatment called “IP”). The remaining plants were continuously grown using Fe-EDDAH but P concentration was reduced to 1/20 as well (“w/o Fe”). The nutrient solution was changed daily to ensure sufficient supply with Fe^{II} and nutrients. All plants were transferred to Fe-free nutrient solution 24 h prior to uptake experiments to remove noncrystallized Fe from the root surface.

Uptake of Methylated (Thio)arsenates in Rice Plants with and without IP. Uptake and later sorption experiments were performed in an electrolyte (ARPW) that mimics natural conditions in the paddy field rhizosphere and sustains rice plant growth for uptake experiments, instead of the widely used NaNO_3 . Therefore, phosphorus (P) concentration in the range of experimentally measured values in rice rhizospheres⁴¹ was chosen, and the concentrations of all other nutrients were adjusted to maintain the same stoichiometry as in the original nutrient solution used for rice growth (Table S2). The pH was adjusted to 6.5, which is at the lower end of pore-water pH in paddy soils under flooded conditions.⁷

Arsenic uptake and translocation in rice plants containing IP and control plants without IP (w/o Fe) were analyzed after exposure to 10 μM MMA, MMMTA, DMA, or DMMTA for 8 h in ARPW (pH 6.5; $n = 4$). Arsenic-spiked ARPW was

renewed every 2 h to limit the previously shown transformation of MMMTA and DMMTA to MMA and DMA in the presence of rice roots.³³ After exposure, roots were washed with ultrapure water to remove As containing nutrient solution. Dry weight for roots and shoots was determined after drying at 60 °C for 2 days (Table S3). Total As and Fe concentrations of dried roots and shoots were determined by ICP-MS after microwave digestion (Mars 5 microwave digestion system, CEM Corp., Matthews, NC) in concentrated HNO₃ (Kraft) and 30% H₂O₂ (VWR) (ratio 1.5:1). Arsenic sorbed to IP and Fe content of IP were calculated by subtracting the mean As or Fe content in the rice roots without IP from the total As or Fe concentration in roots covered with IP ($A_{s\text{ sorbed}} = A_{s\text{ IP}} - \overline{A_{s\text{ w/o Fe}}}$). Quantifying As concentration in the IP directly using the dithionite–citrate–bicarbonate (DCB) extraction method⁴² was not possible because As concentrations in DCB extracts were below limits of quantification (LOQ) (1000-fold dilution of DCB extracts was necessary to enable sample introduction into ICP–MS).

Sorption Experiments of Methylated (Thio)arsenates to Iron Minerals. Sorption of methylated (thio)arsenates to goethite and ferrihydrite was studied because those minerals are reported as major components of IP.^{13–18} The experimental and sampling procedure for the three different sorption experiments (pH, kinetic, and isotherms) followed a general procedure described below with detailed information for each experiment given in the next paragraph. Fe minerals [goethite: 36 mM; ferrihydrite: 3.6 mM ferric iron (Fe^{III})] were pre-equilibrated under anoxic conditions for 16 h in ARPW at the respective pH in 10 mL vials (Sarstedt). Each sample was spiked with MMA, MMMTA, DMA, or DMMTA, shaken on an overhead shaker (13 rpm), and kept anoxic during sorption. After equilibration, samples were centrifuged for 5 min (5000 rpm; Hettich); supernatants were filtered through 0.2 μm filters (CA), and subsamples for As speciation by IC–ICP–MS were flash-frozen on dry ice immediately. Further subsamples for analysis of total As by ICP–MS were stabilized with 2.5% 7 M HNO₃ (Kraft), and the pH was measured in the remaining samples (Figures S6 and S8).

For pH-dependent sorption envelopes, both Fe minerals were pre-equilibrated at pH 4–12 and spiked with 5 μM MMA, MMMTA, DMA, or DMMTA ($n = 1$). Samples were taken after 2 h equilibration time. For sorption kinetics, both Fe-mineral suspensions were pre-equilibrated at pH 6.5, prior to spiking with 5 μM MMA, MMMTA, DMA, or DMMTA ($n = 1$). Sacrifice samples were taken after 10, 20, 30 min, 1, 3, 6, 10, 24, 48, and 72 h. For nonequilibrium sorption isotherms, both Fe-mineral suspensions were pre-equilibrated at pH 6.5 and spiked with 0.5, 5, 50, 100, and 500 μM MMA, MMMTA, DMA, or DMMTA ($n = 3$). Samples were taken after 2 h equilibration time.

X-ray Diffraction. Freeze-dried samples of goethite and ferrihydrite were analyzed by X-ray powder diffraction (XRD) using a Philips X'Pert Pro diffractometer operating in the reflection mode with monochromated Co K α_1 radiation operated at 40 kV and 40 mA, in the 2θ range 15°–90° with a step size of 0.02° and scan speed of 0.66°/min. Comparison between the collected X-ray diffraction pattern of goethite with a reference pattern taken from the Inorganic Crystal Structure Database (Nr. 245057-ICSD) confirmed that the commercial goethite was free of impurities and not altered during purification (Figure S1). The XRD pattern for the synthesized 2-line ferrihydrite revealed two broad characteristic

peaks in line with published references (Figure S2).³⁹ The surface area of goethite (9.0–12.5 m²/g)⁴³ is nearly two orders of magnitude smaller than for ferrihydrite (200–600 m²/g)³⁹ which is in line with the high crystallinity of goethite and amorphous structure of ferrihydrite seen in the XRD spectra. Two powdered rice root samples one covered with IP and one without IP were also analyzed using the same XRD diffractometer; however, no difference between the two samples was observed likely because of the amount of IP being below the detection limit of the instrument (Figure S3). For this reason, an intact rice root with IP was analyzed using a microfocused X-ray diffractometer (Bruker, D8 DISCOVER) equipped with a two-dimensional (2D) solid-state detector (VANTEC500) and a microfocus source (I μ S) with Co K α radiation operated at 40 kV and 500 μA. The X-ray beam was focused to 50 μm using an IFG polycapillary X-ray mini-lens. Different portions of the root sample were chosen according to their bright orange color, and 2D diffraction patterns were collected in the 2θ range 15°–90° for 1000 s/frame (Figure S4). The diffraction patterns present weak, well-defined spots, suggesting the presence of a good crystalline material. The integrated one-dimensional diffraction patterns show diffraction peaks which can be mostly explained with the presence of goethite together with vivianite because of the presence of phosphate in the ARPW (Figure S5). Note, however, that an accurate analysis of such diffraction patterns is hindered by the low intensity of the diffraction peaks and the poor statistic due to the few number of crystals present in the microfocused beam.

As Measurements. Arsenic species were separated by IC (Dionex ICS-3000) using an AS16 column (Dionex AG/AS16 IonPac, 2.5–100 mM NaOH, flow rate 1.2 mL/min)³⁷ and quantified by ICP–MS (XSeries 2, Thermo Fisher) as AsO⁺ (m/z 91) using oxygen as reaction cell gas. Additionally, total As (AsO⁺ m/z 91) and Fe (Fe⁺ m/z 56 using 2 V kinetic energy discrimination with helium as collision gas) concentrations were determined by ICP–MS and the signal drift was corrected using 48 nM rhodium (Rh⁺ m/z 103) as an internal standard added manually to each sample. Quality of ICP–MS measurements was checked by recovery of the certified reference material (TMDA 54.5, Environment Canada 98 ± 4%) and recovery of As spiked into diluted samples prior to measurement (80–103%). The limits of detection (LOD) and of LOQ for As were 2.1 and 2.4 nM for the As uptake in rice plants and 0.9–1.3 nM (both LOD and LOQ) for As sorption to Fe minerals, respectively. The lowest detectable concentrations for As speciation were between 0.4 and 0.8 nM.

Statistics. Two-way analysis of variance with the Tukey post hoc test was performed using SigmaPlot 11.

RESULTS

Uptake of Methylated Thioarsenates in the Presence of IP. Comparing the total As uptake in rice plants covered with IP or without IP after 8 h exposure to 10 μM MMA, MMMTA, DMA, or DMMTA, the largest effect was found for plants exposed to MMA (Figure 1a,b). In comparison to roots without IP, roots with IP accumulated significantly more MMA [2.0 ± 0.3 vs 1.1 ± 0.4 mmol/kg ($P < 0.001$)] and translocated little less As to the shoots [13 ± 3 vs 18 ± 7 μmol/kg ($P = 0.57$)]. Less MMA uptake in shoots by IP sequestration is in line with the highest net As enrichment in IP found in MMA-exposed rice roots (1.3 ± 0.3 μmol As/mmol Fe; Figure 1c). IP-coated roots exposed to DMA showed increased DMA

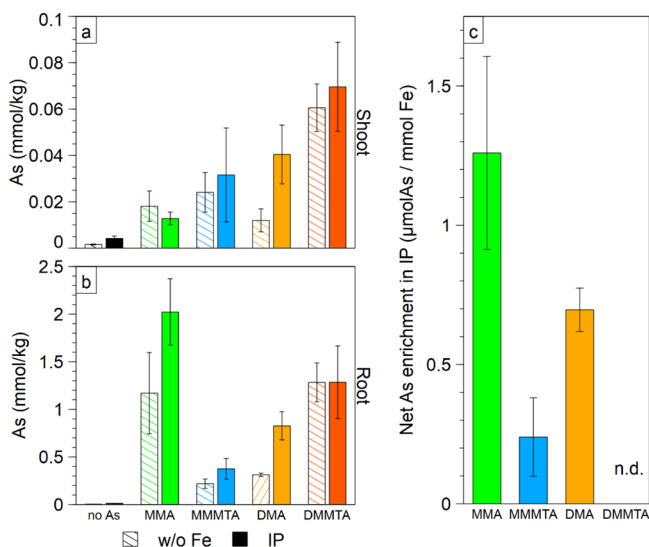


Figure 1. As uptake for rice seedlings grown with root IP and without root IP (w/o Fe) after exposure to 10 μM MMA, MMMTA, DMA, or DMMTA in ARPW for 8 h. Total As concentrations were determined after microwave digestion ($n = 4$); (a) shoot contents, (b) root contents, (c) net As enrichment in IP of rice roots after exposure to 10 μM MMA, MMMTA, DMA, or DMMTA in ARPW for 8 h. Amounts of As and Fe in roots w/o Fe were subtracted to obtain As/Fe ratios in IP ($n = 4$). No net As enrichment in IP was found for rice seedlings exposed to DMMTA.

concentrations in roots [0.8 ± 0.1 compared to 0.3 ± 0.0 mmol/kg in roots without IP ($P = 0.013$)] similar to MMA-exposed roots, but increased As concentrations in shoots as well [40 ± 13 compared to 12 ± 5 $\mu\text{mol/kg}$ in shoots without IP ($P = 0.005$)]. Taking the net As enrichment in roots (0.7 ± 0.1 $\mu\text{mol As/mmole Fe}$; Figure 1c) into account, the results imply that DMA was sorbed to IP to a lesser extent than MMA.

Plants exposed to MMMTA showed slightly higher As concentrations in IP roots [0.4 ± 0.1 compared to 0.2 ± 0.0 mmol/kg in roots without IP ($P = 0.42$)] without effects on As accumulation in shoots [32 ± 20 compared to 24 ± 9 $\mu\text{mol/kg}$ in shoots without IP ($P = 0.42$)]. Compared to MMA and DMA, less spiked MMMTA was sorbed to IP-covered roots, resulting in a lower net As enrichment (0.2 ± 0.1 $\mu\text{mol As/mmole Fe}$; Figure 1c). IP had no effect on As uptake in plants exposed to DMMTA and no sorption of DMMTA to IP was observed.

Sorption Kinetics. Sorption kinetics of methylated (thio)-arsenates on goethite and ferrihydrite were clearly different between the two minerals but the order of sorption was the same for both minerals with a decrease from highest total As sorption after exposure to MMA, followed by MMMTA, DMA, and DMMTA (Figure 2a). Goethite sorbed 56% MMA within the first 10 min (Figure S7) and increased further to a maximum of 87% after 24 h (Figure 2a) while ferrihydrite sorbed MMA completely within the first 10 min (Figure S7). Arsenic speciation revealed that the MMA remaining in the ARPW was stable throughout the experiment (data not shown). Larger differences were observed for spiked MMMTA, where sorption to goethite was much slower than to ferrihydrite (15% sorbed within 10 min compared to 97%, respectively, Figure S7). Sorption to goethite increased slowly and reached values comparable to MMA after 48 h (84% for MMA and 78% for MMMTA; Figure 2a). Ferrihydrite sorbed

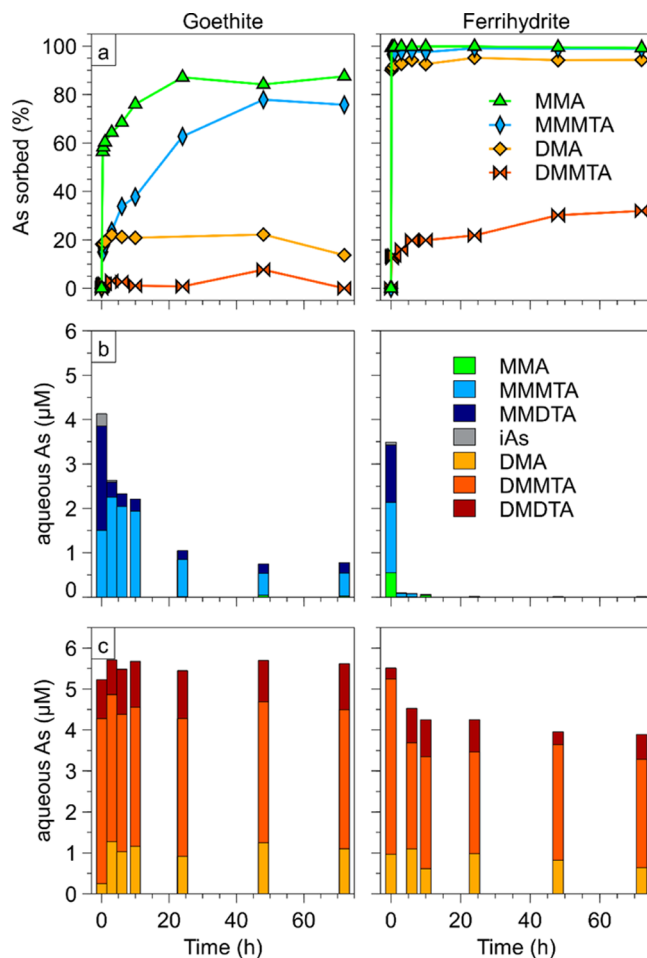


Figure 2. Sorption kinetics for 5 μM MMA, MMMTA, DMA, or DMMTA on goethite (36 mM) and ferrihydrite (3.6 mM) in ARPW after 0–72 h equilibration ($n = 1$). Sorbed total As is calculated as difference between As concentration in control without goethite or ferrihydrite and measured total As concentration in the aqueous phase after equilibration (a). Arsenic speciation for MMMTA (b) and DMMTA (c) is shown as the measured As concentration in the aqueous phase after equilibration; for a higher resolution of changes happening between 0 and 1 h equilibration, please refer to Figure S7.

97% of spiked MMMTA within the first 10 min (Figure S7), sorption after 24 h increased only slightly further on to 99% (Figure 2a). In contrast to experiments with MMA, the As speciation of MMMTA was not stable over time. The MMMTA standard used contained impurities of MMDTA, which originated at least partly from pH adjustment to 6.5 as concentration of MMDTA (up to 57%) increased compared to the synthesized stock solution (13%). MMDTA was transformed to MMMTA within the first 10 min and the remaining 13% of MMDTA was stable for 72 h (Figure 2b). Impurities of MMA in the synthesized stock solution were not detectable after 10 min due to rapid sorption to the Fe minerals. The MMMTA concentration remaining in the ARPW decreased over time (Figure 2b).

DMA was sorbed within the first 10 min (Figure S7) with the quantity of sorption being higher on ferrihydrite than on goethite (90% compared to 18% after 10 min, respectively). No species transformations were found for DMA during sorption, and DMA remained stable for 72 h (data not shown). Sorption of spiked DMMTA on goethite was below 8% with

no clear trend over time (Figure 2a), and As speciation was stable over time (Figure 2c). Spiked DMMTA sorption to ferrihydrite continuously increased over 72 h to 32% without reaching a maximum (Figure 2a). The As speciation revealed slowly decreasing DMMTA concentrations over time. Similar to the MMMTA stock, the DMMTA standard synthesized in our lab contained impurities of DMDTA as well. Dimethyldithioarsenate, in contrast to MMDTA, was stable for 72 h at $\approx 20\%$ (Figure 2c).

Nonequilibrium Sorption Isotherm. Sorption isotherms were determined after 2 h reaction time to limit species transformation, even though equilibrium was not reached in all cases, yet (Figure 3). Both Fe minerals sorbed highest

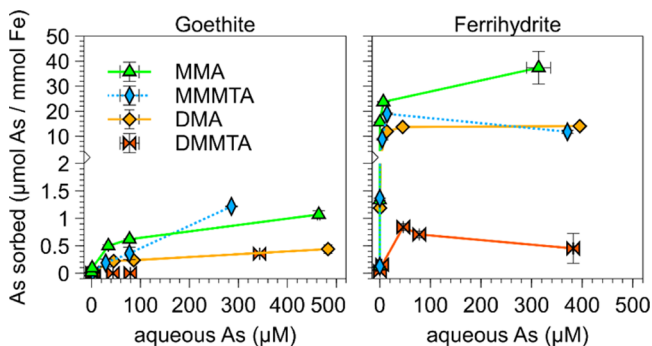


Figure 3. Nonequilibrium sorption isotherm for nominal 0.5–500 μM MMA, MMMTA, DMA, or DMMTA on goethite (36 mM) and ferrihydrite (3.6 mM) in ARPW after 2 h equilibration ($n = 3$). Sorbed As calculated as difference between As concentration in control without goethite or ferrihydrite and measured total As concentration in the aqueous phase normalized to the Fe content; solutions at nominal 100 and 500 μM MMMTA for goethite turned black upon addition of the spike but were clear after filtration indicating precipitation of FeS minerals; solutions at 500 μM spike ferrihydrite remained black even after filtration, indicating the presence of colloids.

quantities of As after exposure to MMA, followed by MMMTA (below 50 μM MMMTA initially spiked to the Fe mineral) and DMA. Sorption on ferrihydrite was 30–50 times higher than on goethite. Similar to the previous experiments, spiked DMMTA was not sorbed on goethite; however, small amounts of spiked DMMTA were sorbed on ferrihydrite independent of the As concentration in the aqueous phase. Arsenic speciation of spiked MMMTA and DMMTA in the aqueous phase showed less transformation of MMDTA to MMMTA and DMDTA to DMMTA with higher As/Fe ratios (increasing As spikes) (Figure S9). The highest transformation of MMMTA to MMA and DMMTA to DMA was found for the lowest As spike (0.5 μM).

pH-Dependent Sorption Envelopes. Sorption of both methylated oxyarsenates and thioarsenates on goethite and ferrihydrite decreased with increasing pH (Figure 4). Decreased sorption of MMA started above pH 5.3 and 7.0 on goethite and ferrihydrite, respectively. Sorption of spiked MMMTA and DMA started to decrease above pH 6.1 and 5.8, on goethite and ferrihydrite, respectively. Spiked DMMTA was not sorbed quantitatively at any pH. Ferrihydrite sorbed spiked MMA, MMMTA, and DMA completely ($\geq 98\%$ for MMA and MMMTA, $\geq 96\%$ for DMA) at low pH values in contrast to goethite, where only MMA was sorbed completely ($\geq 99\%$). Spiked MMMTA and DMA were not absorbed to more than

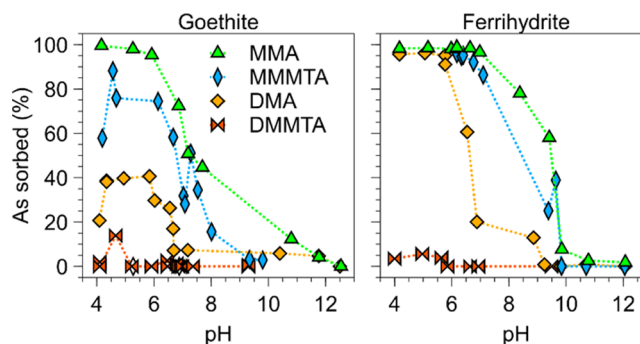


Figure 4. Sorption envelope for 5 μM MMA, MMMTA, DMA, or DMMTA on goethite (36 mM) and ferrihydrite (3.6 mM) in ARPW ($n = 1$). Sorbed As calculated as difference between As concentration in control without goethite or ferrihydrite and measured total As concentration in aqueous phase after 2 h equilibration.

88 and 41%, respectively. The pH of the ARPW itself did not change the As speciation of the spiked As species (Figure S10).

Compared to sorption studies using NaNO_3 as the “standard” electrolyte instead of our ARPW, sorption of MMA and DMA in ARPW started to decrease at lower pH values on goethite (see own data for comparison between ARPW and 10 mM NaNO_3 in Figure S11) and ferrihydrite.¹⁹ Additionally, less DMA was sorbed to goethite in ARPW compared to NaNO_3 (Figure S11).

DISCUSSION

IP is often considered an effective barrier for decreasing the uptake of the inorganic As species arsenite and arsenate in plants.^{22–25} Much less is known about potential mitigating effects of IP on methylated oxyarsenates and nothing so far about methylated thioarsenates. We could show that IP acts as a barrier for MMA (Figure 1), with higher MMA immobilization at the plant roots and slightly decreased translocation to above ground biomass compared to plants without IP. The observed high sorption to IP is in line with our results from sorption studies with synthetic minerals as well as previously published data.^{19,44} At pH 6.5, where we conducted plant uptake experiments, both goethite and ferrihydrite show nearly complete sorption. Formation of weak outer-sphere complexes has been reported for MMA before⁴⁵ which is caused by attraction because of the net positive surface charge of the Fe minerals (pH at the point-of-zero-charge, pH_{pzc} goethite 6.5^{43–8.6},⁴⁴ pH_{pzc} ferrihydrite 8.3¹⁹) and the net negative charge of MMA ($\text{p}K_{\text{a}1}$: 4.2; $\text{p}K_{\text{a}2}$: 8.2). Independent of electrostatic interactions, formation of strong bidentate binuclear inner-sphere complexes via Fe–O–As bonds has been described for MMA.^{19,46} The presence of competing ions, such as phosphate, is known to limit sorption of methylated oxyarsenates, especially when they are bound as outer-sphere complexes.¹⁹ Also in our experiments, we observed some loss in retention of MMA in the presence of phosphate at pH 6.5 (around -20% , Figure S11). However, even if in the presence of IP, some additional MMA would make its way from the IP reservoir at the outside of the plant roots to the inside; MMA is known to be sequestered quite efficiently in root vacuoles via MMA^{III} –phytochelatin (PC) complexes, limiting translocation to shoots.^{47–49}

For DMA, such as for MMA, higher As immobilization at the plant roots was found in the presence of IP than in its absence. Compared to MMA, however, the net As enrichment

in IP was lower (Figure 1c) and translocation to above ground biomass was not decreased but actually increased in the presence of IP. Lower As sorption and a decrease in maximum potential sorption already at $\text{pH} > 6$ was also observed in the sorption studies with goethite and ferrihydrite. A significant extent of DMA sorption was only observed at the highly reactive ferrihydrite (61%, Figure 4), while sorption to goethite, which was the dominant Fe mineral in our IP, was only 26% at $\text{pH} 6.5$. One reason for the lower sorption affinity of DMA compared to MMA might be a higher pK_a value (pK_a : 6.1), so almost 40% of all DMA is noncharged at $\text{pH} 6.5$, potentially decreasing electrostatic interactions with the negatively charged Fe-mineral surfaces. The presence of the second methyl group in DMA might also be a greater steric hindrance to binding.¹⁹ The presence of phosphate further decreases DMA sorption (Figure S11). Some extent of sorption but combined with easy remobilization, for example, in the presence of competing anions such as phosphate,^{19,45} could in fact explain why for DMA the IP does not act as a barrier but rather as a reservoir providing additional DMA for uptake into the plant. Once inside the plant roots, in contrast to MMA, DMA is not complexed by PCs and sequestered into root vacuoles but escapes root storage with enhanced translocation from roots to shoots.

In contrast to the methylated oxyarsenates, MMMTA showed much lower and DMMTA showed no net As enrichment in IP at all (Figure 1c). The much higher As sorption to root IP after exposure to MMA compared to exposure to MMMTA at first glance seems to contradict the much more similar sorption behavior observed in the studies with goethite and especially ferrihydrite. On ferrihydrite, MMMTA sorbed as quickly and completely as MMA, while sorption to goethite was slower and slightly lower with maximum sorption after 48 h at $\text{pH} 6.5$ only reaching around 78% compared to 84% for MMA (Figure 2a). The exact sorption mechanism of MMMTA is unclear at the moment. From studies on inorganic MTA, we know that binding to Fe occurs via the O atom and is lower than binding of the oxyarsenate.^{35,36} The additional S group might be a steric hindrance for binding. MMMTA contains, besides the S group, an additional methyl group. We therefore assume, in comparison to MTA, even lower or no direct binding at all. From the time lag in sorption and from speciation analyses, we propose that MMMTA is first transformed to MMA, which then sorbs. MMMTA is known to be unstable in the presence of oxygen^{30,37} and transforms to MMA within 30 min.³³ Fe^{III} is a very strong oxidant, so transformation of MMMTA to MMA over 72 h can be expected. Slow but continuous transformation of MMMTA could explain the lower sorption of spiked MMMTA compared to MMA and a lack of MMA built-up in the aqueous phase because it is immediately sorbed (Figure 2b). The higher reactivity of ferrihydrite might accelerate the transformation of MMMTA to MMA, explaining higher overall sorption. The observed significantly lower sorption to IP upon exposure to MMMTA fits this proposed mechanism, because during uptake experiments, we exchanged the As-spiked ARPW every 2 h. Previous experiments indicated that rice plant-induced transformation of MMMTA to MMA was less than 10% within the first 2 h of exposure.³³ A higher As/Fe ratio ($\approx 34 \mu\text{mol As}/\text{mmol Fe}$) in the experiments with IP-coated roots compared to Fe-mineral sorption experiments ($0.14 \mu\text{mol As}/\text{mmol Fe}$ for goethite and $1.4 \mu\text{mol As}/\text{mmol Fe}$ for ferrihydrite) further contributes to lower MMMTA

transformation to MMA in the presence of Fe^{III} . If we assume that only MMA but not MMMTA sorbs, the observed low sorption to IP is well explained. For MMDTA, we also saw no evidence for direct sorption; after initial transformation to MMMTA within the first 10 min, remaining MMDTA concentrations did not change any further over time (Figure 2b).

After exposure to DMMTA, very little As sorption was observed on IP and pure goethite, only slightly more (maximum 32% after 72 h) on the highly reactive ferrihydrite. Like for MMMTA, the exact sorption mechanisms are unknown yet. Following a similar argumentation as above, direct binding of DMMTA seems unlikely considering the steric hindrance of one S and two methyl groups. Transformation to DMA is probably low because previous experiments revealed that DMMTA is less sensitive to oxidation than MMMTA³³ and stable in the presence of Fe^{III} for several days.⁵⁰ Arsenic speciation of the aqueous phase revealed little significant trends over time except for a clear decrease in DMMTA both in the presence of goethite and ferrihydrite already after 10 min (Figure S7). For goethite, with little overall sorption (and not much sorption of pure DMA either), the decrease in DMMTA was mirrored in an increase in DMA in solution, probably indicating the transformation pathway from DMMTA to DMA. For ferrihydrite, the DMA concentrations seem to stay constant over time, but this could also be a dynamic equilibrium between some DMA formation from DMMTA and some DMA sorption to ferrihydrite. Like for MMDTA, we also found no evidence for direct sorption of DMDTA, as aqueous concentrations showed no significant trend over time. DMDTA was reported to transform to DMMTA in the presence of Fe^{III} after 15 days,⁵⁰ however, 72 h was not enough time for transformation and DMDTA seemingly persisted without sorption.

■ ENVIRONMENTAL IMPLICATIONS

Our study showed that thiolation of methylated arsenates decreases sorption kinetics and lowers the extent of sorption to the Fe minerals goethite and ferrihydrite as representative endmembers of IP at rice roots. Also for inorganic thioarsenates, less sorption to the Fe minerals goethite, ferrihydrite, or mackinawite was reported before.^{35,36,51} However, there is evidence for direct sorption of the inorganic thioarsenates MTA and TTA,³⁵ while our data showed no evidence for direct sorption of methylated thioarsenates and indicated that transformation to methylated oxyarsenates is a prerequisite to removal by IP at rice roots. Higher transformation of MMMTA to MMA versus DMMTA to DMA will lead to relatively more removal of MMMTA and a very high mobility for DMMTA in the rhizosphere.

In natural paddy soils, a multitude of factors will influence the fate of methylated thioarsenates in the rhizosphere, the contribution of IP to their removal, and finally their uptake in the rice plants. One factor that could lead to higher removal of methylated thioarsenates at IPs in natural paddy soils compared to our experiments is the quantity, distribution, and large diversity of IP formed under different paddy soil conditions and different ROL of rice plants.⁵² The IP formed in our experiments mainly consisted of goethite. Its high crystallinity lowers the available sorption sites and reduces sorption capacity (Figures 1–4). IP consisting mainly of amorphous ferrihydrite could sorb significantly (30–50 times in our study) more MMA, MMMTA, and DMA than goethite;

however, it would still not contribute much to DMMTA removal. Another factor that could lead to sequestration of methylated thioarsenates despite low sorption to IP is co-precipitation with FeS minerals. Methylated thioarsenates form under anoxic conditions in the presence of reduced sulfur from their precursors, methylated oxyarsenates. Paddy soil conditions that sustain formation of (methylated) thioarsenates also enable the formation and precipitation of amorphous FeS, which can scavenge or co-precipitate As. Our MMMTA isotherm studies, for example, showed very high As removal at high aqueous As with a linear increase between 100 and 500 μM spiked MMMTA (Figure 3). We suspect that the process observed here was not only sorption to goethite but also co-precipitation with and sorption to FeS minerals. The excess reduced sulfur in our experiments comes from the synthesis process because MMMTA was synthesized with 10-fold sulfide excess, which could not be removed after synthesis. The Fe-mineral suspensions at high MMMTA concentrations (100 and 500 μM As, corresponding to 1 and 5 mM sulfide) turned black upon addition of the spike, indicating rapid formation of amorphous FeS which could co-precipitate or sorb MMMTA. Colloid formation, such as probably observed at 500 μM MMMTA spike to ferrihydrite, will not contribute to overall As removal from the aqueous phase.

Factors that could decrease removal of methylated thioarsenates, beyond what we predict from our laboratory experiments, are the presence of competing anions, such as phosphate (shown in our study) but potentially also nitrate, sulfate, silica, and so forth, and a high pH. Our experiments were conducted at pH 6.5, which is already at the lower end of typical paddy soil pore water pH values. An increase from, for example, 6.5–7, which is quite common in flooded paddy soils, decreases sorption significantly (around 30% for MMMTA and MMA and around 20% for DMA on goethite, based on our data, Figure 4).

The high mobility of methylated thioarsenates in the rice rhizosphere is directly related to their plant availability, as both MMMTA and DMMTA can be taken up by rice plants and further transported to the xylem³³ and DMMTA, potentially also to the rice grain.^{2,34} Using common acid-based extraction methods for As speciation in rice, highly toxic methylated thioarsenates are converted to and co-determined with their methylated analogues,² which are exempted for regulatory values because of their lower toxicity compared to inorganic As.^{31,32} The occurrence and uptake of MMMTA seems to be less critical because MMA concentrations in the rice grain were often below the detection limit or had only a minor contribution to total As.⁵³ Compared to MMMTA, the high mobility of DMMTA is of greater concern as its uptake and total As translocation to shoots were high³³ and it has been detected in rice grains before, using an extraction method that at least partly preserves DMMTA.³⁴ More studies are needed that monitor the fate of thioarsenates in paddy soils and the rhizosphere and find mitigation strategies to limit uptake and potential grain transport, especially for DMMTA.

■ ASSOCIATED CONTENT

📄 Supporting Information

The Supporting Information is available free of charge on the ACS Publications website at DOI: 10.1021/acs.est.9b04158.

Characterization of Fe minerals; characterization of IP; As speciation of MMMTA and DMMTA for sorption

kinetics, isotherms, and pH-dependent sorption as well as respective pH values; pH-dependent sorption for different electrolytes; composition of ARPW and nutrient solution; and seedling weights (PDF)

■ AUTHOR INFORMATION

Corresponding Author

*E-mail: b.planer-friedrich@uni-bayreuth.de. Phone: +49 921 55 3999.

ORCID

Britta Planer-Friedrich: 0000-0002-0656-4283

Notes

The authors declare no competing financial interest.

■ ACKNOWLEDGMENTS

We acknowledge financial support for a PhD stipend to CK from the German Academic Scholarship Foundation and funding by the German Research Foundation (DFG) Grants PL 302/25 (hydroponic IP studies) and PL 302/26 (synthetic mineral studies). We thank Stefan Will for help with IC–ICP–MS measurements as well as Shubhi Aurora, Nathalia Paola Ceron Espejo, Philipp Knobloch, Eva Voggenreiter, and Christin Wirt for help during the experimental work.

■ REFERENCES

- (1) BfR. Arsen in Reis und Reisprodukten. *Stellungnahme*, 2014; Vol. 018/2015 p58.
- (2) Mantha, M.; Yeary, E.; Trent, J.; Creed, P. A.; Kubachka, K.; Hanley, T.; Shockey, N.; Heitkemper, D.; Caruso, J.; Xue, J.; Rice, G.; Wymer, L.; Creed, J. T. Estimating Inorganic Arsenic Exposure from U.S. Rice and Total Water Intakes. *Environ. Health Perspect.* **2017**, *125*, 057005.
- (3) European Commission, amending Regulation (EC). No 1881/2006 as Regards Maximum Levels of Inorganic Arsenic in Foodstuffs, 2015.
- (4) Chen, H.; Tang, Z.; Wang, P.; Zhao, F.-J. Geographical variations of cadmium and arsenic concentrations and arsenic speciation in Chinese rice. *Environ. Pollut.* **2018**, *238*, 482–490.
- (5) Marin, A. R.; Masscheleyn, P. H.; Patrick, W. H. Soil Redox-Ph Stability of Arsenic Species and Its Influence on Arsenic Uptake by Rice. *Plant Soil* **1993**, *152*, 245–253.
- (6) Masscheleyn, P. H.; Delaune, R. D.; Patrick, W. H. Effect of Redox Potential and Ph on Arsenic Speciation and Solubility in a Contaminated Soil. *Environ. Sci. Technol.* **1991**, *25*, 1414–1419.
- (7) Meharg, A. A.; Zhao, F.-J. *Arsenic & Rice*; Springer: Netherlands, 2012; Vol. 1, p 172.
- (8) Zhao, F.-J.; McGrath, S. P.; Meharg, A. A. Arsenic as a food chain contaminant: mechanisms of plant uptake and metabolism and mitigation strategies. *Annu. Rev. Plant Biol.* **2010**, *61*, 535–559.
- (9) Fan, C.; Liu, G.; Long, Y.; Rosen, B.; Cai, Y. Thiolation in arsenic metabolism: a chemical perspective. *Metallomics* **2018**, *10*, 1368–1382.
- (10) Lomax, C.; Liu, W.-J.; Wu, L.; Xue, K.; Xiong, J.; Zhou, J.; McGrath, S. P.; Meharg, A. A.; Miller, A. J.; Zhao, F.-J. Methylated arsenic species in plants originate from soil microorganisms. *New Phytol.* **2012**, *193*, 665–672.
- (11) Li, R. Y.; Stroud, J. L.; Ma, J. F.; McGrath, S. P.; Zhao, F. J. Mitigation of Arsenic Accumulation in Rice with Water Management and Silicon Fertilization. *Environ. Sci. Technol.* **2009**, *43*, 3778–3783.
- (12) Seyfferth, A. L.; Limmer, M. A.; Dykes, G. E. On the Use of Silicon as an Agronomic Mitigation Strategy to Decrease Arsenic Uptake by Rice. *Adv. Agron.* **2018**, *149*, 49–91.
- (13) Tripathi, R. D.; Tripathi, P.; Dwivedi, S.; Kumar, A.; Mishra, A.; Chauhan, P. S.; Norton, G. J.; Nautiyal, C. S. Roles for root iron

plaque in sequestration and uptake of heavy metals and metalloids in aquatic and wetland plants. *Metallomics* **2014**, *6*, 1789–1800.

(14) Bacha, R. E.; Hossner, L. R. Characteristics of Coatings formed on Rice Roots as Affected by Iron and Manganese Additions I. *Soil Sci. Soc. Am. J.* **1977**, *41*, 931.

(15) Chen, C. C.; Dixon, J. B.; Turner, F. T. Iron Coatings on Rice Roots: Mineralogy and Quantity Influencing Factors I. *Soil Sci. Soc. Am. J.* **1980**, *44*, 635.

(16) Liu, W. J.; Zhu, Y. G.; Hu, Y.; Williams, P. N.; Gault, A. G.; Meharg, A. A.; Charnock, J. M.; Smith, F. A. Arsenic Sequestration in Iron Plaque, Its Accumulation and Speciation in Mature Rice Plants (*Oryza sativa* L.). *Environ. Sci. Technol.* **2006**, *40*, 5730–5736.

(17) Seyfferth, A. L.; Webb, S. M.; Andrews, J. C.; Fendorf, S. Arsenic Localization, Speciation, and Co-Occurrence with Iron on Rice (*Oryza sativa* L.) Roots Having Variable Fe Coatings. *Environ. Sci. Technol.* **2010**, *44*, 8108–8113.

(18) Seyfferth, A. L.; Webb, S. M.; Andrews, J. C.; Fendorf, S. Defining the distribution of arsenic species and plant nutrients in rice (*Oryza sativa* L.) from the root to the grain. *Geochim. Cosmochim. Acta* **2011**, *75*, 6655–6671.

(19) Lafferty, B. J.; Loeppert, R. H. Methyl arsenic adsorption and desorption behavior on iron oxides. *Environ. Sci. Technol.* **2005**, *39*, 2120–2127.

(20) Dixit, S.; Hering, J. G. Comparison of Arsenic(V) and Arsenic(III) Sorption onto Iron Oxide Minerals: Implications for Arsenic Mobility. *Environ. Sci. Technol.* **2003**, *37*, 4182–4189.

(21) Raven, K. P.; Jain, A.; Loeppert, R. H. Arsenite and Arsenate Adsorption on Ferrihydrite: Kinetics, Equilibrium, and Adsorption Envelopes. *Environ. Sci. Technol.* **1998**, *32*, 344–349.

(22) Deng, D.; Wu, S.-C.; Wu, F.-Y.; Deng, H.; Wong, M.-H. Effects of root anatomy and Fe plaque on arsenic uptake by rice seedlings grown in solution culture. *Environ. Pollut.* **2010**, *158*, 2589–2595.

(23) Chen, Z.; Zhu, Y. G.; Liu, W. J.; Meharg, A. A. Direct evidence showing the effect of root surface iron plaque on arsenite and arsenate uptake into rice (*Oryza sativa*) roots. *New Phytol.* **2005**, *165*, 91–7.

(24) Wu, C.; Ye, Z.; Li, H.; Wu, S.; Deng, D.; Zhu, Y.; Wong, M. Do radial oxygen loss and external aeration affect iron plaque formation and arsenic accumulation and speciation in rice? *J. Exp. Bot.* **2012**, *63*, 2961–2970.

(25) Lee, C.-H.; Hsieh, Y.-C.; Lin, T.-H.; Lee, D.-Y. Iron plaque formation and its effect on arsenic uptake by different genotypes of paddy rice. *Plant Soil* **2012**, *363*, 231–241.

(26) Hossain, M. B.; Jahiruddin, M.; Loeppert, R. H.; Panaullah, G. M.; Islam, M. R.; Duxbury, J. M. The effects of iron plaque and phosphorus on yield and arsenic accumulation in rice. *Plant Soil* **2008**, *317*, 167–176.

(27) Planer-Friedrich, B.; Halder, D.; Kerl, C. F.; Schaller, J.; Wang, J.; Martin, M.; Romani, M. *Thioarsenates—So Far Unrecognized Arsenic Species in Paddy Soils*; Goldschmidt Abstracts: Paris, 2017; p 3176.

(28) Stauder, S.; Raue, B.; Sacher, F. Thioarsenates in Sulfidic Waters. *Environ. Sci. Technol.* **2005**, *39*, 5933–5939.

(29) Planer-Friedrich, B.; Suess, E.; Scheinost, A. C.; Wallschläger, D. Arsenic speciation in sulfidic waters: reconciling contradictory spectroscopic and chromatographic evidence. *Anal. Chem.* **2010**, *82*, 10228–10235.

(30) Cullen, W. R.; Liu, Q.; Lu, X.; McKnight-Whitford, A.; Peng, H.; Popowich, A.; Yan, X.; Zhang, Q.; Fricke, M.; Sun, H.; Le, X. C. Methylated and thiolated arsenic species for environmental and health research - A review on synthesis and characterization. *J. Environ. Sci.* **2016**, *49*, 7–27.

(31) Naranmandura, H.; Iyata, K.; Suzuki, K. T. Toxicity of dimethylmonothioarsinic acid toward human epidermoid carcinoma A431 cells. *Chem. Res. Toxicol.* **2007**, *20*, 1120–1125.

(32) Naranmandura, H.; Carew, M. W.; Xu, S.; Lee, J.; Leslie, E. M.; Weinfeld, M.; Le, X. C. Comparative toxicity of arsenic metabolites in human bladder cancer EJ-1 cells. *Chem. Res. Toxicol.* **2011**, *24*, 1586–1596.

(33) Kerl, C. F.; Schindele, R. A.; Brüggewirth, L.; Colina Blanco, A. E.; Rafferty, C.; Clemens, S.; Planer-Friedrich, B. Methylated Thioarsenates and Monothioarsenate Differ in Uptake, Transformation, and Contribution to Total Arsenic Translocation in Rice Plants. *Environ. Sci. Technol.* **2019**, *53*, 5787–5796.

(34) Ackerman, A. H.; Creed, P. A.; Parks, A. N.; Fricke, M. W.; Schwegel, C. A.; Creed, J. T.; Heitkemper, D. T.; Vela, N. P. Comparison of a Chemical and Enzymatic Extraction of Arsenic from Rice and an Assessment of the Arsenic Absorption from Contaminated Water by Cooked Rice. *Environ. Sci. Technol.* **2005**, *39*, 5241–5246.

(35) Couture, R.-M.; Rose, J.; Kumar, N.; Mitchell, K.; Wallschläger, D.; Van Cappellen, P. Sorption of arsenite, arsenate, and thioarsenates to iron oxides and iron sulfides: a kinetic and spectroscopic investigation. *Environ. Sci. Technol.* **2013**, *47*, 5652–5659.

(36) Suess, E.; Planer-Friedrich, B. Thioarsenate formation upon dissolution of orpiment and arsenopyrite. *Chemosphere* **2012**, *89*, 1390–1398.

(37) Wallschläger, D.; London, J. Determination of Methylated Arsenic-Sulfur Compounds in Groundwater. *Environ. Sci. Technol.* **2008**, *42*, 228–234.

(38) Hinrichsen, S.; Geist, F.; Planer-Friedrich, B. Inorganic and methylated thioarsenates pass the gastrointestinal barrier. *Chem. Res. Toxicol.* **2015**, *28*, 1678–1680.

(39) Schwertmann, U.; Cornell, R. M. *Iron Oxides in the Laboratory: Preparation and Characterization*; Wiley-VCH: Weinheim, New York, 2000; Vol. 2.

(40) Kerl, C. F.; Rafferty, C.; Clemens, S.; Planer-Friedrich, B. Monothioarsenate Uptake, Transformation, and Translocation in Rice Plants. *Environ. Sci. Technol.* **2018**, *52*, 9154–9161.

(41) Wang, Y.; Yuan, J.-H.; Chen, H.; Zhao, X.; Wang, D.; Wang, S.-Q.; Ding, S.-M. Small-scale interaction of iron and phosphorus in flooded soils with rice growth. *Sci. Total Environ.* **2019**, *669*, 911–919.

(42) Fu, Y.-Q.; Yang, X.-J.; Ye, Z.-H.; Shen, H. Identification, separation and component analysis of reddish brown and non-reddish brown iron plaque on rice (*Oryza sativa*) root surface. *Plant Soil* **2016**, *402*, 277–290.

(43) Buchholz, A.; Laskov, C.; Haderlein, S. B. Effects of Zwitterionic buffers on sorption of ferrous iron at goethite and its oxidation by CCl_4 . *Environ. Sci. Technol.* **2011**, *45*, 3355–3360.

(44) Kersten, M.; Daus, B. Silicic acid competes for dimethylarsinic acid (DMA) immobilization by the iron hydroxide plaque mineral goethite. *Sci. Total Environ.* **2015**, *508*, 199–205.

(45) Adamescu, A.; Mitchell, W.; Hamilton, I. P.; Al-Abadleh, H. A. Insights into the surface complexation of dimethylarsinic acid on iron (oxyhydr)oxides from ATR-FTIR studies and quantum chemical calculations. *Environ. Sci. Technol.* **2010**, *44*, 7802–7807.

(46) Shimizu, M.; Arai, Y.; Sparks, D. L. Multiscale assessment of methylarsenic reactivity in soil. 1. Sorption and desorption on soils. *Environ. Sci. Technol.* **2011**, *45*, 4293–4299.

(47) Mishra, S.; Mattusch, J.; Wennrich, R. Accumulation and transformation of inorganic and organic arsenic in rice and role of thiol-complexation to restrict their translocation to shoot. *Sci. Rep.* **2017**, *7*, 40522.

(48) Raab, A.; Schat, H.; Meharg, A. A.; Feldmann, J. Uptake, translocation and transformation of arsenate and arsenite in sunflower (*Helianthus annuus*): formation of arsenic-phytochelatin complexes during exposure to high arsenic concentrations. *New Phytol.* **2005**, *168*, 551–558.

(49) Raab, A.; Williams, P. N.; Meharg, A.; Feldmann, J. Uptake and translocation of inorganic and methylated arsenic species by plants. *Environ. Chem.* **2007**, *4*, 197.

(50) Kim, Y.-T.; Lee, H.; Yoon, H.-O.; Woo, N. C. Kinetics of Dimethylated Thioarsenicals and the Formation of Highly Toxic Dimethylmonothioarsinic Acid in Environment. *Environ. Sci. Technol.* **2016**, *50*, 11637–11645.

(51) Burton, E. D.; Johnston, S. G.; Planer-Friedrich, B. Coupling of arsenic mobility to sulfur transformations during microbial sulfate

reduction in the presence and absence of humic acid. *Chem. Geol.* **2013**, *343*, 12–24.

(52) Seyfferth, A. L. Abiotic effects of dissolved oxyanions on iron plaque quantity and mineral composition in a simulated rhizosphere. *Plant Soil* **2015**, *397*, 43–61.

(53) Zhao, F.-J.; Zhu, Y.-G.; Meharg, A. A. Methylated arsenic species in rice: geographical variation, origin, and uptake mechanisms. *Environ. Sci. Technol.* **2013**, *47*, 3957–3966.

Supporting Information

Environmental Science & Technology

Iron plaque at rice roots: no barrier for methylated thioarsenates

Carolin F. Kerl[†], Tiziana Boffa Ballaran[‡], Britta Planer-Friedrich^{†}*

[†]Environmental Geochemistry, Bayreuth Center for Ecology and Environmental Research (BayCEER), University of Bayreuth, D-95440 Bayreuth, Germany

[‡] Bayerisches Geoinstitut BGI, University of Bayreuth, D-95440 Bayreuth, Germany

* Corresponding author phone: +49 921 55 3999, E-mail: b.planer-friedrich@uni-bayreuth.de

(S15 pages, 11 figures, 3 tables)

CONTENTS

Figure SI 1 X-ray diffraction pattern of goethite	2
Figure SI 2 X-ray diffraction pattern of ferrihydrite	3
Figure SI 3 X-ray diffraction pattern of rice root with and without IP	4
Figure SI 4 Example of a 2D diffraction pattern collected for a portion of a rice root	5
Figure SI 5 μ -X-ray diffraction pattern of rice root with IP	6
Figure SI 6 pH values of sorption kinetics on goethite and ferrihydrite	7
Figure SI 7 As speciation of sorption kinetics on goethite and ferrihydrite during first hour	8
Figure SI 8 pH values of non-equilibrium sorption isotherm on goethite and ferrihydrite	9
Figure SI 9 As speciation of non-equilibrium sorption isotherm on goethite and ferrihydrite	10
Figure SI 10 As speciation of pH dependent sorption envelope on goethite and ferrihydrite	11
Figure SI 11 pH dependent sorption envelope of goethite comparing different electrolytes	12
Table SI 1 Nutrient solution	13
Table SI 2 Artificial rhizosphere pore water	14
Table SI 3 Seedling dry weights for uptake experiments	15

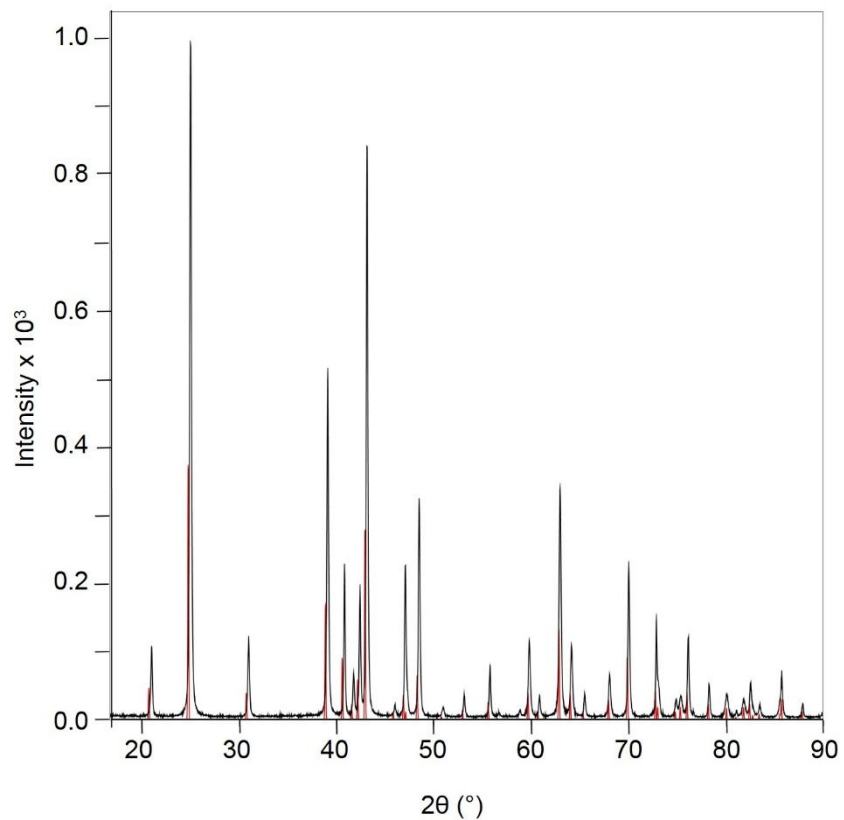


Figure SI 1. Measured X-ray diffraction pattern of α -goethite (black line) mineral used for sorption experiments compared with the goethite pattern reported in the Inorganic Crystal Structure Database (Nr. 245057-ICSD) (red line).

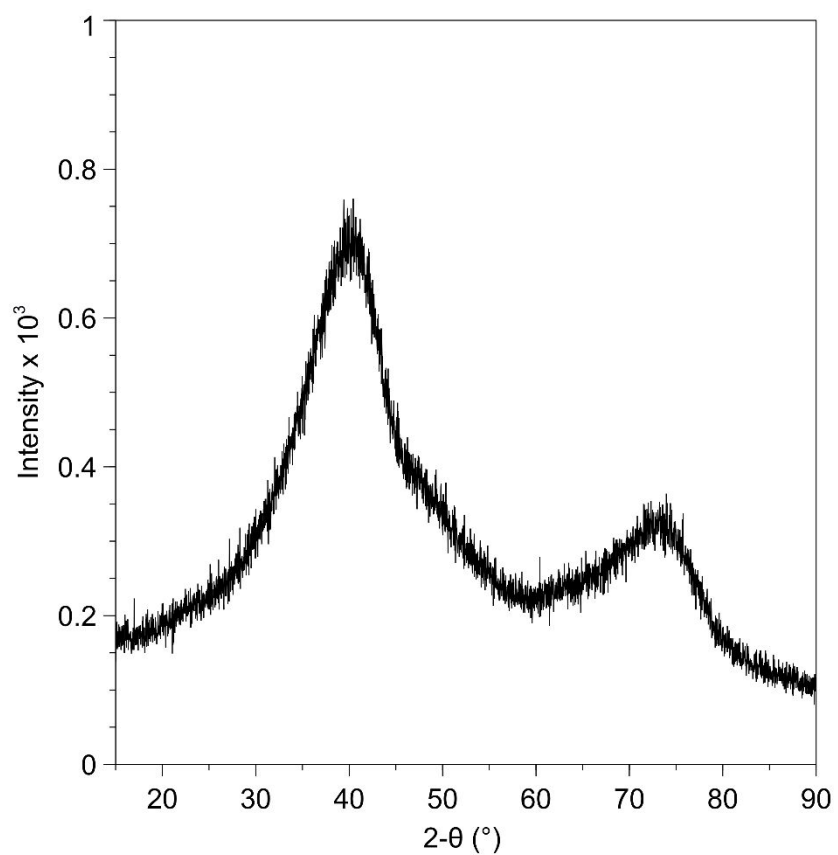


Figure SI 2. X-ray diffraction pattern of a 2-line ferrihydrite mineral used for sorption experiments.

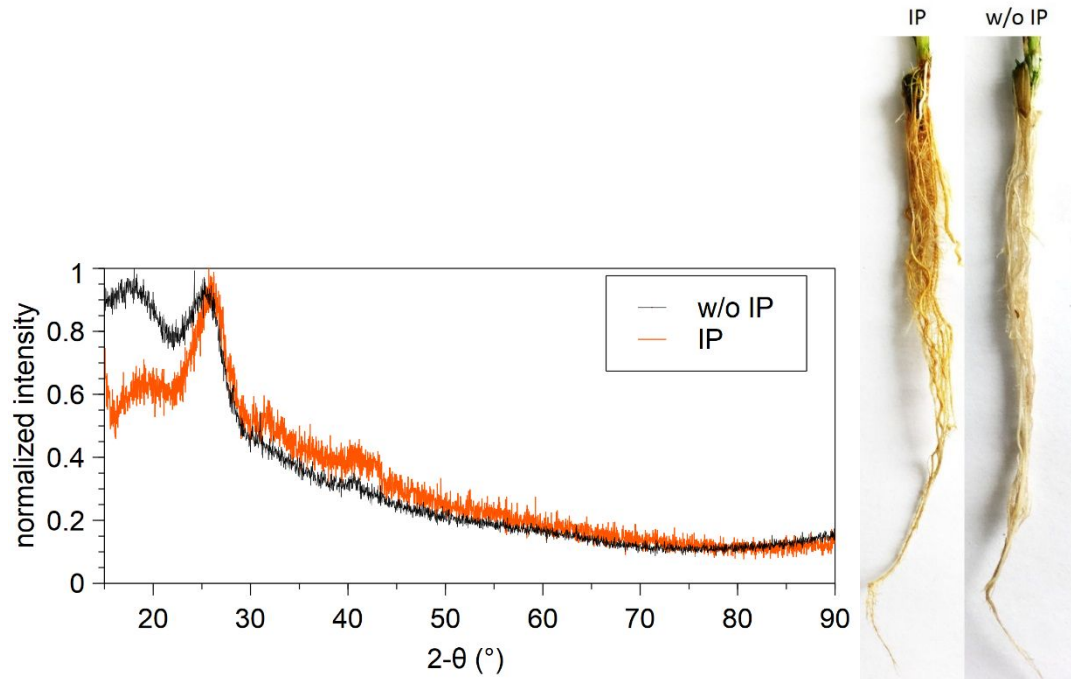


Figure SI 3. Bulk X-ray diffraction (XRD) pattern were obtained from grounded rice roots covered with IP (orange line, left picture) and roots without IP (black line, right picture) used for uptake experiments. The results showed that bulk XRD is not sensitive enough for determining IP compared to the background noise of rice roots w/o IP.

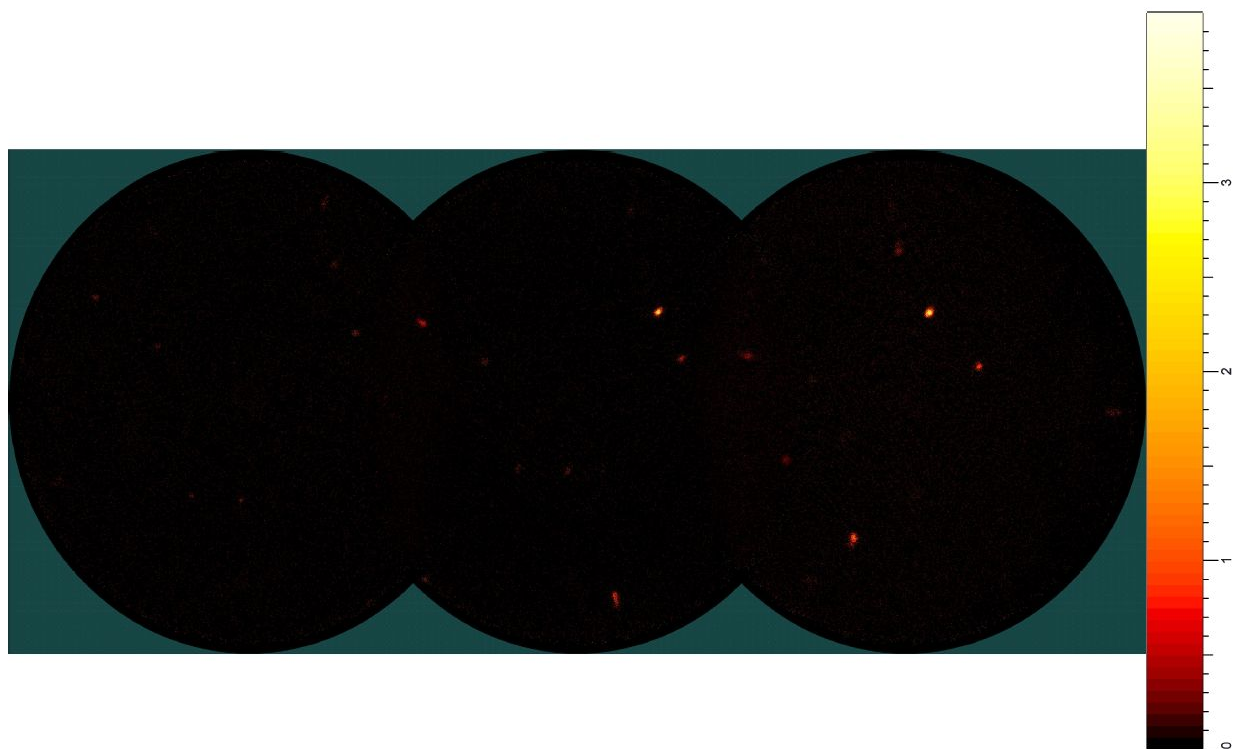


Figure SI 4. Example of a 2D diffraction pattern collected for a portion of a rice root with IP. The pattern has been collected with a diffraction beam focused down to 50-100 microns. The few diffraction spots visible in the frames suggest, therefore, that only few large grains of IP are present in the area covered by the X-ray beam and therefore only few planes obey the diffraction geometry, giving rise to well defined spots instead of Debye rings as expected for a statistically oriented powdered sample. The color chart shows the signal intensity, with lowest intensity in black and highest intensity in white.

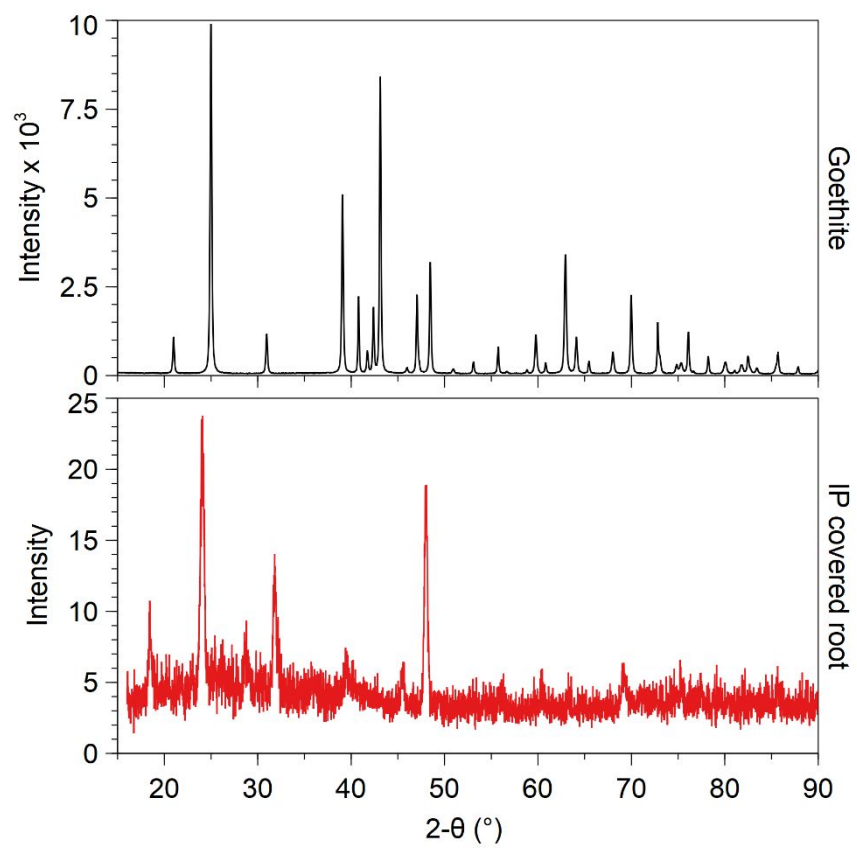


Figure SI 5. 1D X-ray diffraction pattern of rice root covered with IP (red line) obtained by integrating the 2D frames collected with the micro-focused diffractometer compared to goethite.

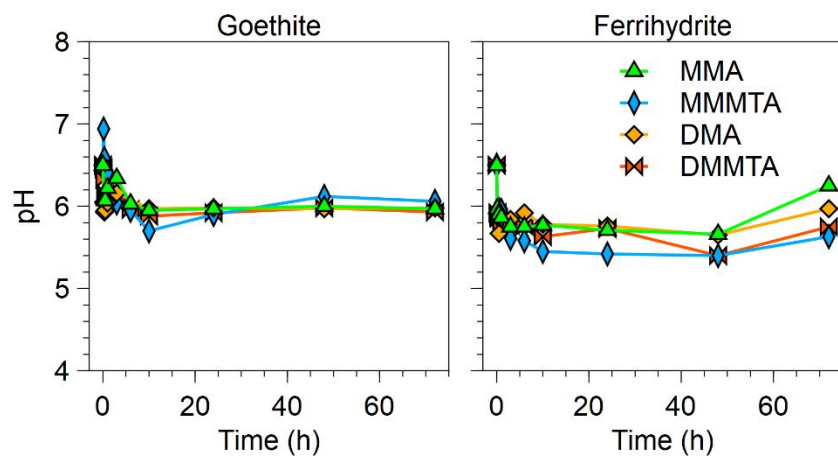


Figure SI 6. pH values of sorption kinetics for 5 μ M MMA, MMMTA, DMA, or DMMTA on goethite (36 mM) and 2-line ferrihydrite (3.6 mM) in ARPW after 0-72 h equilibration (n=1).

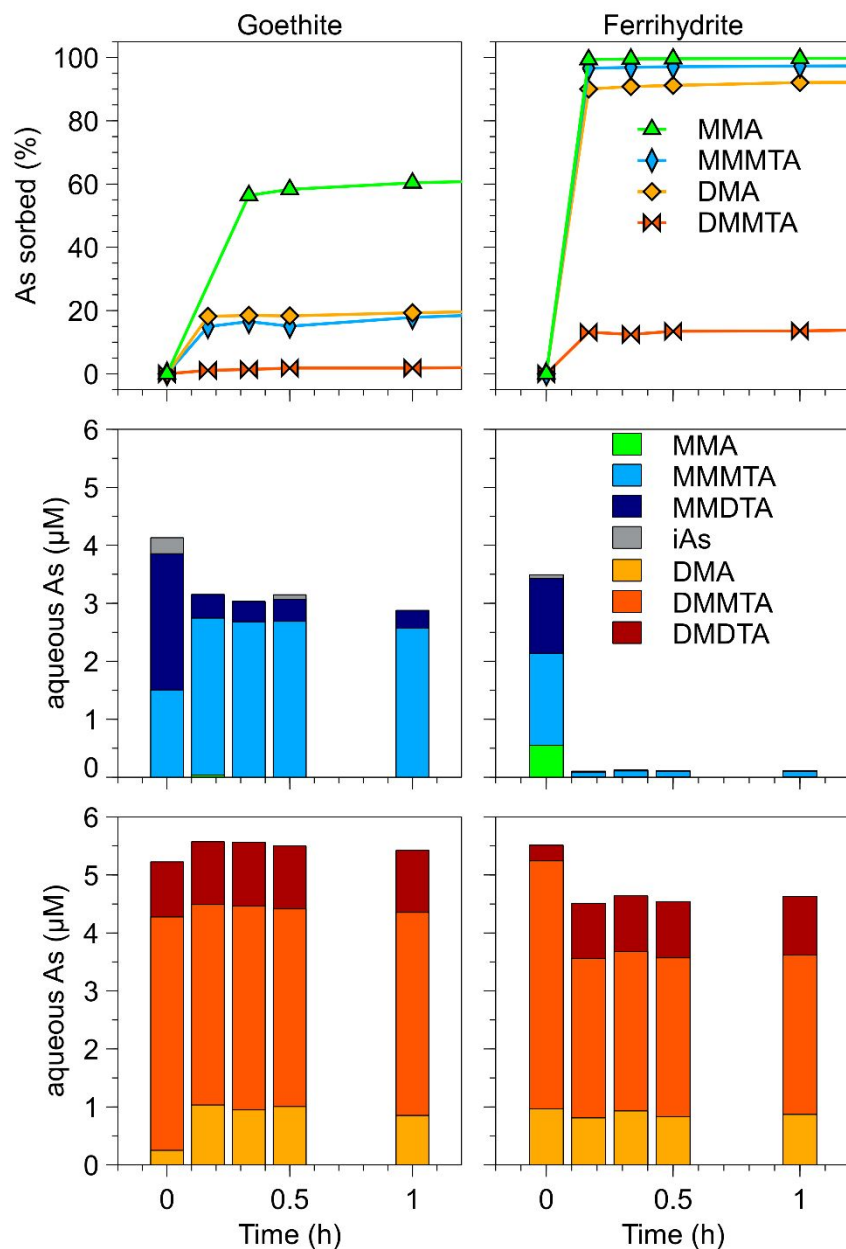


Figure SI 7. Sorption kinetics for 5 μM MMA, MMMTA, DMA, or DMMTA on goethite (36 mM) and 2-line ferrihydrite (3.6 mM) in ARPW after 0-1 h equilibration ($n=1$). Sorbed total As is calculated as difference between As concentration in control without goethite or 2-line ferrihydrite and measured total As concentration in aqueous phase after equilibration (upper panel). As speciation for MMMTA (middle panel) and DMMTA (lower panel) is shown as measured As concentration in the aqueous phase after equilibration.

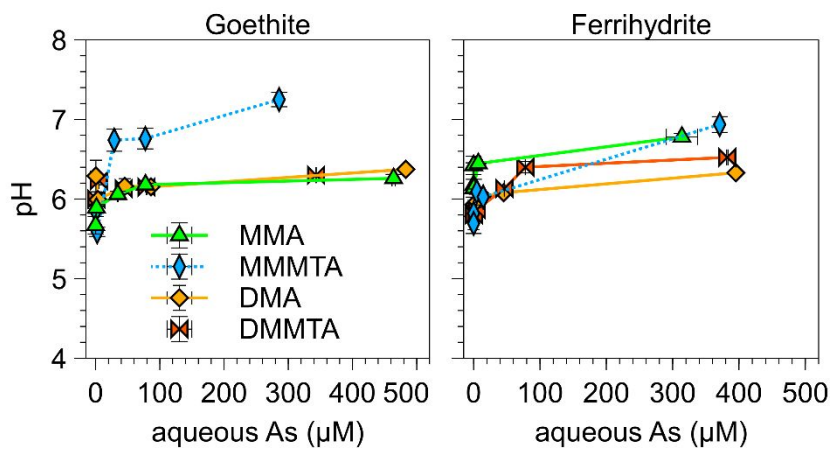


Figure SI 8. pH values of non-equilibrium sorption isotherm for 0.5-500 μM MMA, MMMTA, DMA, or DMMTA on goethite (36 mM) and 2-line ferrihydrite (3.6 mM) in ARPW after 2 h equilibration (n=3).

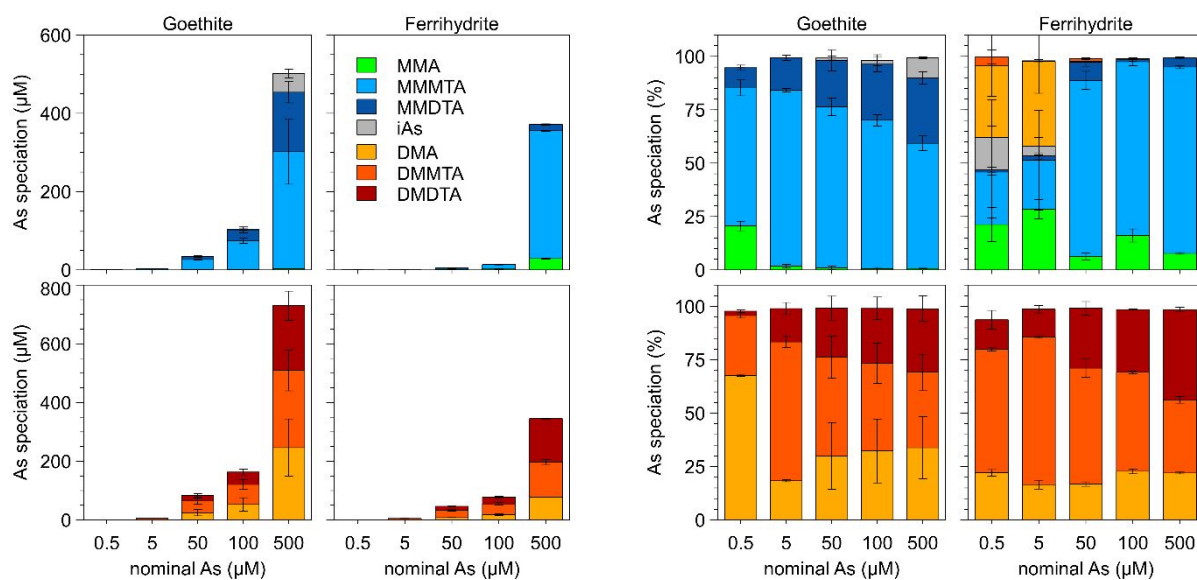


Figure SI 9. As speciation of non-equilibrium sorption isotherms for 0.5-500 μM MMMTA, or DMMTA on goethite (36 mM) and 2-line ferrihydrite (3.6 mM) in ARPW after 2 h equilibration ($n=3$). As speciation shown as measured As concentration in the aqueous phase after 2 h equilibration (left side) and As speciation in percent (right side).

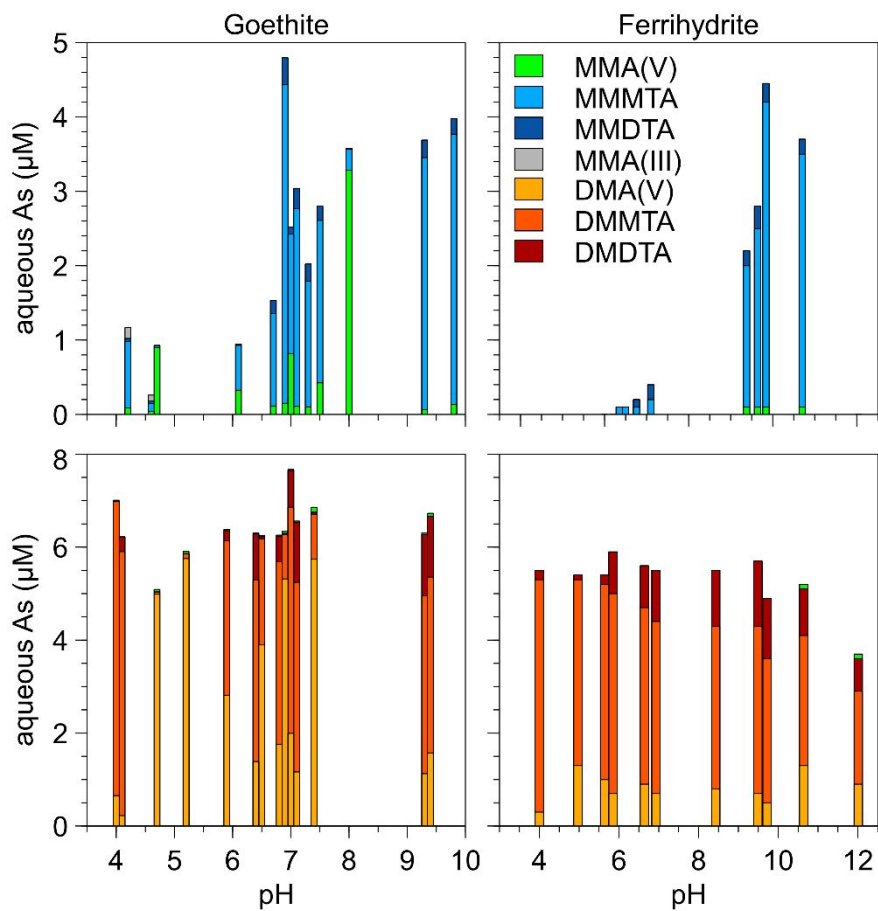


Figure SI 10. As speciation of pH dependent sorption envelope for 5 μM MMMTA, or DMMTA on goethite (36 mM) and ferrihydrite (3.6 mM) in ARPW ($n=1$). As speciation shown as measured As concentration in aqueous phase after 2 h equilibration.

pH dependent sorption experiments were performed analogue to experiments in ARPW. Goethite (36 mM ferric iron Fe^{III}) was pre-equilibrated for 16 h in ARPW, ARPW without phosphate and in 10 mM NaNO_3 at the respective pH. Each sample in 10 mL vials (Sarsteadt) was spiked with MMA or DMA and kept anoxic during sorption. After 2 h equilibration, samples were centrifuged 5 min (5000 rpm; Hettich), supernatants were filtered through 0.2 μm filters (cellulose-acetate, Machery-Nagel), and sub-samples for analysis of totals As by ICP-MS were stabilized with 2.5% 7 M HNO_3 (Kraft) and pH was measured in the remaining sample.

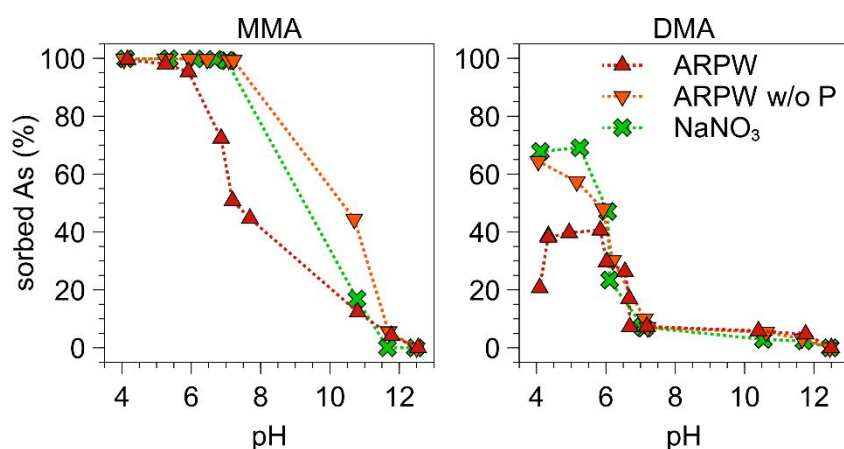


Figure SI 11. Sorption envelope for 5 μM MMA and DMA on goethite (36 mM) in ARPW, ARPW without P and 10 mM NaNO_3 ($n=1$). Sorbed As calculated as difference between As concentration in control without goethite and measured total As concentration in aqueous phase after 2 h equilibration.

Table SI 1. Composition of nutrient solution used for plant growth.

Nr.	Macronutrients	Concentration (mg/L)	Vendor
1	Ca(NO ₃) ₂ *4H ₂ O	1000	Grüssing
2	KCl	120	Grüssing
3	KH ₂ PO ₄	250*	Grüssing
4	MgSO ₄ *7H ₂ O	250	Merck
5	Fe-EDDAH (5.7% Fe)	20**	Duchefa Biochemie
Nr.	Micronutrients	Concentration (µg/L)	Vendor
1	KI	27	Grüssing
2	LiCl	27	Fluka
3	CuSO ₄ *5H ₂ O	55	Grüssing
4	ZnSO ₄ *7H ₂ O	111	Roth
5	H ₃ BO ₃	55	Merck
6	Al ₂ (SO ₄) ₃	55	Alfa Aesar
7	MnCl ₂ *4H ₂ O	388	AppliChem
8	NiSO ₄ *7H ₂ O	55	Aldrich
9	Co(NO ₃) ₂ *6H ₂ O	55	Fluka
10	KBr	27	Merck
11	(NH ₄) ₆ Mo ₇ O ₂₄	55	Fluka

* 12.5 mg/L during IP formation and in control treatment

** 100 mg/L Fe(II)Cl₂ during IP formation; plants in control treatment were grown using Fe-EDDAH

Table SI 2. Composition of artificial rhizosphere pore water used for sorption experiments.

Nr.	Macronutrients	Concentration (mg/L)	Vendor
1	Ca(NO ₃) ₂ *4H ₂ O	10	Grüssing
2	KCl	1.2	Grüssing
3	KH ₂ PO ₄	2.5	Grüssing
4	MgSO ₄ *7H ₂ O	2.5	Merck

Nr.	Micronutrients	Concentration (µg/L)	Vendor
1	KI	0.3	Grüssing
2	LiCl	0.3	Fluka
3	CuSO ₄ *5H ₂ O	0.6	Grüssing
4	ZnSO ₄ *7H ₂ O	1.1	Roth
5	H ₃ BO ₃	0.6	Merck
6	Al ₂ (SO ₄) ₃	0.6	Alfa Aesar
7	MnCl ₂ *4H ₂ O	3.9	AppliChem
8	NiSO ₄ *7H ₂ O	0.6	Aldrich
9	Co(NO ₃) ₂ *6H ₂ O	0.6	Fluka
10	KBr	0.3	Merck
11	(NH ₄) ₆ Mo ₇ O ₂₄	0.6	Fluka

Table SI 3. Seedling dry weights for uptake experiments.

		Uptake					
		root dry weight in (g)			shoot dry weight in (g)		
IP	no As	0.0182	±	0.0051	0.0366	±	0.0058
	MMA^V	0.0177	±	0.0026	0.0331	±	0.0096
	MMMTA	0.0165	±	0.0030	0.0284	±	0.0094
	DMA^V	0.0182	±	0.0040	0.0317	±	0.0078
	DMMTA	0.0258	±	0.0076	0.0495	±	0.0245
Control	no As	0.0259		0.0015	0.0536		0.0046
	MMA^V	0.0194	±	0.0051	0.0446	±	0.0206
	MMMTA	0.0232	±	0.0035	0.0510	±	0.0115
	DMA^V	0.0302	±	0.0049	0.0695	±	0.0121
	DMMTA	0.0213	±	0.0033	0.0492	±	0.0136

List of publications

The following publications/manuscripts have been published or are submitted during the work on this thesis:

Wang, J.; **Kerl, C. F.**; Hu, P.; Martin, M.; Mu, T.; Brüggewirth, L.; Wu, G.; Said-Pullicino, D.; Romani, M.; Wu, L.; Planer-Friedrich, B., Thiolated arsenic species observed in rice paddy pore-waters. *Nature Geoscience* **2020**. DOI: 10.1038/s41561-020-0533-1.

Kerl, C. F.; Rafferty, C.; Clemens, S.; Planer-Friedrich, B., Monothioarsenate Uptake, Transformation, and Translocation in Rice Plants. *Environ. Sci. Technol.* **2018**, *52*, (16), 9154-9161. DOI: 10.1021/acs.est.8b02202

Kerl, C. F.; Schindele, R. A.; Brüggewirth, L.; Colina Blanco, A. E.; Rafferty, C.; Clemens, S.; Planer-Friedrich, B., Methylated thioarsenates and monothioarsenate differ in uptake, transformation, and contribution to total arsenic translocation in rice plants. *Environ. Sci. Technol.* **2019**. DOI: 10.1021/acs.est.9b00592

Kerl, C. F.; Boffa Balaran, T.; Planer-Friedrich, B., Iron plaque of rice plants: no barrier for methylated thioarsenates. *Environ. Sci. Technol.* **2019**, *53*, (23): 13666-13674. DOI: 10.1021/acs.est.9b04158.

Other publications:

Kerl, C. F.; Lohmayer, R.; Bura-Nakic, E.; Vance, D.; Planer-Friedrich, B., Experimental Confirmation of Isotope Fractionation in Thiomolybdates Using Ion Chromatographic Separation and Detection by Multicollector ICPMS. *Anal. Chem.* **2017**, *89*, (5), 3123-3129. DOI: 10.1021/acs.analchem.6b04898

Mehlhorn, J.; Lohmayer, R.; Boeing, F.; **Kerl, C. F.**; Kaasalainen, H.; Stefánsson, A.; Planer-Friedrich, B., Thiomolybdates and thiotungstates in geothermal waters: comparison to thioarsenates and thioantimonates. Submitted to *Environmental Science & Technology*.

Muehe, E. M.; Wang, T.; **Kerl, C. F.**; Planer-Friedrich, B.; Fendorf, S., Rice production threatened by coupled stresses of climate and soil arsenic. *Nat. Comm.* **2019**, *10*, (4985), doi:10.1038/s41467-019-12946-4

Eberle, A.; Besold, J.; **Kerl, C. F.**; Lezama-Pacheco, J. S.; Fendorf, S. Planer-Friedrich, B., Ambivalent Role of Reduced Sulfur for the Fate of Arsenic in Peatlands: Sequestration at Acidic and Mobilization at Neutral to Alkaline Conditions. Submitted to *Environmental Science & Technology*.

Supervised theses

Bachelor

The following Bachelor thesis has been co-supervised during the work on this thesis:

1. Pinzer, S. (2018): Toxizität von Monothioarsenat unter dem Einfluss von Silizium und Phosphat in Reis, Bachelor Thesis, University of Bayreuth, Environmental Geochemistry.

Results of this project are included in study 2 of this thesis.

Master

The following Master theses have been co-supervised during the work on this thesis:

1. Eberle, A. (2018): Sulfur-induced remobilisation of arsenic from natural organic matter, Master Thesis, University of Bayreuth, Environmental Geochemistry.

Results of this project are included in co-author publication.

2. Schindele, R.A. (2018): Uptake and transformation of methylated thioarsenates in rice, Master Thesis, University of Bayreuth, Environmental Geochemistry.

Results of this project are included in study 3 of this thesis.

3. Brüggewirth, L. (2018): Effect of root radial oxygen loss on arsenic speciation in the rice rhizosphere, Master Thesis, University of Bayreuth, Environmental Geochemistry.

Results of this project are included in study 3 of this thesis.

4. Breuninger, E. (2018): Isotope Fractionation During Sorption of Different Thiomolybdate Species to Marine Phytoplankton Using IC-Separation & Detection by MC-ICP-MS, Master Thesis, University of Bayreuth, Environmental Geochemistry.

5. Colina Blanco, A.E (2019): Arsenic in rice in Costa Rica, Master Thesis, University of Bayreuth, Environmental Geochemistry.

(Eidesstattliche) Versicherungen und Erklärungen

(§ 9 Satz 2 Nr. 3 PromO BayNAT)

Hiermit versichere ich eidesstattlich, dass ich die Arbeit selbstständig verfasst und keine anderen als die von mir angegebenen Quellen und Hilfsmittel benutzt habe (vgl. Art. 64 Abs. 1 Satz 6 BayHSchG).

(§ 9 Satz 2 Nr. 3 PromO BayNAT)

Hiermit erkläre ich, dass ich die Dissertation nicht bereits zur Erlangung eines akademischen Grades eingereicht habe und dass ich nicht bereits diese oder eine gleichartige Doktorprüfung endgültig nicht bestanden habe.

(§ 9 Satz 2 Nr. 4 PromO BayNAT)

Hiermit erkläre ich, dass ich Hilfe von gewerblichen Promotionsberatern bzw. -vermittlern oder ähnlichen Dienstleistern weder bisher in Anspruch genommen habe noch künftig in Anspruch nehmen werde.

(§ 9 Satz 2 Nr. 7 PromO BayNAT)

Hiermit erkläre ich mein Einverständnis, dass die elektronische Fassung meiner Dissertation unter Wahrung meiner Urheberrechte und des Datenschutzes einer gesonderten Überprüfung unterzogen werden kann.

(§ 9 Satz 2 Nr. 8 PromO BayNAT)

Hiermit erkläre ich mein Einverständnis, dass bei Verdacht wissenschaftlichen Fehlverhaltens Ermittlungen durch universitätsinterne Organe der wissenschaftlichen Selbstkontrolle stattfinden können.

.....
Ort, Datum, Unterschrift